Novel insights into the

Pathophysiology

— of Group II —

Pulmonary Hypertension

Impact on the pulmonary vasculature and right ventricle

R.W.B. van Duin

Novel insights into the

Pathophysiology

— of Group II —

Pulmonary Hypertension

Impact on the pulmonary vasculature and right ventricle

Richard Willem Benjamin van Duin

Novel Insights into the Pathophysiology of Group II Pulmonary Hypertension

Thesis Erasmus Medical Center, Rotterdam

ISBN: 978-94-6416-431-2
Print: Ridderprint | www.ridderprint.nl
Cover art: Corpus mechanica - Cardiopulmonary bypass by Nohablalogica

Novel insights into the

Pathophysiology of Group II Pulmonary Hypertension

Impact on the pulmonary vasculature and right ventricle

Nieuwe inzichten in de

Pathofysiologie van groep II pulmonale hypertensie

Impact op de longvaten en het rechter ventrikel

Proefschrift

ter verkrijging van de graad van doctor aan de
Erasmus Universiteit Rotterdam

op gezag van de rector magnificus
Prof. dr. F.A. van der Duijn Schouten
en volgens besluit van het College voor Promoties.

De openbare verdediging zal plaatsvinden op
dinsdag 30 maart 2021 om 10:30 uur

door

Richard Willem Benjamin van Duin

geboren te Spijkenisse.

Erasmus University Rotterdam

Promotiecommissie:

Promotoren:	prof. dr. D.J.G.M. Duncker prof. dr. D. Merkus
Overige leden:	prof. dr. I.K.M. Reiss prof. dr. H.J. Bogaard prof. dr. B. Ibanez

The studies in this thesis have been conducted at the Laboratory of the Division of Experimental Cardiology, Department of Cardiology, Erasmus University Medical Center, Rotterdam, The Netherlands.

Financial support by the Dutch Heart Foundation for the publication of this thesis is gratefully acknowledged.

The research described in this thesis was supported by a grant of the Dutch Heart Foundation (PHAEDRA 2012B008).

CONTENTS

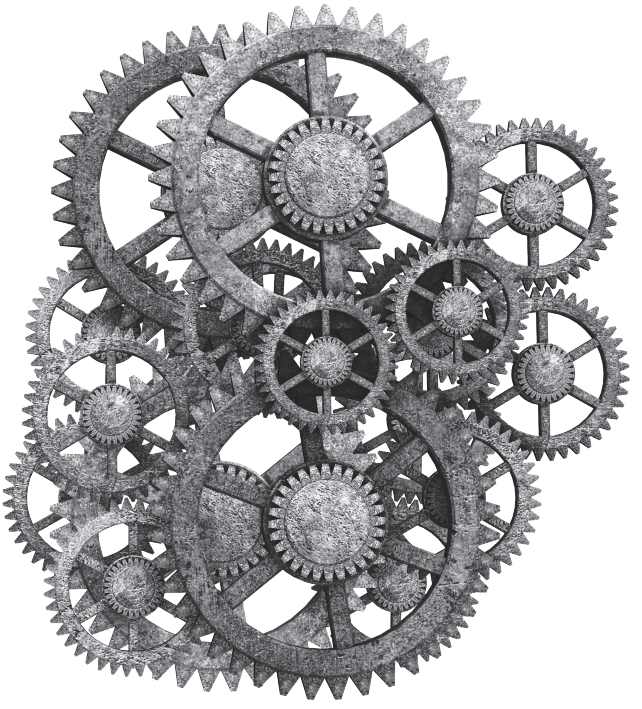

1

Chapter 1

Introduction and outline of this thesis

GENERAL INTRODUCTION

Pulmonary hypertension is a pathophysiological disorder that is defined as a mean pulmonary arterial pressure of >25 mmHg at rest (1). Symptoms include shortness of breath, fatigue, swelling of the legs and exercise intolerance. There are many forms of pulmonary hypertension and each form has its own aetiology and pathophysiology. Some forms of pulmonary hypertension originate from the lungs itself, for instance when the pulmonary vasculature is constricted and stiffened. Other forms originate from the legs, where thrombi are formed that follow the blood stream to the lungs and ultimately cause multiple emboli. By far the most prevalent form of pulmonary hypertension originates from dysfunction of the heart (1,2). Treatment of this form of pulmonary hypertension is challenging and mostly consists of symptomatic treatment as well as treatment of the underlying heart disease (3). However, therapies specifically targeting the pulmonary vasculature in this form of pulmonary hypertension are lacking. This thesis aims to elucidate pathophysiological mechanisms in this form of pulmonary hypertension to ultimately provide insights in possible treatment options. This chapter will first describe the basic anatomy and physiology of the cardiovascular system and a more detailed description of the pathophysiology of pulmonary hypertension. Finally, this chapter will describe the aim and outline of this thesis.

THE NEED FOR OXYGEN AND NUTRIENTS

Every living cell needs oxygen and nutrients to create energy, while waste products like carbon dioxide need to be removed. Unicellular organisms can extract both oxygen and nutrients from their surroundings by diffusion. Our bodies however, consist of so many cells that only a tiny fraction of these cells are in direct contact with the “outside”. The majority of these outer cells are dead skin-cells, and do not even have the capability to acquire the needed oxygen and nutrients from their surroundings. The only locations where oxygen diffuses into and carbon dioxide is removed from our bodies are the lungs, and the main location for nutrient uptake is our digestive system. To transport both oxygen and nutrients to all of our ~100

trillion cells, evolution blessed us with three things: blood, as a medium to contain oxygen and nutrients; blood vessels, as a road infrastructure to reach all cells; and at the centre of this all, our heart, which is the pump that creates the driving force that moves our blood (4,5).

THE HUMAN HEART AND CIRCULATORY SYSTEM

Our heart is roughly the size of our fist, and weighs ~300 grams. It contracts an average of 60 times per minute at rest, pumping about 5 litres of blood through our circulation each minute. Anatomically (Figure 1), the heart consists of two sides, the right side, and the left side. Both sides are divided in two chambers, separated by valves. The chambers that collect blood are the so-called atria, the chambers that eject blood are the ventricles. In order to collect and distribute oxygen and nutrients to all the cells of our body, blood is continuously circulating. Deoxygenated blood is collected in the right atrium. During diastole, blood flows from the right atrium into the right ventricle, facilitated by the atrial contraction. As the ventricle contracts, blood is pumped through the pulmonary arteries to the lungs. In the lungs, the blood is oxygenated and carbon dioxide is removed. The now oxygen-rich blood is transported through the pulmonary veins, and collected in the left atrium. During diastole, the blood flows into the left ventricle facilitated by the left atrial contraction. During systole, a powerful contraction of the left ventricle propels the blood through the aorta, and via the conductance arteries and the resistance arteries to all the organs and supporting tissues. Here, in the capillary beds it supplies the surrounding tissue with oxygen and nutrients, and absorbs carbon dioxide and waste products. The blood is then transported through the venules, the large veins and the venae cava superior and inferior, back to the right atrium (4,6).

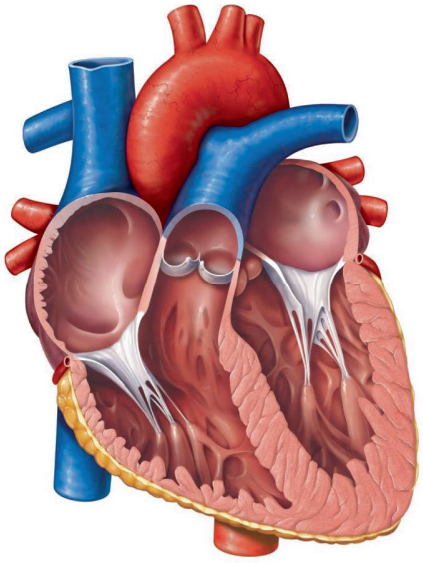

Figure 1. Anatomy of the heart. Figure adapted from (7).

Pressure, flow and resistance

The driving force that moves the blood through the circulation is generated by the contraction of the heart. In order to contract an average of 60 times a minute, the heart muscle itself (myocardium) needs a continuous supply of oxygen (6). This is realized by the coronary circulation. At the base of the aorta, two coronary arteries originate. The right coronary artery originates from the right aortic sinus and supplies the right atrium and ventricle, and in some animal species including humans, part of the posterior wall of the left ventricle, with oxygen-rich blood. The left coronary artery originates from the left aortic sinus, and divides into two branches near its origin: the left anterior descending coronary artery, which predominantly supplies the front side (anterior) of the heart, and the left circumflex coronary artery, which curves to the back (lateral and posterior wall) (6,8). Together, the coronary arteries receive 5% of the total amount of blood that passes through the aorta, even though the weight of the heart is less than 0,5% of total body weight (8,9). During the quick passage through the myocardium, 60-80% of the oxygen is extracted and utilized even at rest. This is

much higher than any other organ of the body (8-10). Oxygen is used to generate energy, which allows the heart to pump the blood through the entire circulation.
The amount of blood that is pumped out of a ventricle per minute is called the cardiac output. Vascular resistance is calculated as the pressure drop through a circulatory system divided by the blood flow. William Harvey (1578-1657) was the first to describe the circulatory system as a closed circuit of two serial circuits in his book 'De Motu Cordis' published in 1628. He extensively described the systemic and pulmonary circulations, that both originate from, and terminate in the heart, implying that flow through both circuits must be equal, and thus cardiac output of the right ventricle equals that of the left ventricle. In contrast, pressure and vascular resistance of the pulmonary and systemic circulations are very different (11). The similarities and differences of these two circulations will be further described in the next two paragraphs.

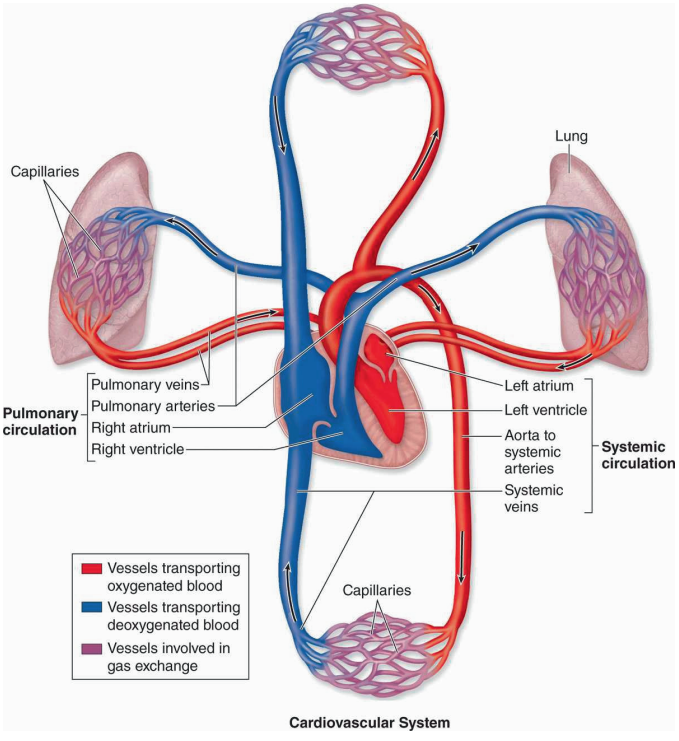

Figure 2. Schematic representation of the circulatory system. Figure adapted from (12).

The systemic circulation

The part of the circulatory system that delivers oxygen rich blood to the body, and collects deoxygenated blood to transport back to the heart is called the systemic circulation (Figure 2). The systemic circulation has a high pressure and high resistance. Blood is pumped into the aorta under a mean arterial pressure of ~95 mmHg. Arteries that carry the blood to all regions of the body branch off the aorta. These arteries divide again into smaller arteries, and subsequently into arterioles. As a vast network in the organs and tissues, the arterioles diverge into capillaries. Here, oxygen from the blood diffuses into the cells while carbon dioxide and waste products diffuse out of the cells and into the blood. At rest, an average of 30-40% of the oxygen content is extracted from the blood in the various organs, depending on the activity of the tissue and the amount of blood this tissue receives. The capillaries converge into venules, which connect to smaller, and then larger veins, and ultimately drain into the venae cava superior (upper body) and inferior (lower body), which finally drain into the right atrium. The pressure under which the blood enters the right atrium is ~5 mmHg. The pressure drop of ~85 mmHg between the aorta and the right atrium implies a big resistance in the systemic circulation. While the aorta and the bigger arteries pose a low resistance to flow, and act primarily as conduits, it is the small arteries and arterioles that contain up to 80% of total resistance and determine distribution of flow to various organs and tissues.

The pulmonary circulation

The part of the circulation that is responsible for circulating blood through the lungs and back to the left atrium is called the pulmonary circulation (Figure 2). The main purpose of the pulmonary circulation is to oxygenate blood, and remove carbon dioxide out of the blood, and into the air. Air is breathed in through the nose or mouth, and flows through the trachea, which divides into the left and right main bronchus. These bronchi diverge multiple times into finer and finer tubes called bronchioles, the finest of which are called the terminal bronchioles. These terminal bronchioles finally end into a cluster of air-sacs called alveoli (Figure 3). The arteries of the pulmonary circulation, the only arteries in the body that carry oxygen-poor blood, follow a similar

path of divergence after divergence as the airways, until finally a fine web of capillaries surrounds each alveolus. This close contact enables free diffusion of oxygen from the air in the alveolus, into the capillary blood and of carbon dioxide from the blood to the alveolus. The blood is then collected in the pulmonary venules, which converge into the pulmonary veins, the only veins that carry oxygen-rich blood, and back to the heart where it enters the left atrium (4). Because of the close contact, and very thin layer, between the alveolus and the capillaries, the pressure in the capillaries must be very low. Otherwise, not only gas, but also fluids would pass the barrier and enter the lungs. Indeed, pressure in the pulmonary circulation is much lower than that in the systemic circulation. Blood is pumped from the right ventricle into the pulmonary artery under a low mean pressure of ~15 mmHg, and is finally collected in the left atrium under a pressure of ~8 mmHg (11). The pressure drop of only ~7 mmHg under the same cardiac output as the systemic circulation implies that the vascular resistance of the pulmonary circulation is over ten times lower than that of the systemic circulation.

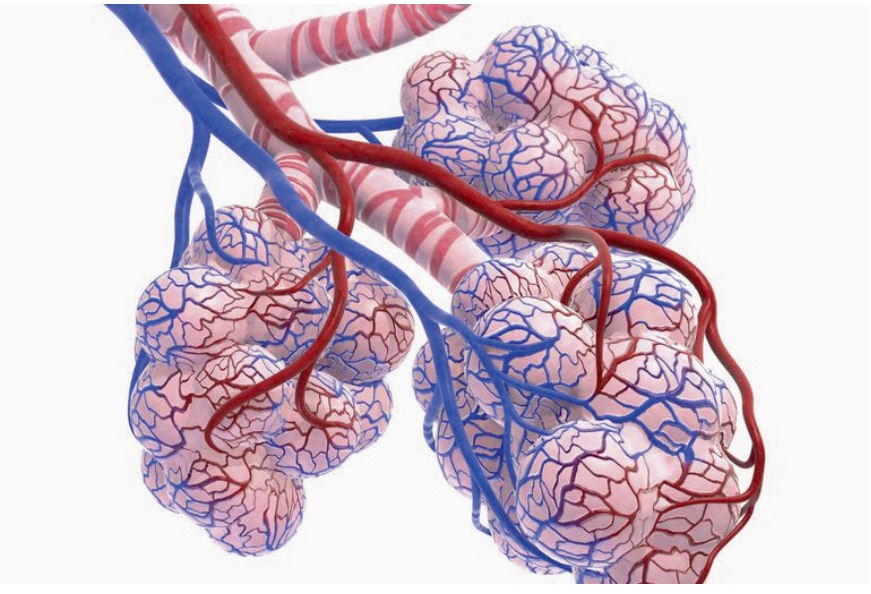

Figure 3. Schematic representation of a bronchiole with alveoli and the capillary network. Figure adapted from (13).

Determinants of vascular resistance

Different organs need different amounts of oxygen at different moments, depending on their activity. During exercise, cardiac output increases to match oxygen delivery to the increased oxygen demand of the muscles. In order to increase cardiac output, heart rate and contractile force of the heart, so-called contractility, will increase. As a consequence, oxygen demand in the myocardium also increases. At the same time, because of the increased flow, pulmonary artery pressure would increase if pulmonary vascular resistance would remain unchanged. To regulate flow and pressure, vascular resistance can be adjusted by the regulation of vascular diameters. Changes in vascular diameter and thus vascular resistance, can be ascribed to both passive and active influences (14).

Passive influences on vascular resistance

There are several passive factors that determine vascular diameter, and hence local blood flow. In de coronary circulation, the coronary arteries are embedded within the myocardium, especially the smaller branches penetrate deep into the cardiac tissue. As the heart contracts, the muscle cells, or cardiomyocytes shorten and thicken. Because of this thickening of all cardiomyocytes surrounding the coronary vasculature, the blood vessels are stretched and squeezed, temporarily reducing flow. Because of this extravascular compression, myocardial perfusion, particularly of the muscular left ventricle, mainly occurs during diastole. Distribution of flow is determined by the structure of the vasculature, i.e. the size, number and branching pattern of the vessels. Vessel diameter is not fixed, as an increase in transmural pressure distends the vessels, thereby increasing their diameter. When looking at the pulmonary circulation, passive influences on blood flow consist of passive distension of the vasculature, as a consequence of increased pulmonary arterial pressure. Another passive component altering vascular resistance is the recruitment of previously unperfused vessels. The subsequent distension of the recruited vessels lowers the vascular resistance even more. These passive mechanisms attenuate the increase of pulmonary arterial pressure during exercise, while cardiac output markedly increases. Although passive influences on pulmonary vascular resistance

are important and very fascinating, this thesis will mainly focus on active regulation of vascular resistance (15).

Active regulation of vascular resistance

Active regulation of vascular resistance is the result of the adaptation of vessel diameter by contraction or relaxation of smooth muscle cells in the vessel wall. To understand active regulation, the structure of the vessel wall will briefly be described. The vessel wall comprises three layers. The inner layer, which is the only layer in direct contact with the circulating blood, is called the Tunica Intima, and consists mostly of endothelial cells (Figure 4). Around this layer is the Tunica Media, which consists mainly of smooth muscle cells. The most outer layer is the Tunica Adventitia, which consists mostly of connective tissue. These layers are supported by elastic layers called the lamina elastica interna (between the Tunica Intima and Media) and the laminae elastica externa (between the Tunica Media and Adventitia) (16).

Regulation of vascular tone is the result of an intricate interplay between vasoconstrictors and vasodilators: factors that cause contraction, or relaxation of the smooth muscle cells within the Tunica Media. These smooth muscle cells are highly specialized cells that express various contractile proteins, ion channels and signalling molecules. Key in the contraction or relaxation of the smooth muscle cell is the concentration of free calcium (Ca^{2+}) in the cytosol. When this concentration increases, myosin light chain kinase (MLCK) is activated, and phosphorylates the myosin light chain. This allows cycling of cross bridges between myosin and actin, contracting the smooth muscle cell. The dephosphorylation of the myosin light chain is achieved by myosin light chain phosphatase (MLCP), relaxing the smooth muscle cell (14,17,18).

Contraction of the smooth muscle cell is thus regulated by activation of the contractile proteins myosin and actin. This activation can be electromechanical, initiated by stretch and intraluminal pressure, or pharmacological, when vasoactive substances activate receptors on the cell-surface or within the smooth muscle cells (17,19). Many of the vasoactive factors that cause pharmacological activation originate from the endothelium. Some are vasodilator factors, such as nitric oxide (NO), prostacyclin (PGI_2) and endothelium derived hyperpolarizing factors (EDHFs), and some are vasoconstrictor factors, such as endothelin-1 (ET-1) and thromboxane A_2 (TXA_2)

(14,18). This thesis will mainly focus on the vasodilator nitric oxide and the vasoconstrictor endothelin.

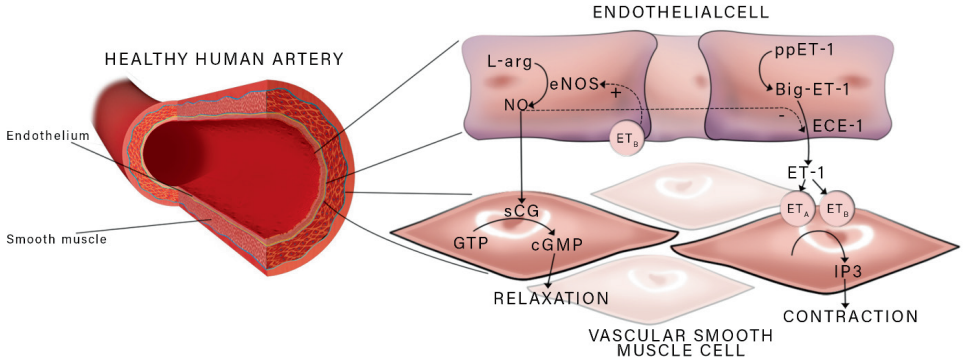

Figure 4. Vascular anatomy of human artery, and schematic representation of the nitric oxide- and endothelin pathways. Figure adapted from (20).

Nitric oxide

In 1980, Furchgott and Zawadski found that acetylcholine could only cause relaxation of smooth muscle cells in the presence of endothelial cells. They concluded that there is a relaxing factor produced in the endothelial cell, that can be activated by acetylcholine, and exert a relaxing effect on the smooth muscle cells. Now we know that this relaxing factor is in fact the gaseous compound nitric oxide (NO). NO is formed by the enzyme nitric oxide synthase (NOS), which converts the amino acid L-arginine to NO (Figure 4). NO then diffuses to the smooth muscle cell, where it activates the enzyme soluble guanylyl cyclase, which increases the conversion rate of guanosine triphosphate (GTP) to cyclic guanosine monophosphate (cGMP). cGMP has a relaxing effect on the smooth muscle cell by promoting Ca^{2+} release from the sarcoplasmic reticulum and activation of K^{+} channels. NO-signalling is terminated through removal of cGMP by phosphodiesterase 5 (PDE5), which removes cGMP by hydrolysing it to 5' GMP (21). NO is continuously produced, and is a very potent vasodilator. In addition, NO can inhibit platelet and leukocyte adherence to the endothelium, promote endothelial and prevent smooth muscle–cell migration and proliferation, and regulate gene expression. These actions make NO an important player in regulation of vascular function as well as vascular remodelling (22).

Endothelin

In 1982, de Mey and Vanhoutte reported that endothelial cells can stimulate the contraction of vascular smooth muscle cells of the media by an unknown mechanism (23). In the following years, the endothelial release of a vasoconstrictor substance was further investigated and reported (24-26). Finally, in 1988 Yanagisawa et al. sequenced the substance and named it endothelin (ET) (27). There are three forms of ET, being ET-1, ET-2 and ET-3. This thesis will focus on ET-1, which is the major isoform produced in and secreted from endothelial cells (28). It is one of the most potent vasoconstrictors. ET-1 is synthesized from its precursor big-ET by endothelin-converting enzyme (ECE)-1 (Figure 4). Big-ET, in its turn, is cleaved from preproendothelin (29,30). ET-1 is not only produced by endothelial cells, but also by vascular and airway smooth muscle cells, cardiomyocytes, leucocytes and macrophages. Endothelial ET is released ab-luminally, i.e. towards the underlying smooth muscle cells, where it binds to endothelin receptors. There are two types of endothelin receptors, namely ET_A- and ET_B-receptors. Smooth muscle cells express both types of receptors. Binding of ET-1 to the ET_A- and ET_B-receptors on smooth muscle cells increases intracellular Ca^{2+}-concentration via two pathways. Ca^{2+} is recruited from the sarcoplasmic reticulum by activation of the inositol triphosphate (IP_3) receptor and by opening of the Ca^{2+} channels on the cellular membrane, allowing extracellular Ca^{2+} into the cell. ET_B-receptors are also present on endothelial cells, and cause vasodilation upon binding of ET-1, by the activation of both NO and PGI_2. These ET_B-receptors are also responsible for ET-1 clearance from the circulation (31). The distribution of these two receptor-subtypes depends on the type of vessel. Compared with arteries, veins show a lower ET_A:ET_B receptor ratio (32). Within the pulmonary arterial bed, ET_A- as well as ET_B-receptors have stronger medial expression in the proximal, compared to distal arteries. In contrast, endothelial ET_B-expression is stronger in distal pulmonary arteries (33).

While ET-1 is produced and cleared in the entire body, the main site for both production and clearance is the pulmonary vasculature (34). The pulmonary vasculature clears about 80% of circulating ET-1 (28). In addition to the regulation of vascular tone, ET-1 also promotes vascular smooth muscle cell growth and proliferation. This appears to be ET_A receptor-mediated (33).

PULMONARY HYPERTENSION

Pulmonary hypertension (PH) is a pathophysiological disorder that is defined by a mean pulmonary arterial pressure (mPAP) of >25 mmHg at rest (1), although at this moment, the definition is under heavy debate (35-40) and the mPAP threshold may be lowered to > 20 mmHg as mPAP ≥ 20 mmHg (41) at rest for a prolonged period of time is already associated with increased morbidity and mortality (42-49). PH may involve multiple clinical conditions, and may present as a complication of a multitude of cardiovascular and respiratory diseases, increasing morbidity and mortality (1). There are different types of pulmonary hypertension, with different aetiologies.

Aetiologies of pulmonary hypertension

For a long time, PH was subdivided into primary and secondary PH. In the former, patients were diagnosed with PH of an unexplained aetiology, while in the latter, the increased mPAP was the result of an underlying disease. In 1998, at the World Symposium on Pulmonary Hypertension in Evian, France, a clinical classification was formed and taken into use (50). It comprised five groups of PH, categorized by aetiologies. Since then, new insights in the disease, and the management of the disease have led to many updates of the classification. Figure 5 displays the most recent classification of pulmonary hypertension. A note on terminology: Pulmonary arterial hypertension (PAH) is often wrongfully used to indicate any form of pulmonary hypertension, when in fact PAH only comprises group I PH, where the disease starts with alterations in the pulmonary arterial wall.

Pulmonary hypertension associated with left heart disease

While PH has many different aetiologies, in 65 – 80% of all cases PH is due to left heart disease, i.e. WHO classification group II (2). In this group of PH, left heart failure (LHF), valvular disease, inflow-/outflow-tract obstructions or congenital or acquired pulmonary vein stenosis cause an upstream pressure increase in the pulmonary vasculature (1). By far the biggest subgroup op group II PH is PH caused by LHF. Exact percentages vary per study, but on average, 60% of LHF patients has PH (51).

1 Pulmonary arterial hypertension
1.1 Idiopathic Pulmonary arterial hypertension
1.2 Heritable Pulmonary arterial hypertension
1.3 Drug- and toxin-induced Pulmonary arterial hypertension
1.4 Pulmonary arterial hypertension associated with:
1.4.1 Connective tissue disease
1.4.2 HIV infection
1.4.3 Portal hypertension
1.4.4 Congenital heart disease
1.4.5 Schistosomiasis
1.5 Pulmonary arterial hypertension long-term responders to calcium channel blockers
1.6 Pulmonary arterial hypertension with overt features of venous/capillaries involvement
1.7 Persistent PH of the newborn syndrome
2 PH due to left heart disease
2.1 PH due to heart failure with preserved left ventricular ejection fraction
2.2 PH due to heart failure with reduced left ventricular ejection fraction
2.3 Valvular heart disease
2.4 Congenital/acquired cardiovascular conditions leading to post-capillary PH
3 PH due to lung diseases and/or hypoxia
3.1 Obstructive lung disease
3.2 Restrictive lung disease
3.3 Other lung disease with mixed restrictive/obstructive pattern
3.4 Hypoxia without lung disease
3.5 Developmental lung disorders
4 PH due to pulmonary artery obstructions
4.1 Chronic thromboembolic PH
4.2 Other pulmonary artery obstructions
5 PH with unclear and/or multifactorial mechanisms
5.1 Haematological disorders
5.2 Systemic and metabolic disorders
5.3 Others
5.4 Complex congenital heart disease

Figure 5. Classification of pulmonary hypertension. Figure adapted from (1).

Considering a total amount of 26 million people suffering from LHF worldwide, the prevalence of PH group II is enormous (52). Heart failure is the condition where the heart is unable to supply the body with the necessary cardiac output. Heart failure can be attributed to either the inability of the left ventricle to contract sufficiently, or to fill sufficiently. The first being called heart failure with reduced ejection fraction (HFrEF), and the latter being called heart failure with preserved ejection fraction (HFpEF). Myocardial infarction is the primary cause of HFrEF, whereas in HFpEF old age and the metabolic syndrome are the most important risk factors (6,53).

Pulmonary hypertension associated with pulmonary vein stenosis

An often-overlooked cause of PH type II is partial pulmonary vein stenosis (PVS). In PVS, one or more of the pulmonary veins are narrowed (Figure 6), hampering outflow of blood from the lungs into the left atrium, thereby increasing pulmonary vascular resistance and pressure. In the adult population, PVS may occur as an, albeit rare, consequence of radio-frequency ablation of atrial tissue around the pulmonary veins to treat atrial fibrillation (54). While twenty years ago, PVS was reported in 30-40% of patients after this procedure, new techniques improved clinical efficacy and decreased the incidence of PVS to approximately 1% (55-57). PVS in the paediatric population is a severe congenital anomaly associated with poor outcome (58). Paediatric PVS is rare (0.4% of congenital heart diseases) (59), and can occur as a singular anomaly, but is generally associated with congenital heart defects (univentricular heart disease, ventricular septal defect, atrial septal defect or persistent arterial duct), lung disease (bronchopulmonary dysplasia (BPD)), or Down syndrome or other trisomies (60-63).

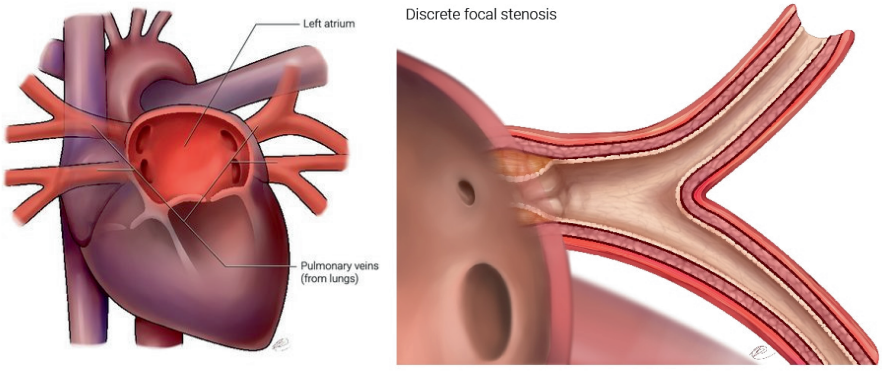

Figure 6. Schematic representation of the left atrium and pulmonary veins (left) and pulmonary vein stenosis (right). Figure adapted from (64).

Pre- or post-capillary pulmonary hypertension

Contrary to group I PH, which initiates in the pulmonary arteries, and is therefore referred to as pre-capillary pulmonary hypertension, group II PH initiates either in the pulmonary veins or in the left ventricle or atrium, and is referred to as post-

capillary pulmonary hypertension. When the increase in pulmonary pressure is purely passive, it is referred to as isolated post-capillary PH (IpcPH). However, when left untreated, IpcPH can cause abundant pulmonary vasoconstriction and even vascular remodelling (65-67). This form of post-capillary pulmonary hypertension also displays pre-capillary aspects, and is thus called combined pre- and post-capillary PH (CpcPH). CpcPH is a chronic, progressive disease with a worse prognosis than IpcPH (68). Haemodynamic profiling can help to distinguish between pre-capillary PH, IpcPH and CpcPH. While all forms of PH have mPAP>25 mmHg, pre-capillary PH has a pulmonary arterial wedge pressure (PAWP) of <15 mmHg. The PAWP is the pressure measured with a pulmonary catheter, distal to an inflated balloon, and an estimation of the pressure in the left atrium. IpcPH and CpcPH are defined as a PAWP of >15 mmHg (1). To further discriminate between IpcPH and CpcPH, the transpulmonary pressure gradient (TPG), pulmonary vascular resistance (PVR) and / or diastolic pressure gradient (DPG) should be assessed. TPG is calculated as mPAP - PAWP, DPG is calculated as diastolic PAP - mean PAWP. TPG<15 mmHg, DPG<7 mmHg and/or PVR<3 WU (wood units; mmHg·l/min) define IpcPH, while TPG>15 mmHg, DPG>7 mmHg and/or PVR>3 WU define CpcPH (1,69). While IpcPH can be treated by treating only the underlying condition (1), CpcPH requires treatment of pulmonary vascular remodelling as well as the primary disease, as treatment of the primary disease alone is no longer able to arrest the progression of CpcPH (3).

The right ventricle in pulmonary hypertension

In contrast to the systemic circulation and left ventricle, the relatively low mean arterial pressure in the pulmonary circulation does not require a lot of power from the right ventricle under normal circumstances. Indeed, early studies in dogs showed that even complete ablation of the RV-free wall, and ligation of the coronary arteries supplying this region, does not alter peripheral venous or pulmonary systolic or diastolic pressures (70,71). This suggests that the motion of the interventricular septum alone is sufficient to move blood from the systemic venous system into the

pulmonary circulation. When looking at a cross-section of the heart, a clear difference can be seen in muscle thickness between the right and left ventricle (figure 7).

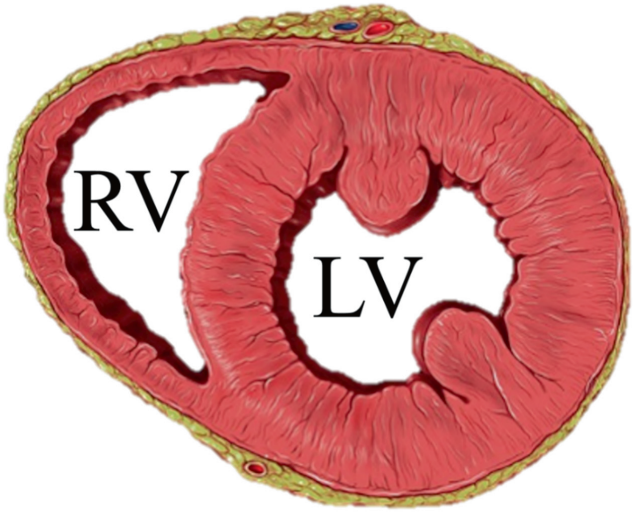

Figure 7. Schematic short axis cross-section of the left (LV) and right ventricle (RV). Figure adapted from (76).

While a systemic pressure increase of 10 mmHg would not burden the left ventricle, because its afterload would only increase by 11%, the same absolute increase does imply a 66% increase of afterload for the right ventricle. Franciosa et al (72) proposed that it is the inability of the right ventricle to overcome the increase in afterload that limits the exercise capacity in patients with left ventricular failure, a concept that was recently confirmed by Kim et al (73). Understandably, pulmonary hypertension principally affects the right ventricle. The gradual increase in afterload over time results in structural remodelling of the RV. This can be either adaptive remodelling, or maladaptive remodelling. Adaptive remodelling comprises concentric hypertrophy, and unchanged systolic and diastolic function. Maladaptive remodelling comprises eccentric remodelling, RV dilatation and reduced RV function (74). Maladaptive remodelling ultimately leads to RV failure. Even in PH group II as a result of left heart failure, the patient actually may ultimately die of right heart failure (75).

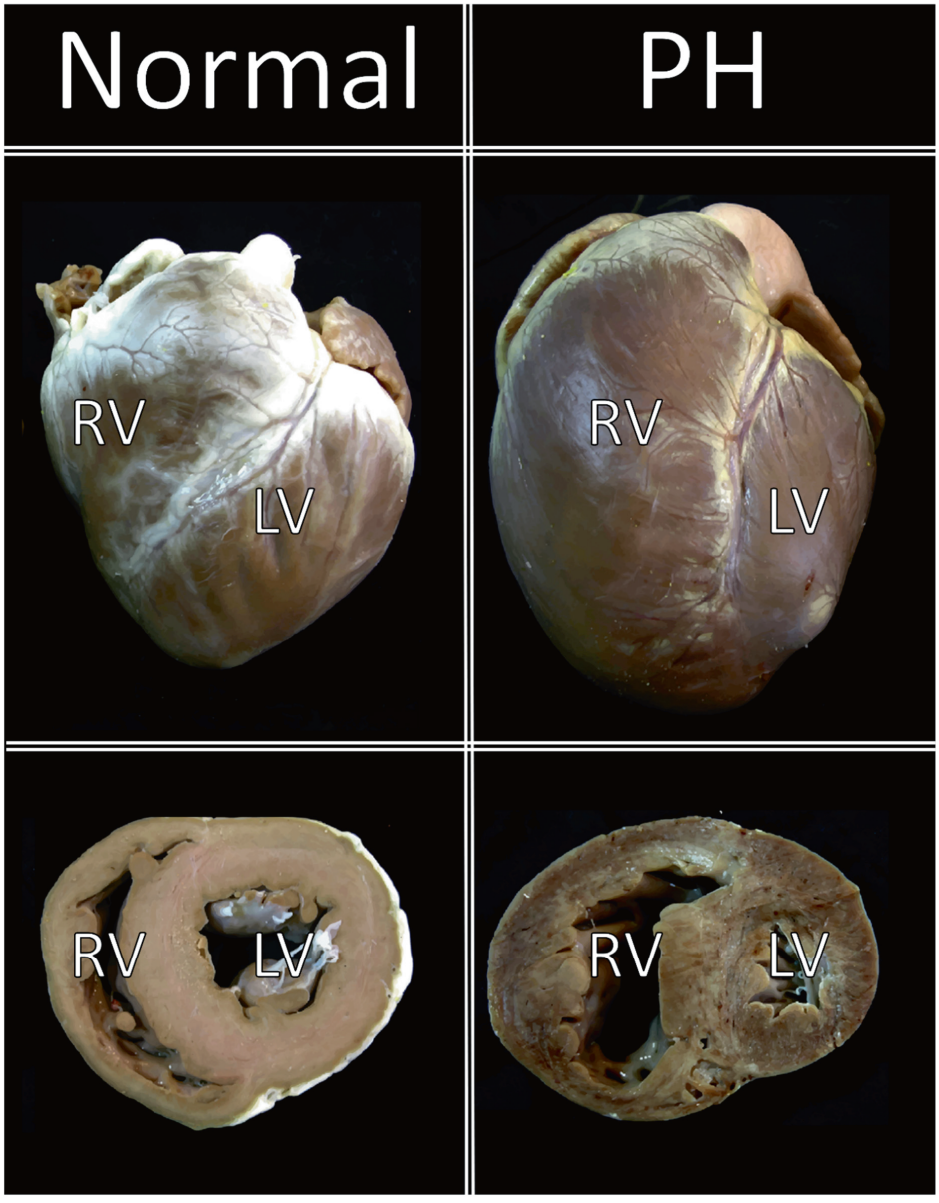

Figure 8. Macroscopic pictures of a normal swine heart on the left side, and a remodelled swine heart on the right. Upper panels show the whole heart. Lower panels show a cross-section. LV: Left Ventricle, RV: right ventricle. Figure adapted from (77).

Treatment options in group II pulmonary hypertension

The current guidelines of the European Society of Cardiology for treatment of group II PH recommend the treatment of the LV, to optimize volume status, to take care of co-morbidities and to take caution in using pulmonary vasodilators (1). However, while IpcPH can be treated by treating only the underlying condition (1), CpcPH is characterized by pre-capillary structural and functional vascular remodelling resembling pulmonary arterial hypertension (PAH; WHO classification type I PH) and requires treatment of pulmonary vascular remodelling as well as the primary disease, as treatment of the primary disease alone is no longer able to arrest the progression of CpcPH (3,65-67). The use of PAH vasodilation therapy however, can be perilous in type II PH, as vasodilation increases flow, while the outflow remains hampered, potentially resulting in a further increase in capillary pressure and pulmonary oedema. Use of first line vasodilator therapy like inhaled nitric oxide (NO), administration of NO-donors, or phosphodiesterase-5 (PDE5)-inhibitors, therefore may increase dyspnoea by causing pulmonary oedema (3).

AIM AND OUTLINE OF THIS THESIS

The aim of this thesis is to characterize (patho-)physiological mechanisms in group II pulmonary hypertension. Specifically, we aim to investigate 1) how the pulmonary vasculature reacts to a post-capillary pressure increase, 2) if and what structural and functional changes in the vasculature occur, 3) if, when and how IpcPH turns into CpcPH and 4) how the right ventricle adapts to an increased afterload. Characterizing mechanisms of pulmonary and right ventricular remodelling are necessary first steps towards reducing morbidity and mortality caused by this disease.

In order to study changes in pulmonary vascular haemodynamics over time in a large animal model for pulmonary hypertension, we first describe a surgical chronic catheterization method in **chapter 2**. This technique enables serial haemodynamic measurements and the collection of serial arterial as well as venous blood samples over time. Also, as animals are fully awake, with minimal discomfort of the implanted catheters, we can challenge the cardiopulmonary system by exercising the animals on a treadmill, while haemodynamics are recorded. This allows us to study early physiological adaptations, and early signs of pulmonary hypertension. We utilized the techniques described in **chapter 2** in a swine model for myocardial infarction in **chapter 3**. In this chapter, following a myocardial infarction of the left ventricle, swine developed mild pulmonary hypertension. We investigated the possibility to utilize PDE5-inhibition to boost the NO-pathway in order to ameliorate pulmonary haemodynamics in these animals. In **chapter 4**, we describe and characterize a swine model for more severe pulmonary hypertension as a result of pulmonary venous banding, which mimics pulmonary hypertension as a result of either left heart disease, or pulmonary vein stenosis. By applying the chronic instrumentation described in **chapter 2**, we were able to study the transition from IpcPH to CpcPH. We studied functional and structural remodelling of the pulmonary microvasculature and changes in the endothelin-pathway. When pulmonary hypertension is the result of pulmonary vein stenosis, it has a mixed phenotype with high pressure / low flow (HP/LF)-vasculature draining into stenotic pulmonary veins, and high pressure / high flow (HP/HF)-vasculature draining into unaffected pulmonary veins. The pulmonary venous banding swine model introduced in **chapter 4** was further investigated in

chapter 5. In this chapter we studied the NO-pathway in vivo, both at rest and during exercise. After sacrifice we investigated how pulmonary vessels isolated from the HP/LF and HP/HF territories are acutely affected by therapies that alter the NO-pathway, using wire-myography. Finally, in **chapter 6**, we investigated how the chronic increase in pulmonary arterial pressure affects the right ventricle, in the pulmonary venous banding swine model. We assessed right ventricular structural and functional changes. Furthermore, we used exercise to challenge the cardio-pulmonary system and unmask right ventricular dysfunction. We aimed to establish right ventricular oxygen delivery reserve as a determinant for right ventricular functional reserve during exercise. In **chapter 7**, we integrate and discuss the results presented in this thesis and provide a broader perspective of their implications before concluding with recommendations for future research.

REFERENCES

1. Galie N, Humbert M, Vachiery JL et al. 2015 ESC/ERS Guidelines for the Diagnosis and Treatment of Pulmonary Hypertension. Rev Esp Cardiol (Engl Ed) 2016;69:177.
2. Rosenkranz S, Gibbs JS, Wachter R, De Marco T, Vonk-Noordegraaf A, Vachiery JL. Left ventricular heart failure and pulmonary hypertension. Eur Heart J 2016;37:942-54.
3. Lundgren J, Radegran G. Pathophysiology and potential treatments of pulmonary hypertension due to systolic left heart failure. Acta Physiol (Oxf) 2014;211:314-33.
4. Boron WF, Boulpaep EL. Medical Physiology. Updated edition 2ed. Philadelphia, Pennsylvania: Elsevier, 2012.
5. Widmaier EP, Raff H, Strang KT. Cardiovascular Physiology. Vander's Human Physiology. New York: McGraw-Hill, 2011:353-433.
6. Braunwald E ZD ZD, Libby P, Bonow R. Braunwald's Heart Disease: A Textbook of Cardiovascular Medicine. 11 ed: Elsevier - Health Sciences Division, 2018.
7. Doe J. Schematic representation of the cardiac anatomy. 2019.
8. Rehman S, Rehman A. Physiology, Coronary Circulation. 2020.
9. Feigl EO. Coronary physiology. Physiological reviews 1983;63:1-205.
10. Duncker DJ, Bache RJ. Regulation of coronary blood flow during exercise. Physiological reviews 2008;88:1009-86.
11. Berne RM LM, Koeppen BM. Physiology. 4 ed. St Louis, Missouri, 1998.
12. Doe J. Diagram of the cardiovascular system. 2019.
13. Kindersley D. Alveoli: Structure, Function, and Disorders of the Lungs. 2016.
14. Laughlin MH, Davis MJ, Secher NH et al. Peripheral Circulation. Comprehensive Physiology: John Wiley & Sons, Inc., 2012.
15. Klabunde R. Cardiovascular Physiology Concepts. 2nd ed: Lippincott Williams & Wilkins, 2011.
16. Gartner L. Textbook of Histology. Elsevier 2016:672.
17. Somlyo AP SA. Signal transduction and regulation in smooth muscle. Nature 1994;372:231-236.
18. Merkus D, de Beer VJ, Houweling B, Duncker DJ. Control of pulmonary vascular tone during exercise in health and pulmonary hypertension. Pharmacol Ther 2008;119:242-63.
19. Ogut O, Brozovich FV. Regulation of force in vascular smooth muscle. Journal of molecular and cellular cardiology 2003;35:347-55.
20. Stam K. A novel preclinical model for chronic thrombo-embolic pulmonary hypertension. Development, validation and characterization. ISBN 978-94-6380-443-1 2019:20.
21. Rybalkin SD, Yan C, Bornfeldt KE, Beavo JA. Cyclic GMP phosphodiesterases and regulation of smooth muscle function. Circ Res 2003;93:280-91.
22. Rudic RD, Sessa WC. Nitric oxide in endothelial dysfunction and vascular remodeling: clinical correlates and experimental links. Am J Hum Genet 1999;64:673-7.

23. De Mey JG, Vanhoutte PM. Heterogeneous behavior of the canine arterial and venous wall. Importance of the endothelium. Circ Res 1982;51:439-47.
24. Gillespie MN, Owasoyo JO, McMurtry IF, O'Brien RF. Sustained coronary vasoconstriction provoked by a peptidergic substance released from endothelial cells in culture. The Journal of pharmacology and experimental therapeutics 1986;236:339-43.
25. Hickey KA, Rubanyi G, Paul RJ, Highsmith RF. Characterization of a coronary vasoconstrictor produced by cultured endothelial cells. Am J Physiol 1985;248:C550-6.
26. O'Brien RF, Robbins RJ, McMurtry IF. Endothelial cells in culture produce a vasoconstrictor substance. Journal of cellular physiology 1987;132:263-70.
27. Yanagisawa M, Kurihara H, Kimura S et al. A novel potent vasoconstrictor peptide produced by vascular endothelial cells. Nature 1988;332:411-5.
28. Kawanabe Y, Nauli SM. Endothelin. Cell Mol Life Sci 2011;68:195-203.
29. Rubanyi GM, Polokoff MA. Endothelins: molecular biology, biochemistry, pharmacology, physiology, and pathophysiology. Pharmacological reviews 1994;46:325-415.
30. Schiffrin EL, Touyz RM. Vascular biology of endothelin. Journal of cardiovascular pharmacology 1998;32 Suppl 3:S2-13.
31. Dupuis J, Goresky CA, Fournier A. Pulmonary clearance of circulating endothelin-1 in dogs in vivo: exclusive role of ETB receptors. J Appl Physiol (1985) 1996;81:1510-5.
32. Sandoo A, van Zanten JJ, Metsios GS, Carroll D, Kitas GD. The endothelium and its role in regulating vascular tone. Open Cardiovasc Med J 2010;4:302-12.
33. Schneider MP, Boesen EI, Pollock DM. Contrasting actions of endothelin ET(A) and ET(B) receptors in cardiovascular disease. Annual review of pharmacology and toxicology 2007;47:731-59.
34. Dupuis J SD, Cernacek P, et al. Human pulmonary circulation is an important site for both clearance and production of endothelin -1. Circulation 1996;94:1578-1584.
35. Simonneau G, Hoeper MM. The revised definition of pulmonary hypertension: exploring the impact on patient management. Eur Heart J Suppl 2019;21:K4-K8.
36. Rosenkranz S, Diller GP, Dumitrescu D et al. [Hemodynamic Definition of Pulmonary Hypertension: Commentary on the Proposed Change by the 6th World Symposium on Pulmonary Hypertension]. Dtsch Med Wochenschr 2019;144:1367-1372.
37. Maron BA, Choudhary G, Tedford RJ, Brittain E. Correspondence on the debate regarding the haemodynamic definition of pulmonary hypertension. Eur Respir J 2019;53.
38. Kovacs G, Olschewski H. Debating the new haemodynamic definition of pulmonary hypertension: much ado about nothing? Eur Respir J 2019;54.
39. Hoeper MM, Humbert M. The new haemodynamic definition of pulmonary hypertension: evidence prevails, finally! Eur Respir J 2019;53.
40. Gibbs JSR, Torbicki A. Proposed new pulmonary hypertension definition: is 4 mm(Hg) worth re-writing medical textbooks? Eur Respir J 2019;53.
41. Galie N, McLaughlin VV, Rubin LJ, Simonneau G. An overview of the 6th World Symposium on Pulmonary Hypertension. Eur Respir J 2019;53.

42. Torbicki A. Hypertension: Definition of pulmonary hypertension challenged? Nat Rev Cardiol 2016;13:250-1.

43. Maron BA, Hess E, Maddox TM et al. Association of Borderline Pulmonary Hypertension With Mortality and Hospitalization in a Large Patient Cohort: Insights From the Veterans Affairs Clinical Assessment, Reporting, and Tracking Program. Circulation 2016;133:1240-8.

44. Douschan P, Kovacs G, Avian A et al. Mild Elevation of Pulmonary Arterial Pressure as a Predictor of Mortality. Am J Respir Crit Care Med 2018;197:509-516.

45. Kim NH, Delcroix M, Jais X et al. Chronic thromboembolic pulmonary hypertension. Eur Respir J 2019;53.

46. Kovacs G, Maier R, Aberer E et al. Borderline pulmonary arterial pressure is associated with decreased exercise capacity in scleroderma. Am J Respir Crit Care Med 2009;180:881-6.

47. Kovacs G, Avian A, Tscherner M et al. Characterization of patients with borderline pulmonary arterial pressure. Chest 2014;146:1486-1493.

48. Kolte D, Lakshmanan S, Jankowich MD, Brittain EL, Maron BA, Choudhary G. Mild Pulmonary Hypertension Is Associated With Increased Mortality: A Systematic Review and Meta-Analysis. J Am Heart Assoc 2018;7:e009729.

49. Nishihara T, Yamamoto E, Tokitsu T et al. New Definition of Pulmonary Hypertension in Patients with Heart Failure with Preserved Ejection Fraction. Am J Respir Crit Care Med 2019;200:386-388.

50. Simonneau G, Galie N, Rubin LJ et al. Clinical classification of pulmonary hypertension. J Am Coll Cardiol 2004;43:5S-12S.

51. Guazzi M. Pulmonary Hypertension and Heart Failure: A Dangerous Liaison. Heart failure clinics 2018;14:297-309.

52. Savarese G, Lund LH. Global Public Health Burden of Heart Failure. Card Fail Rev 2017;3:7-11.

53. Gevaert AB, Boen JRA, Segers VF, Van Craenenbroeck EM. Heart Failure With Preserved Ejection Fraction: A Review of Cardiac and Noncardiac Pathophysiology. Front Physiol 2019;10:638.

54. Cappato R. Pulmonary Vein Stenosis Following Radiofrequency Ablation of Atrial Fibrillation: Has It Become a Clinically Negligible Complication? JACC Clin Electrophysiol 2017;3:599-601.

55. Chen SA, Hsieh MH, Tai CT et al. Initiation of atrial fibrillation by ectopic beats originating from the pulmonary veins: electrophysiological characteristics, pharmacological responses, and effects of radiofrequency ablation. Circulation 1999;100:1879-86.

56. Arentz T, Jander N, von Rosenthal J et al. Incidence of pulmonary vein stenosis 2 years after radiofrequency catheter ablation of refractory atrial fibrillation. Eur Heart J 2003;24:963-9.

57. Cappato R, Calkins H, Chen SA et al. Updated worldwide survey on the methods, efficacy, and safety of catheter ablation for human atrial fibrillation. Circ Arrhythm Electrophysiol 2010;3:32-8.

58. Backes CH, Nealon E, Armstrong AK et al. Pulmonary Vein Stenosis in Infants: A Systematic Review, Meta-Analysis, and Meta-Regression. J Pediatr 2018;198:36-45 e3.

59. Pazos-Lopez P, Garcia-Rodriguez C, Guitian-Gonzalez A et al. Pulmonary vein stenosis: Etiology, diagnosis and management. World J Cardiol 2016;8:81-8.

60. Seale AN, Webber SA, Uemura H et al. Pulmonary vein stenosis: the UK, Ireland and Sweden collaborative study. Heart 2009;95:1944-9.

61. Gowda S, Bhat D, Feng Z, Chang CH, Ross RD. Pulmonary vein stenosis with Down syndrome: a rare and frequently fatal cause of pulmonary hypertension in infants and children. Congenit Heart Dis 2014;9:E90-7.

62. Mahgoub L, Kaddoura T, Kameny AR et al. Pulmonary vein stenosis of ex-premature infants with pulmonary hypertension and bronchopulmonary dysplasia, epidemiology, and survival from a multicenter cohort. Pediatr Pulmonol 2017;52:1063-1070.

63. Laux D, Rocchisani MA, Boudjemline Y, Gouton M, Bonnet D, Ovaert C. Pulmonary Hypertension in the Preterm Infant with Chronic Lung Disease can be Caused by Pulmonary Vein Stenosis: A Must-Know Entity. Pediatr Cardiol 2016;37:313-21.

64. PVSnetwork.org. Pulmonary veins and pulmonary vein stenosis. 2012.

65. Gerges M, Gerges C, Pistritto AM et al. Pulmonary Hypertension in Heart Failure. Epidemiology, Right Ventricular Function, and Survival. Am J Respir Crit Care Med 2015;192:1234-46.

66. Miller WL, Grill DE, Borlaug BA. Clinical features, hemodynamics, and outcomes of pulmonary hypertension due to chronic heart failure with reduced ejection fraction: pulmonary hypertension and heart failure. JACC Heart Fail 2013;1:290-299.

67. Vanderpool RR, Naeije R. Progress in Pulmonary Hypertension with Left Heart Failure. Beyond New Definitions and Acronyms. Am J Respir Crit Care Med 2015;192:1152-4.

68. Tatebe S, Fukumoto Y, Sugimura K et al. Clinical significance of reactive post-capillary pulmonary hypertension in patients with left heart disease. Circ J 2012;76:1235-44.

69. Naeije R, D'Alto M. The Diagnostic Challenge of Group 2 Pulmonary Hypertension. Prog Cardiovasc Dis 2016;59:22-9.

70. P BAC. The Question of the Function of the Right Ventricular Myocardium: An Experimental Study. Circulation 1950;1:724-732.

71. Starr I JWA, Meade R H. The absence of conspicuous increments of venous pressure after severe damage to the RV of the dog, with discussion of the relation between clinical congestive heart failure and heart disease. Am Heart J 1943;26:291–301.

72. Franciosa JA, Baker BJ, Seth L. Pulmonary versus systemic hemodynamics in determining exercise capacity of patients with chronic left ventricular failure. Am Heart J 1985;110:807-13.

73. Kim J, Di Franco A, Seoane T et al. Right Ventricular Dysfunction Impairs Effort Tolerance Independent of Left Ventricular Function Among Patients Undergoing Exercise Stress Myocardial Perfusion Imaging. Circ Cardiovasc Imaging 2016;9.

74. van de Veerdonk MC, Bogaard HJ, Voelkel NF. The right ventricle and pulmonary hypertension. Heart failure reviews 2016;21:259-71.

75. Vonk Noordegraaf A, Chin KM, Haddad F et al. Pathophysiology of the right ventricle and of the pulmonary circulation in pulmonary hypertension: an update. Eur Respir J 2019;53.

76. Lynch Pj. Short axis of left and right ventricle. 2010.

77. Pereda D, Garcia-Alvarez A, Sanchez-Quintana D et al. Swine model of chronic postcapillary pulmonary hypertension with right ventricular remodeling: long-term characterization by cardiac catheterization, magnetic resonance, and pathology. J Cardiovasc Transl Res 2014;7:494-506.

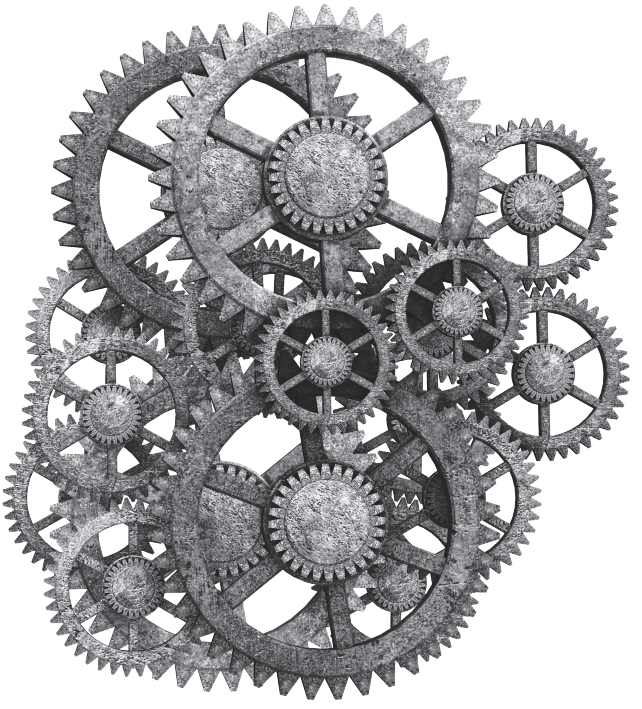

2

Chapter 2

Surgical placement of catheters for long-term cardiovascular exercise testing in swine

Daphne P de Wijs-Meijler, Kelly Stam, Richard WB van Duin, Annemarie Verzijl, Irwin K Reiss, Dirk J Duncker, Daphne Merkus

•

JOURNAL OF VISUALIZED EXPERIMENTS. FEB 2016

ABSTRACT

This protocol describes the surgical procedure to chronically instrument swine and the procedure to exercise swine on a motor-driven treadmill. Early cardiopulmonary dysfunction is difficult to diagnose, particularly in animal models, as cardiopulmonary function is often measured invasively, requiring anaesthesia. As many anaesthetic agents are cardio depressive, subtle changes in cardiovascular function may be masked. In contrast, chronic instrumentation allows for measurement of cardiopulmonary function in the awake state, so that measurements can be obtained under quiet resting conditions, without the effects of anaesthesia and acute surgical trauma. Furthermore, when animals are properly trained, measurements can also be obtained during graded treadmill exercise.

Flow probes are placed around the aorta or pulmonary artery for measurement of cardiac output and around the left anterior descending coronary artery for measurement of coronary blood flow. Fluid-filled catheters are implanted in the aorta, pulmonary artery, left atrium, left ventricle and right ventricle for pressure measurement and blood sampling. In addition, a 20 G catheter is positioned in the anterior interventricular vein to allow coronary venous blood sampling.

After a week of recovery, swine are placed on a motor-driven treadmill, the catheters are connected to pressure and flow meters, and swine are subjected to a five-stage progressive exercise protocol, with each stage lasting 3 min. Haemodynamic signals are continuously recorded and blood samples are taken during the last 30 sec of each exercise stage.

The major advantage of studying chronically instrumented animals is that it allows serial assessment of cardiopulmonary function, not only at rest but also during physical stress such as exercise. Moreover, cardiopulmonary function can be assessed repeatedly during disease development and during chronic treatment, thereby increasing statistical power and hence limiting the number of animals required for a study.

INTRODUCTION

Adequate cardiopulmonary function is essential to supply the body with oxygen and nutrients, particularly during conditions of increased metabolic demand such as during exercise (1). The cardiopulmonary response to exercise is characterized by a number of adaptations in cardiac function, i.e., an increase in heart rate, contractility and stroke volume, and microvascular function, i.e., vasodilation in the vascular beds supplying exercising muscles as well as in the pulmonary vasculature, and vasoconstriction in the vascular beds supplying the gastrointestinal system as well as inactive muscles (1). Impaired exercise capacity is an early hallmark of cardiopulmonary dysfunction, and cardiopulmonary exercise testing is used as an effective method to delineate between cardiac dysfunction, vascular dysfunction and/or pulmonary dysfunction in patients with impaired exercise capacity (2). Early cardiopulmonary dysfunction is difficult to diagnose, particularly in animal models, as cardiopulmonary function is often measured invasively, requiring anaesthesia, with many anaesthetic agents possessing cardio depressive properties (3). Chronic instrumentation allows for measurement of cardiopulmonary function in the awake state, and when the animals are fully adjusted to the laboratory conditions measurements can be obtained under quiet resting conditions without the effects of anaesthesia and acute surgical trauma. Furthermore, when the animals are appropriately trained, measurements can also be obtained during graded treadmill exercise (4,5). More specifically, left and right ventricular function can be assessed and related to myocardial perfusion, while regulation of vasomotor tone in the coronary, systemic and pulmonary microcirculation can be determined. The use of fluid-filled catheters allows measurement of pressure as well as taking blood samples without imposing additional stress on the animals. Another advantage of studying chronically instrumented animals is that cardiopulmonary exercise testing can be repeated allowing the use of an animal as its own control, either during disease development or during chronic treatment, thereby increasing statistical power and hence limiting the number of animals required for a study. Cardiopulmonary anatomy of swine closely resembles that of humans and it is possible to induce various forms of cardiopulmonary disease, such as diabetes (6), myocardial infarction (7),

pulmonary hypertension (8,9) and pacing-induced heart failure (10,11). Moreover, the size of swine allows chronic instrumentation, and repeated blood sampling of sufficient quantity to analyse not only blood gases, but also to perform neurohumoral measurements and/or to search for biomarkers of disease. This protocol describes the surgery used to chronically instrument swine as well as the protocol for exercising the swine on a motor-driven treadmill.

PROTOCOL

Procedures involving animal subjects have been approved by the Animal Care Committee at Erasmus Medical Centre Rotterdam (NL). Swine with weights between 6 and 80 kg have been successfully instrumented using this protocol.

1. Adaptation of the Animals to Human Handling

1. After arrival in the facility, house the animals solitarily but enable them to interact with each other.

2. Accustomise swine to human handling and transportation from the animal facility to the experimental laboratory, by handling the animal at least once a day for one week.

3. Train the animals appropriately for exercise experiments on a motor-driven treadmill by exercising them on the treadmill for a minimum of three times before surgery.

4. Animals should be fasted O/N before surgery to prevent nausea, vomiting and thereby potential aspiration of stomach fluids.

2. Preparation for Surgery

1. Sedation

1. Prepare medication for sedation in a 10 ml syringe. Premedication consists of tiletamine/zolazepam (5 mg/kg), xylazine, (2.25 mg/kg) and atropine (1 mg).

2. Inject the medication intramuscularly in the trapezius muscle with a 19 G 1.5'' needle to sedate the pig.

3. Wait for approximately 10 min and check for muscle relaxation and unconsciousness to confirm appropriate and stable level of sedation.

4. Place a 20 G peripheral safety catheter in an ear vein for subsequent intravenous administration of anaesthesia and/or fluids.

2. Intubation and Ventilation

1. Place the animal on a table and/or trolley in supine position.

2. Open the mouth of the animal with an oral spreader.

3. In case of insufficient relaxation of the jaws or presence of swallowing reflexes, which hinder intubation, administer thiopental (10 mg/ kg) intravenously via the ear vein catheter. Alternatively, the pig could be masked with isoflurane to induce sedation.

4. Use a conventional laryngoscope with a light and a Miller blade to allow the laryngoscopist to directly view the larynx. If there is laryngospasm, apply 2% lidocaine to the cords and larynx to reduce the spasm and allow intubation.

5. Insert an intubating stylet into the endotracheal tube to make the tube conform better to the upper airway anatomy and pass the tube through the mouth and between the vocal cords into the trachea.

6. Inflate the balloon cuff with a 10 ml syringe to help secure it in place, to prevent leakage of respiratory gases, and to protect the airways from possible aspiration of stomach fluid.

7. Connect the tube to a breathing filter (heat and moisture exchanger) and to the mechanical ventilator.

8. Place the animal on its right side on the surgical table.

9. To achieve pO2 levels of 100-120 mmHg, ventilate the animal with a mixture of oxygen and nitrogen (1:2 v/v), using the following ventilator settings: Pressure control mode: positive end-expiratory pressure (PEEP) 4 cmH2O; peak inspiratory

pressure 16 - 18 cmH2O; breathing frequency depending on the size of the animal (for a 20 kg animal, decrease frequency with increasing body weight) this should result in a tidal volume of ~10 ml/kg, monitor ventilation with capnography.

10. Monitor temperature using a rectal thermometer and maintain temperature between 37 - 39 ºC using a heat lamp or heat mat. Moreover, monitor heart rate with electrocardiography.

3. Anaesthesia

1. Induce and maintain anaesthesia preferably by adding 2.0% of isoflurane (v/v) to the ventilation gas-mixture or alternatively by intravenous administration of fentanyl (10 µg/kg/h) via the ear vein catheter.

2. Check adequate depth of anaesthesia by testing pain reflexes with a hind leg toe pinch before starting surgery. When necessary, add additional anaesthesia or wait for a few minutes. Check pain reflexes regularly throughout the surgery.

4. Fluids and Antibiotics

1. Administer the first dose of amoxicillin (25 mg/kg) intravenously via the ear vein catheter.

2. Connect a transfusion system to the ear vein catheter to enable slow infusion of glucose 10% (500 ml) during surgery.

5. Sterilization of Surgical Site

1. Shave and clean the skin of the animal over an area of approximately 25 cm width from the vertebral column all the way to the left axilla.

2. Scrub the moisturized skin with povidone-iodine scrub (75 mg/ml) for approximately 5 min.

3. Remove the povidone-iodine soap from the skin with wet sterile gauzes, before sterilizing the skin with povidone-iodine lotion (100 mg/ ml).

4. Cover the animal with sterile surgical drapes to reduce bacterial transfer and subsequent contamination of the surgical site.

3. Surgery

1. Opening the Thorax (Thoracotomy)

1. Make an incision in the skin, starting 1 cm caudal to the left inferior angle of the scapula down to the left axilla (Figure 1). Use diathermy to cauterize blood vessels in the skin to prevent excessive bleeding.

2. Cut through the serratus muscle and pectoralis major muscle, using the cutting modality of the diathermy. Also use diathermy to cauterize blood vessels in the muscle layer to prevent excessive bleeding.

3. Use blunt dissection to carefully divide the intercostal muscle of the fourth left intercostal space with a mosquito clamp. Now the costal surface of the left lung covered with visceral and parietal pleura should be exposed.

4. To enter the pleural cavity, carefully pierce both layers of the pleura and tear them open.

5. Use a thoracic retractor to separate the edges of the wound and the ribs and to forcefully drive tissues apart to obtain good exposure of the pleural cavity.

6. Push away the left lung in the caudal direction and keep it in place with a wet gauze. Now the heart and great vessels should be clearly exposed.

2. Placement of Catheters and Flow Probes (Figure 1)

1. Use blunt dissection to remove ~2 cm2 of the surrounding connective tissue of the descending thoracic aorta.

2. Perform a purse-string suture, consisting of three stitches, in the aortic wall with a non-absorbable USP3-0 braided silk suture (Ø0.2 mm).

3. Penetrate the aortic vessel wall with a stainless steel 16 G needle in the middle of the purse-string suture.

4. Insert the tip of the fluid-filled catheter (until the ring) into the aorta, pull the purse-string suture firmly together and tie the two strings of the suture.

5. To keep the catheter in place, wind the suture 3 times around the catheter above the ring and again tie the two strings of the suture. Further secure the catheter with a new stitch approximately 1 cm cranial from the insertion place.

6. Connect the fluid-filled catheter to the calibrated pressure transducer, which is connected to the computer, to monitor the mean arterial pressure during the surgery. Obtain an arterial blood gas to verify or adjust for correct ventilation settings.

7. Open the pericardium with a crossed cut. Be aware to keep the phrenic nerve that runs over the pericardium intact.

8. Identify the pulmonary artery and pull it slightly in the caudal direction with a Farabeuf retractor. Now the ascending aorta and aortic arch should be exposed. Monitor mean arterial pressure while retracting the pulmonary artery.

9. Make a small cut (~1 cm) in the connective tissue between the ascending aorta and the pulmonary artery using Metzenbaum scissors, to be able to dissect either the ascending aorta or the pulmonary artery with a large curved mosquito clamp to place the flow probe.

10. Place the rubber band of the flow probe around the vessel. To make this easier, place a suture through one end of the rubber band, place this suture around the vessel and pull it until the rubber band surrounds the vessel.

11. Fix the flow probe measurement device on the rubber band. Connect the flow probe to the computer and check the cardiac output signal on the computer to confirm a correct placement of the flow probe.

12. Place fluid-filled catheters in the pulmonary artery, right ventricle, left ventricle and left atrium at the same manner as described for the aortic fluid-filled catheter (3.2.2 - 3.2.5). Note that it is not necessary to remove connective tissue before performing a purse-string suture in these structures.

13. Expose and dissect the proximal part of the left anterior descending coronary artery by first lifting the tissue with a forceps and making a small (2 - 3 mm) cut with Metzenbaum scissors, followed by carefully teasing the tissue away from the artery

with a cotton swab. Ensure complete dissection of the coronary artery by passing a small straight angled mosquito clamp underneath.

14. Make a stitch parallel to the anterior interventricular coronary vein with a suture, which is connected to the coronary venous catheter.

15. Puncture the coronary vein with the 20 G needle of the coronary venous catheter and insert the cannula of the catheter intravenously.

16. Remove the needle and secure the catheter with the already performed stitch (3.2.14). Further secure the catheter with a new stitch approximately 1cm from the place of initial puncture.

17. Place the coronary flow probe around the previously dissected left anterior descending coronary artery. When the artery is constricted and is hardly visible, use lidocaine 10% spray to relax the vessel to get a better exposure of the vessel. Check the signal of the coronary flow on the computer to confirm a correct placement of the flow probe (Figure 2).

3. Tunnelling

1. Tunnel the flow probes individually through the third left intercostal space beneath the muscle and above the rib by using a large curved mosquito clamp.

2. Tunnel the fluid-filled catheters through either the third or the fifth left intercostal space by piercing the intercostal muscle. Clamp off the fluid-filled catheters and remove the three-way stopcock to minimize the piercing area and prevent leakage of the fluid-filled catheters during the tunnelling.

3. Fix the flow probes and the fluid-filled catheters with non-absorbable USP2-0 braided silk (Ø0.3 mm) by means of a purse string suture on the intercostal muscle. This suture also serves to prevent air leakage after re-instating negative intrathoracic pressure.

4. Make three incisions in the skin approximately 2 cm sinister and parallel to the vertebral column, approximately 3 cm in length 3 cm apart of each other.

5. Pierce a trochar beneath the left latissimus dorsi muscle from rostral incision site to the incisions on the back. Tunnel the flow probes and fluid catheters to the back within this trochar.

6. Place the stopcocks on the fluid-filled catheters and remove the clamp. Withdraw blood to remove clots and air bubbles and fill the fluid-filled catheters with 1,000 IU/ml heparin. Coronary venous catheters should be filled with 5,000 IU/ml heparin.

4. Closing the Thorax

1. Make an incision with a length of approximately 1.5 cm, 8 cm caudal and parallel to the first incision.

2. Lead the drain from the pleural cavity through the sixth intercostal muscles subcutaneously to this incision with a large curved mosquito clamp. Connect the drain to the suction device to remove any remaining fluid and reinstate negative pressure in the pleural cavity during the closing of the thorax.

3. Relieve and inflate the lung with an end-inspiratory hold. Ensure adequate filling of the lung by visual monitoring.

4. Close the thorax by pulling the ribs of the fourth intercostal space together at two separate sites with non-absorbable USP6 braided polyester (Ø0.8 mm).

5. Close the serratus muscle and pectoralis major muscle with a running stitch and the skin with a running subcuticular suture using nonabsorbable USP2-0 braided silk (Ø0.3 mm)

6. Suture the incisions on the dorsal side with non-absorbable USP2-0 braided polyester (Ø0.3 mm) between the catheters. First tie a knot directly onto the skin to close the incision, then fixate the catheters to the suture with a knot 1 cm from the skin. For the flow probes, use an absorbable USP2-0 braided polyglactin (Ø0.3 mm) suture to prevent cutting of the suture in the flow probe wire (Figure 1).

7. Carefully remove the drain while applying pressure on the cranial side of the incision to maintain negative pressure in the pleural cavity. Close the incision with a purse string suture using non-absorbable USP2-0 braided polyester (Ø0.3 mm) and seal the wound with petroleum jelly.

5. Termination of anaesthesia and recovery from surgery

1. Stop anaesthesia when all incision sites are closed.

2. Provide analgesia by administering buprenorphine (0.015 mg/kg) i.m. in the gracilis muscle.

3. Stop the ventilation when the animal is breathing independently and disconnect the tracheal tube from the ventilator. Check regularly if the animal is breathing sufficiently.

4. Place gauze pads between exteriorization sites of the catheters to absorb wound fluid.

5. To protect the external segments of the catheters, give the animal an elastic vest and package the catheters between two pieces of artificial sheepskin.

6. Deflate the balloon of the tracheal tube and extubate when the animal regains its swallowing reflex.

7. Provide long-term analgesia by means of a Fentanyl slow-release patch (12 μg/hr for a 20 kg pig; adjust strength according to bodyweight). Place the patch on a thin part of the skin (such as the lower abdomen) to ensure adequate delivery of analgesia.

8. House the animal separately for the entire post-operative period. Provide a heating lamp for the first week after surgery to keep the animal warm.

9. Supply enough fluid i.v. if the animal is not drinking independently.

10. Flush the fluid-filled catheters daily, by first withdrawing blood to remove clots, then refilling with saline and finally with heparinized saline (1,000 - 5,000 IU/ml) to prevent blood clot formation. Take care not to infuse any air bubbles while flushing the catheters.

11. Administer amoxicillin (25 mg/kg) i.v. daily for 6 days after surgery to prevent post-surgical infections.

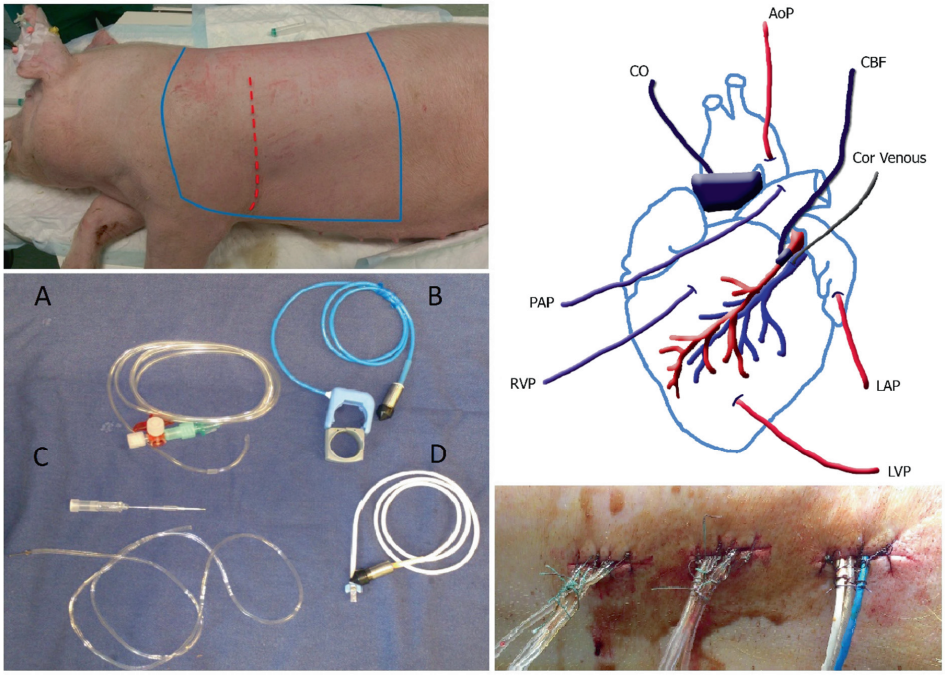

Figure 1. Overview of the Surgery. Top left panel: The sterile area of the animal, which should be shaved and sterilized lies between the bleu lines. The incision site is depicted as the red dotted line. Bottom left panel: Picture of catheters and flow probes: fluid-filled catheter (A), aorta/ pulmonary flow probe including rubber band (B), coronary venous catheter including 20 G needle (C) and the coronary flow probe (D). Top right panel: Schematic overview of placement of the catheters and flow probes. MAP, mean arterial pressure; Cor venous, coronary venous catheter; LAP, left atrial pressure; LVP left ventricular pressure; RVP, right ventricular pressure; PAP, pulmonary artery pressure; CO, cardiac output; CBF, coronary blood flow. Bottom right panel: Tunnelled catheters exiting the back secured with a stitch and a knot at approximately 1 cm distance along the suture.

4. Treadmill Experiment (Figure 2)

1. Flush the fluid-filled catheters as described (3.5.10) and attach the flushed catheters to the pressure transducers. Measure the rectal temperature to be able to obtain temperature corrected blood gas values.

2. Flush the pressure transducers with saline to prevent damping of the signals due to air bubbles. Attach the pressure transducers to the elastic vest on the dorsal side.

3. Connect the pressure transducers and flow probes to the amplifier. Start measuring in the computer program and calibrate the pressure transducers and flow probes with

0 mmHg being open to the air (and closed to animal) and 100 mmHg using a manometer.

4. Switch the three-way stopcock in a way that the fluid catheters have an open connection with the pressure transducers. Note that the blood pressures can now be obtained. Check signals for shape and amplitude (Figure 2).

5. If required, connect an extension line to either of the fluid catheters for sampling of mixed venous and arterial blood.

6. Measure haemodynamics when the animal is lying as well as standing quietly on the treadmill. Average blood pressures are measured over a timeframe of 10 sec.

7. Obtain arterial and mixed venous blood samples by first withdrawing 5 ml of blood using a 10 ml syringe so that 1 ml of pure blood can be obtained using a heparinized 1 ml syringe. For the coronary venous blood samples, a 2 ml syringe is used instead of the 10 ml syringe and withdrawal of 1 ml is sufficient to obtain pure blood.

8. Keep the sealed 1 ml syringes on ice before processing the blood samples with a blood gas analyser to determine the metabolic and ventilatory condition of the animal.

9. Subject the swine to a five-stage exercise protocol on the treadmill, 3 min per speed, 1 - 5 km/hr (~85% of maximal heart rate). Obtain haemodynamics and blood gases after 1.5 - 2 min per speed on each speed as in the resting position.

10. After the exercise protocol close the stopcocks and check if drift has occurred in the 0 mmHg calibration, make a note of this calibration. Remove the pressure transducers of the fluid-filled catheters and disconnect the flow probes.

11. Flush the fluid-filled catheters with saline and heparin (1,000 - 5,000 IU/ml). Protect the catheters and flow probes by putting them beneath the elastic vest between two pieces of artificial sheepskin. The animal can now be returned to its cage.

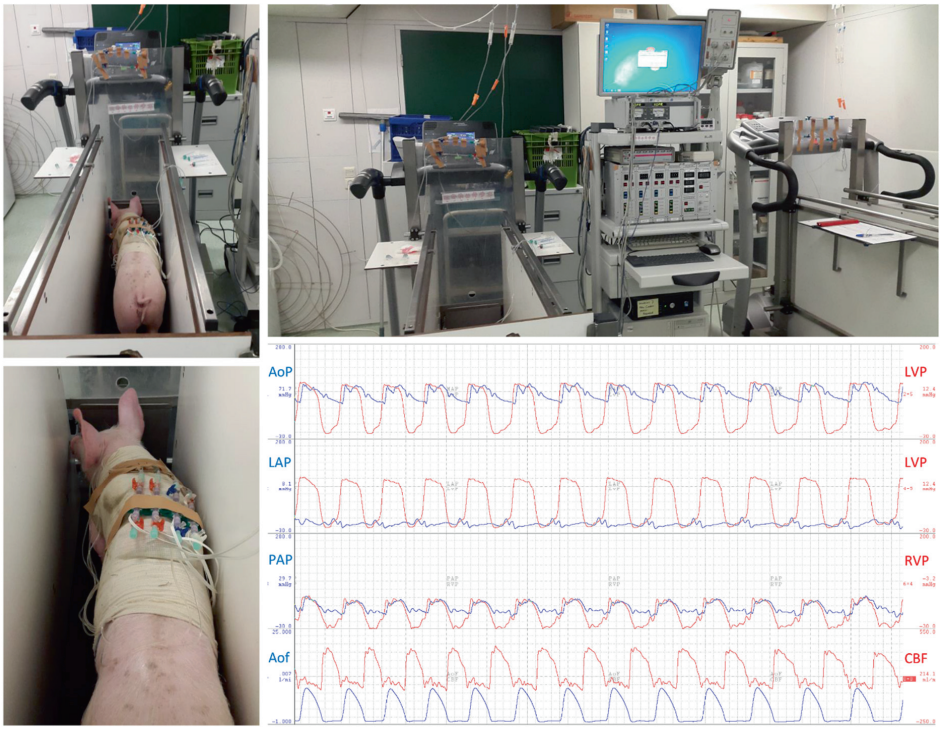

Figure 2. Treadmill Experiment. Left panels: Instrumented swine on the treadmill. Fluid-filled catheters are connected to the pressure transducers, placed on the back of the swine. Top right panel: Overview of the total experimental set-up, including treadmill, amplifier and recording computer. Bottom right panel: Typical example of recorded haemodynamic data. From top to bottom; aortic pressure (AoP, blue) and left ventricular pressure (LVP, red); left atrial pressure (LAP, blue) and left ventricular pressure (red); pulmonary artery pressure (PAP, blue) and right ventricular pressure (RVP, red); aortic flow/cardiac output (AoF, blue); coronary blood flow (CBF, red).

REPRESENTATIVE RESULTS

Exercise up to 5 km/hr resulted in a doubling of cardiac output from 4.3 ± 0.3 to 8.5 ± 0.7 L/min which was principally accomplished by an increase in heart rate from 137 ± 7 to 256 ± 8 beats per min in combination with a small increase in stroke volume from 32 ± 2 to 36 ± 3 ml (Figure 3). The increase in stroke volume was facilitated by an increase in left ventricular contractility, as evidenced by an increase in the maximum of the first derivative of left ventricular pressure dP/dtmax together with an increased rate of relaxation of the left ventricle and an increase in left atrial pressure, being the filling pressure of the left ventricle (Figure 3). The increase in cardiac output together with an increase in haemoglobin concentration (from 8.5 ± 0.4 to 9.2 ± 0.4 g/dl) and an increase in body oxygen extraction from 45 ± 1 to 71 ± 1% allowed a tripling of body oxygen consumption (Figure 3). Systemic vasodilation occurred as evidenced by an increase in systemic vascular conductance and a decrease in systemic vascular resistance, which accommodated the increase in cardiac output almost completely, so that mean aortic pressure increased only slightly (Figure 3). Exercise also resulted in modest vasodilation in the pulmonary circulation, as evidenced by a 33 ± 8% increase in pulmonary vascular conductance. However, the 101 ± 8% increase in cardiac output, together with the increase in left atrial pressure (from 3 ± 1 to 10 ± 1 mmHg), resulted in an increase in pulmonary artery pressure and thereby in an increase in right ventricular afterload (Figure 3). The increase in heart rate, together with the slight increase in arterial pressure resulted in an increase in left ventricular myocardial oxygen consumption, which was principally met by an increase in coronary blood flow which, in combination with the increase in haemoglobin concentration resulted in an increase in myocardial oxygen delivery (from 310 ± 37 to 738 ± 68 μmol/min). The increase in myocardial oxygen demand was commensurate with the increase in myocardial oxygen supply, as myocardial oxygen extraction (79.8 ± 1.9% at rest 81.6 ± 1.9% during maximal exercise) was essentially maintained constant, resulting in an unchanged coronary venous oxygen saturation and coronary venous oxygen tension (Figure 3).

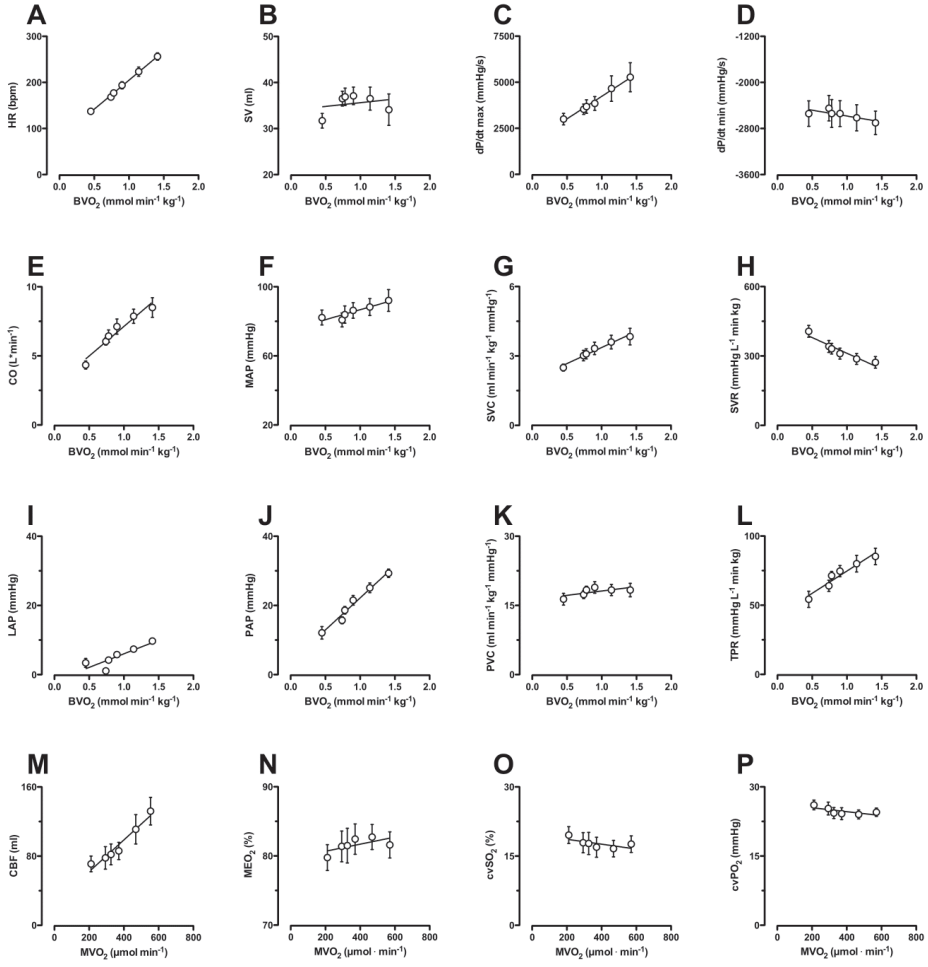

Figure 3. Typical Haemodynamic Response to Exercise. Body oxygen consumption (BVO2) was used as an index for exercise intensity (x-axes of panel A-L). Shown are the responses of heart rate (HR, panel A), stroke volume (SV, panel B), maximum and minimum of the first derivative of left ventricular pressure (dP/dtmax, panel C and dP/dtmin, panel D resp) as indices of contractility and rate of relaxation, cardiac output (CO, panel E), mean arterial pressure (MAP, panel F), systemic vascular conductance (SVC, panel G), systemic vascular resistance (SVR, panel H), Pulmonary artery pressure (PAP, panel J), left atrial pressure (LAP, panel I), pulmonary vascular conductance (PVC, panel K). Total pulmonary resistance (TPR index for right ventricular afterload increased during exercise, Panel L). The increase in heart rate, together with the slight increase in arterial pressure resulted in an increase in left ventricular myocardial oxygen consumption (x-axes of panels M-P), which was principally met by an increase in coronary blood flow (CBF, panel M), as myocardial oxygen extraction (MEO2, panel N), coronary venous oxygen saturation (CVSO2, panel O) and coronary venous oxygen tension (cvPO2, panel P) were minimally affected. All data are presented as mean with standard error of the mean (SEM).

DISCUSSION

The present study describes the surgery for chronical instrumentation of swine as well as the protocol for exercising the instrumented swine on a motor-driven treadmill while measuring haemodynamics and taking blood samples for measurement of oxygen content in arterial, mixed venous and coronary venous blood.

Critical Steps within the Protocol

There are several critical steps within the protocol that start already during the intubation procedure. Thiopental (2.1.5) is a respiratory depressive agent, therefore requiring swift intubation upon administration. Also, it is important to carefully monitor ventilator settings during the procedure. Thus, when the thoracic cavity is opened (step 3.1.4), this results in a loss of the negative intrathoracic pressure. To compensate for this loss and to prevent alveolar collapse, ventilation requires positive end expiratory pressure (PEEP). Moreover, ventilator settings (peak inspiratory pressure) should be adjusted to maintain a tidal volume of ~10 ml/kg. Also note that when the left lung is pushed away (3.1.6.) tidal volume is likely to be decreased because only part of the left lung is ventilated. Ventilator settings should be adjusted based on blood gasses.

Another important note with respect to haemodynamic measurements with fluid filled catheters is that there is a hydrostatic pressure difference between the pressure transducer and the insertion site of the fluid-filled catheter into the cardiovascular system. The height difference between the level of the pressure transducer pressure on the elastic vest (4.2), and the insertion point of the catheter should be estimated during surgery and at sacrifice of the animal and corrected for by interpolation either pre- or post- processing of the data.

Another important point to consider when using this technique is that blood loss, either during surgery or during repeated blood sampling should be minimized, despite the fact that swine are relatively large and consequently have a large blood volume (65 ml/kg). During surgery, blood loss during insertion of the catheters can be minimized by simply applying compression on the puncture wounds. According to

animal experimentation guidelines, up to 10% of the circulating blood volume can be taken on a single occasion from normal, healthy animals with minimal adverse effects, but it will take an animal about 14 days to replenish this amount of blood (12). This means that the recovery from surgery is prolonged when a significant amount of blood is lost.

During the repeated blood sampling during the exercise experiments, a maximum of 1.0% of an animal's circulating blood volume, or 0.6 ml/ kg can be removed every 24 hr 15. This also means that the amount of blood that is sampled during treadmill exercise, should be well-planned and that, after removal of the initial clots that are invariably present in the lumen of the catheter near the tip at the interface with the blood, the remaining blood withdrawn to flush the lines should be given back to the animals.

Modifications and Troubleshooting

Implanted fluid-filled catheters should be flushed daily to prevent malfunctioning because of blood clot formation. Depending on the amount of blood clots in the fluid filled catheters, the amount of heparin in each line can be varied from 1,000 IU/ml to 5,000 IU/ml. The amount of heparin should be kept to a minimum in the first week after surgery to prevent bleeding from surgical incision wounds due to the presence of the anticoagulant heparin.

However, even when flushed daily, some fluid-filled catheters will get clogged. When this happens, try withdrawing blood with a smaller 2 ml syringe by applying minimal and/or pulsatile suction. It can take several minutes before the catheter will be unclogged. When this does not work, carefully flush a small amount of saline into the catheter and immediately try to withdraw blood. Be aware that infusion can result in a release of thrombus into the circulation and embolism of distal organs, depending on the site of the catheter. When careful flushing does not work, connect the clogged line to a pressure-transducer to check if there is still a haemodynamic signal. If there is no signal, the fluid filled line should be sealed by several knots and cut off.

Interpretation and Limitations

When all points as mentioned above are taken into account, the combination of haemodynamic measurements and blood samples allows for interpretation of the exercise response in terms of whole body and myocardial oxygen consumption, which are better measures for exercise intensity than treadmill speed alone (7,13-15).

In order to meet the increased metabolic requirements of the body, exercise requires changes in cardiac function as well as changes in local perfusion. Tissue perfusion is regulated by changes in diameter of the small arteries and arterioles of the vascular bed supplying the tissue. Myriad vasoactive factors, derived from neurohumoral systems, the endothelium and local metabolites interact to determine vascular tone and ensure adequate tissue perfusion (1,5,13,16). Changes in systemic and pulmonary vascular resistance or the inverse, vascular conductance, can be calculated from the blood pressure and flow signals and interpreted in terms of changes in vasomotor tone in the systemic and pulmonary vasculature. Intuitively, vascular resistance is often used to assess changes in vascular tone. However, in our research group, we advocate the use of conductance although conductance and resistance are mathematically related, with conductance being flow normalized for pressure, and resistance equalling pressure divided by flow. Although conductance and resistance are interchangeable if one investigates the effect of only a single stimulus (i.e., exercise) (7,17), interpretation of the two parameters can differ when combining exercise with pharmacological interventions, to investigate the contributions of various vasoactive systems to regulation of vascular tone (4,5,7,15,18).

During exercise, the systemic circulation transforms from a system at rest that is characterized by a low flow and a high resistance (i.e., low conductance) into a system with high flow and low resistance, (high conductance). As such, pharmacological vasodilation has different consequences for conductance and resistance during rest versus exercise. The decrease in resistance that is produced by a pharmacological vasodilator at rest is large while the increase in conductance is only small. In contrast, during exercise the same degree of vasodilation translates into a large increase in conductance, but only a small decrease in resistance. Thus, when conductance is used, a greater vasodilation seems to occur during exercise, while when looking at

resistance vasodilation appears to be larger at rest. Interpretation of the data thus differs when using resistance or conductance. Although the choice between resistance and conductance may seem rather arbitrary, in physics the variable that undergoes the primary change is designated as the numerator of the index for a response (7,17,18). Since during exercise aortic blood pressure remains fairly constant whereas cardiac output increases markedly, the most appropriate parameter to describe the systemic vascular response to exercise would appear to be systemic vascular conductance (cardiac output / aortic blood pressure), rather than resistance. Moreover, the systemic circulation consists of a multitude of vascular beds from a variety of organs that are principally perfused in a parallel manner. Since parallel resistors add up reciprocally, while parallel conductors add up in a linear manner, any change in conductance of a particular regional vascular bed translates into an identical (absolute) change of the total systemic vascular conductance. This consideration lends further support to the use of vascular conductance to describe the systemic vascular responses to exercise and pharmacological interventions.

The choice for either resistance or conductance to describe the vascular responses to exercise in the pulmonary bed appears to be less obvious, because exercise produced increases in cardiac output as well as pulmonary artery pressure (7,17). A choice for either resistance or conductance is also less critical, in view of the relatively minor exercise-induced changes in PVR and PVC as compared to the degree of vasodilation produced by, for example, ET-receptor blockade (7). As a result, the use of either resistance or conductance to characterize the vascular effects of a pharmacological vasodilator in the pulmonary circulation will yield similar conclusions.

In the coronary circulation, interpretation of the data is even more complex as systemic administration of pharmacological antagonists of endogenous vasoactive substances results not only in alterations in coronary resistance vessel tone, but often also produce pronounced changes in systemic haemodynamic variables (7,15,17,19). These altered haemodynamics influence cardiac work, and thereby cause changes in coronary blood flow resulting from changes in metabolic requirements of the heart or from autoregulation, rather than as a direct effect of the intervention on coronary vascular tone. For example, blockade of an endogenous vasoconstrictor system decreases mean aortic pressure, as a consequence of systemic vasodilation, and elicits

auto regulatory adjustments in coronary microvascular tone. Moreover, baroreceptor reflex activation acts to increase heart rate and myocardial contractility. Such changes in heart rate and/or blood pressure subsequently will result in alterations in myocardial metabolism, requiring an adjustment in myocardial oxygen supply and hence in coronary blood flow.

To take into account the effects of such drug-induced alterations in myocardial oxygen consumption, investigators examine the relation between coronary venous oxygen levels and myocardial oxygen consumption (MVO2) (4,5), as this approach allows assessment of regulation of coronary resistance vessel tone independently of changes in myocardial oxygen demand. Administration of a vasodilator will increase myocardial oxygen delivery at a given level of MVO2. As this increase in oxygen delivery occurs without a change in oxygen consumption, myocardial oxygen extraction will decrease, thereby leading to increases in coronary venous oxygen content and hence in an upward shift of the relation between MVO2 and coronary venous oxygen levels. It is therefore imperative to measure both myocardial oxygen demand as well as myocardial oxygen supply in order to correctly study the regulation coronary resistance vessel tone (4,5).

Notwithstanding its elegance and usefulness, some investigators have pointed out the limitations of this approach (20). Thus, plotting MVO2 versus coronary venous PO2 or coronary venous SO2 could be considered to be inappropriate because these variables are actually part of the equation to compute MVO2. Consequently, MVO2 is not a variable that is independent of coronary venous PO2 or SO2. Alternatively, investigators should consider using another index of myocardial work, the rate-pressure product (RPP), which is the product of heart rate and left ventricular systolic pressure. However, as RPP and MVO2 are almost linearly related, substituting RPP for MVO2 yields virtually identical results (15), and the relation between MVO2 and coronary venous oxygen levels is considered a sensitive way of studying alterations in coronary vasomotor tone.

Significance with Respect to Existing Methods

Another method commonly used to assess changes in regulation of vascular tone is the use of isolated coronary and pulmonary small arteries or arterioles in a pressure or wire myograph (6,15,21). The advantage of myograph studies is that vessels can be studied independent of surrounding tissue and without potentially confounding effect from circulating factors. These in vitro techniques are therefore complementary to the in vivo measurements. However, in vivo and in vitro techniques sometimes give opposing results. For example, the response to the potent vasoconstrictor endothelin was reduced in the intact coronary circulation after myocardial infarction, but was augmented in isolated coronary small arteries from swine with myocardial infarction as compared to healthy control swine (21). This difference between the in vivo and in vitro data was due to an increased suppression of the vasoconstrictor influence of endothelin by prostanoids in vivo (21).

Future Applications

Given the proposed role of changes in coronary microvascular function in both left and right ventricular dysfunction, assessment of these changes in relevant models of cardiovascular disease is required. The use of chronically instrumented animals allows correlations of the severity of the disease with microvascular (dys) function. Moreover, both coronary and pulmonary microvascular function may appear normal under basal resting conditions, while microvascular dysfunction may be revealed under cardiovascular stress, such as during exercise.

Several swine models of cardiopulmonary disease, such as diabetes (6), myocardial infarction (22), pulmonary hypertension (8,9) and pacing induced heart failure (10) are available and could be combined with chronic instrumentation. A potential drawback is that, when commercially available swine breeds such as Yorkshire, Landrace, Large White etc. are used, adult swine are very large and may therefore be difficult to handle. Therefore, juvenile swine are often used. However, as juvenile swine grow rapidly, positioning and function of flow probes and pressure catheters and patency of fluid-filled catheters may become compromised, limiting the duration of serial measurements within individual animals to approximately 10 weeks. An

alternative is the use of adult miniature swine, such as Yucatan or Gottingen swine, of which the adult weight is 40 - 60 kg (23).

In conclusion, the use of chronically instrumented animals allows serial assessment of cardiopulmonary function either during development of disease or evaluation of treatment, thereby increasing statistical power and limiting the number of animals required for a study.

REFERENCES

1. Laughlin MH, Davis MJ, Secher NH et al. Peripheral circulation. Comprehensive Physiology 2012;2:321-447.
2. Datta D, Normandin E, ZuWallack R. Cardiopulmonary exercise testing in the assessment of exertional dyspnea. Annals of thoracic medicine 2015;10:77-86.
3. Vatner SF, Braunwald E. Cardiovascular control mechanisms in the conscious state. The New England journal of medicine 1975;293:970-6.
4. Duncker DJ, Bache RJ. Regulation of coronary blood flow during exercise. Physiological reviews 2008;88:1009-86.
5. Tune JD, Gorman MW, Feigl EO. Matching coronary blood flow to myocardial oxygen consumption. Journal of applied physiology 2004;97:404-15.
6. van den Heuvel M, Sorop O, Koopmans SJ et al. Coronary microvascular dysfunction in a porcine model of early atherosclerosis and diabetes. American journal of physiology Heart and circulatory physiology 2012;302:H85-94.
7. Zhou Z, de Beer VJ, de Wijs-Meijler D et al. Pulmonary vasoconstrictor influence of endothelin in exercising swine depends critically on phosphodiesterase 5 activity. Am J Physiol Lung Cell Mol Physiol 2014;306:L442-52.
8. Pereda D, Garcia-Alvarez A, Sanchez-Quintana D et al. Swine model of chronic postcapillary pulmonary hypertension with right ventricular remodeling: long-term characterization by cardiac catheterization, magnetic resonance, and pathology. J Cardiovasc Transl Res 2014;7:494-506.
9. Mercier O, Sage E, Izziki M et al. Endothelin A receptor blockade improves regression of flow-induced pulmonary vasculopathy in piglets. The Journal of thoracic and cardiovascular surgery 2010;140:677-83.
10. Spinale FG, Hendrick DA, Crawford FA, Smith AC, Hamada Y, Carabello BA. Chronic supraventricular tachycardia causes ventricular dysfunction and subendocardial injury in swine. The American journal of physiology 1990;259:H218-29.
11. Yarbrough WM, Spinale FG. Large animal models of congestive heart failure: a critical step in translating basic observations into clinical applications. Journal of nuclear cardiology : official publication of the American Society of Nuclear Cardiology 2003;10:77-86.
12. Gross DR. Animal Models in Cardiovascular Research. 3 ed: Springer, 2009.
13. Duncker DJ, Stubenitsky R, Verdouw PD. Autonomic control of vasomotion in the porcine coronary circulation during treadmill exercise: evidence for feed-forward beta-adrenergic control. Circ Res 1998;82:1312-22.
14. Stubenitsky R, Verdouw PD, Duncker DJ. Autonomic control of cardiovascular performance and whole body O2 delivery and utilization in swine during treadmill exercise. Cardiovasc Res 1998;39:459-74.
15. Zhou Z, de Beer VJ, Bender SB et al. Phosphodiesterase-5 activity exerts a coronary vasoconstrictor influence in awake swine that is mediated in part via an increase in endothelin production. American journal of physiology Heart and circulatory physiology 2014;306:H918-27.

16. Merkus D, Duncker DJ. Perspectives: Coronary microvascular dysfunction in post-infarct remodelled myocardium. European Heart Journal Supplements 2014;16:A74-A79.
17. de Beer VJ, de Graaff HJ, Hoekstra M, Duncker DJ, Merkus D. Integrated control of pulmonary vascular tone by endothelin and angiotensin II in exercising swine depends on gender. Am J Physiol Heart Circ Physiol 2010;298:H1976-85.
18. Lautt WW. Resistance or conductance for expression of arterial vascular tone. Microvascular research 1989;37:230-6.
19. Merkus D, Visser M, Houweling B, Zhou Z, Nelson J, Duncker DJ. Phosphodiesterase 5 inhibition-induced coronary vasodilation is reduced after myocardial infarction. American journal of physiology Heart and circulatory physiology 2013;304:H1370-81.
20. Heusch G. The paradox of alpha-adrenergic coronary vasoconstriction revisited. J Mol Cell Cardiol 2011;51:16-23.
21. Merkus D, Houweling B, van den Meiracker AH, Boomsma F, Duncker DJ. Contribution of endothelin to coronary vasomotor tone is abolished after myocardial infarction. Am J Physiol Heart Circ Physiol 2005;288:H871-80.
22. Haitsma DB, Bac D, Raja N, Boomsma F, Verdouw PD, Duncker DJ. Minimal impairment of myocardial blood flow responses to exercise in the remodeled left ventricle early after myocardial infarction, despite significant hemodynamic and neurohumoral alterations. Cardiovasc Res 2001;52:417-28.
23. Bender SB, van Houwelingen MJ, Merkus D, Duncker DJ, Laughlin MH. Quantitative analysis of exercise-induced enhancement of early- and late-systolic retrograde coronary blood flow. Journal of applied physiology 2010;108:507-14.

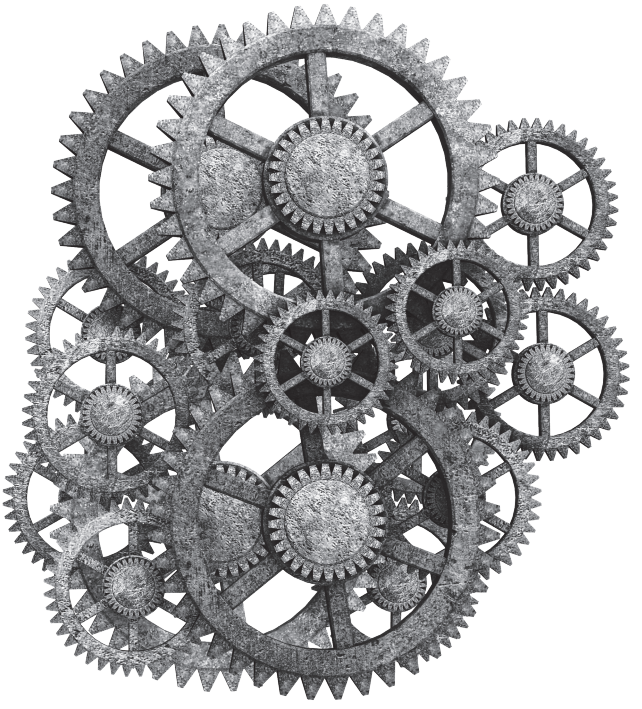

3

Chapter 3

Pulmonary vasodilation by phosphodiesterase 5-inhibition is enhanced and nitric oxide-independent in early pulmonary hypertension after myocardial infarction

Richard WB van Duin, Birgit Houweling,
André Uitterdijk, Dirk J Duncker, Daphne Merkus

•

THE AMERICAN JOURNAL OF PHYSIOLOGY - HEART
AND CIRCULATORY PHYSIOLOGY. FEB 2018

ABSTRACT

Myocardial infarction (MI) may result in pulmonary hypertension (PH). Inhibition of phosphodiesterase 5 (PDE5), the enzyme responsible for the breakdown of cGMP in vascular smooth muscle, has become part of the contemporary therapeutic armamentarium for pulmonary arterial hypertension and may also be beneficial for PH secondary to MI. Nitric oxide (NO) is an important activator of cGMP-synthesis and can be enhanced in early PH and decreased in severe PH. In the present study we investigated if PDE5-inhibition ameliorates pulmonary haemodynamics in swine with PH secondary to MI and whether NO is essential. The PDE5-inhibitor EMD360527 was administered in awake, chronically instrumented swine with or without MI. At rest, PDE5-inhibition produced pulmonary vasodilation as evidenced by decrease in pulmonary vascular resistance, which was more pronounced in MI (n=5) compared to normal swine (n=10; $P \leq 0.01$) and was accompanied by an increase in stroke volume in MI swine. Both pulmonary vasodilation and increased stroke volume were maintained during exercise, suggesting that this therapy may improve exercise capacity in patients with PH secondary to MI. Interestingly, prior inhibition of NO significantly enhanced ($P \leq 0.01$) pulmonary vasodilation by PDE5-inhibition in both normal (n=8) and MI swine (n=5; $P \leq 0.05$ vs normal). This suggests that the increased vasodilator responses to PDE5-inhibition after MI were not due to an increase in NO-induced cGMP production. These observations indicate that PDE5-inhibition represents an interesting pharmacotherapeutic approach in early PH following a recent MI, to prevent overt PH.

New and noteworthy

This research article is the first to describe that pulmonary vasodilation to PDE5-inhibition is enhanced and NO-independent in resting and exercising swine with PH as a result of MI. This suggests that PDE5-inhibition can normalize pulmonary haemodynamics in post-capillary PH following a recent MI and may improve exercise capacity.

INTRODUCTION

Myocardial infarction (MI) can result in post-capillary pulmonary hypertension (PH), i.e. a passive increase of pulmonary arterial pressure as a direct result of increased left atrial pressure (1-3). When left untreated, this condition can progress to combined pre- and post-capillary PH, formerly known as "out-of-proportion PH" a chronic, progressive disease with high mortality and limited treatment options (4-6). In prolonged PH, endothelial dysfunction accounts for an imbalance between vasodilators (e.g. nitric oxide (NO) and prostacyclin) and vasoconstrictors (e.g. endothelin) (7-9). This imbalance between production of vasodilators and vasoconstrictors likely contributes to the sustained state of pulmonary vasoconstriction after MI. However, endothelial dysfunction appears to be principally associated with severe PH, while in early, mild PH, NO-production by NO-synthase (NOS) is maintained or even enhanced (7). Thus, in early stage PH the pulmonary vasoconstriction may lead to increased shear stress, thereby stimulating NO-production and counteracting the development of PH (10-12). These observations suggest that the early response to PH is an increased synthesis of NO to normalize pulmonary vasoconstriction until chronic PH eventually results in endothelial dysfunction introducing pre-capillary aspects to the originally isolated post-capillary PH. Indeed, in our swine model of PH secondary to MI, the vasodilator influence of NO is maintained (13), at a time when endothelin-induced pulmonary vasoconstriction is enhanced (14).

NO-induced vasodilation is mediated through production of cyclic guanosine monophosphate (cGMP) by soluble guanylate cyclase (GC) and reduction of intracellular Ca^{2+} concentration. NO-signalling is terminated through removal of cGMP by phosphodiesterase 5 (PDE5), which removes cGMP by hydrolysing it to 5' GMP (15). Inhibition of PDE5 has shown to be of benefit for the alleviation of pulmonary arterial hypertension by enhancing the vasodilator influence of NO (16-18). In a previous study we showed that in normal swine, inhibition of PDE5 results in vasodilation of the pulmonary vascular bed (19).

Another enzyme that is capable of producing cGMP is particulate GC, which is activated through natriuretic peptides, including atrial natriuretic peptide (ANP)

(20). While NO-production is enhanced in early PH and decreased in later stages of PH and heart failure (HF) (12), ANP levels are elevated in patients with acute MI, HF after MI, and PH (21,22) as well as in our porcine model of early PH secondary to MI (23,24). The increased circulating levels of ANP may result in elevated levels of cGMP in pulmonary vascular smooth muscle cells, thereby further enhancing the pulmonary vasodilator effects of PDE5-inhibition. The elevated ANP levels after MI, in combination with the maintained NO-induced vasodilation, led us to hypothesize that the vasodilator effect of PDE5-inhibition in the pulmonary circulation is maintained or even increased after MI, which would make PDE5-inhibition a very suitable therapeutic strategy for normalizing pulmonary haemodynamics in early PH after a recent MI, to prevent overt PH. To test this hypothesis, and to investigate the importance of NO in the pulmonary vascular response to PDE5-inhibition, we studied chronically instrumented swine with early PH secondary to a recent MI, in the awake state both in the absence and presence of NOS-inhibition, at rest and during staged sub-maximal treadmill exercise.

METHODS

Studies were performed in accordance with the "Guiding Principles in the Care and Use of Laboratory Animals" as approved by the Council of the American Physiological Society, and with written approval of the Animal Care Committee of the Erasmus MC Rotterdam. Twenty-two crossbred Landrace x Yorkshire swine of either sex (2-3 months old, 25±1 kg) entered the study.

Surgical procedures

After one week of acclimatization to the animal facilities and treadmill experiments using positive encouragement with food, swine (n=22) were chronically instrumented as described previously (25). In short, swine were sedated with an intramuscular (i.m.) injection of ketamine (30 mg · kg^{-1} Anisane, Raamsdonksveer, The Netherlands) and midazolam (2 mg · kg^{-1} Actavis, Baarn, The Netherlands), anaesthetised with an intravenous (i.v.) bolus administration of thiopental (10 mg · kg^{-1} Rotexmedica, Trittau, Germany), intubated and ventilated with a mixture of O_2 and N_2O (1:2) Anaesthesia was maintained with midazolam (1 mg · kg^{-1} per hour i.v. Actavis, Baarn, Netherlands) and fentanyl (10 µg · kg^{-1} per hour i.v. Hameln Pharmaceuticals, Hameln, Germany). Under sterile conditions, the chest and pericardium were opened via the fourth left intercostal space and a fluid-filled polyvinylchloride catheter was inserted into the aortic arch, the pulmonary artery and the left atrium for blood pressure measurement (Combitrans® pressure transducers, Braun, Melsungen, Germany) and blood sampling. An electromagnetic flow probe (14-15 mm, Skalar Medical, Delft, The Netherlands) was positioned around the ascending aorta for measurement of cardiac output (CO). Body core temperature was monitored and maintained using heating pads (26). Fluid status was maintained with a saline drip (100 ml · hr^{-1} i.v.).

In all 22 swine the proximal part of the left coronary circumflex artery (LCx) was dissected free, and in 9 animals the LCx was permanently occluded with a silk suture to produce MI (24,27-29). Successful production of MI was visually ascertained by ST elevation and epicardial discoloration of the area at risk. Catheters were tunneled to

the back, the wound was closed and animals were allowed to recover, receiving analgesia (0.3 mg buprenorphine i.m. Indivior, Slough, United Kingdom) for 2 sequential days and antibiotic prophylaxis consisting of amoxicillin (25 mg · kg^{-1} i.v. Centrafarm B.V. Etten-Leur, The Netherlands) and gentamycin (5 mg · kg^{-1} i.v. Eurovet, Bladel, The Netherlands) for 5 days.

Experimental protocols

Studies were performed 11±4 days following surgery.

Effect of PDE5-inhibition

After haemodynamic measurements consisting of left atrial, aortic and pulmonary arterial blood pressures, heart rate and CO, blood samples, and rectal temperature were obtained at rest, swine (Table 1; 12 normal and 5 MI) were subjected to a four-stage sub-maximal exercise protocol on a motor driven treadmill (1-4 km · h^{-1}) as described before (CON experiment) (25). Haemodynamic variables were continuously recorded and blood samples collected during the last 60 seconds of each 3 minutes exercise stage, at a time when haemodynamics had reached a steady state. After 90 minutes of rest, the PDE5-inhibitor EMD360527 (EMD, Merck, Darmstadt, Germany) was administered by an infusion of 300 µg · kg^{-1} · min^{-1} i.v. and after ten minutes of infusion the exercise protocol was repeated, with continuous infusion of EMD during the entire protocol (EMD experiment). This dose of EMD was based on a previous dose-response study in normal swine (19). In the present study, EMD infusion resulted in plasma levels of 8210±690 ng ml^{-1} in MI swine (n=6), which was similar to the plasma levels in normal swine (6715±630 ng ml^{-1}; n=6).

Effect of PDE5-inhibition after NOS-inhibition: On a different day (4±3 days prior/after PDE5-run), the NOS-inhibitor N^{ω}-nitro-L-Arginine (NLA, Sigma-Aldrich, Zwijndrecht, Netherlands) was administered to swine (Table 1; 10 normal and 5 MI, of which 9 normal and 2 MI had also participated in the above described protocol) at a dose of 20 mg · kg^{-1} i.v. prior to the first exercise protocol (NLA experiment) (19,30,31). After 90 minutes of rest, the PDE5-inhibitor was administered as described above and the exercise protocol was repeated (NLA+EMD experiment).

Table 1. Schematic representation of the overlap and bodyweights of swine used in different protocols

	Con - EMD	NLA - NLA+EMD
Con - EMD	**N: n=12; 26±1kg**	N: n=9
	MI:n=5; 25±1kg	MI: n=2
NLA - NLA+EMD	-	**N: n=10; 25±1 kg**
	-	**MI: n=5; 25±1kg**

Blood Gas Measurements

Blood samples were kept in iced syringes. Measurements of PO_2 (mmHg), PCO_2 (mmHg) and pH were subsequently performed with a blood gas analyzer (Acid-Base Laboratory Model 505, Radiometer, Copenhagen, Denmark). O_2 saturation and Hb (g/dl) were measured with a haemoximeter (OSM3, Radiometer). Arterial and venous blood O_2 content (CaO_2 and CvO_2) were computed as (Hb·0.621·O_2-saturation) + (0.00131·PO_2) and multiplied by 2.241 to convert from µMol/ml to ml/100 ml (vol%). Arteriovenous O_2 difference (a-vO_2; vol%) was computed as CaO_2-CvO_2. Body O_2 consumption (BVO_2; ml · min^{-1} · kg^{-1}) was calculated as the product of a-vO_2 and CO corrected for bodyweight (31).

Data Analysis

Digital recording and off-line haemodynamic analyses have been described previously (13). Systemic vascular resistance (SVR) was computed as mean aortic blood pressure divided by CO. Pulmonary vascular resistance (PVR) was defined as mean pulmonary arterial pressure (PAP) minus mean left atrial pressure (LAP) divided by CO. Due to malfunction of flow probes, CO was not measured in 2 normal animals in both the CON – EMD and the NLA – NLA+EMD experiments.

Statistical analysis

To test the effect of exercise and drug treatment (EMD in presence or absence of NLA) within the normal and MI groups, a two way repeated measures ANCOVA was performed. The interaction between exercise and drug treatment was assessed using a mixed model analysis with PAP and PVR as dependent variables, NLA and EMD as

independent variables, and BVO_2 as a co-variate. The effect of MI on haemodynamics and on the effect of drug treatment was assessed using a two-way repeated measures ANOVA. Statistical significance was accepted when $P \leq 0.05$. Data are presented as mean±S.E.M.

RESULTS

One MI swine died during surgery, due to nonconvertible ventricular fibrillation.

Effects of exercise and MI

In normal swine (n=10), exercise up to 4 km h^{-1} resulted in an increase in CO that was exclusively mediated by an increase in heart rate (Table 2). Mean aortic blood pressure was minimally affected, implying that the increase in CO was balanced by an equivalent decrease in SVR. Both mean PAP and LAP approximately doubled in response to exercise, with the increase in transpulmonary pressure gradient (TPG; PAP-LAP) paralleling the increase in CO, so that PVR remained essentially unchanged during exercise (Fig. 1).

In MI swine (n=5), CO was on average 10-15% lower than in normal swine, due to a 10-20% lower stroke volume (both $P \leq 0.05$ by two-way ANOVA; Table 2). Despite the slightly lower CO, mean PAP increased from 18±3 mmHg in normal to 25±3 mmHg in MI swine, which was principally the result of a higher mean LAP after MI (both $P \leq 0.05$ by two-way ANOVA; Table 3), while PVR was not significantly different between MI and normal swine. Similar to normal swine, PAP increased in MI swine in response to exercise as a result of the exercise-induced increases in LAP and CO, while PVR remained unchanged (Table 3; Fig. 1).

Table 2 Systemic hemodynamics of swine at rest and during exercise before and after administration of EMD and NLA

					Exercise level (km h^{-1})							
	n	Treatment	MI	Rest	1		2		3		4	
HR	12	Control	-	139 ± 3	170 ± 4	*	183 ± 4	*	202 ± 7	*	240 ± 8	*
(bpm)		EMD	-	156 ± 5	178 ± 4	*†	193 ± 6	*	218 ± 8	*†	244 ± 9	*
	5	Control	+	156 ± 8	180 ± 2	*‡	187 ± 3	*	207 ± 5	*	222 ± 6	*
		EMD	+	171 ± 3	192 ± 3	*†	201 ± 3	*†	213 ± 5	*	233 ± 7	*
	10	NLA	-	112 ± 4	125 ± 3	*	132 ± 3	*	150 ± 4	*	193 ± 9	*
		NLA+EMD	-	122 ± 7	135 ± 7	*	147 ± 7	*	164 ± 7	*	199 ± 9	*
	5	NLA	+	122 ± 7	143 ± 6	*‡	154 ± 6	*‡	173 ± 8	*‡	191 ± 8	*
		NLA+EMD	+	150 ± 7 †‡	156 ± 5		175 ± 13		187 ± 12		206 ± 12	*
SV	10	Control	-	40 ± 2	39 ± 2		39 ± 2	*	37 ± 2	*	36 ± 2	*
(ml)		EMD	-	38 ± 3	38 ± 2		38 ± 2		39 ± 2	†	39 ± 2	†
	5	Control	+	31 ± 2 ‡	31 ± 1	‡	32 ± 2		32 ± 1		32 ± 1	
		EMD	+	34 ± 1 †	33 ± 1	†	34 ± 1		35 ± 1	†	34 ± 1	
	8	NLA	-	39 ± 3	40 ± 3	*	41 ± 3	*	40 ± 3		38 ± 3	
		NLA+EMD	-	43 ± 4	43 ± 4		44 ± 4		44 ± 4		42 ± 4	†
	5	NLA	+	31 ± 1	32 ± 1		32 ± 1	*	32 ± 1		32 ± 1	
		NLA+EMD	+	34 ± 1 †	34 ± 1	†	34 ± 1	†	34 ± 1	†	34 ± 1	
CO	10	Control	-	5.4 ± 0.3	6.4 ± 0.3	*	7.0 ± 0.3	*	7.4 ± 0.3	*	8.5 ± 0.3	*
(L min^{-1})		EMD	-	5.9 ± 0.3	6.8 ± 0.2	*	7.2 ± 0.3	*	8.4 ± 0.2	*†	9.3 ± 0.3	*†
	5	Control	+	4.8 ± 0.2	5.6 ± 0.2	*	6.0 ± 0.3	*	6.6 ± 0.2	*	7.1 ± 0.3	*‡
		EMD	+	5.8 ± 0.2 †	6.4 ± 0.1	*†	6.8 ± 0.3	*†	7.4 ± 0.3	*†‡	8.0 ± 0.2	*†‡
	8	NLA	-	4.3 ± 0.2	5.0 ± 0.3	*	5.5 ± 0.4	*	6.1 ± 0.4	*	7.3 ± 0.3	*
		NLA+EMD	-	5.1 ± 0.3	5.7 ± 0.3	*†	6.3 ± 0.3	*†	7.0 ± 0.4	*†	8.2 ± 0.4	*†
	5	NLA	+	4.1 ± 0.2	4.9 ± 0.2	*	5.2 ± 0.1	*	5.8 ± 0.4	*	6.2 ± 0.3	*
		NLA+EMD	+	5.6 ± 0.4 †	5.7 ± 0.2	†	6.6 ± 0.9		6.9 ± 0.4		7.5 ± 0.7	*
MAP	12	Control	-	87 ± 3	84 ± 3		85 ± 3		86 ± 3		89 ± 3	
(mmHg)		EMD	-	76 ± 3	74 ± 2	†	76 ± 3	†	78 ± 2	†	80 ± 2	*†
	5	Control	+	80 ± 5	82 ± 5		81 ± 5		82 ± 5		81 ± 4	
		EMD	+	69 ± 4 †	72 ± 4	†	73 ± 5	*†	73 ± 4	*†	73 ± 4	*†
	10	NLA	-	112 ± 3	111 ± 2		112 ± 3		115 ± 4		116 ± 3	
		NLA+EMD	-	105 ± 5	105 ± 4	†	106 ± 4	†	105 ± 4	†	106 ± 3	†
	5	NLA	+	108 ± 3	108 ± 2		112 ± 2		112 ± 2		109 ± 4	
		NLA+EMD	+	99 ± 4	101 ± 2		100 ± 1		99 ± 4		98 ± 5	
SVR	10	Control	-	15.9 ± 1.1	12.9 ± 0.7	*	12.0 ± 0.6	*	11.4 ± 0.5	*	10.2 ± 0.4	*
(mmHg		EMD	-	12.7 ± 0.7	10.6 ± 0.3	*†	10.2 ± 0.4	*†	9.1 ± 0.3	*†	8.4 ± 0.3	*†
L min^{-1})	5	Control	+	16.7 ± 1.6	14.9 ± 1.3		13.5 ± 1.2	*	12.5 ± 0.9	*	11.4 ± 0.9	*
		EMD	+	12.0 ± 0.8 †	11.3 ± 0.7	†	10.9 ± 0.9	*†	10.0 ± 0.6	*†	9.2 ± 0.4	*†
	8	NLA	-	26.8 ± 1.6	22.7 ± 1.3	*	21.4 ± 1.5	*	19.3 ± 1.3	*	16.1 ± 0.7	*
		NLA+EMD	-	21.0 ± 1.7	18.8 ± 1.4	*†	16.9 ± 0.9	*†	15.1 ± 0.6	*†	12.9 ± 0.5	*†
	5	NLA	+	26.4 ± 0.8	22.1 ± 0.5	*	21.4 ± 0.3	*	19.3 ± 1.1	*	17.3 ± 0.6	*
		NLA+EMD	+	17.7 ± 0.8 †	17.9 ± 0.3	†	16.0 ± 1.7		14.6 ± 1.2		13.1 ± 1.3	*

HR: Heart Rate, SV: Stroke Volume, CO: Cardiac Output, MAP: Mean Arterial Pressure, SVR: Systemic Vascular Resistance (MAP/CO), EMD: EMD360527, NLA: N_{ω}-nitro-L-Arginine. Data are mean ± S.E.M.; *P≤0.05 vs rest; †P≤0.05 vs corresponding control experiment, ‡P≤0.05 vs corresponding normal swine.

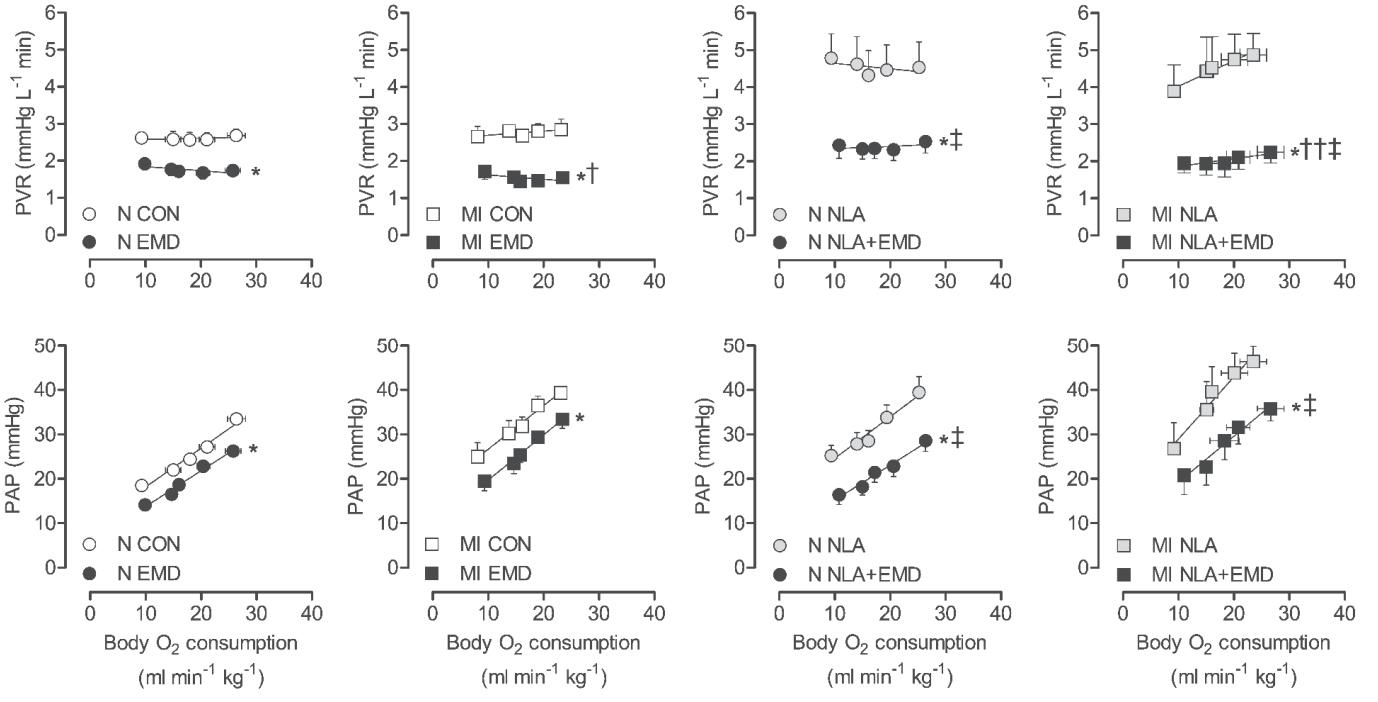

Figure 1: Effect of PDE5-inhibition on pulmonary vascular resistance and pulmonary arterial pressure in normal and MI swine. Shown are the effects of the PDE5-inhibitor EMD alone and after prior administration of the NOS-inhibitor NLA in normal swine (circles) and MI swine (squares) on pulmonary vascular resistance (PVR; upper panels) and pulmonary arterial pressure (PAP; lower panels) as a function of body O_2 consumption. Control exercise results are shown as open symbols, exercise results in the presence of antagonists are shown as solid symbols. *P≤0.05 effect of EMD vs corresponding Control, † P≤0.05 †† P≤0.1 different effect of EMD in MI vs N, ‡P≤0.05 different effect of NLA+EMD vs EMD alone. Normal CON - EMD: n=12 (n=10 for PVR), MI CON - EMD: n=5, Normal NLA - NLA+EMD: n=10 (n=8 for PVR), MI NLA - NLA+EMD n=5

Effects of PDE5-inhibition

In accordance with a previous study from our laboratory (19), administration of the PDE5-inhibitor EMD produced vasodilation in the systemic bed of both normal (n=12) and MI swine (n=5; Table 2), reflected by a decrease in SVR (Table 3) and an increase in mixed venous oxygen content (Table 4) at rest. Systemic vasodilation was maintained during exercise in normal swine and slightly waned in MI swine (Table 2) and was accompanied by a decrease in oxygen extraction (Table 4). Interestingly, the increase in CO was larger in MI than in normal animals (Table 2) mainly because stroke volume in the MI group increased in response to PDE5-inhibition whereas it tended to decrease in the normal group (Fig 2). PAP and PVR decreased after administration of the PDE5-inhibitor EMD, indicating vasodilation of the pulmonary vascular bed (Table 3; Fig. 1). The overall change in PVR was larger in MI swine than in normal swine ($P \leq 0.01$ by ANOVA). During exercise the vasodilator effect of EMD on the pulmonary vasculature increased in both normal and MI swine (both $P \leq 0.05$; Fig. 1). There was a strong correlation between left atrial pressure and effect of PDE5-inhibition on PVR in normal ($r^2=0.89$; $P \leq 0.05$) and MI ($r^2=0.72$; $P \leq 0.1$) swine (Fig 3), so that a higher LAP was associated with a greater decrease in PVR.

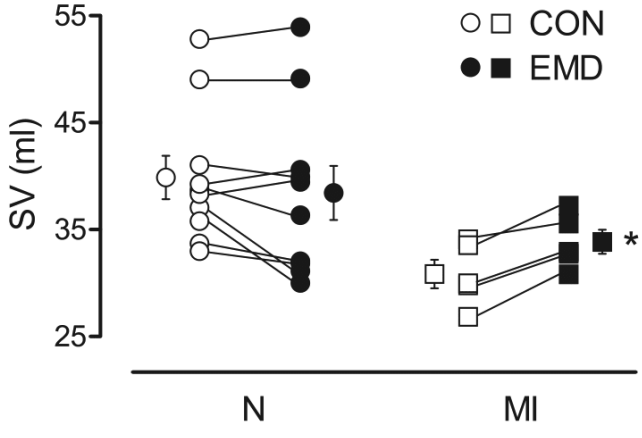

Figure 2. Effect of PDE5-inhibition on stroke volume. Shown are the effects of PDE5-inhibitor EMD on stroke volume in resting normal swine (N) and swine with a recent myocardial infarction (MI), plotted as individual data and means±SE before (open symbols) and in the presence of (solid symbols) PDE5-inhibition. *P≤0.05 effect EMD

Effects of combined NLA and EMD during exercise

Administration of the NOS-inhibitor NLA resulted in a marked increase in aortic blood pressure, caused by systemic vasoconstriction in both normal (n=10) and MI swine (n=5; Table 2). This vasoconstriction was maintained during exercise. In the pulmonary circulation, NOS-inhibition also resulted in marked vasoconstriction, reflected by an increase in PVR, which during exercise was maintained in normal swine and even increased in MI swine (Fig. 1).

Following NOS-inhibition by NLA, administration of the PDE5-inhibitor EMD produced an increase in CO and a decrease in mean aortic pressure in both normal and MI swine, implying a decrease in SVR at rest, that slightly waned during exercise (Table 2). Inhibition of PDE5 also caused vasodilation of the pulmonary vascular bed, demonstrated by a decrease in PVR at rest, as well as during exercise in both normal and MI swine (Table 3, Fig. 1). Strikingly, in both experimental groups, the effect of PDE5-inhibition after inhibition of NOS was larger than the effect of PDE5-inhibition under control conditions ($P \leq 0.01$ By ANCOVA; Fig. 1), indicating that despite the loss of NOS-activity, the availability of, or sensitivity to, cGMP was increased. The change in PVR upon PDE5-inhibition after prior NLA administration was larger in MI compared to normal swine ($P \leq 0.01$ by ANCOVA; Fig. 1), which correlated with the higher levels of LAP after NLA in MI compared to normal swine (Fig 3).

Table 3 Pulmonary hemodynamics of swine at rest and during exercise before and after administration of EMD and NLA

					Exercise level (km h^{-1})							
	n	Treatment	MI	Rest	1		2		3		4	
LAP	12	Control	-	5 ± 1	6 ± 1		7 ± 1	*	9 ± 1	*	11 ± 1	*
(mmHg)		EMD	-	3 ± 1	5 ± 1		6 ± 1	*	9 ± 1	*	11 ± 1	*
	5	Control	+	12 ± 3 ‡	15 ± 3	‡	16 ± 3	*‡	18 ± 3	*‡	19 ± 2	*‡
		EMD	+	10 ± 2 ‡	13 ± 2	*‡	16 ± 2	*‡	19 ± 2	*‡	21 ± 3	*‡
	10	NLA	-	6 ± 1	7 ± 1		8 ± 1		10 ± 1	*	10 ± 1	*
		NLA+EMD	-	5 ± 2	7 ± 2		8 ± 2		8 ± 2	*	10 ± 2	*
	5	NLA	+	11 ± 3	14 ± 3	‡	16 ± 2	‡	16 ± 2	‡	16 ± 2	‡
		NLA+EMD	+	10 ± 3	12 ± 3		15 ± 2	‡	17 ± 2	*‡	19 ± 2	‡
PAP	12	Control	-	18 ± 1	22 ± 1	*	24 ± 1	*	27 ± 1	*	34 ± 1	*
(mmHg)		EMD	-	14 ± 1 †	17 ± 1	†	19 ± 1	*†	23 ± 1	*†	26 ± 1	*†
	5	Control	+	25 ± 3 ‡	30 ± 3	‡	32 ± 2	‡	37 ± 2	*‡	39 ± 2	*‡
		EMD	+	20 ± 2 †‡	23 ± 2	*†‡	25 ± 2	*†‡	29 ± 1	*†‡	33 ± 2	*†‡
	10	NLA	-	25 ± 2	28 ± 3		29 ± 2		34 ± 3	*	39 ± 4	*
		NLA+EMD	-	16 ± 2 †	18 ± 2	†	21 ± 2	*†	23 ± 2	*†	29 ± 2	*†
	5	NLA	+	27 ± 6	36 ± 6		39 ± 6		44 ± 4	*	46 ± 3	*
		NLA+EMD	+	21 ± 4	23 ± 4		28 ± 4		32 ± 4	*†	36 ± 3	*†
TPG	12	Control	-	14 ± 1	16 ± 1	*	17 ± 1	*	19 ± 1	*	22 ± 1	*
(mmHg)		EMD	-	11 ± 1 †	12 ± 1	†	12 ± 1	†	14 ± 1	*†	15 ± 1	*†
	5	Control	+	13 ± 2	16 ± 1		16 ± 1		18 ± 1	*	20 ± 2	*
		EMD	+	10 ± 2	10 ± 1	†	10 ± 1	†	11 ± 1	†	12 ± 1	*†
	10	NLA	-	20 ± 2	22 ± 2		22 ± 2		25 ± 2	*	31 ± 3	*
		NLA+EMD	-	12 ± 1 †	13 ± 1	†	15 ± 1	†	16 ± 1	*†	20 ± 2	*†
	5	NLA	+	16 ± 3	22 ± 4		24 ± 4		27 ± 4	*	30 ± 4	*
		NLA+EMD	+	11 ± 2	11 ± 2	†	13 ± 3		15 ± 2	*†	17 ± 2	*†
PVR	10	Control	-	2.6 ± 0.2	2.6 ± 0.2		2.6 ± 0.2		2.6 ± 0.2		2.7 ± 0.2	
(mmHg		EMD	-	1.9 ± 0.2 †	1.8 ± 0.2	†	1.7 ± 0.2	†	1.7 ± 0.2	†	1.7 ± 0.2	†
L min^{-1})	5	Control	+	2.7 ± 0.3	2.8 ± 0.1		2.7 ± 0.2		2.8 ± 0.2		2.8 ± 0.3	
		EMD	+	1.7 ± 0.2 †	1.6 ± 0.1	†	1.4 ± 0.2	*†	1.5 ± 0.1	*†	1.6 ± 0.1	†
	8	NLA	-	4.8 ± 0.7	4.6 ± 0.7		4.3 ± 0.7		4.5 ± 0.7		4.5 ± 0.7	
		NLA+EMD	-	2.4 ± 0.4 †	2.3 ± 0.3	†	2.3 ± 0.3	†	2.3 ± 0.3	†	2.5 ± 0.3	†
	5	NLA	+	3.9 ± 0.7	4.4 ± 0.9		4.6 ± 0.9		4.8 ± 0.7		4.9 ± 0.6	
		NLA+EMD	+	1.9 ± 0.3	1.9 ± 0.3	†	1.9 ± 0.4	†	2.1 ± 0.3	*†	2.2 ± 0.3	*†

LAP: mean Left Atrial Pressure, PAP: mean Pulmonary Arterial Pressure TPG: Trans-pulmonary Pressure Gradient (PAP-LAP), PVR: Pulmonary Vascular Resistance ((PAP-LAP)/CO), EMD: EMD360527, NLA: N_{ω}-nitro-L-Arginine. Data are mean ± S.E.M.; *P≤0.05 vs rest; †P≤0.05 vs corresponding control experiment, ‡P≤0.05 vs corresponding normal swine.

Table 4 Oximetry of swine at rest and during exercise before and after administration of EMD and NLA

					Exercise level (km h^{-1})			
	n	Treatment	MI	Rest	1	2	3	4
CaO_2	12	Control	-	10.2 ± 0.4	10.6 ± 0.4	11.4 ± 0.3 *	11.5 ± 0.3 *	11.7 ± 0.2 *
(vol%)		EMD	-	10.7 ± 0.3	11.0 ± 0.2	11.1 ± 0.2	11.1 ± 0.2 †	11.3 ± 0.2 †
	5	Control	+	9.9 ± 0.6	10.7 ± 0.5 *	10.9 ± 0.5 *	11.1 ± 0.3 *	11.1 ± 0.3 *
		EMD	+	10.1 ± 0.5	10.5 ± 0.3	10.3 ± 0.2 ‡	10.5 ± 0.2 †	10.4 ± 0.2 †‡
	10	NLA	-	10.5 ± 0.4	11.3 ± 0.4 *	11.5 ± 0.4 *	11.9 ± 0.4 *	12.3 ± 0.3 *
		NLA+EMD	-	10.7 ± 0.4	11.5 ± 0.4	11.4 ± 0.4	11.7 ± 0.4 *	12.1 ± 0.3 *
	5	NLA	+	10.8 ± 0.5	11.8 ± 0.5	11.6 ± 0.5	12.2 ± 0.5	12.4 ± 0.5 *
		NLA+EMD	+	10.6 ± 0.5	10.9 ± 0.5	11.3 ± 0.5 *	11.4 ± 0.4 *†	12.0 ± 0.3 *†
CvO_2	12	Control	-	5.7 ± 0.3	4.4 ± 0.2 *	4.5 ± 0.2 *	4.1 ± 0.2 *	3.7 ± 0.2 *
(vol%)		EMD	-	6.3 ± 0.2 †	5.2 ± 0.2 *†	5.2 ± 0.3 *†	4.6 ± 0.3 *†	4.0 ± 0.2 *†
	5	Control	+	5.7 ± 0.4	4.6 ± 0.4 *	4.2 ± 0.3 *	3.9 ± 0.4 *	3.0 ± 0.5 *
		EMD	+	6.1 ± 0.4 †	4.8 ± 0.3 *	4.5 ± 0.4 *	4.0 ± 0.4 *	3.0 ± 0.5 *‡
	10	NLA	-	4.8 ± 0.4	4.0 ± 0.3 *	3.8 ± 0.3 *	3.6 ± 0.2 *	3.3 ± 0.3 *
		NLA+EMD	-	5.3 ± 0.6	4.6 ± 0.4 *	4.2 ± 0.4 *	4.0 ± 0.4 *	3.7 ± 0.3 *
	5	NLA	+	5.2 ± 0.3	4.1 ± 0.5	4.0 ± 0.5	3.6 ± 0.5 *	3.1 ± 0.5 *
		NLA+EMD	+	5.7 ± 0.4	4.4 ± 0.5 *	4.5 ± 0.6 *	3.9 ± 0.6 *	3.7 ± 0.6 *
a-vO_2	12	Control	-	4.5 ± 0.2	6.2 ± 0.3 *	6.9 ± 0.2 *	7.4 ± 0.3 *	8.1 ± 0.2 *
(vol%)		EMD	-	4.3 ± 0.2	5.8 ± 0.1 *	5.9 ± 0.2 *†	6.4 ± 0.2 *†	7.3 ± 0.2 *†
	5	Control	+	4.1 ± 0.3	6.1 ± 0.1 *	6.7 ± 0.2 *	7.2 ± 0.3 *	8.1 ± 0.3 *
		EMD	+	4.0 ± 0.2	5.7 ± 0.3 *	5.8 ± 0.2 *†	6.5 ± 0.2 *†	7.3 ± 0.4 *†
	10	NLA	-	5.7 ± 0.3	7.3 ± 0.3 *	7.7 ± 0.3 *	8.3 ± 0.3 *	9.0 ± 0.2 *
		NLA+EMD	-	5.3 ± 0.3	6.9 ± 0.2 *	7.2 ± 0.2 *	7.7 ± 0.2 *	8.3 ± 0.2 *†
	5	NLA	+	5.6 ± 0.2	7.7 ± 0.2 *	7.6 ± 0.1 *	8.6 ± 0.2 *	9.4 ± 0.3 *
		NLA+EMD	+	4.9 ± 0.2 †	6.6 ± 0.2 *	6.9 ± 0.1 *†	7.5 ± 0.3 *	8.3 ± 0.4 *†
BVO_2	10	Control	-	9.3 ± 0.6	15.0 ± 1.4 *	18.0 ± 1.0 *	21.1 ± 1.4 *	26.4 ± 1.6 *
($ml\ min^{-1}\ kg^{-1}$)		EMD	-	9.9 ± 0.6	14.7 ± 0.7 *	16.0 ± 0.7 *†	20.4 ± 1.2 *	25.8 ± 1.4 *
	5	Control	+	8.1 ± 0.8	13.8 ± 0.6 *	16.1 ± 0.9 *	19.0 ± 0.8 *	23.1 ± 0.5 *
		EMD	+	9.3 ± 0.5	14.7 ± 0.6 *	15.8 ± 0.4 *	19.0 ± 0.6 *	23.4 ± 0.6 *
	8	NLA	-	9.4 ± 0.4	14.0 ± 0.9 *	16.1 ± 1.0 *	19.4 ± 0.9 *	25.2 ± 0.9 *
		NLA+EMD	-	10.8 ± 1.0	15.0 ± 0.8 *	17.2 ± 0.9 *	20.6 ± 0.8 *	26.4 ± 1.0 *
	5	NLA	+	9.2 ± 1.0	15.1 ± 1.2 *	16.0 ± 1.1 *	20.1 ± 2.4 *	23.5 ± 2.4 *
		NLA+EMD	+	11.0 ± 1.0 †	15.0 ± 0.6 *	18.3 ± 2.6 *	20.8 ± 2.1 *	26.6 ± 2.4 *
Hb	12	Control	-	7.6 ± 0.3	8.0 ± 0.3	8.6 ± 0.2 *	8.7 ± 0.2 *	8.8 ± 0.2 *
(g/dl^{-1})		EMD	-	8.0 ± 0.2	8.3 ± 0.2	8.4 ± 0.2	8.4 ± 0.2 †	8.6 ± 0.2 *†
	5	Control	+	7.5 ± 0.4	8.2 ± 0.3	8.4 ± 0.2 *	8.7 ± 0.1 *	8.6 ± 0.1 *
		EMD	+	7.8 ± 0.3	8.2 ± 0.2	8.1 ± 0.2	8.2 ± 0.1 †	8.4 ± 0.1
	10	NLA	-	7.7 ± 0.3	8.3 ± 0.3 *	8.4 ± 0.3 *	8.8 ± 0.3 *	9.2 ± 0.2 *
		NLA+EMD	-	7.8 ± 0.3	8.5 ± 0.3 *	8.4 ± 0.3 *	8.7 ± 0.3 *	9.0 ± 0.3 *
	5	NLA	+	7.9 ± 0.3	8.8 ± 0.2	8.7 ± 0.2	9.1 ± 0.3	9.3 ± 0.3 *
		NLA+EMD	+	7.9 ± 0.3	8.2 ± 0.3	8.5 ± 0.3	8.6 ± 0.2 *†	8.9 ± 0.2 *†

CaO_2: Arterial O_2 content, CvO_2: Venous O_2 content, a-vO_2:Arteriovenous O_2 difference, BVO_2: Body O_2 consumption, Hb: Hemoglobin, EMD: EMD360527, NLA: N_ω-nitro-L-Arginine. Data are mean ± S.E.M.; *P≤0.05 vs rest; †P≤0.05 vs corresponding control experiment, ‡P≤0.05 vs corresponding normal swine.

DISCUSSION

The main findings of the present study are that *(i)* PDE5-inhibition results in vasodilation in the pulmonary circulation of normal swine and swine with a recent MI, both at rest and during exercise; *(ii)* The pulmonary vasodilation produced by PDE5-inhibition was slightly larger in MI compared to normal swine, and *(iii)* in both normal and MI swine, the effect of PDE5-inhibition was similarly enhanced after prior inhibition of NOS, preserving the larger effect of PDE5-inhibition in MI swine.

The cGMP/PDE5-pathway in pulmonary hypertension

In the present study we found that vasodilation by PDE5-inhibition in swine with early PH secondary to MI was not only well maintained, but was even slightly more pronounced than in normal swine, particularly during exercise, indicating that either cGMP-levels were higher or that PDE5-activity was increased. Elevated levels of cGMP could have resulted from increased NOS-activity, as has been reported in early stages of PH (11,12), which is the stage that our porcine post-MI model of early PH likely represents. In this porcine model, we have previously shown that the pulmonary vasodilator influence of NO is maintained (13), although it cannot be excluded that increased NOS-activity in that study was accompanied by a similar increase in PDE5-activity. Indeed, several studies in animal models demonstrated that cGMP and PDE5-activity are increased and hence that the NO-cGMP pathway is altered in PH (32-35). Two of these studies showed that the net result of these alterations in the NO-pathway are elevated levels of cGMP (33,34). However, in the present study, inhibition of PDE5, in the presence of NOS-inhibition, still produced a greater decrease in PVR in MI compared to normal swine. The observation that the increased vasodilator response to PDE5-inhibition in PH was not attenuated after inhibition of NO-synthase, suggests that this increased response was NO-independent.

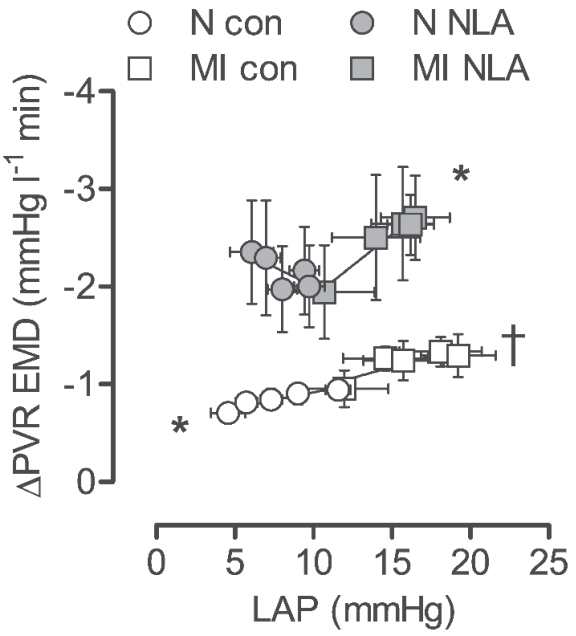

Figure 3. Correlation between change in PVR and LAP. Shown are the changes in PVR produced by inhibition of PDE5 with EMD plotted as a function of left atrial pressure without NOS-inhibition in normal swine (N; white circles; r^2=0.89; P≤0.05) and swine with myocardial infarction (MI; white squares; r^2=0.72; P≤0.1), and after NOS-inhibition with NLA (N; grey circles r^2=0.54; P=0.16 and MI; grey squares; r^2=0.96; P≤0.01). *P≤0.05; †P≤0.1 slope≠0. N CON: n=12, MI CON n=5, N NLA: n=10, MI NLA: n=5. Values are means±SE.

cGMP can also be produced through activation of particulate GC, for example by natriuretic peptides such as ANP. ANP is stored within atrial secretory granules and is released in response to increased wall stress or pressure (36). In the present study the effect of PDE5-inhibition increased during exercise, when LAP increased as well. Indeed, there was a correlation between LAP and the change in PVR as a result of PDE5-inhibition in both normal and MI swine (Fig. 3), consistent with the concept that ANP-signaling via particulate GC could have contributed to cGMP-production. In PH secondary to MI atrial pressures are increased and can thereby contribute to elevated levels of ANP that are found in patients with PH (37). In accordance with these findings, we have previously shown that ANP levels are elevated in our model of early PH (23,24). To further elucidate the potential involvement of ANP we plotted ANP levels as a function of LAP, obtained in those studies (Fig 4), and observed a strong correlation between LAP and ANP in normal (r^2=0.90; P=0.05) and especially in MI swine MI (r^2=0.93; P≤0.05). The increased vasodilator effect on PDE5-inhibition in MI swine in the present study could thus have been the result of these elevated levels of

ANP. Future studies with an ANP receptor antagonist (38-42) are needed to test this hypothesis.

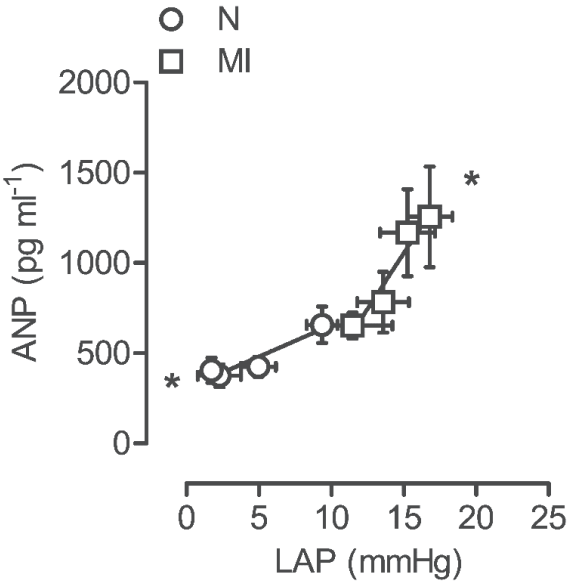

Figure 4. Historical data: Correlation between ANP plasma levels and LAP. Historical data from our lab (24) showing the correlation between left atrial pressure and arterial plasma levels of ANP in normal swine (N; circles; r^2=0.90; P≤0.05) and swine with a recent myocardial infarction (MI; squares r^2=0.93; P≤0.05) swine, at rest and during incremental exercise under control conditions. *P≤0.05 slope≠0. N: n=8, MI: n=9. Values are means±SE.

Clinical relevance

Employment of PDE5-inhibition for the alleviation of pulmonary haemodynamics could be applicable to both early PH after MI, when NO-production is maintained and ANP is upregulated, as well as in later stages of PH with chronic HF, when NO-production is reduced, but natriuretic peptide levels are further increased. In chronic HF, natriuretic peptide levels in plasma are increased, but do not translate into increased cGMP (43). While the reduced ratio of plasma cGMP to plasma natriuretic peptides can be explained, at least in part, by reduced natriuretic peptide receptor expression (44,45), it may also be caused by impaired downstream signalling due to increased PDE5-activity. Thus, Forfia et al. (46) demonstrated that acute PDE5-inhibition in dogs with tachypacing-induced HF restored the ratio of plasma cGMP to plasma natriuretic peptides. The haemodynamic response to PDE5-inhibition was similar to the responses to exogenous natriuretic peptides (46).

PDE5-inhibitors are already widely used to reduce PVR and PAP and thereby alleviate the workload of the right ventricle in patients with PAH. While many PAH-therapies

have proven ineffective (47-49) or even detrimental (50,51) for other forms of PH, recent trials showed decreased PAP, pulmonary capillary wedge pressure and improved function of the right ventricle and the pulmonary vasculature with PDE5-inhibition in PH due to systolic left HF (52,53). Moreover, whereas other PAH-therapies have been associated with increased LV filling pressures, leading to acute pulmonary edema in PH secondary to left HF (8,54), Guazzi et al. showed that PDE5-inhibition not only improved pulmonary and right ventricular function, but also left ventricular function (55). This crucial feature prevents pulmonary edema and makes this vasodilator therapy particularly suited for treatment of PH due to left HF. Interestingly, in our MI swine PDE5-inhibition not only decreased PVR, but also improved cardiac function, indicated by an increased stroke volume. Whether this was mediated by improved left and/or right ventricular function remains to be determined although consistent with previous studies (28), we observed no significant changes in left ventricular contraction or relaxation rate (not shown) and no change in left ventricular filling pressure upon PDE5-inhibition (Table 3).

The present study indicates that not only patients with overt left HF, but also subjects with early PH secondary to MI could benefit from the pulmonary vasodilator capacity of PDE5-inhibition. Moreover, this vasodilator effect is enhanced after MI in comparison with normal healthy conditions, probably as a result of increased cGMP availability that appeared to be independent of NO-signaling. Importantly, these findings suggest that when patients develop endothelial dysfunction and exhibit decreased NOS-activity as a result of aggravation of PH, inhibition of PDE5 can still result in pulmonary vasodilation and decrease PAP and PVR.

Patients with PH have a decreased exercise capacity because of an increase in right-ventricular afterload. Indeed, Franciosa et al (56) proposed that it is the inability of the right ventricle to overcome the increase in afterload that limits the exercise capacity in patients with left ventricular failure, a concept that was recently confirmed by Kim et al (57). The present study was not designed to test whether PDE5 inhibition was capable of increasing exercise capacity, as true maximal exercise in swine can only be obtained using adverse conditioning. However, comparison of our data (maximal BVO_2's of 26.4±1.6 and 23.1±0.5 ml min^{-1} kg^{-1} for N and MI swine, respectively (Table 4), and maximal heart rate of ~240 bpm for both groups) to

maximal exercise capacity in untrained swine as obtained by the groups of White (maximal BVO_2 of 49.2 ml min^{-1} $kg^{-1,}$ maximal heart rate of 272 bpm (58)) and extrapolated from Armstrong (maximal BVO_2 of 43.6 ml min^{-1} kg^{-1} (59)), suggest that the swine exercised at 60% of maximal BVO_2 and at 88% of maximal heart rate. The discrepancy between BVO_2 and heart rate appears to be due to the lower haemoglobin levels in our swine (8.8±0.2 g dl^{-1}, Table 4) as compared to those in previous studies (12.5±0.6 g dl^{-1} (59)). Importantly, even though swine exercised at sub-maximal levels, the present study shows that not only the decreases in PAP and PVR but also the increase in stroke volume following PDE5-inhibition are maintained during exercise, suggesting that this therapy may improve exercise capacity in patients with PH secondary to MI. In support of this concept, Lewis et al. performed a small trial with long-term treatment of oral PDE5-inhibition in HF with PH, and reported an increased exercise capacity with no adverse effects (60). Moreover, recent meta-analyses showed that PDE5 inhibition indeed improves exercise capacity in patients with HF with reduced, but not with preserved ejection fraction.(61-63)

CONCLUSIONS

PDE5-inhibition results in vasodilation of the pulmonary vascular bed of normal swine and MI swine, both at rest and during exercise. After MI, PDE5-inhibition produced pulmonary vasodilation that was not only maintained but even slightly greater compared to normal swine. Moreover, in both normal and MI swine, inhibition of NOS similarly enhanced the effect of subsequent PDE5-inhibition, indicating that this increased response in MI swine was not NO-mediated. These observations suggest that PDE5-inhibition holds promise as a pharmacotherapeutic strategy to normalize pulmonary haemodynamics in post-capillary PH following a recent MI, in order to prevent progressive pre- and post-capillary PH.

REFERENCES

1. Guazzi M, Galie N. Pulmonary hypertension in left heart disease. Eur Respir Rev 2012;21:338-46.
2. Guazzi M, Borlaug BA. Pulmonary hypertension due to left heart disease. Circulation 2012;126:975-90.
3. Rosenkranz S, Gibbs JS, Wachter R, De Marco T, Vonk-Noordegraaf A, Vachiery JL. Left ventricular heart failure and pulmonary hypertension. Eur Heart J 2016;37:942-54.
4. Vanderpool RR, Naeije R. Progress in Pulmonary Hypertension with Left Heart Failure. Beyond New Definitions and Acronyms. Am J Respir Crit Care Med 2015;192:1152-4.
5. Gerges M, Gerges C, Pistritto AM et al. Pulmonary Hypertension in Heart Failure. Epidemiology, Right Ventricular Function, and Survival. Am J Respir Crit Care Med 2015;192:1234-46.
6. Miller WL, Grill DE, Borlaug BA. Clinical features, hemodynamics, and outcomes of pulmonary hypertension due to chronic heart failure with reduced ejection fraction: pulmonary hypertension and heart failure. JACC Heart Fail 2013;1:290-299.
7. Budhiraja R, Tuder RM, Hassoun PM. Endothelial dysfunction in pulmonary hypertension. Circulation 2004;109:159-65.
8. Moraes DL, Colucci WS, Givertz MM. Secondary pulmonary hypertension in chronic heart failure: the role of the endothelium in pathophysiology and management. Circulation 2000;102:1718-23.
9. Tuder R CC, Geraci M, et al. Prostacyclin synthase expression is decreased in lungs from patients with severe pulmonary hypertension. Am J Resp Crit Care Med 1999;159:1925-32.
10. Black SM, Fineman JR, Steinhorn RH, Bristow J, Soifer SJ. Increased endothelial NOS in lambs with increased pulmonary blood flow and pulmonary hypertension. Am J Physiol Heart Circ Physiol 1998;275:H1643-1651.
11. Archer S, Rich S. Primary Pulmonary Hypertension : A Vascular Biology and Translational Research "Work in Progress". Circulation 2000;102:2781-2791.
12. Hampl V, Herget J. Role of nitric oxide in the pathogenesis of chronic pulmonary hypertension. Physiological reviews 2000;80:1337-72.
13. Haitsma DB, Merkus D, Vermeulen J, Verdouw PD, Duncker DJ. Nitric oxide production is maintained in exercising swine with chronic left ventricular dysfunction. Am J Physiol Heart Circ Physiol 2002;282:H2198-209.
14. Houweling B, Merkus D, Sorop O, Boomsma F, Duncker DJ. Role of endothelin receptor activation in secondary pulmonary hypertension in awake swine after myocardial infarction. J Physiol 2006;574:615-26.
15. Rybalkin SD, Yan C, Bornfeldt KE, Beavo JA. Cyclic GMP phosphodiesterases and regulation of smooth muscle function. Circ Res 2003;93:280-91.
16. Galie N, Ghofrani HA, Torbicki A et al. Sildenafil Citrate Therapy for Pulmonary Arterial Hypertension 10.1056/NEJMoa050010. N Engl J Med 2005;353:2148-2157.

17. Oudiz RJ, Brundage BH, Galie N et al. Tadalafil for the treatment of pulmonary arterial hypertension: a double-blind 52-week uncontrolled extension study. J Am Coll Cardiol 2012;60:768-74.
18. Galie N, Brundage BH, Ghofrani HA et al. Tadalafil therapy for pulmonary arterial hypertension. Circulation 2009;119:2894-903.
19. Houweling B, Quispel J, Beier N, Verdouw PD, Duncker DJ, Merkus D. Endothelial dysfunction enhances the pulmonary and systemic vasodilator effects of phosphodiesterase-5 inhibition in awake swine at rest and during treadmill exercise. Experimental biology and medicine (Maywood, NJ 2012;237:201-10.
20. Levin ER, Gardner DG, Samson WK. Natriuretic peptides. N Engl J Med 1998;339:321-8.
21. Yap LB, Ashrafian H, Mukerjee D, Coghlan JG, Timms PM. The natriuretic peptides and their role in disorders of right heart dysfunction and pulmonary hypertension. Clin Biochem 2004;37:847-56.
22. Silver MA. The natriuretic peptide system: kidney and cardiovascular effects. Curr Opin Nephrol Hypertens 2006;15:14-21.
23. van Kats JP, Duncker DJ, Haitsma DB et al. Angiotensin-converting enzyme inhibition and angiotensin II type 1 receptor blockade prevent cardiac remodeling in pigs after myocardial infarction: role of tissue angiotensin II. Circulation 2000;102:1556-63.
24. Haitsma DB, Bac D, Raja N, Boomsma F, Verdouw PD, Duncker DJ. Minimal impairment of myocardial blood flow responses to exercise in the remodeled left ventricle early after myocardial infarction, despite significant hemodynamic and neurohumoral alterations. Cardiovasc Res 2001;52:417-28.
25. De Wijs-Meijler DP, Stam K, van Duin RW et al. Surgical Placement of Catheters for Long-term Cardiovascular Exercise Testing in Swine. J Vis Exp 2016:e53772.
26. Duncker DJ, Klassen CL, Ishibashi Y, Herrlinger SH, Pavek TJ, Bache RJ. Effect of temperature on myocardial infarction in swine. Am J Physiol 1996;270:H1189-99.
27. van der Velden J, Merkus D, Klarenbeek BR et al. Alterations in myofilament function contribute to left ventricular dysfunction in pigs early after myocardial infarction. Circ Res 2004;95:e85-95.
28. Merkus D, Visser M, Houweling B, Zhou Z, Nelson J, Duncker DJ. Phosphodiesterase 5 inhibition-induced coronary vasodilation is reduced after myocardial infarction. Am J Physiol Heart Circ Physiol 2013;304:H1370-81.
29. van der Velden J, Merkus D, de Beer V et al. Transmural heterogeneity of myofilament function and sarcomeric protein phosphorylation in remodeled myocardium of pigs with a recent myocardial infarction. Front Physiol 2011;2:83.
30. Duncker DJ, de Beer VJ, Merkus D. Alterations in vasomotor control of coronary resistance vessels in remodelled myocardium of swine with a recent myocardial infarction. Med Biol Eng Comput 2008;46:485-97.
31. Duncker DJ, Stubenitsky R, Tonino PA, Verdouw PD. Nitric oxide contributes to the regulation of vasomotor tone but does not modulate O(2)-consumption in exercising swine. Cardiovasc Res 2000;47:738-48.

32. Hanson KA, Ziegler JW, Rybalkin SD, Miller JW, Abman SH, Clarke WR. Chronic pulmonary hypertension increases fetal lung cGMP phosphodiesterase activity. Am J Physiol Lung Cell Mol Physiol 1998;275:L931-941.

33. Cohen AH, Hanson K, Morris K et al. Inhibition of cyclic 3'-5'-guanosine monophosphate-specific phosphodiesterase selectively vasodilates the pulmonary circulation in chronically hypoxic rats. J Clin Invest 1996;97:172-9.

34. Black SM, Sanchez LS, Mata-Greenwood E, Bekker JM, Steinhorn RH, Fineman JR. sGC and PDE5 are elevated in lambs with increased pulmonary blood flow and pulmonary hypertension. Am J Physiol Lung Cell Mol Physiol 2001;281:L1051-1057.

35. Li D, Zhou N, Johns RA. Soluble guanylate cyclase gene expression and localization in rat lung after exposure to hypoxia. Am J Physiol 1999;277:L841-7.

36. de Bold AJ, Ma KK, Zhang Y, de Bold ML, Bensimon M, Khoshbaten A. The physiological and pathophysiological modulation of the endocrine function of the heart. Can J Physiol Pharmacol 2001;79:705-14.

37. Nootens M, Kaufmann E, Rector T et al. Neurohormonal activation in patients with right ventricular failure from pulmonary hypertension: relation to hemodynamic variables and endothelin levels. J Am Coll Cardiol 1995;26:1581-5.

38. Delporte C, Winand J, Poloczek P, Von Geldern T, Christophe J. Discovery of a potent atrial natriuretic peptide antagonist for ANPA receptors in the human neuroblastoma NB-OK-1 cell line. Eur J Pharmacol 1992;224:183-8.

39. Poirier H, Labrecque J, Deschenes J, DeLean A. Allotopic antagonism of the non-peptide atrial natriuretic peptide (ANP) antagonist HS-142-1 on natriuretic peptide receptor NPR-A. Biochem J 2002;362:231-7.

40. Zhang PL, Jimenez W, Mackenzie HS et al. HS-142-1, a potent antagonist of natriuretic peptides in vitro and in vivo. J Am Soc Nephrol 1994;5:1099-105.

41. Toki S, Morishita Y, Sano T, Matsuda Y. HS-142-1, a novel non-peptide ANP antagonist, blocks the cyclic GMP production elicited by natriuretic peptides in PC12 and NG108-15 cells. Neurosci Lett 1992;135:117-20.

42. Norling LL, von Geldern T, Chevalier RL. Maturation of A71915-dependent inhibition of atrial natriuretic peptide-stimulated cyclic GMP production in isolated rat glomeruli. Biol Neonate 1994;66:294-301.

43. Diez J. Chronic heart failure as a state of reduced effectiveness of the natriuretic peptide system: implications for therapy. Eur J Heart Fail 2017;19:167-176.

44. Singh G, Kuc RE, Maguire JJ, Fidock M, Davenport AP. Novel snake venom ligand dendroaspis natriuretic peptide is selective for natriuretic peptide receptor-A in human heart: downregulation of natriuretic peptide receptor-A in heart failure. Circ Res 2006;99:183-90.

45. Tsutamoto T, Kanamori T, Morigami N, Sugimoto Y, Yamaoka O, Kinoshita M. Possibility of downregulation of atrial natriuretic peptide receptor coupled to guanylate cyclase in peripheral vascular beds of patients with chronic severe heart failure. Circulation 1993;87:70-5.

46. Forfia PR, Lee M, Tunin RS, Mahmud M, Champion HC, Kass DA. Acute phosphodiesterase 5 inhibition mimics hemodynamic effects of B-type natriuretic peptide and potentiates B-

type natriuretic peptide effects in failing but not normal canine heart. J Am Coll Cardiol 2007;49:1079-88.

47. McMurray JJ, Teerlink JR, Cotter G et al. Effects of tezosentan on symptoms and clinical outcomes in patients with acute heart failure: the VERITAS randomized controlled trials. JAMA 2007;298:2009-19.
48. McLaughlin V, Channick RN, Ghofrani HA et al. Bosentan added to sildenafil therapy in patients with pulmonary arterial hypertension. Eur Respir J 2015;46:405-13.
49. Packer M, McMurray J, Massie BM et al. Clinical effects of endothelin receptor antagonism with bosentan in patients with severe chronic heart failure: results of a pilot study. J Card Fail 2005;11:12-20.
50. Califf RM, Adams KF, McKenna WJ et al. A randomized controlled trial of epoprostenol therapy for severe congestive heart failure: The Flolan International Randomized Survival Trial (FIRST). Am Heart J 1997;134:44-54.
51. Gottlieb SS. The impact of finally publishing a negative study: new conclusions about endothelin antagonists. J Card Fail 2005;11:21-2.
52. Reichenbach A, Al-Hiti H, Malek I et al. The effects of phosphodiesterase 5 inhibition on hemodynamics, functional status and survival in advanced heart failure and pulmonary hypertension: a case-control study. Int J Cardiol 2013;168:60-5.
53. Guazzi M, Vicenzi M, Arena R, Guazzi MD. Pulmonary hypertension in heart failure with preserved ejection fraction: a target of phosphodiesterase-5 inhibition in a 1-year study. Circulation 2011;124:164-74.
54. Rich S, Rabinovitch M. Diagnosis and treatment of secondary (non-category 1) pulmonary hypertension. Circulation 2008;118:2190-9.
55. Guazzi M, Vicenzi M, Arena R, Guazzi MD. PDE5 inhibition with sildenafil improves left ventricular diastolic function, cardiac geometry, and clinical status in patients with stable systolic heart failure: results of a 1-year, prospective, randomized, placebo-controlled study. Circ Heart Fail 2011;4:8-17.
56. Franciosa JA, Baker BJ, Seth L. Pulmonary versus systemic hemodynamics in determining exercise capacity of patients with chronic left ventricular failure. Am Heart J 1985;110:807-13.
57. Kim J, Di Franco A, Seoane T et al. Right Ventricular Dysfunction Impairs Effort Tolerance Independent of Left Ventricular Function Among Patients Undergoing Exercise Stress Myocardial Perfusion Imaging. Circ Cardiovasc Imaging 2016;9.
58. White FC, McKirnan MD, Breisch EA, Guth BD, Liu YM, Bloor CM. Adaptation of the left ventricle to exercise-induced hypertrophy. J Appl Physiol (1985) 1987;62:1097-110.
59. Armstrong RB, Delp MD, Goljan EF, Laughlin MH. Distribution of blood flow in muscles of miniature swine during exercise. J Appl Physiol (1985) 1987;62:1285-98.
60. Lewis GD, Lachmann J, Camuso J et al. Sildenafil improves exercise hemodynamics and oxygen uptake in patients with systolic heart failure. Circulation 2007;115:59-66.
61. De Vecchis R, Cesaro A, Ariano C, Giasi A, Cioppa C. Phosphodiesterase-5 Inhibitors Improve Clinical Outcomes, Exercise Capacity and Pulmonary Hemodynamics in Patients With Heart Failure With Reduced Left Ventricular Ejection Fraction: A Meta-Analysis. J Clin Med Res 2017;9:488-498.

62. Jiang R, Wang L, Zhu CT et al. Comparative effectiveness of sildenafil for pulmonary hypertension due to left heart disease with HFrEF. Hypertens Res 2015;38:829-39.

63. Wu X, Yang T, Zhou Q, Li S, Huang L. Additional use of a phosphodiesterase 5 inhibitor in patients with pulmonary hypertension secondary to chronic systolic heart failure: a meta-analysis. Eur J Heart Fail 2014;16:444-53.

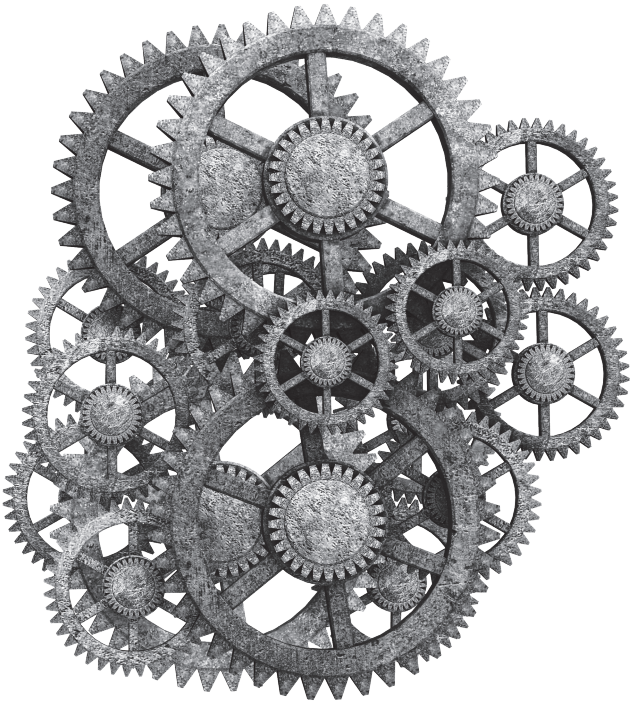

4

Chapter 4

Transition from post-capillary pulmonary hypertension to combined pre- and post-capillary pulmonary hypertension in swine: A key role for endothelin

Richard WB van Duin, Kelly Stam, Zongye Cai,
André Uitterdijk, Ana García Álvarez, Borja Ibanez,
AH Jan Danser, Irwin K Reiss, Dirk J Duncker, Daphne Merkus

•

THE JOURNAL OF PHYSIOLOGY. FEB 2019

ABSTRACT

Passive, isolated post-capillary pulmonary hypertension (IpcPH) secondary to left heart disease may progress to combined pre- and post-capillary or 'active' PH (CpcPH) characterized by chronic pulmonary vascular constriction and remodelling. The mechanisms underlying this 'activation' of passive PH remain incompletely understood. Here we investigate the role of the vasoconstrictor endothelin-1 (ET) in the progression from IpcPH to CpcPH in a swine model for post-capillary PH. Swine underwent pulmonary vein banding (PVB n=7) or sham-surgery (Sham n=6) and were chronically instrumented four weeks later. Haemodynamics were assessed for eight weeks, at rest and during exercise, before and after administration of ET receptor-antagonist tezosentan. After sacrifice, the pulmonary vasculature was investigated by histology, RT-qPCR and myograph experiments. Pulmonary arterial pressure and resistance increased significantly over time. mRNA-expression of prepro-endothelin-1 and endothelin converting enzyme-1 in the lung was increased, while ET_A-expression was unchanged, and ET_B-expression was downregulated. This was associated with increased plasma ET-levels from week 10 onward and a more pronounced vasodilation to in-vivo administration of tezosentan at rest and during exercise. Myograph experiments showed decreased endothelium-dependent vasodilation to Substance P and increased vasoconstriction to KCl in PVB swine consistent with increased muscularization observed with histology. Moreover, maximal vasoconstriction to ET was increased whereas ET-sensitivity was decreased. In conclusion, PVB swine gradually developed PH with structural and functional vascular remodelling. From week 10 onward, the pulmonary ET-pathway was upregulated, likely contributing to pre-capillary activation of the initially isolated post-capillary PH. Inhibition of the ET-pathway could thus potentially provide a pharmacotherapeutic target for early stage post-capillary PH.

INTRODUCTION

Pulmonary hypertension (PH) is a pathophysiological disorder that is defined by a mean pulmonary arterial pressure (mPAP) of >25 mmHg at rest (1). While PH has many different aetiologies, in 65 – 80% of all cases PH is due to left heart disease, i.e. WHO classification group II (1,2). In this group of PH, left heart failure (HF), valvular disease, inflow-/outflow-tract obstructions or congenital or acquired pulmonary vein stenosis cause an upstream pressure increase in the pulmonary vasculature. Initially, this isolated post-capillary PH (IpcPH) is purely passive, i.e. a direct consequence of the increased pulmonary venous pressure. However, when left untreated, IpcPH has the potential to progress to active, combined pre- and post-capillary PH (CpcPH), a chronic progressive disease characterized by marked pulmonary vasoconstriction and vascular remodelling (3-5) with a worse prognosis than IpcPH (6). While IpcPH can be treated by correcting only the underlying condition (1), CpcPH requires treatment of pulmonary vascular remodelling as well as the primary disease, as treatment of the primary disease alone is no longer able to arrest the progression of CpcPH (7). Hence, understanding the time course of the transition from IpcPH to CpcPH as well as its underlying mechanism is essential. IpcPH is defined as a mPAP of >25 mmHg, with a pulmonary capillary wedge pressure (PCWP) >15 mmHg and a diastolic pressure gradient (difference between diastolic PAP and PCWP) <7 mmHg and/or a pulmonary vascular resistance (PVR) ≤3 Wood units (WU), while CpcPH is defined as a diastolic pressure gradient of ≥7 mmHg and/or a PVR >3 WU (8). Discriminating IpcPH from CpcPH requires right heart catheterization to measure PCWP. Such an invasive procedure is not suitable for a longitudinal clinical study. In contrast, pre-clinical animal models for post-capillary PH are available but most haemodynamic data are acquired at only one or two time-points, often under anaesthesia (9-12). In PH, not only vasoconstriction, but potentially also vascular remodelling may be due to an imbalance between vasoconstrictors and vasodilators, which may involve downregulation of the nitric oxide- and prostacyclin-pathways, and upregulation of the endothelin (ET)-pathway (13,14). Although changes in these pathways have been well characterized in both experimental (12,15-18) as well as clinical studies of PH (19-23), the contribution of alterations in these pathways to the

transition from IpcPH to CpcPH remains incompletely understood. Here, we hypothesize that the transition from IpcPH to CpcPH is mediated, at least in part, by increased activity of the ET-pathway. To test this hypothesis, we investigated the progression of PH using chronically instrumented swine (24), in a recently developed swine model of group II PH by pulmonary vein banding (PVB) (10,11,25). Repeated measurements of pulmonary haemodynamics in awake swine were performed between 5-12 weeks after PVB, during the progression of PH while evaluating the activity of the ET-pathway. Since exercise testing allows detection of perturbations in cardiopulmonary function that may not be apparent under quiet resting conditions, and thus facilitates the assessment of disease severity (26), we performed measurements both at rest and during graded treadmill exercise.

METHODS

Ethical approval

Studies were performed in accordance with the "Guiding Principles in the Care and Use of Laboratory Animals" as approved by the Council of the American Physiological Society, and with approval of the Animal Care Committee of the Erasmus University Medical Centre (EMC3158, 109-13-09). The authors understand the ethical principles under which the Journal of Physiology operates and hereby declare that this work complies with the animal ethics checklist outlined by Grundy (27).

Sample size calculations

Experiments were designed to minimise the number of animals used. To calculate minimal sample size, a power analysis was performed using specialized software (G*Power 3.0) (28). Assuming a similar increase in PVR at 3 months post PVB as in a previous study (11), and a similar decrease in PVR after administration of tezosentan as reported previously (17), a two-tailed approach with assumed α-error probability of 0.5 and a power of 80% led to a sample size of n=5 per experimental group. Taken into consideration a drop-out of 25% as a result of (post-)surgical complications, and a 10% drop-out due to malfunction of the catheters, target group size was set to n=8. Thirteen animals completed the protocol and are included in the final analyses.

Study design

Fifteen crossbred Landrace x Yorkshire swine of either sex (9±1 kg) underwent non-restrictive inferior pulmonary vein banding (n=9) or sham operation (n=6). Four weeks later, all surviving 14 animals (22±1 kg) were chronically instrumented to enable weekly monitoring of haemodynamics and blood gases in animals in the awake state. In the following 8 weeks, animals performed bi-weekly exercise experiments under control conditions and after administration of an ET_A/ET_B-receptor antagonist. After 12 weeks, the surviving 13 animals (62±2 kg) were sacrificed and tissues were harvested.

Pulmonary vein banding

Swine underwent banding of the inferior venous confluence as described by Pereda et al. (11). Briefly, swine were sedated with an intramuscular (i.m.) injection of tiletamine/zolazepam (5 mg kg^{-1}, Virbac, Barneveld, The Netherlands), xylazine, (2.25 mg kg^{-1}, AST Pharma, Oudewater, The Netherlands) and atropine (1 mg), anaesthetised with intravenous (i.v.) bolus administration of thiopental (10 mg kg^{-1} Rotexmedica, Trittau, Germany), intubated and ventilated with a mixture of O_2 and N_2 (1:2) to which isoflurane (2% vol/vol Pharmachemie, Haarlem, the Netherlands) was added. Animals received antibiotic prophylaxis prior to the procedure (0.75 ml Depomycine, 200.000 IU ml^{-1} procainebenzylpenicilline, 200 mg ml^{-1} dihydrostreptomycine, Intervet Schering-Plough, Boxmeer, Netherlands). Under sterile conditions, the chest was opened via the fifth right intercostal space and the inferior venous confluence, draining both inferior pulmonary lobes, was exposed and separated from surrounding lung tissue using blunt dissection. A surgical loop (Braun Medical Inc., Bethlehem, PA, USA) was passed around the vein near the left atrium and secured at the resting diameter with a silk suture. The ribs were secured using non-absorbable USP6 braided polyester (Ø0.8 mm) and the wound was closed in layers using silk sutures. Anaesthesia was terminated and animals were extubated once spontaneous ventilation was restored. Animals received analgesia (0.3 mg buprenorphine i.m. Indivior, Slough, United Kingdom) and a fentanyl slow-release patch (6 µg h^{-1}, 48 hrs) and were transferred back to the animal facilities once awake. Six swine (8±1 kg) underwent a sham procedure, performed exactly as described above where the inferior venous confluence was exposed and dissected free, but not banded. In the PVB group, one animal died immediately after the banding procedure upon commencement of spontaneous breathing, due to acute pulmonary oedema. Taking humane endpoints into account, one animal was prematurely euthanized 6 weeks after banding due to severe HF. Data from these animals have been excluded from analysis. In the sham group, all animals survived until the end of follow up, resulting in group sizes of n=7 for PVB and n=6 for sham.

Chronic instrumentation

Four weeks after PVB or sham procedure, swine were anaesthetised and ventilated as described above and chronically instrumented as described previously (24). Briefly, under sterile conditions, the chest and pericardium were opened via the fourth left intercostal space and fluid-filled polyvinylchloride catheters (Braun Medical Inc., Bethlehem, PA, USA) were inserted into the aortic arch, the pulmonary artery, the right ventricle, and the left atrium for blood pressure measurement and blood sampling. A transit time flowprobe (Transonic Systems Inc., Ithaca, NY, USA) was positioned around the ascending aorta for measurement of cardiac output. Catheters were tunnelled to the back and the chest was closed. Animals were allowed to recover, receiving a single shot of buprenorphine i.m. (0.3 mg) and a fentanyl slow-release patch (12 μg h^{-1}, 48 hrs) for analgesia and antibiotic prophylaxis consisting of amoxicillin (25 mg kg^{-1} i.v. Centrafarm B.V. Etten-Leur, The Netherlands) and gentamycin (5 mg kg^{-1} i.v. Eurovet, Bladel, The Netherlands) for 7 consecutive days post-surgery. Once fully awake, animals were transferred back to the animal facilities.

Experimental protocols

Resting haemodynamic measurements were obtained each week, while exercise studies were performed 6, 8, 10 and 12 weeks following the PVB procedure. Swine were transferred to a customized, motor-driven treadmill and the fluid-filled catheters were connected to pressure transducers (Combitrans pressure transducers, Braun, Melsungen, Germany). Transducers and flowprobe were connected to amplifiers and haemodynamics were recorded at rest and during four-stage incremental treadmill exercise (1-4 km h^{-1}, 3 min per speed). Heart rate, cardiac output and left atrial, aortic, right ventricular and pulmonary arterial blood pressures were continuously recorded and blood samples were collected during the last 60 seconds of each 3 minutes exercise stage, at a time when haemodynamics had reached a steady state. After 60 minutes of rest, at a time when haemodynamics had returned to baseline, the ET_A/ET_B-receptor antagonist tezosentan (gift from Dr Clozel, Actelion Pharmaceuticals Ltd.) was administered by an infusion of 300 μg kg^{-1} min^{-1} i.v. After ten minutes of infusion the exercise protocol was repeated, with continuous infusion

of 100 μg kg^{-1} min^{-1} i.v. during the entire protocol. Due to recurrent crippleness, one PVB animal and one sham animal did not participate in all exercise experiments, reducing the number of animals to 5 in the sham group and 6 in the PVB group. Moreover, due to technical failure, flow probe data of one PVB animal were not available, reducing the number of animals to 5 for flow-related parameters (cardiac output, stroke volume, systemic and pulmonary vascular resistance, body oxygen consumption).

Blood Gas Measurements

Arterial and mixed venous blood samples were kept in iced syringes before being processed by a blood gas analyser (ABL 800, Radiometer, Denmark). Measurements included pO2 (mmHg), pCO2 (mmHg), oxygen saturation (%), lactate and haemoglobin (grams per decilitre). Body O2-consumption (BVO2) was calculated as the product of cardiac output and the difference in O2-content between arterial and mixed venous blood, where blood O2-content (μmol ml-1) was computed as (Hb·0.621·O2-saturation) + (0.00131·PO2) (29).

Data Analysis

Digital recording and off-line haemodynamic analyses were described previously (30). CO was corrected for bodyweight (cardiac index, CI). Total pulmonary vascular resistance index (tPVRi) and systemic vascular resistance index (SVRi) were calculated as mPAP/CI and mean arterial pressure MAP/CI respectively. Stroke volume index was computed as CI divided by heart rate and body oxygen consumption index (BVO_2i) as BVO_2 divided by bodyweight.

Sacrifice

Upon completion of follow up, i.e. 12 weeks after banding or sham surgery, animals were sedated with i.v. tiletamine/zolazepam (5 mg kg^{-1}), xylazine, (2.25 mg kg^{-1}) and atropine (1 mg) and anaesthetised with pentobarbital sodium (i.v. 6-12 mg kg^{-1} h^{-1}). An endotracheal tube was placed, and animals were ventilated with a mixture of O_2

and N_2 (1:2). Following sternotomy, the heart was arrested and immediately excised together with the lungs. Parts of the upper and lower lobe of the right lung were snap frozen in liquid nitrogen for molecular analyses, or processed for histology. Other parts of the upper and lower lobe were placed in cold Krebs buffer for dissection of pulmonary small arteries for wire-myograph experiments. The left and right ventricle of the heart were weighed separately to assess right ventricular hypertrophy.

Plasma ET measurements

Two-weekly blood samples were collected in EDTA-coated tubes, centrifuged for 10 minutes at 1460g and 4°C and plasma was subsequently aliquoted and cryopreserved at -80°C until analysis. For measurement of plasma ET-levels, an ET enzyme-linked immunosorbent assay (ELISA)-kit was used according to the manufacturer's protocol (Enzo Life Sciences International Inc., NY, USA).

Real-Time Quantitative PCR of lung tissue

For measurement of prepro-ET-1 (PPET), ET converting enzyme-1 (ECE), ET-receptor A (ET_A) and ET-receptor B (ET_B) mRNA levels, lung tissue was snap frozen in liquid nitrogen after excision. Small pieces of tissue (<30 mg) were homogenized by adding RLT lysisbuffer (Qiagen, Venlo, The Netherlands) and 2-mercaptoethanol (Sigma-Aldrich, Zwijndrecht, The Netherlands) using a homogenizer. After a proteinase K (Invitrogen, Breda, The Netherlands) treatment at 55°C for 10 min, total RNA was isolated using RNeasy Fibrous Tissue Mini Kit (Qiagen, Venlo, The Netherlands). RNA was eluted in RNase-free water and the concentration was determined using a NanoDrop (NanoDrop1000, Thermo Fisher Scientific, Bleiswijk, the Netherlands). RNA integrity was confirmed by Bioanalyzer (2100 Bioanalyzer, Agilent, Santa Clara, California, USA). cDNA was synthesized from 500 ng of total RNA with SensiFAST cDNA Synthesis Kit (Bioline, London, UK). RT-qPCR (CFX-96, Bio-Rad, Hercules, California, USA) was performed with SensiFAST SYBR & Fluorescein Kit (Bioline, London, UK). Target gene mRNA levels were normalized against β-actin, glyceraldehyde-3-phosphate dehydrogenase (GADPH), and Cyclophilin using the CFX manager software (Bio-Rad, Hercules, California, USA). Relative gene expression data

were calculated using the ΔΔCt method. Expression relative to sham was calculated by dividing individual expressions of PVB as well as sham animals by mean sham expression.

Wire myograph experiments

In vitro pulmonary vessel experiments were performed as previously described (31,32). In short, pulmonary small arteries were dissected and stored overnight in oxygenated (95% O_2/5% CO_2) Krebs bicarbonate solution (composition in mM: 118 NaCl, 4.7 KCl, 2.5 $CaCl_2$, 1.2 $MgSO_4$, 1.2 KH_2PO_4, 25 $NaHCO_3$, glucose 8.3; pH 7.4) at 4 °C. The next day, 2 mm segments were obtained and mounted on wire myographs in separate organ baths with oxygenated Krebs bicarbonate solution at 37 °C. Following a stabilization period of 30 minutes, internal vessel diameter was set to a tension equivalent of 0.9 times the estimated diameter at 20 mmHg effective transmural force. After pre-constriction using 100 nM of the synthetic thromboxane analogue U46619, endothelial integrity was ascertained by administration of the endothelium-dependent vasodilator substance P (10 nM). Maximal constriction was tested by exposure of the vessels to 100 mM KCl. After 30 minutes of stabilization in fresh buffer solution, vessels were incubated with either no blocker, the ET_A-blocker BQ123 (10^{-6} M) or the ET_B-blocker BQ788 (10^{-8} M). To test contraction to ET, vessels were subjected to incremental dosages from 10^{-10} to $3x10^{-7}$ M ET. Constriction to ET was calculated as percentage of maximal constriction to KCl 100 mM. Data was analysed using designated software (Labchart 8.0, AD instruments, Sydney, Australia), and concentration response curves were created using Prism (version 5.0, Graphpad Software, Inc., La Jolla, CA, USA) and StatView (version 5.0, SAS Institute, Cary, North Carolina, USA).

Histology

Tissue from the upper and lower lobe of the right lung was fixed in 3.5-4% buffered formaldehyde for at least 48 hours and subsequently dehydrated in incremental alcohol solutions, xylene and finally embedded in paraffin wax. Transverse sections (4.5 μm) were cut, using a microtome, and mounted on glass slides. Resorcin-Fuchsin-

von Gieson (RF) staining was performed to discriminate the internal- and external elastic lamina in small pulmonary arteries. Using the Hamamatsu NanoZoomer Digital Pathology (NDP) slide scanner (Hamamatsu Nanozoomer 2.0HT, Hamamatsu Photonics K.K., Japan), whole section images were obtained. Morphometric measurements of pulmonary small arteries were performed using NDP viewer (Hamamatsu). Both internal- and external elastic lamina areas were measured and assuming circularity of the vessels, inner and outer radius were calculated as $r = \sqrt{(area/\pi)}$. Wall-to-lumen ratio was calculated as (outer – inner radius)/inner radius, and relative lumen area as outer/inner area. To ensure that pulmonary veins were excluded from analysis, vessels in close proximity to the intersegmental septae were excluded from analysis. Only transversely cut vessels with an outer diameter of 50-150 μm were analysed.

Statistical analysis

SPSS (version 21.0 IBM, Armonk, NY, USA) was used for statistical analysis. Statistical analysis was performed using a t-test, or one-way or two-way ANOVA for repeated measures, followed by post-hoc testing with Bonferroni, when appropriate. Concentration response curves were analysed by regression analyses using Prism (version 5, GraphPad Software, La Jolla, CA, USA) and Statview (version 5.0). Statistical significance was accepted when $P \leq 0.05$ (two-tailed). Data are presented as means ± SEM. Individual data below the [1st quartile – 1.5 * Interquartile range] and above the [3rd quartile + 1.5 * Interquartile range] thresholds were considered outliers, and were excluded from statistical analyses.

RESULTS

Induction of pulmonary hypertension

Already after 5 weeks, pulmonary vein banding resulted in an increased tPVRi of 129±6 vs 105±5 mmHg l^{-1} min kg in sham animals ($P \leq 0.05$). This increased resistance was reflected in pulmonary hypertension, mPAP=29±1 mmHg vs 21±1 mmHg in sham ($P \leq 0.01$). Both tPVRi and mPAP increased over time, reflecting the progressive nature of PH (Fig 1; wk12 tPVRi: 255±31 vs 116±10 mmHg l^{-1} min kg; mPAP: 39±1 vs 20±2 mmHg; both $P \leq 0.01$). Resting systemic haemodynamics remained unchanged as compared to sham group (Table 1) and cardiac index, while transiently higher in PVB group at week 5 and 7, remained essentially similar in both groups (Fig 1). PVB resulted in a markedly lower arterial pO_2 from 7 weeks after banding, which persisted until follow up at 12 weeks (Table 2, 87±4 vs 101±4 mmHg, $P \leq 0.05$) and arterial oxygen saturation tended to be lower at 12 weeks (96±1 vs 98±1, $P=0.06$). Mixed venous pO_2 and oxygen saturation, arterial and mixed venous pCO_2 and haemoglobin were similar between PVB and sham animals.

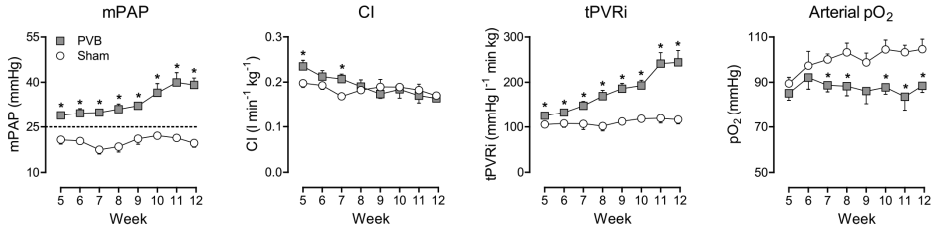

Figure 1. Haemodynamic progression of pulmonary hypertension. Progression of mean pulmonary artery pressure (mPAP), cardiac index (CI), total pulmonary vascular resistance index (tPVRi) and arterial partial oxygen pressure (pO_2) at rest over time. PVB: Pulmonary vein banding (n=7 for mPAP, n=6 for CI and tPVRi), Sham n=6. *P≤0.05 vs sham. By two-way ANOVA for repeated measures with Bonferroni posthoc test. Values are means ± SEM. Dotted line represents clinical threshold for PH.

Right ventricular remodelling

At sacrifice, bodyweight and left ventricle to bodyweight ratio were similar between groups (Fig 2). Both the right ventricle to bodyweight ratio (1.74±0.11 vs 1.29±0.06 g kg^{-1}) and the Fulton Index, calculated as ratio of right ventricular to left ventricular weight (0.59±0.03 vs 0.44±0.01 g g^{-1}) were increased, indicating right ventricular hypertrophy.

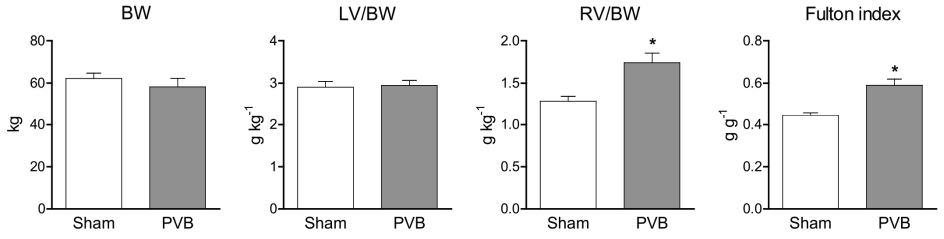

Figure 2. Right ventricular remodelling. Right ventricular mass increased in PVB animals (n=7) as compared to sham animals (n=6). LV: Left Ventricle, RV: Right ventricle, BW: Bodyweight *P≤0.05 vs sham by unpaired t-test (two-sided). Values are means ± SEM.

Response to exercise

At all timepoints during follow-up, exercise up to 4 km h^{-1} produced an increase in mPAP in sham animals that was the consequence of an increase in LAP in combination with an increase in CI, while tPVRi remained essentially unchanged (Fig 3). Arterial O_2-saturation remained virtually unaffected in sham animals, but decreased significantly with exercise in PVB animals (Table 2). From week 6 until week 10, the exercise-induced increases in LAP (not shown) and CI (Fig 3) were similar in PVB as compared to sham animals, and although resting mPAP and tPVRi were higher in PVB as compared to sham, the exercise-induced increases in mPAP and tPVRi were similar. In week 12, CI was lower during exercise in PVB animals than in sham animals (Fig 3, CI at 4 km h^{-1}: 0.23±0.01 vs 0.28±0.02 P≤0.05) which was almost entirely attributed to a decreased heart rate in PVB animals compared to sham animals (Table 1, heart rate at 4 km h^{-1}: 198±6 vs 256±9 beats min^{-1} P≤0.05). Despite this attenuated increase in CI, the exercise-induced increase in mPAP was similar in PVB as compared to sham animals, as a result of the higher tPVRi in PVB animals.

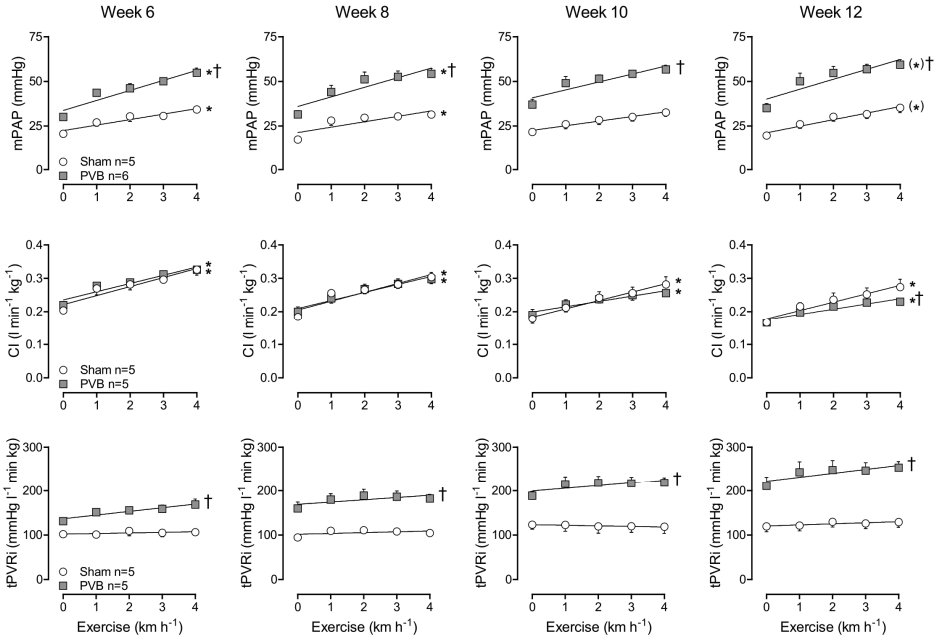

Figure 3. Haemodynamic response to exercise. Haemodynamic response to exercise in week 6, 8, 10 and 12. mPAP: mean pulmonary arterial pressure, CI: cardiac index, tPVRi: total pulmonary vascular resistance index. PVB: pulmonary vein banding. *P≤0.05 effect exercise, †P≤0.05 vs sham. (*) P=0.7 by two-way ANOVA for repeated measures. Values are means ± SEM.

Table 1: Haemodynamics at rest and during exercise before and after administration of tezosentan.

						Exercise (km h^{-1})					
	n	Group	Treatment	Rest		2			4		
HR	5	Sham	Control	133	± 10	195	± 7	*	256	± 9	*
(bpm)	5		Tezosentan	160	± 12 ‡	203	± 13	*	263	± 11	*
	6	PVB	Control	131	± 7	173	± 6	*†	198	± 6	*†
	6		Tezosentan	145	± 3	180	± 5	*	208	± 9	*†
MAP	5	Sham	Control	96	± 3	101	± 2		103	± 3	
(mmHg)	5		Tezo	86	± 4	88	± 1	‡	95	± 2	‡
	6	PVB	Control	86	± 5	86	± 4	†	84	± 6	†
	6		Tezosentan	73	± 3 ‡†	77	± 3	‡†	78	± 4	†
LAP	5	Sham	Control	3	± 0.5	6.8	± 0.9		9	± 0.3	*
(mmHg)	5		Tezosentan	6.3	± 2.9	8.8	± 1.3		13.3	± 1	‡
	6	PVB	Control	5.7	± 1.4	9.4	± 1.2	*	12.8	± 1.9	*
	6		Tezosentan	4.4	± 1.7	7.8	± 1.3	*‡	13.7	± 2.8	*
mPAP	5	Sham	Control	20	± 1	30	± 3	*	35	± 3	*
(mmHg)	5		Tezosentan	20	± 2	28	± 3	*	35	± 3	*
	6	PVB	Control	35	± 2 †	55	± 4	*†	59	± 3	*†
	6		Tezosentan	33	± 3 †	48	± 4	*‡†	57	± 3	*†
CI	5	Sham	Control	0.17	± 0.01	0.24	± 0.02	*	0.28	± 0.02	*
($l\ min^{-1}\ kg^{-1}$)	5		Tezosentan	0.19	± 0.01	0.24	± 0.01	*	0.28	± 0.02	*
	5	PVB	Control	0.17	± 0.01	0.22	± 0.01	*	0.23	± 0.01	*
	5		Tezosentan	0.18	± 0.01	0.22	± 0.01	*	0.23	± 0.01	*
SVi	5	Sham	Control	1.29	± 0.13	1.23	± 0.12		1.09	± 0.11	
($ml\ kg^{-1}$)	5		Tezosentan	1.23	± 0.12	1.2	± 0.12		1.09	± 0.1	
	5	PVB	Control	1.28	± 0.07	1.27	± 0.08		1.2	± 0.07	
	5		Tezosentan	1.25	± 0.09	1.24	± 0.08		1.14	± 0.07	
SVRi	5	Sham	Control	575	± 26	437	± 41	*	381	± 28	*
($mmHg\ l^{-1}\ min\ kg$)	5		Tezosentan	453	± 29 ‡	375	± 22		343	± 29	
	5	PVB	Control	522	± 44	405	± 33	*	364	± 38	*
	5		Tezosentan	411	± 44 ‡	351	± 29	‡	334	± 25	*

Haemodynamics obtained 12 weeks after banding. HR: Heart Rate, MAP: Mean Arterial Pressure, LAP: mean Left Atrial Pressure, mPAP: mean Pulmonary Arterial Pressure, CI: Cardiac Index, SVi: Stroke Volume index (CI/HR), SVRi: Systemic Vascular Resistance index (MAP/CI). Data are means ± SEM. *P≤0.05 vs rest, ‡P≤0.05 vs corresponding control experiment, †P≤0.05 vs corresponding sham.

Table 2: Blood gas analyses at rest and during exercise before and after administration of tezosentan

						Exercise (km hr^{-1})			
	n	Group	Treatment	Rest		2		4	
pO_2 art	5	Sham	Control	101 ±	4	89 ±	4 *	90 ±	5 *
(mmHg)	5		Tezosentan	98 ±	2	95 ±	6	90 ±	5
	6	PVB	Control	87 ±	4 †	69 ±	4 *†	65 ±	4 *†
	6		Tezosentan	82 ±	3 †	67 ±	4 *†	63 ±	4 *†
pO_2 mv	5	Sham	Control	42 ±	1	35 ±	1 *	30 ±	1 *
(mmHg)	5		Tezo	46 ±	1 ‡	38 ±	2 *	30 ±	2 *
	6	PVB	Control	41 ±	2	31 ±	2 *	27 ±	2 *
	6		Tezosentan	42 ±	2	34 ±	2 *	28 ±	2 *
saO_2 art	5	Sham	Control	98 ±	1	95 ±	1 *	96 ±	1
(%)	5		Tezosentan	97 ±	1	96 ±	1	96 ±	1
	6	PVB	Control	96 ±	1	90 ±	3	88 ±	2 *†
	6		Tezosentan	95 ±	1	89 ±	2 *†	86 ±	3 *†
saO_2 mv	5	Sham	Control	55 ±	1	40 ±	2 *	31 ±	3 *
(%)	5		Tezosentan	63 ±	2 ‡	48 ±	5 *‡	31 ±	4 *
	6	PVB	Control	56 ±	2	35 ±	3 *	25 ±	3 *
	6		Tezosentan	58 ±	3	41 ±	2 *	28 ±	4 *
pCO_2 art	5	Sham	Control	40 ±	2	43 ±	2 *	37 ±	3
(mmHg)	5		Tezosentan	41 ±	2	39 ±	2 ‡	35 ±	2 *
	6	PVB	Control	38 ±	3	37 ±	1 †	36 ±	2
	6		Tezosentan	40 ±	2	39 ±	2	36 ±	2
pCO_2 mv	5	Sham	Control	49 ±	1	52 ±	2	53 ±	3
(mmHg)	5		Tezosentan	47 ±	2	49 ±	2	48 ±	2
	6	PVB	Control	48 ±	2	47 ±	2	49 ±	3
	6		Tezosentan	44 ±	3	43 ±	2	44 ±	3
Hb	5	Sham	Control	9.4 ±	0.4	11 ±	0.3 *	11.2 ±	0.3 *
(g dl^{-1})	5		Tezosentan	9.9 ±	0.6	10.5 ±	0.2	10.9 ±	0.3
	6	PVB	Control	9.4 ±	0.7	10 ±	0.5	10.4 ±	0.8
	6		Tezosentan	9.5 ±	0.6	10.1 ±	0.6	10.6 ±	0.6
Lac	5	Sham	Control	0.78 ±	0.07	0.88 ±	0.07 *	1.86 ±	0.28 *
(mmol l^{-1})	5		Tezosentan	0.72 ±	0.06	0.78 ±	0.05	2.46 ±	0.53 *
	6	PVB	Control	0.87 ±	0.04	0.8 ±	0.04	1.77 ±	0.33 *
	6		Tezosentan	0.83 ±	0.05	0.78 ±	0.05	1.95 ±	0.52

Table 2 continued

					Exercise (km hr^{-1})	
	n	Group	Treatment	Rest	2	4
BVO_2i ($mmol\ min^{-1}\ kg^{-1}$)	5	Sham	Control	0.43 ± 0.03	0.92 ± 0.08 *	1.26 ± 0.09 *
	5		Tezosentan	0.4 ± 0.03	0.75 ± 0.05 *	1.25 ± 0.06 *
	6	PVB	Control	0.42 ± 0.04	0.75 ± 0.03 *	1 ± 0.02 *†
	6		Tezosentan	0.42 ± 0.05	0.65 ± 0.02 *	0.92 ± 0.01 *‡†

Blood gas analyses obtained 12 weeks after banding. pO_2: partial oxygen pressure, saO_2: oxygen saturation, pCO_2:partial carbondioxide pressure, Hb: hemoglobin, Lac: lactate, BVO_2i: body-oxygen consumption index (CI*arterio-venous oxygen difference), art: arterial, mv: mixed venous. Data are means ± SEM. *P≤0.05 vs rest, ‡P≤0.05 vs corresponding control experiment, †P≤0.05 vs corresponding sham.

Plasma ET-levels and effect of ET_A/ET_B-blockade by tezosentan

Plasma ET-levels were similar between PVB and sham animals in week 6 and 8 (Fig 4), and ET_A/ET_B-blockade by tezosentan at rest resulted in vasodilation that was similar in PVB and sham groups in week 6 (Fig 5; ΔtPVRi: -21±4 vs -18±7 mmHg l^{-1} min kg *P*=N.S.) and week 8 (ΔtPVRi: -19±8 vs -10±5 mmHg l^{-1} min kg *P*=N.S.). Consistent with the higher plasma ET-levels in PVB as compared to sham animals in week 10 (Fig 4), tezosentan-induced vasodilation was significantly more pronounced in PVB than in sham animals at rest at this timepoint (Fig 5, resting ΔtPVRi week 10: -43±5 vs -8±3 mmHg l^{-1} min kg *P*≤0.01) although this effect waned during exercise. In week 12, plasma ET-levels remained higher in PVB as compared to sham, and the tezosentan-induced vasodilation was now higher in PVB than in sham animals both at rest (Fig 5, ΔtPVRi -33±9 vs -12±8 mmHg l^{-1} min kg *P*≤0.05), and at all exercise intensities.

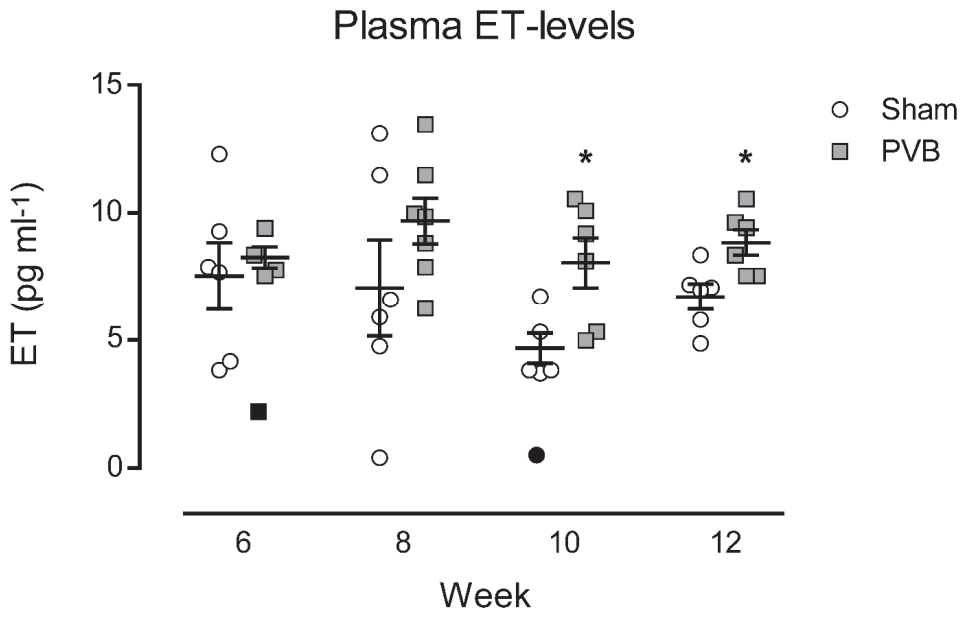

Figure 4. Plasma ET-levels over time in PVB and sham animals. *P≤0.05 vs sham by unpaired t-test (two-sided). Values are individual animals and means ± SEM. Data below the [1st quartile – 1.5 * Interquartile range] and above the [3rd quartile + 1.5 * Interquartile range] thresholds were considered outliers (black symbols), and were excluded from statistical analyses and from means ± SEM calculations.

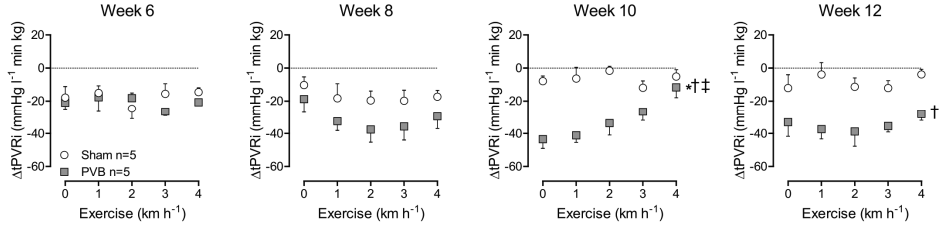

Figure 5. Vasodilation by ET_A/ET_B-blocker tezosentan in rest and during exercise over time. Vasodilation by ET_A/ET_B-blocker tezosentan had a more pronounced effect on PVB animals in week 10 and 12, ΔtPVRi: delta total pulmonary vascular resistance index: tPVRi with tezosentan – tPVRi without tezosentan. PVB: pulmonary vein banding n=5, Sham n=5. *P≤0.05 effect exercise; †P≤0.05 vs sham; ‡P≤0.05 effect exercise PVB vs effect exercise sham by two-way ANOVA. Values are means ± SEM.

Gene expression

PVB lung tissue showed no change in expression of the ET_A-receptor while expression of PPET and ECE was upregulated (Fig 6). In the lower lobes, this was accompanied by a down-regulation of the ET_B-receptor, which is the ET-clearance receptor, while in the upper lobe, expression of the ET_B-receptor was maintained. Altogether, these data suggest an increased ET-production and a decreased ET-clearance in the lungs and point towards the lungs as the origin of the increased circulating ET-levels.

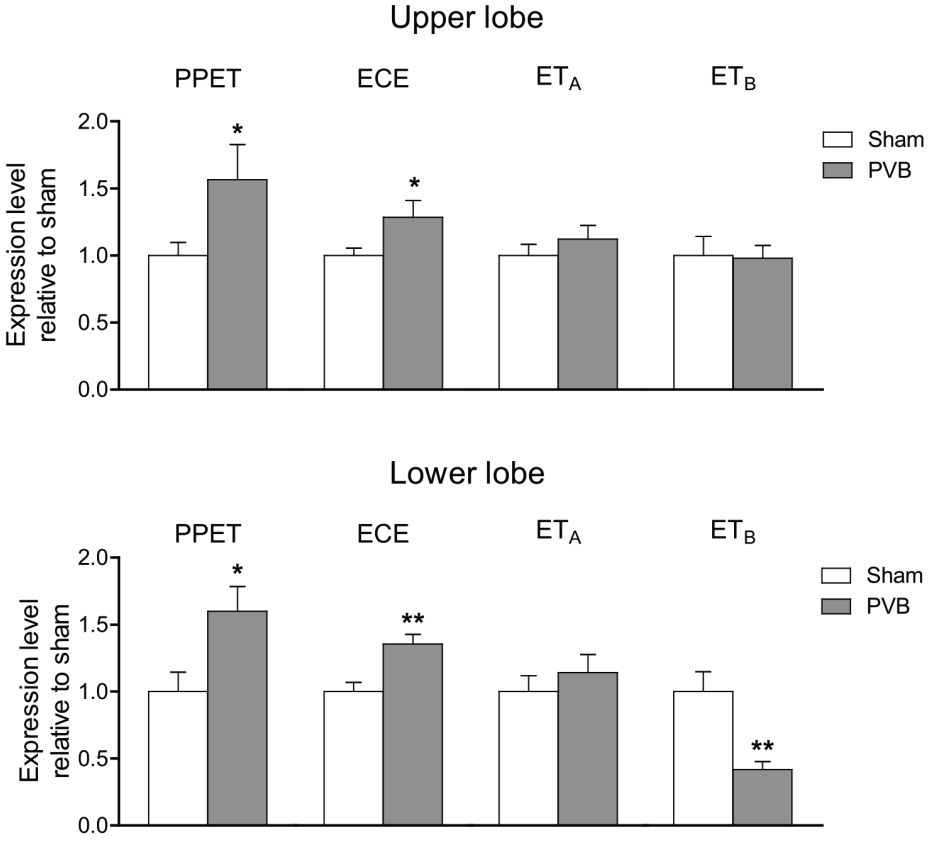

Figure 6. Gene expressions. Expression of prepro-endothelin-1 (PPET), endothelin converting enzyme 1 (ECE), and receptors ET_A and ET_B in the upper and lower lobes of PVB and sham animals relative to the corresponding mean expression of sham animals. *P≤0.05, **P≤0.01 by unpaired t-test (two tailed). Values are means ± SEM

Pulmonary microvascular structure and function

Histological assessment of small pulmonary arteries revealed increased wall thickness in PVB as compared to sham (Fig 7, 16.1±0.9 µm vs 13.6±0.4 µm, $P \leq 0.05$), resulting in an increased wall/lumen ratio (0.73±0.05 vs 0.54±0.01 $P \leq 0.01$) and a decreased relative lumen area (0.36±0.02 vs 0.44±0.01 $P \leq 0.01$).

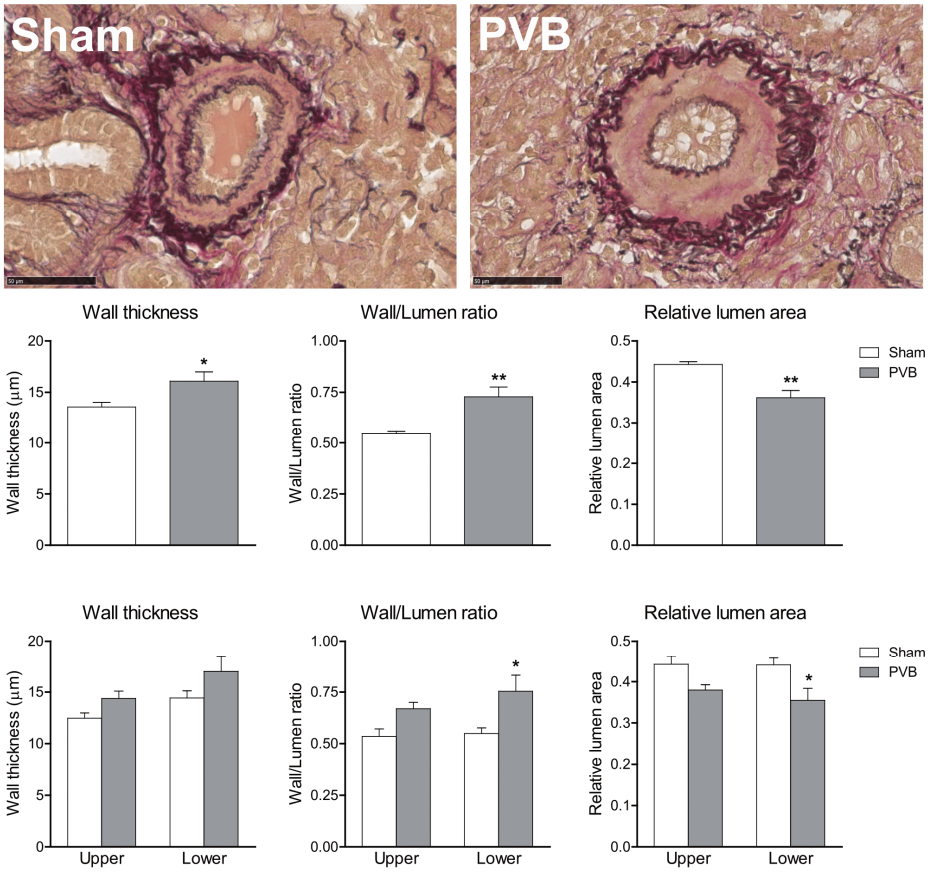

Figure 7. Pulmonary microvascular structure. Typical examples (upper panels) and histological assessment of small pulmonary arteries (Ø 50-150 µm) showing differences in wall thickness, wall/lumen ratio and relative lumen area between PVB and sham groups (middle panels) and between upper and lower lobes of these groups (lower panels). *P≤0.05 vs corresponding sham, **P≤0.01 vs corresponding sham by two-way ANOVA with Bonferroni's post-hoc test when appropriate. Values are means ± SEM. Scalingbar = 50 µm.

To elucidate the potential difference between the upper and lower lobes, data were split into four groups, PVB upper lobe, PVB lower lobe, sham upper lobe and sham

lower lobe, which showed that differences between PVB and sham groups, were essentially similar in both lobes, but reached statistical significance only in the lower lobes (Fig 7, lower panel).

Vasoconstriction in response to KCl 100 mM and U46619 was increased in vessels isolated from both upper and lower lobes from PVB as compared to sham animals (Fig 8). These effects reflect the medial hypertrophy of the pulmonary small arteries observed histologically. Endothelial function, as determined by vasodilation to substance P was similar between upper and lower lobes from sham animals. In PVB animals, the vasodilator response to substance P in the upper lobe was not different from that in the upper lobe of sham swine. However, vasodilation to substance P was significantly reduced in pulmonary small arteries from the lower lobe of PVB animals (Fig 8).

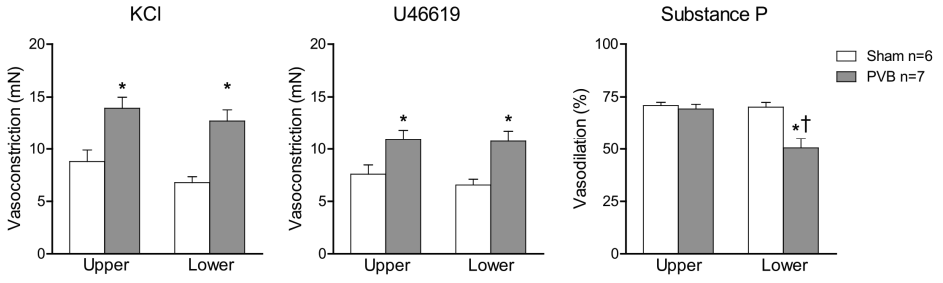

Figure 8. Vascular function. Vasoconstriction response to 100 mM KCl and U46619 was bigger in PVB group compared to sham group, whereas endothelium-dependent vasodilatation to Substance P was reduced in the lower, but not upper lobes of swine with PVB. Vasodilation by substance P was impaired in PVB lower lobes, but not in upper lobes. *P≤0.05 vs corresponding sham, †P≤0.05 vs corresponding upper lobe by two-way ANOVA with Bonferroni's post-hoc testing. KCl- and U46619 data are given as absolute values, Substance P data as percentage of dilation after constriction by U46619. Values are means ± SEM.

Administration of exogenous ET resulted in vasoconstriction in both sham and PVB animals. While absolute maximal vasoconstriction to ET was higher in PVB than sham animals (16.6±2.4mN vs 9.9±1.6mN $P \leq 0.05$), constriction relative to maximal KCl-induced vasoconstriction was lower in PVB (121±10% vs 161±7% $P \leq 0.01$), and sensitivity to ET was reduced in PVB animals (Fig 9; logEC50 8.3±0.2 vs 7.6±0.2 $P \leq 0.05$).

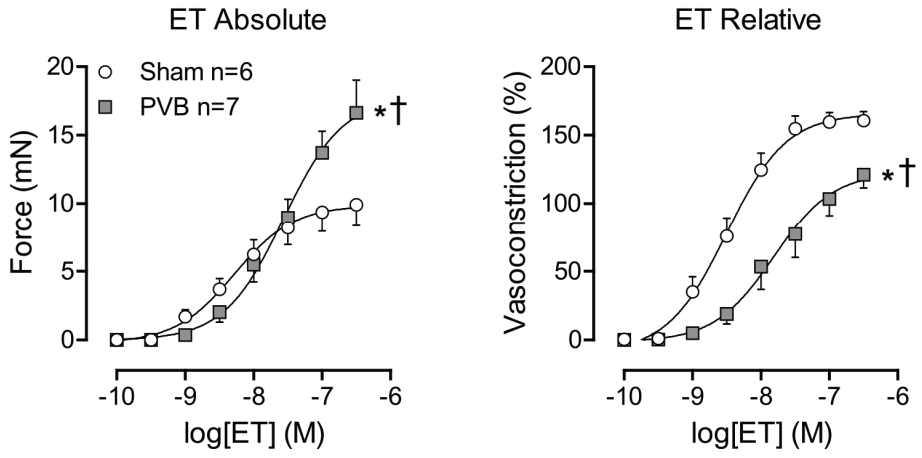

Figure 9. Response to exogenous endothelin. Vasoconstriction by administration of exogenous endothelin-1 (ET) to isolated small pulmonary arteries. Data is presented as absolute constriction (mN, left panel) and as percentage of maximal vasoconstriction by administration of 100 mM KCl (%, right panel). *P≤0.05 vs sham top, †P≤0.05 vs sham EC50 by regression analyses. Values are means ± SEM.

Vessels were incubated with BQ123 or BQ788 to obtain ET_A- or ET_B-blockade, and exposed to exogenous ET. The resulting concentration response curves were compared to those of vessels only exposed to exogenous ET. Under no condition did BQ788 affect the ET concentration response curve, while BQ123 reduced the ET effects, except in the sham lower lobes (Fig 10).

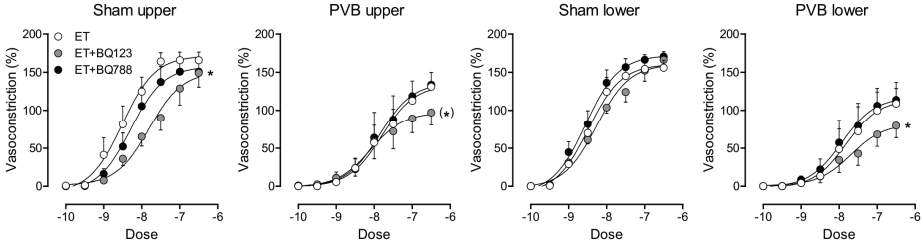

Figure 10. Response to exogenous endothelin with and without ET_A- or ET_B-blockade. Vasoconstriction by administration of exogenous endothelin-1 (ET) to isolated small pulmonary arteries of the sham upper and lower lobes, and PVB upper and lower lobes. Vessels were first incubated with either BQ123 for ET_A-blockade, BQ788 for ET_B-blockade, or no receptor blocker at all. Data are presented as percentage of maximal vasoconstriction by administration of 100mM KCl. *P≤0.05 vs ET, (*) P=0.06 by regression analyses. Values are means ± SEM.

DISCUSSION

The main findings in this study are that *(i)* non-restrictive banding of the confluence of the lower pulmonary veins in swine resulted in PH; *(ii)* within 12 weeks after banding, the initially isolated post-capillary PH progressed to combined pre-/post-capillary PH with structural and functional changes in pre-capillary pulmonary vessels; *(iii)* from 10 weeks after banding until sacrifice at 12 weeks, the ET-pathway was upregulated, actively contributing to the increased pulmonary vascular resistance.

Model Validation

This swine model for group II PH originates in the group of Ibanez et al. (10,11,25). To date, pulmonary hypertension and RV function have been studied under anaesthesia in this model, and revealed a marked increase in mPAP, PVR, and vessel wall thickness that, after 4 months follow up, resulted in structural and functional changes in the RV and, in a subset of animals, resulted in RV failure. In the present study, we performed serial measurements of systemic and pulmonary haemodynamics and blood gases in awake swine at rest as well as during graded treadmill exercise. Moreover, the chronic instrumentation allows for serial testing of vasoactive compounds – to study over time the mechanisms that control pulmonary vascular tone – and the serial collection of blood samples. The current study demonstrates that this porcine group II PH model has excellent inter-study and inter-group reproducibility, as the present findings at 12 weeks (mPAP and PVR, as well as pulmonary vascular remodelling) are very similar to those of the Ibanez group at three months (10,11). The additional chronic instrumentation, and subsequent exercise testing unmasked a mild chronotropic incompetence that has also been shown in PH (33), and has been ascribed to impaired autonomic control (34,35). The impaired increase in heart rate in PVB vs sham resulted in an attenuated increase in cardiac index and is consistent with the exercise intolerance in group II PH (33,36). Clinically, group II PH is comprised of a variety of different aetiologies, including left HF, valvular disease, inflow-/outflow-tract obstructions and, congenital or acquired,

pulmonary vein stenosis. The pulmonary vein banding swine model is well suited to study the progression and pathophysiology of all forms of group II PH. With translation to PH as a result of left HF, both with reduced or preserved ejection fraction, it can be both a drawback as well as an advantage that there is no actual left HF. On the one hand, this model could be missing circulating factors originating from left HF such as elevated natriuretic peptides and troponins (37), while on the other hand, we are able to study the isolated pulmonary vascular pathogenesis of CpcPH without influence of the left side of the heart. A limitation of this swine model, however, is that the conventional methods of calculating PVR ((mPAP-PCWP)/CO or (mPAP-LAP)/CO) do not result in true vascular resistance, as the resistance of the band around the lower pulmonary veins is also taken into account. Also the new parameter for differentiation between IpcPH and CpcPH, i.e. the diastolic pressure gradient, is not directly applicable in this model. In the present study, tPVRi (PAP/CI) was used to indicated changes in RV afterload as, with the current haemodynamic measurements, changes in vascular resistance of the upper and lower lobes cannot be distinguished from the changes in resistance induced by PVB.

Oxygenation

The venous confluence drains both inferior (caudal) pulmonary lobes, which account for 80% of total lung mass in swine (10). As the animal grows while the band maintains a fixed venous stenosis diameter, blood flow to the lower lobes is gradually restricted, likely resulting in redistribution of the blood flow to the middle and upper pulmonary lobes. The increased flow to these lobes decreases capillary transit time, reflected by a reduced arterial pO_2 and, to a lesser extent in arterial SO_2, in PVB animals (38). It could further be speculated that a decreased diffusion capacity in swine with PVB contributes to the decreased oxygenation at rest as is also observed in severe pulmonary arterial hypertension (PAH) and severe PH in HF (39,40). However, measurement of diffusion capacity requires respiratory mask-testing which is technically challenging in swine and was not performed in the present study.

During exercise, the increase in cardiac output further decreases transit time which resulted in decreased arterial pO_2 and arterial O_2-saturation in PVB swine. In

exercising sham animals, arterial O_2-saturation remained relatively constant, although arterial PO_2 decreased slightly, but to a lesser extent than in swine with PVB. Tezosentan did not alter cardiac output, and arterial oxygenation. Importantly, the observation that arterial pO_2 was unaffected by tezosentan infusion suggests that tezosentan did not result in pulmonary oedema.

Pulmonary microvascular remodelling in PH: role of ET

Twelve weeks after induction of pulmonary vein banding, pulmonary small arteries demonstrated muscularization and thickening of the vascular wall, resulting in a relative reduction of the vascular lumen. This finding is consistent with the observation that pulmonary vascular remodelling in group II PH mainly consists of medial hypertrophy and muscularization of arterioles (41). Consistent with the increased muscularization, we found that maximal contraction of these vessels was also increased, which was accompanied by alterations in the ET-pathway, a well-known mediator of vascular remodelling (42-44). It has been shown that the ET-pathway is upregulated in PAH (1,45). Because of the abluminal release, circulating plasma ET-levels are thought to be the result, at least in part, of spillover from the junctions between endothelial and smooth muscle cells and can therefore not be equated to ET-activity in pathological states (45). However, plasma ET-levels are upregulated in PAH and correlate with disease severity and haemodynamics (19,46). In addition to increased ET-levels, ET-signalling may also be increased via upregulation of ET-receptors. For example, ET_A-receptors have been reported to be upregulated, while ET_B-receptors may be up- or downregulated, depending on the type of PH, in clinical and experimental PH (47-49). We previously showed that in swine with PH secondary to myocardial infarction plasma ET-levels were increased, and infusion of exogenous ET resulted in a more pronounced pulmonary vasoconstriction compared to normal swine (15). This increased response to ET appeared to be the result of an increased ET_A-mediated vasoconstriction. Also, plasma ET-levels are increased in chronic HF, and correlate with the severity of symptoms and pulmonary haemodynamics (21,50). This is accompanied by upregulation of ET_A-, and downregulation of ET_B-receptors (51-53).

The observation that ET_A+ET_B-blockade by tezosentan produced a more pronounced vasodilation in awake PVB than sham animals confirms increased ET-activity in type II PH in vivo. The present study showed an increased expression of PPET and ECE in lung tissue, and higher plasma ET-levels in PVB as compared to sham at 10 and 12 weeks after PVB. As indicated in figure 4, two outliers were identified and removed from statistical analyses. Although this decreased the variation within groups, it did not alter statistical significance. The increased expression of PPET and ECE, as well as the increased plasma ET-levels are consistent with data that show that the lungs are the primary source of ET-1 (54,55), although the contribution of other organs cannot be excluded in the present study as PPET- or ECE-expression was only measured in lung tissue. Furthermore, it appeared that the plasma ET-levels decreased over time in the sham-operated swine, while these levels in PVB swine increased only slightly. Swine received the banding or sham surgery at the age of three weeks and were studied until the age of sixteen weeks. The observation that in sham animals, plasma ET-levels decreased over time is consistent with decreasing plasma ET-levels over time in the first months after birth in humans (56).

The higher plasma ET-levels in PVB were accompanied by a decreased expression of ET_B-receptors, that are responsible for ET-clearance, in the lower lobes. In the present study, the ET_A-receptor was the main receptor responsible for ET-induced vasoconstriction, since ET_B-receptor blockade did not affect this constriction in pulmonary small arteries from either sham or PVB animals. The maximal constriction to exogenous ET was increased, which likely reflects the increased muscularization of the pulmonary small arteries, as the response to KCl was similarly increased. Moreover, the normalized concentration response curve was shifted to the right in PVB pulmonary small arteries, suggesting desensitization of the pulmonary vasculature to ET. Although this desensitization was not accompanied by a decrease in ET_A-receptor expression, it is possible that changes in pulmonary vascular ET_A-receptor expression remained undetected as ET-receptor expression was measured in bulk lung-tissue expression, and hence expression in endothelial and smooth muscle cells cannot be distinguished from expression in bronchi and alveoli.

Interestingly, the vasodilator response to ET-receptor blockade with tezosentan was blunted during exercise at 10 weeks, but not at twelve weeks, suggesting progressive

activation of the ET-system and/or suppression of ET-mediated constriction during exercise. The latter is consistent with our previous findings that during exercise, nitric oxide blunts the vasoconstrictor effect of ET (57). The attenuated vasodilation to tezosentan during exercise at week 10 might thus be the result of an increase in nitric oxide during exercise, that is no longer present at 12 weeks after PVB.

Clinical Relevance

Our study is the first to show that ET is upregulated in group II PH without an underlying disease that causes neurohumoral activation, such as myocardial infarction or HF. The fact that an initially purely mechanical increase of pulmonary pressure and resistance induces over-activation of the ET-pathway suggests that the ET-pathway might be an interesting target for therapy in this group of patients.

To date, a number of clinical trials have been performed with a variety of ET-receptor antagonists (ERA's) in chronic HF, with generally rather disappointing results (58-66). It should be noted however, that all experimental ERA's were tested in the presence of conventional medical HF therapy, including angiotensin-converting-enzyme inhibitors, ß-blockers and angiotensin-II- and aldosterone receptor antagonists. It cannot be excluded that the added effect of ERA's was limited because of blunted neurohumoral activity by these other drugs. Indeed, in another clinical study, acute administration of darusentan produced a dose-dependent change in CI, SVR, PVR, MAP, mPAP and PCWP when conventional medical therapy was interrupted (67), whereas in the HEAT and EARTH trials, where medication was continued, darusentan produced no additional pulmonary haemodynamic effects (58,62). Moreover, while in some clinical trials, ERA's did improve haemodynamic variables, including PCWP, PVR, SVR, CI and right atrial pressure (61-63), none resulted in improved outcome or clinical status. It is therefore important to note that in the present study the acute effect of ERA's were investigated, and that these results may not directly translate to positive long-term studies. Future studies are thus required to investigate the pulmonary effects of chronic therapy with ERA's in group II PH.

The current guidelines of the European Society of Cardiology for treatment of group II PH recommend the treatment of the LV, to optimize volume status, to take care of

co-morbidities and to take caution in using pulmonary vasodilators (1). We believe a distinction must be made between group II PH as a result of left HF, and non-HF causes of group II PH. Non HF causes of group II PH include pulmonary vein stenosis, which can be either congenital, or as a result of radiofrequency ablation in treatment of atrial fibrillation (68-70). Pulmonary vein stenosis causes a passive increase in PVR and mPAP, as was also shown in the present study. We also observed that the ET-pathway is upregulated as early as 10 weeks after inducing the stenosis, and that ET contributes to an active increase of PVR and mPAP. Consequently, inhibiting the ET-pathway could be beneficial in this group of patients to stop progression from IpcPH to CpcPH, especially because the most serious adverse effects in the clinical trials in HF patients (worsening of HF, peripheral/pulmonary oedema) might not apply to non-HF patients. Recently, the FDA approved Dual-receptor antagonist bosentan for treatment of PH in children. While it will mainly be under investigation as treatment of PAH, bosentan could also be utilized in treatment of children with PH as a result of congenital pulmonary vein stenosis. The observation in this study that ET-induced vasoconstriction in isolated pulmonary small arteries appeared to be entirely dependent on ET_A-receptors, suggests ET_A-blockade alone might be preferable over dual ERA's.

CONCLUSIONS

Banding of the confluence of both inferior pulmonary veins in swine resulted in a progressive increase in pulmonary arterial pressure and resistance, which could be measured from week 5 until week 12 after banding, in the awake state, by chronic instrumentation. From week 10 onward, the pulmonary endothelin pathway was upregulated, likely contributing to pre-capillary activation of the initially isolated post-capillary pulmonary hypertension and leading to structural and functional vascular remodelling. Inhibition of the endothelin pathway could thus potentially provide a pharmacotherapeutic target for early stage post-capillary pulmonary hypertension, especially in post-capillary pulmonary hypertension with normal left heart function.

REFERENCES

1. Galie N, Humbert M, Vachiery JL et al. 2015 ESC/ERS Guidelines for the Diagnosis and Treatment of Pulmonary Hypertension. Rev Esp Cardiol (Engl Ed) 2016;69:177.
2. Rosenkranz S, Gibbs JS, Wachter R, De Marco T, Vonk-Noordegraaf A, Vachiery JL. Left ventricular heart failure and pulmonary hypertension. Eur Heart J 2016;37:942-54.
3. Gerges M, Gerges C, Pistritto AM et al. Pulmonary Hypertension in Heart Failure. Epidemiology, Right Ventricular Function, and Survival. Am J Respir Crit Care Med 2015;192:1234-46.
4. Miller WL, Grill DE, Borlaug BA. Clinical features, hemodynamics, and outcomes of pulmonary hypertension due to chronic heart failure with reduced ejection fraction: pulmonary hypertension and heart failure. JACC Heart Fail 2013;1:290-299.
5. Vanderpool RR, Naeije R. Progress in Pulmonary Hypertension with Left Heart Failure. Beyond New Definitions and Acronyms. Am J Respir Crit Care Med 2015;192:1152-4.
6. Tatebe S, Fukumoto Y, Sugimura K et al. Clinical significance of reactive post-capillary pulmonary hypertension in patients with left heart disease. Circ J 2012;76:1235-44.
7. Lundgren J, Radegran G. Pathophysiology and potential treatments of pulmonary hypertension due to systolic left heart failure. Acta Physiol (Oxf) 2014;211:314-33.
8. Naeije R, D'Alto M. The Diagnostic Challenge of Group 2 Pulmonary Hypertension. Prog Cardiovasc Dis 2016;59:22-9.
9. Endo M, Yamaki S, Hata M, Saiki Y, Tabayashi K. Pulmonary vascular changes induced by unilateral pulmonary venous obstruction. Pediatr Cardiol 2002;23:420-5.
10. Garcia-Alvarez A, Fernandez-Friera L, Garcia-Ruiz JM et al. Noninvasive monitoring of serial changes in pulmonary vascular resistance and acute vasodilator testing using cardiac magnetic resonance. J Am Coll Cardiol 2013;62:1621-31.
11. Pereda D, Garcia-Alvarez A, Sanchez-Quintana D et al. Swine model of chronic postcapillary pulmonary hypertension with right ventricular remodeling: long-term characterization by cardiac catheterization, magnetic resonance, and pathology. J Cardiovasc Transl Res 2014;7:494-506.
12. Dai ZK, Tan MS, Chai CY et al. Upregulation of endothelial nitric oxide synthase and endothelin-1 in pulmonary hypertension secondary to heart failure in aorta-banded rats. Pediatr Pulmonol 2004;37:249-56.
13. Budhiraja R, Tuder RM, Hassoun PM. Endothelial dysfunction in pulmonary hypertension. Circulation 2004;109:159-65.
14. Moraes DL, Colucci WS, Givertz MM. Secondary pulmonary hypertension in chronic heart failure: the role of the endothelium in pathophysiology and management. Circulation 2000;102:1718-23.
15. Houweling B, Merkus D, Sorop O, Boomsma F, Duncker DJ. Role of endothelin receptor activation in secondary pulmonary hypertension in awake swine after myocardial infarction. J Physiol 2006;574:615-26.
16. Merkus D, de Beer VJ, Houweling B, Duncker DJ. Control of pulmonary vascular tone during exercise in health and pulmonary hypertension. Pharmacol Ther 2008;119:242-63.

17. Merkus D, Houweling B, de Beer VJ, Everon Z, Duncker DJ. Alterations in endothelial control of the pulmonary circulation in exercising swine with secondary pulmonary hypertension after myocardial infarction. J Physiol 2007;580:907-23.
18. van Duin RWB, Houweling B, Uitterdijk A, Duncker DJ, Merkus D. Pulmonary vasodilation by phosphodiesterase 5 inhibition is enhanced and nitric oxide independent in early pulmonary hypertension after myocardial infarction. Am J Physiol Heart Circ Physiol 2018;314:H170-H179.
19. Giaid A, Yanagisawa M, Langleben D et al. Expression of endothelin-1 in the lungs of patients with pulmonary hypertension. N Engl J Med 1993;328:1732-9.
20. Meoli DF, Su YR, Brittain EL, Robbins IM, Hemnes AR, Monahan K. The transpulmonary ratio of endothelin 1 is elevated in patients with preserved left ventricular ejection fraction and combined pre- and post-capillary pulmonary hypertension. Pulm Circ 2018;8:2045893217745019.
21. Cody RJ, Haas GJ, Binkley PF, Capers Q, Kelley R. Plasma endothelin correlates with the extent of pulmonary hypertension in patients with chronic congestive heart failure. Circulation 1992;85:504-9.
22. Porter TR, Taylor DO, Cycan A et al. Endothelium-dependent pulmonary artery responses in chronic heart failure: influence of pulmonary hypertension. J Am Coll Cardiol 1993;22:1418-24.
23. Cooper CJ, Jevnikar FW, Walsh T, Dickinson J, Mouhaffel A, Selwyn AP. The influence of basal nitric oxide activity on pulmonary vascular resistance in patients with congestive heart failure. Am J Cardiol 1998;82:609-14.
24. De Wijs-Meijler DP, Stam K, van Duin RW et al. Surgical Placement of Catheters for Long-term Cardiovascular Exercise Testing in Swine. J Vis Exp 2016:e53772.
25. Aguero J, Ishikawa K, Hadri L et al. Characterization of right ventricular remodeling and failure in a chronic pulmonary hypertension model. Am J Physiol Heart Circ Physiol 2014;307:H1204-15.
26. Keusch S, Bucher A, Muller-Mottet S et al. Experience with exercise right heart catheterization in the diagnosis of pulmonary hypertension: a retrospective study. Multidiscip Respir Med 2014;9:51.
27. Grundy D. Principles and standards for reporting animal experiments in The Journal of Physiology and Experimental Physiology. J Physiol 2015;593:2547-9.
28. Faul F, Erdfelder E, Lang AG, Buchner A. G*Power 3: a flexible statistical power analysis program for the social, behavioral, and biomedical sciences. Behav Res Methods 2007;39:175-91.
29. Duncker DJ, Stubenitsky R, Tonino PA, Verdouw PD. Nitric oxide contributes to the regulation of vasomotor tone but does not modulate O(2)-consumption in exercising swine. Cardiovasc Res 2000;47:738-48.
30. Haitsma DB, Merkus D, Vermeulen J, Verdouw PD, Duncker DJ. Nitric oxide production is maintained in exercising swine with chronic left ventricular dysfunction. Am J Physiol Heart Circ Physiol 2002;282:H2198-209.

31. Mulvany MJ, Halpern W. Contractile properties of small arterial resistance vessels in spontaneously hypertensive and normotensive rats. Circ Res 1977;41:19-26.
32. Zhou Z, de Beer VJ, de Wijs-Meijler D et al. Pulmonary vasoconstrictor influence of endothelin in exercising swine depends critically on phosphodiesterase 5 activity. Am J Physiol Lung Cell Mol Physiol 2014;306:L442-52.
33. Oliveira RKF, Faria-Urbina M, Maron BA, Santos M, Waxman AB, Systrom DM. Functional impact of exercise pulmonary hypertension in patients with borderline resting pulmonary arterial pressure. Pulm Circ 2017;7:654-665.
34. Wensel R, Jilek C, Dorr M et al. Impaired cardiac autonomic control relates to disease severity in pulmonary hypertension. Eur Respir J 2009;34:895-901.
35. Bristow MR, Minobe W, Rasmussen R et al. Beta-adrenergic neuroeffector abnormalities in the failing human heart are produced by local rather than systemic mechanisms. J Clin Invest 1992;89:803-15.
36. Caravita S, Faini A, Deboeck G et al. Pulmonary hypertension and ventilation during exercise: Role of the pre-capillary component. J Heart Lung Transplant 2017;36:754-762.
37. Gaggin HK, Januzzi JL, Jr. Biomarkers and diagnostics in heart failure. Biochim Biophys Acta 2013;1832:2442-50.
38. Yuba K. A study on the pulmonary functions and the pulmonary circulation in cardio-pulmonary diseases. II. Pulmonary capillary blood flow and pulmonary capillary mean transit time in cardio-pulmonary diseases. Jpn Circ J 1971;35:1399-409.
39. Trip P, Girerd B, Bogaard HJ et al. Diffusion capacity and BMPR2 mutations in pulmonary arterial hypertension. Eur Respir J 2014;43:1195-8.
40. Hoeper MM, Meyer K, Rademacher J, Fuge J, Welte T, Olsson KM. Diffusion Capacity and Mortality in Patients With Pulmonary Hypertension Due to Heart Failure With Preserved Ejection Fraction. JACC Heart Fail 2016;4:441-9.
41. Dickinson MG, Bartelds B, Borgdorff MA, Berger RM. The role of disturbed blood flow in the development of pulmonary arterial hypertension: lessons from preclinical animal models. Am J Physiol Lung Cell Mol Physiol 2013;305:L1-14.
42. Shimoda LA, Laurie SS. Vascular remodeling in pulmonary hypertension. J Mol Med (Berl) 2013;91:297-309.
43. Shao D, Park JE, Wort SJ. The role of endothelin-1 in the pathogenesis of pulmonary arterial hypertension. Pharmacol Res 2011;63:504-11.
44. Shimoda LA, Sham JS, Liu Q, Sylvester JT. Acute and chronic hypoxic pulmonary vasoconstriction: a central role for endothelin-1? Respir Physiol Neurobiol 2002;132:93-106.
45. Kawanabe Y, Nauli SM. Endothelin. Cell Mol Life Sci 2011;68:195-203.
46. Stewart DJ, Levy RD, Cernacek P, Langleben D. Increased plasma endothelin-1 in pulmonary hypertension: marker or mediator of disease? Ann Intern Med 1991;114:464-9.
47. Bauer M, Wilkens H, Langer F, Schneider SO, Lausberg H, Schafers HJ. Selective upregulation of endothelin B receptor gene expression in severe pulmonary hypertension. Circulation 2002;105:1034-6.

48. Gosselin R, Gutkowska J, Baribeau J, Perreault T. Endothelin receptor changes in hypoxia-induced pulmonary hypertension in the newborn piglet. Am J Physiol 1997;273:L72-9.

49. Sauvageau S, Thorin E, Villeneuve L, Dupuis J. Change in pharmacological effect of endothelin receptor antagonists in rats with pulmonary hypertension: role of ETB-receptor expression levels. Pulm Pharmacol Ther 2009;22:311-7.

50. Pacher R, Stanek B, Hulsmann M et al. Prognostic impact of big endothelin-1 plasma concentrations compared with invasive hemodynamic evaluation in severe heart failure. J Am Coll Cardiol 1996;27:633-41.

51. Ponicke K, Vogelsang M, Heinroth M et al. Endothelin receptors in the failing and nonfailing human heart. Circulation 1998;97:744-51.

52. Zolk O, Quattek J, Sitzler G et al. Expression of endothelin-1, endothelin-converting enzyme, and endothelin receptors in chronic heart failure. Circulation 1999;99:2118-23.

53. Staniloae C, Dupuis J, White M et al. Reduced pulmonary clearance of endothelin in congestive heart failure: a marker of secondary pulmonary hypertension. J Card Fail 2004;10:427-32.

54. Dupuis J, Goresky CA, Fournier A. Pulmonary clearance of circulating endothelin-1 in dogs in vivo: exclusive role of ETB receptors. J Appl Physiol (1985) 1996;81:1510-5.

55. Dupuis J, Stewart DJ, Cernacek P, Gosselin G. Human pulmonary circulation is an important site for both clearance and production of endothelin-1. Circulation 1996;94:1578-84.

56. Yoshibayashi M, Nishioka K, Nakao K et al. Plasma endothelin levels in healthy children: high values in early infancy. J Cardiovasc Pharmacol 1991;17 Suppl 7:S404-5.

57. Houweling B, Merkus D, Dekker MM, Duncker DJ. Nitric oxide blunts the endothelin-mediated pulmonary vasoconstriction in exercising swine. J Physiol 2005;568:629-38.

58. Anand I, McMurray J, Cohn JN et al. Long-term effects of darusentan on left-ventricular remodelling and clinical outcomes in the EndothelinA Receptor Antagonist Trial in Heart Failure (EARTH): randomised, double-blind, placebo-controlled trial. Lancet 2004;364:347-54.

59. Coletta AP, Cleland JG. Clinical trials update: highlights of the scientific sessions of the XXIII Congress of the European Society of Cardiology--WARIS II, ESCAMI, PAFAC, RITZ-1 and TIME. Eur J Heart Fail 2001;3:747-50.

60. Kalra PR, Moon JC, Coats AJ. Do results of the ENABLE (Endothelin Antagonist Bosentan for Lowering Cardiac Events in Heart Failure) study spell the end for non-selective endothelin antagonism in heart failure? Int J Cardiol 2002;85:195-7.

61. Louis A, Cleland JG, Crabbe S et al. Clinical Trials Update: CAPRICORN, COPERNICUS, MIRACLE, STAF, RITZ-2, RECOVER and RENAISSANCE and cachexia and cholesterol in heart failure. Highlights of the Scientific Sessions of the American College of Cardiology, 2001. Eur J Heart Fail 2001;3:381-7.

62. Luscher TF, Enseleit F, Pacher R et al. Hemodynamic and neurohumoral effects of selective endothelin A (ET(A)) receptor blockade in chronic heart failure: the Heart Failure ET(A) Receptor Blockade Trial (HEAT). Circulation 2002;106:2666-72.

63. McMurray JJ, Teerlink JR, Cotter G et al. Effects of tezosentan on symptoms and clinical outcomes in patients with acute heart failure: the VERITAS randomized controlled trials. JAMA 2007;298:2009-19.

64. Packer M, McMurray J, Massie BM et al. Clinical effects of endothelin receptor antagonism with bosentan in patients with severe chronic heart failure: results of a pilot study. J Card Fail 2005;11:12-20.
65. Koller B, Steringer-Mascherbauer R, Ebner CH et al. Pilot Study of Endothelin Receptor Blockade in Heart Failure with Diastolic Dysfunction and Pulmonary Hypertension (BADDHY-Trial). Heart Lung Circ 2017;26:433-441.
66. Vachiery JL, Delcroix M, Al-Hiti H et al. Macitentan in pulmonary hypertension due to left ventricular dysfunction. Eur Respir J 2018;51.
67. Spieker LE, Mitrovic V, Noll G et al. Acute hemodynamic and neurohumoral effects of selective ET(A) receptor blockade in patients with congestive heart failure. ET 003 Investigators. J Am Coll Cardiol 2000;35:1745-52.
68. Manzar S. Congenital pulmonary vein stenosis. J Coll Physicians Surg Pak 2007;17:374-5.
69. Latson LA, Prieto LR. Congenital and acquired pulmonary vein stenosis. Circulation 2007;115:103-8.
70. Fender EA, Packer DL, Holmes DR, Jr. Pulmonary vein stenosis after atrial fibrillation ablation. EuroIntervention 2016;12 Suppl X:X31-X34.

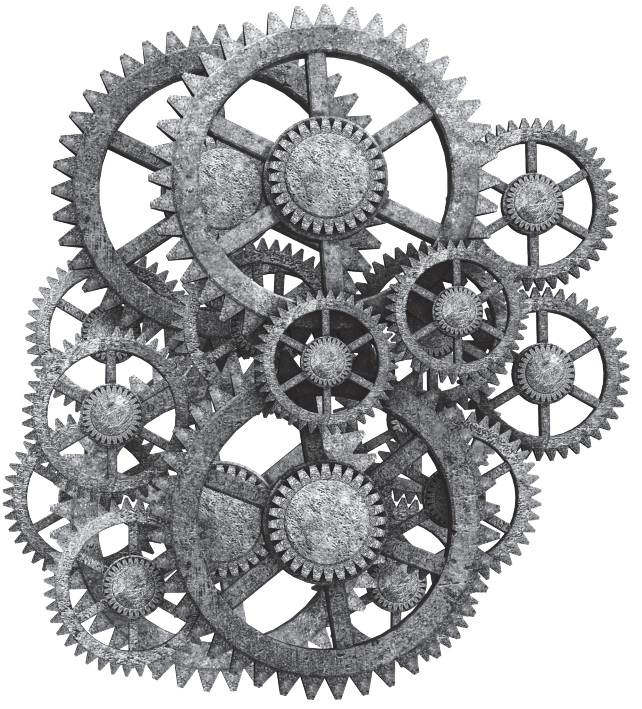

5

Chapter 5

Intervening with the nitric oxide pathway to alleviate pulmonary hypertension in pulmonary vein stenosis

Richard WB van Duin, Kelly Stam, Zongye Cai,
André Uitterdijk, Beatrijs Bartelds, AH Jan Danser,
Irwin K Reiss, Dirk J Duncker, Daphne Merkus

•

JOURNAL OF CLINICAL MEDICINE. AUG 2019

ABSTRACT

Pulmonary hypertension (PH) as a result of pulmonary vein stenosis (PVS) is extremely difficult to treat. The ideal therapy should not target the high-pressure/low-flow (HP/LF) vasculature that drains into stenotic veins, but only the high-pressure/high-flow (HP/HF) vasculature draining into unaffected pulmonary veins, reducing vascular resistance and pressure without risk of pulmonary oedema. We aimed to assess the activity of the nitric oxide (NO) pathway in PVS during the development of PH, and investigate whether interventions in the NO pathway differentially affect vasodilation in the HP/HF vs. HP/LF territories. Swine underwent pulmonary vein banding (PVB; n = 7) or sham surgery (n = 6) and were chronically instrumented to assess progression of PH. Pulmonary sensitivity to exogenous NO (sodium nitroprusside, SNP) and the contribution of endogenous NO were assessed bi-weekly. The pulmonary vasodilator response to phosphodiesterase-5 (PDE5) inhibition was assessed 12 weeks after PVB or sham surgery. After sacrifice, 12 weeks post-surgery, interventions in the NO pathway on pulmonary small arteries isolated from HP/LF and HP/HF territories were further investigated. There were no differences in the in vivo pulmonary vasodilator response to SNP and the pulmonary vasoconstrictor response to endothelial nitric oxide synthase (eNOS) inhibition up to 8 weeks after PVB as compared to the sham group. However, at 10 and 12 weeks post-PVB, the in vivo pulmonary vasodilation in response to SNP was larger in the PVB group. Similarly, the vasoconstriction to eNOS inhibition was larger in the PVB group, particularly during exercise, while pulmonary vasodilation in response to PDE5 inhibition was larger in the PVB group both at rest and during exercise. In isolated pulmonary small arteries, sensitivity to NO donor SNP was similar in PVB vs. sham groups irrespective of HP/LF and HP/HF, while sensitivity to the PDE5 inhibitor sildenafil was lower in PVB HP/HF and sensitivity to bradykinin was lower in PVB HP/LF. In conclusion, both NO availability and sensitivity were increased in the PVB group. The increased nitric oxide sensitivity was not the result of a decreased PDE5 activity, as PDE5 activity was even increased. Some vasodilators differentially effect HP/HF vs. HP/LF vasculature.

INTRODUCTION

Pulmonary hypertension (PH) is a chronic disease characterised by a mean pulmonary arterial pressure (mPAP) > 25 mmHg at rest (1). PH can have many different aetiologies, which are categorised into five groups by the WHO. The most prevalent is group II PH, in which left heart failure (LHF), valvular disease, or obstructions of the inflow/outflow tract of the left ventricle cause an upstream pressure increase in the pulmonary vasculature (1,2). An often-overlooked cause of group II PH is partial pulmonary vein stenosis (PVS).

In PVS, one or more of the pulmonary veins are narrowed, hampering outflow of blood from the lungs into the left atrium, thereby increasing pulmonary vascular resistance. In the adult population, PVS may occur as an, albeit rare, consequence of radio-frequency ablation of atrial tissue around the pulmonary veins to treat atrial fibrillation (3). PVS in the paediatric population is a severe congenital anomaly associated with poor outcomes (4). Paediatric PVS can occur as a singular anomaly, but is generally associated with congenital heart defects (univentricular heart disease, ventricular septal defect, atrial septal defect or persistent arterial duct), lung disease (bronchopulmonary dysplasia (BPD)) or Down syndrome or other trisomies (5–8). PVS is a challenging disease. Treatment of the stenosis itself, either through catheterisation or by means of surgery, often results in restenosis (7). The resulting initially passive, isolated post-capillary PH (IpcPH) may progress to active, combined pre- and post-capillary PH (CpcPH), characterised by pre-capillary structural and functional vascular remodelling resembling pulmonary arterial hypertension (PAH; WHO classification group I PH) (9–11). The use of PAH vasodilation therapy, however, can be perilous in group II PH, as vasodilation increases flow, while the outflow remains hampered, potentially resulting in an increase in capillary pressure and pulmonary oedema. Use of first-line vasodilator therapies like inhaled nitric oxide (NO), administration of NO donors or phosphodiesterase-5 (PDE5) inhibitors may therefore increase dyspnoea by causing pulmonary oedema (12). To this day, crucial information about the effects of these therapies in PH due to PVS is lacking. Unlike LHF-induced PH, PVS-induced PH has a mixed or double phenotype. The pulmonary vasculature draining into the stenotic pulmonary veins experiences a high pressure

with a relatively low flow (HP/LF), while the pulmonary vasculature draining into the remaining unaffected pulmonary veins experiences a high pressure with a relatively high flow (HP/HF) because of flow redistribution (13). The ideal therapy would target only the HP/HF vasculature, lowering PAP with no detrimental effects associated with increased flow. To date, it is unclear whether vasodilator therapies differentially affect these two different lung regions. Therefore, we aimed to (i) assess the activity of the NO pathway in PVS-induced PH during the transition from IpcPH to CpcPH, and (ii) investigate the effect of an NO donor and a PDE5 inhibitor on the HP/HF and HP/LF phenotypes separately. To investigate this, we used a recently developed swine model of post-capillary PH by pulmonary vein banding (PVB) (14–16) that slowly progresses from IpcPH to CpcPH (17). Chronic instrumentation allowed for repeated measurements of pulmonary haemodynamics in awake swine 5–12 weeks after PVB, during the progression of PH, while evaluating the activity of the NO pathway. Since exercise testing allows detection of perturbations in cardiopulmonary function that may not be apparent under resting conditions, which facilitates the assessment of disease severity (18), we performed measurements both at rest and during graded treadmill exercise.

METHODS

Animal Experimentation

All experiments were performed conforming to the "Guiding Principles in the Care and Use of Laboratory Animals," which are supported by the Council of the American Physiological Society, and with the approval of the Erasmus University Medical Centre Animal Care Committee (EMC3158, 109-13-09).

Outline of This Study

Non-restrictive inferior pulmonary vein banding (n = 7) or sham operation (n = 6) was performed on crossbred Landrace x Yorkshire swine of either sex (8 ± 2 kg). After 4 weeks, all 13 animals (23 ± 3 kg) underwent chronic instrumentation, allowing weekly haemodynamic measurements as well as determination of blood gases in awake animals. In the 8 weeks after chronic instrumentation, all animals performed biweekly exercise experiments, both under control conditions and in the presence of an endothelial nitric oxide synthase (eNOS) inhibitor. Animals also underwent two-weekly resting experiments, during which incremental doses of the NO donor sodium nitroprusside (SNP) were administered. After 12 weeks, a control exercise experiment was performed, followed by an exercise experiment after administration of the PDE5 inhibitor sildenafil. After completion of all experiments, in week 12, all 13 animals (61 ± 8 kg) were sacrificed, after which tissues were excised. Isolated small pulmonary arteries upstream of both banded (HP/LF) and unbanded (HP/HF) pulmonary veins were subsequently isolated, and responses to the NO donor and PDE5 inhibitor were assessed.

Pulmonary Vein Banding

Banding of the inferior venous confluent was performed on swine (n = 7, 9 ± 2 kg) as described by Pereda et al. (16). In short, swine received an intramuscular (i.m.) injection of tiletamine/zolazepam (5 mg kg^{-1}, Virbac, Barneveld, the Netherlands), xylazine, (2.25 mg kg^{-1}, AST Pharma, Oudewater, the Netherlands) and atropine (0.5

mg) for sedation, and were subsequently anaesthetised with an intravenous (i.v.) bolus of thiopental (10 mg kg^{-1} Rotexmedica, Trittau, Germany). After relaxation of the vocal chords, an endotracheal tube was inserted and secured and ventilation was started (O_2:N_2 (1:2)). Anaesthesia was maintained by adding isoflurane (2% vol/vol, Pharmachemie, Haarlem, the Netherlands) to the gas mixture. Prior to the banding procedure, antibiotic prophylaxis was administered (0.75 mL depomycine, 200.000 IU mL^{-1} procainebenzylpenicilline, 200 mg mL^{-1} dihydrostreptomycine, Intervet Schering-Plough, Boxmeer, the Netherlands). The skin on the right side of the animal was disinfected using iodine antiseptic solution, and the procedure was performed under sterile conditions. Through the fifth right intercostal space, the chest was opened and blunt dissection was used to expose and dissect the inferior venous confluence, which drains both inferior pulmonary lobes. Near the atrium, a surgical loop (Braun Medical Inc., Bethlehem, PA, USA) was placed around the inferior venous confluent and fixed at the resting diameter using a silk suture. To secure the ribs and close the thorax, non-absorbable USP6 braided polyester (Ø0.8 mm) was used and the skin was closed in layers using silk sutures. Administration of isoflurane was discontinued, allowing the animal to restore spontaneous ventilation, upon which the endotracheal tube was removed. Analgesia was administered by means of an i.m. injection (0.3 mg buprenorphine i.m. Indivior, Slough, UK) and a fentanyl slow-release patch (6 µg h^{-1}, 48 h). Once fully awake, animals were transferred back to the animal facilities. A sham procedure was performed on six additional swine (8 ± 2 kg) as described above, where the vein was exposed and dissected free, but not banded. One PVB animal died directly after the procedure because of acute pulmonary oedema at the onset of spontaneous ventilation. Another PVB animal suffered from severe HF and was prematurely sacrificed 6 weeks after banding. The numbers of animals reported in the methods section and the data presented in the results section do not include these animals. All sham animals completed the entire study.

Chronic instrumentation

The protocol for the chronic instrumentation performed has been previously described in great detail (19). In brief, swine were sedated, anaesthetised and

ventilated as described above, and the chest and pericardium were opened via the fourth left intercostal space under sterile conditions. To allow haemodynamic measurements and extraction of blood samples, fluid-filled polyvinylchloride catheters (Braun Medical Inc., Bethlehem, PA, USA) were inserted into the pulmonary artery (2×), the aortic arch, the left atrium (2×) and the right ventricle. A transit-time flow probe (Transonic Systems Inc., Ithaca, NY, USA) was also placed around the ascending aorta to allow measurement of cardiac output. All catheters were tunnelled to the back and the thorax and wound were closed. Anaesthesia was terminated and analgesia was administered (buprenorphine i.m. (0.3 mg) and a fentanyl slow-release patch (12 μg h^{-1}, 48 h)). Animals were allowed to recover and were transferred to the animal facilities once fully awake. Antibiotic prophylaxis was administered for seven consecutive days after the chronic instrumentation procedure in the form of 25 mg kg^{-1} amoxicillin i.v. (Centrafarm B.V. Etten-Leur, the Netherlands) and 5 mg kg^{-1} gentamycin i.v. (Eurovet, Bladel, the Netherlands).

Experimental Protocols

Experiments were performed at 6, 8, 10, and 12 weeks after PVB. Swine were placed on an adapted motor-driven treadmill and implanted catheters were connected to pressure transducers (Combitrans pressure transducers, Braun, Melsungen, Germany). Transducers and the transit-time flowprobe were connected to an amplifier. Cardiac output, heart rate and aortic, pulmonary arterial, right ventricular and left atrial blood pressures were continuously recorded. Haemodynamic measurements and blood samples were taken while the animal was resting quietly, after which a four-stage incremental treadmill exercise was initiated (1–4 km h^{-1}, 3 min per speed). At rest and during the last minute of each exercise stage, when haemodynamics were steady, haemodynamic measurements were performed, and blood samples were collected. After the exercise experiments, animals received 60 min of rest, to allow haemodynamics to return to baseline. Thereafter, the eNOS inhibitor N^{ω}-nitro-L-arginine (NLA; 20 mg kg^{-1}, dissolved in saline to 5 mg mL^{-1}) was administered by an infusion of 50 mg min^{-1} i.v. Ten minutes after complete NLA administration, the exercise experiment was repeated. On a different day, with a

minimum of 2 days in between, swine were transferred to a small enclosure and fluid-filled catheters were connected to pressure transducers and amplifiers, as described above. While resting quietly, haemodynamics were continuously recorded. After baseline measurements, sodium nitroprusside (SNP) was continuously administered in incremental doses of 0.5, 1, 2, 3, 4 and 5 μg kg^{-1} min^{-1} through the second fluid-filled catheter implanted in the main pulmonary artery. Each dose was administered for 10 min, and haemodynamic measurements were performed in the final minutes of each dose.

Flowprobe data of one PVB animal were not available because of technical failure. Consequently, the number of animals for flow-related parameters (cardiac output, stroke volume, vascular resistance) was reduced to six. One sham animal as well as one PVB animal suffered from recurrent lameness and did not perform all exercise experiments, resulting in an available group size of five sham animals and six PVB animals (five for PVB flow-related parameters).

Twelve weeks after PVB or sham operation, swine (PVB n = 4, Sham n = 5) were transferred to the treadmill, catheters were connected and an exercise experiment under control conditions was performed as described above. After 60 min of rest, allowing haemodynamics to return to baseline, 10 mg of the PDE5 inhibitor sildenafil was administered in 10 min through the second catheter implanted in the main pulmonary artery. Ten minutes after completion of administration, the exercise protocol was repeated.

Blood Gas Measurements

pO_2 (mmHg) was determined in the collected arterial blood samples using a blood gas analyser (ABL 800, Radiometer, Denmark).

Data Analysis

Haemodynamic data were recorded digitally and analysed offline, as described previously (20). CO was corrected for bodyweight (cardiac index, CI). Total pulmonary vascular resistance index (tPVRi) and systemic vascular resistance index

(SVRi) were calculated as the ratio of mPAP and CI and MAP and CI, respectively. Stroke volume index was calculated as CI/heart rate.

Sacrifice

After completion of follow-up, 12 weeks after PVB or sham surgery, animals were sacrificed. Animals were sedated, as described above, and anaesthetised with pentobarbital sodium (i.v. 6–12 mg kg^{-1} h^{-1}). After intubation, animals were ventilated with a mixture of O_2 and N_2 (1:2). Sternotomy was performed to expose the heart and lungs. Ventilation was terminated, and the heart was arrested and immediately excised together with the lungs. Parts of the upper (cranial) and lower (caudal) lobe of the right lung were placed in cold Krebs buffer for dissection of pulmonary small arteries for wire-myograph experiments, and parts were snap-frozen for protein isolation to determine eNOS expression.

Wire-Myograph Experiments

In vitro pulmonary vessel experiments were performed as described previously (21,22). Briefly, pulmonary small arteries were isolated and stored overnight in oxygenated (95% O_2/5% CO_2) Krebs bicarbonate solution (composition in mM: 118 NaCl, 4.7 KCl, 2.5 $CaCl_2$, 1.2 $MgSO_4$, 1.2 KH_2PO_4, 25 $NaHCO_3$, glucose 8.3; pH 7.4) at 4 °C. The following day, segments 2 mm in length were cut and installed on wire myographs in separate organ baths filled with oxygenated Krebs bicarbonate solution at 37 °C. Following a half hour stabilisation period, internal vessel diameter was set to a tension equivalent to 0.9 times the estimated diameter at 20 mmHg effective transmural force. Vessels were exposed to 100 nM of the synthetic thromboxane analogue U46619 to induce pre-constriction, and endothelial integrity was ascertained subsequently by exposure to the endothelium-dependent vasodilator substance P (10 nM). To test maximal constriction, 100 mM KCl was administered, after which the vessels were washed and allowed to stabilise in fresh buffer solution for half an hour. After preconstriction with 100 nM U46619, vessels were subjected to one of three experimental protocols: incremental concentrations of the NO donor SNP (10^{-9}–10^{-5} M); the PDE5 inhibitor sildenafil (10^{-10}–10^{-5} M); or the endothelium-

dependent vasodilator bradykinin (10^{-10}–10^{-7} M), in the absence or presence of pre-incubation with L-N$^{\omega}$-nitroarginine methyl ester (L-NAME, 10^{-4} M), 30 min before administrating bradykinin. In each protocol, four–six vessel segments per lobe per group were used.

The designated software was used to analyse data (Labchart 8.0, AD instruments, Sydney, Australia) and to create concentration response curves (Prism 5.0, Graphpad Software, Inc., La Jolla, CA, USA).

eNOS Protein Expression

Snap-frozen lung samples were homogenised to determine total eNOS protein expression, as well as eNOS monomer and dimer protein expression. For eNOS monomer and dimer fraction detection, low temperature sodium dodecyl sulfate–polyacrylamide gel electrophoresis (SDS-PAGE) was performed, as described previously (23). In brief, all gels and buffers were equilibrated at 4 °C before electrophoresis, and during electrophoresis, the buffer tank was placed in an ice bath to maintain low temperature. SDS-PAGE for total eNOS protein content and housekeeping protein α-tubulin was performed at room temperature. Subsequently, the proteins were transferred to nitrocellulose membranes and the blots were probed with primary, anti-eNOS (1:500, Transduction Laboratory) and anti-α-tubulin (1:10,000, Imgenex). All blots were analysed using the Odyssey system (LI-COR). Band intensities were determined, and the ratio of the intensity of the eNOS monomer and dimer as well as eNOS and α-tubulin were calculated and expressed as arbitrary units (A.U.). Monomer:α-tubulin and dimer:α-tubulin were calculated as monomer ÷ (monomer + dimer) × eNOS ÷ α-tubulin and dimer ÷ (monomer + dimer) × eNOS ÷ α-tubulin, respectively.

Statistical Analysis

Statistical analyses were performed using SPSS (version 21.0 IBM, Armonk, NY, USA) and comprised unpaired (two tailed) *t*-test, or one-way or two-way ANOVA for repeated measures, followed by post-hoc testing with Bonferroni when appropriate. Statistical analyses on concentration response curves consisted of regression

analyses using Prism (version 5, GraphPad Software, La Jolla, CA, USA). Data were considered statistically significant when $p \leq 0.05$ (two-tailed). Data are presented as means ± SEM.

RESULTS

Induction of Pulmonary Hypertension

Pulmonary vein banding resulted in an increased tPVRi as early as 6 weeks after banding (Table 1, 132 ± 4 vs. 107 ± 9 mmHg L^{-1} min kg in sham ($p \leq 0.05$)). Together with the maintained CI, this resulted in an increased mPAP (Table 1, 30 ± 2 vs. 20 ± 1 mmHg in sham ($p \leq 0.001$)). Both tPVRi and mPAP increased over time (tPVRi week 12: 244 ± 26 vs. 116 ± 10 mmHg L^{-1} min kg in sham ($p \leq 0.01$)), mPAP week 12: 39 ± 2 vs. 20 ± 1 mmHg in sham ($p \leq 0.001$)), reflecting the progressive nature of PH. Pulmonary vein banding had minor effects on the systemic circulation at rest, as only MAP tended to be lower 12 weeks after banding, while LAP, HR, CI, SVi and SVRi were unaltered compared to sham (Table 1).

Response to Exercise

Exercise up to 4 km h^{-1} produced an increase in mPAP in sham animals that was the consequence of an increased CI and LAP and a maintained tPVRi (Table 1). The exercise-induced increase in LAP was similar in the PVB animals, although, 8 weeks after banding, LAP was lower in PVB compared to sham. From week 6 until week 10, the exercise-induced increase in CI (Table 1) was similar in PVB compared to sham animals, although the CI during exercise was lower in PVB in week 10 as compared to week 6. Furthermore, in week 12, CI was lower during exercise in PVB animals than in sham animals (Table 1, CI at 4 km h^{-1}: 0.23 ± 0.01 vs. 0.28 ± 0.02 $p \leq 0.05$), which was principally due to an attenuated exercise-induced increase in heart rate in PVB animals compared to sham animals (Table 1, heart rate at 4 km h^{-1}: 207 ± 6 vs. 251 ± 10 beats min^{-1} $p \leq 0.05$). Despite this attenuated increase in CI, the exercise-induced increase in mPAP was similar in PVB compared to sham animals, as a result of the higher tPVRi in PVB animals that was only significantly elevated further by exercise in week 6 (Table 1).

Table 1: Hemodynamics at rest and during exercise over the development of post capillary PH.

				Week								
	n	Group		6		8		10		12		
MAP	5	Sham	Rest	90 ± 1		81 ± 4		92 ± 5		95 ± 4		
(mmHg)	5		Exercise	93 ± 4		92 ± 5		98 ± 4		102 ± 3		
	6	PVB	Rest	86 ± 5		85 ± 4		80 ± 4		86 ± 3		(†)
	6		Exercise	90 ± 2		88 ± 3		83 ± 4	†	86 ± 7		(†)
LAP	5	Sham	Rest	6.0 ± 2.1		3.8 ± 1.2		4.0 ± 1.2		3.1 ± 1.0		
(mmHg)	5		Exercise	9.5 ± 1.2		9.0 ± 0.8	*	7.9 ± 0.9	(*)	10.1 ± 1.1		*
	6	PVB	Rest	4.1 ± 0.9		3.5 ± 1.3		6.4 ± 1.3		7.1 ± 1.6		
	6		Exercise	7.2 ± 0.9	*	5.9 ± 0.8	†	10.1 ± 1.7		12.8 ± 1.9		*(‡)
mPAP	5	Sham	Rest	20 ± 1		17 ± 2		22 ± 1		20 ± 1		
(mmHg)	5		Exercise	34 ± 1	*	31 ± 1	*	32 ± 2	*	35 ± 3		*
	6	PVB	Rest	30 ± 2	†	31 ± 2	†	36 ± 3	†	39 ± 2		†‡
	6		Exercise	51 ± 2	†*	56 ± 3	†*	56 ± 2	†*	62 ± 3		†*‡
HR	5	Sham	Rest	152 ± 12		136 ± 10		138 ± 12		132 ± 9		
(bpm)	5		Exercise	259 ± 10	*	228 ± 15	*	243 ± 19	*	251 ± 10		*
	5	PVB	Rest	147 ± 8		139 ± 4		136 ± 10		135 ± 5		
	5		Exercise	246 ± 11	*	238 ± 11	*	206 ± 8	(†)*‡	207 ± 6		†*‡
CI	5	Sham	Rest	0.19 ± 0.01		0.19 ± 0.01		0.19 ± 0.01		0.17 ± 0.01		
($l\ min^{-1}\ kg^{-1}$)	5		Exercise	0.32 ± 0.01	*	0.30 ± 0.01	*	0.29 ± 0.02	*	0.28 ± 0.02		*
	5	PVB	Rest	0.21 ± 0.01		0.19 ± 0.01		0.18 ± 0.02		0.16 ± 0.01		(‡)
	5		Exercise	0.32 ± 0.01	*	0.28 ± 0.02	*	0.25 ± 0.01	*‡	0.23 ± 0.01		†*‡

SVi	5	Sham	Rest	1.30	±	0.09		1.39	±	0.09		1.41	±	0.13		1.31	±	0.11	
(ml kg^{-1})	5		Exercise	1.26	±	0.06		1.36	±	0.11		1.23	±	0.14		1.11	±	0.10	
	5	PVB	Rest	1.41	±	0.09		1.35	±	0.09		1.38	±	0.05		1.21	±	0.06	
	5		Exercise	1.26	±	0.06		1.19	±	0.05		1.25	±	0.06		1.10	±	0.06	
SVRi	5	Sham	Rest	472	±	18		439	±	28		488	±	24		562	±	26	(‡)
(mmHg l^{-1} min kg)	5		Exercise	288	±	13	*	309	±	22	*	340	±	22	*	378	±	27	*(‡)
	5	PVB	Rest	390	±	32	†	471	±	52		455	±	59		534	±	38	(‡)
	5		Exercise	270	±	13	*	319	±	27	*	325	±	24	(*)	391	±	45	*
tPVRi	5	Sham	Rest	107	±	9		94	±	11		118	±	7		116	±	10	
(mmHg l^{-1} min kg)	5		Exercise	106	±	6		105	±	7		111	±	10		128	±	11	
	5	PVB	Rest	132	±	4	†	169	±	14	†	192	±	12	†‡	244	±	26	†‡
	5		Exercise	155	±	7	†*	201	±	16	†(‡)	218	±	11	†‡	274	±	14	†‡
pO_{2art}	5	Sham	Rest	98	±	4		102	±	4		103	±	4		102	±	4	
(mmHg)	5		Exercise	84	±	4	*	86	±	3	*	87	±	3	*	92	±	5	
	6	PVB	Rest	92	±	5		87	±	5	†	88	±	3	†	88	±	3	†
	6		Exercise	68	±	3	†*	63	±	2	†*	66	±	3	†*	65	±	3	†*

Hemodynamics obtained 6, 8, 10 and 12 weeks after banding at rest and during exercise (4 km hr^{-1}). MAP: Mean Arterial Pressure, LAP: mean Left Atrial Pressure, mPAP: mean Pulmonary Arterial Pressure, HR: Heart Rate, CI: Cardiac Index, SVi: Stroke Volume index (CI/HR), SVRi: Systemic Vascular Resistance index (MAP/CI), tPVRi: total Pulmonary Vascular Resistance index (mPAP/CI), pO_{2art}: Arterial partial oxygen pressure. Data are means ± SEM. *P≤0.05 vs rest, ‡P≤0.05 vs week 6, †P≤0.05 vs sham. ()P≤0.1

Nitric Oxide Production and Sensitivity

To assess the vasoactive effect of endogenous NO production, the eNOS inhibitor NLA was administered. In week 6 and 8, vasoconstriction response to NLA was similar in PVB and sham animals, reflected by the similar increase in SVRi and tPVRi both at rest and during exercise (Figures 1 and 2). While in week 10 and 12, the increase in SVRi upon NLA administration was similar in PVB and sham, the increase in tPVRi was significantly more pronounced in PVB animals, especially during exercise (Figure 2), suggesting an augmented, exercise-induced increase of NO production. To investigate NO sensitivity, the NO donor SNP was administered (0.5–5 μg kg^{-1} min^{-1}). While systemic sensitivity to SNP was transiently lower in PVB animals at week 6, there was no statistically significant difference in ΔSVRi, and thus NO sensitivity, at weeks 8, 10 or 12. In the pulmonary vasculature however, the NO sensitivity was significantly increased in PVB animals at week 10, and tended to be increased at week 12 (p = 0.09, Figure 2). Our data suggest that both endogenous NO production during exercise and NO sensitivity were increased after PVB.

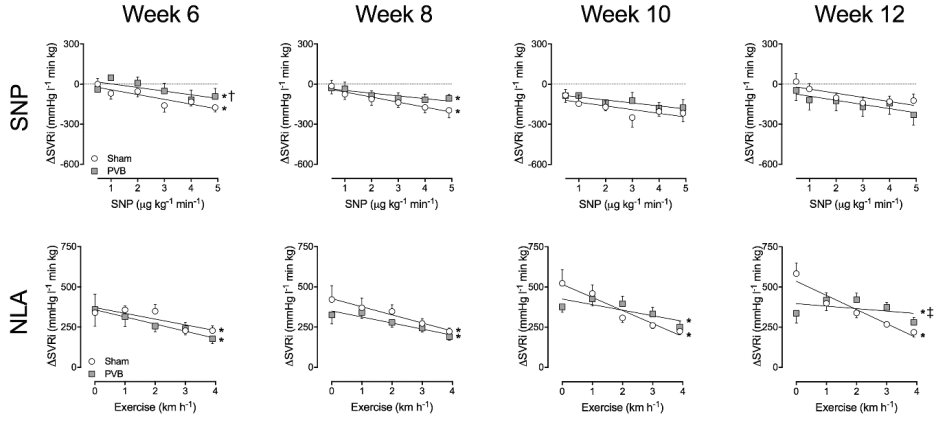

Figure 1. Systemic vasodilation by different doses of the nitric oxide donor sodium nitroprusside (SNP, upper panel), and the endothelial nitric oxide synthase inhibitor Nω-nitro-L-arginine (NLA). Data is at rest and during graded treadmill exercise (lower panels) at 6, 8, 10 and 12 weeks after pulmonary vein banding (PVB) or sham surgery. ΔSVRi: Change in systemic vascular resistance index; * p ≤ 0.05 effect exercise; † p ≤ 0.05 vs. sham; ‡ p ≤ 0.05 effect exercise PVB vs. effect exercise sham by two-way ANOVA. Values are means ± SEM.

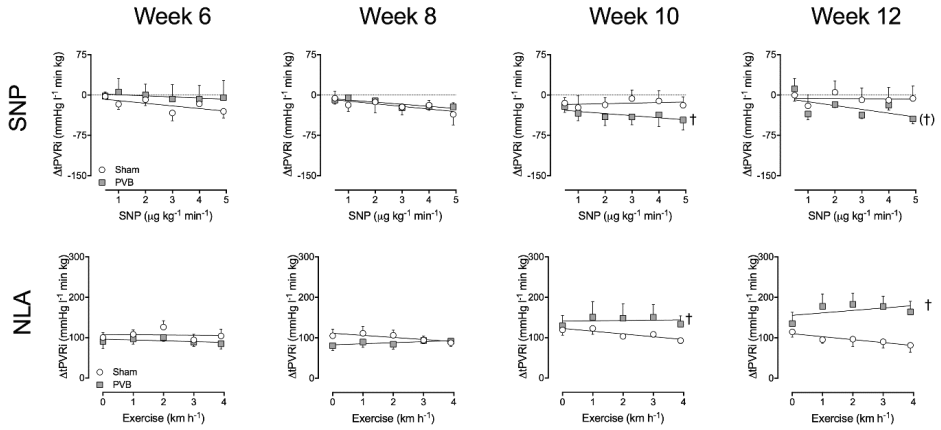

Figure 2. Pulmonary vasodilation by different doses of the nitric oxide donor sodium nitroprusside (SNP, upper panel), and the endothelial nitric oxide synthase inhibitor Nω-nitro-L-arginine (NLA). Data is at rest and during graded treadmill exercise (lower panels) at 6, 8, 10 and 12 weeks after pulmonary vein banding (PVB) or sham surgery. ΔtPVRi: Change in total pulmonary vascular resistance index; * $p \leq 0.05$ effect exercise; † $p \leq 0.05$, (†) $p \leq 0.10$ vs. sham. Values are means ± SEM.

5

Contribution of PDE5

To test if the increased sensitivity to NO was due to a decreased PDE5 activity, the PDE5 inhibitor sildenafil was administered at week 12. In sham animals, PDE5 inhibition resulted in a small decrease in SVRi and tPVRi at rest, as well as during exercise (Figure 3). In PVB animals, PDE5 inhibition resulted in considerable vasodilation in both the systemic and pulmonary vasculature at rest. During exercise, this effect waned in the systemic vasculature, but was unaltered in the pulmonary vasculature. This indicates that the increased NO sensitivity cannot be attributed to decreased PDE5 activity. Importantly, pulmonary vasodilation due to sildenafil was not accompanied by a further decrease in pO_{2art} (Figure 3), indicating that sildenafil did not induce pulmonary oedema.

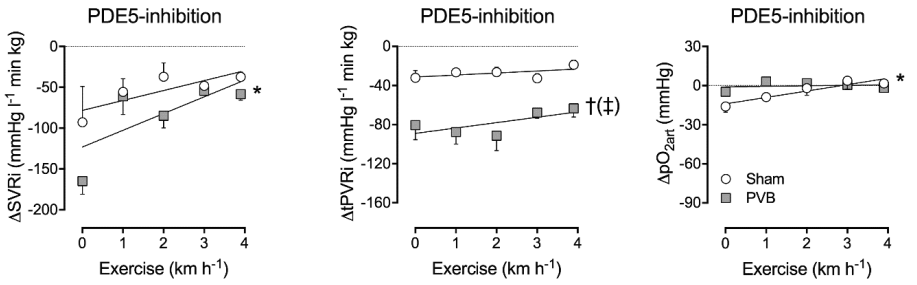

Figure 3. Effect of PDE5-inhibition. Changes in systemic vascular resistance index (ΔSVRi, left panel), total pulmonary vascular resistance index (ΔtPVRi, middle panel) and arterial partial oxygen pressure (ΔpO_{2art}, right panel), induced by vasodilation to phosphodiesterase-5 (PDE5) inhibitor sildenafil, at rest and during graded treadmill exercise. * $p \leq 0.05$ effect exercise; † $p \leq 0.05$ vs. sham; (‡) $p \leq 0.10$ effect exercise PVB different from effect exercise sham by two-way ANOVA. Values are means ± SEM.

Regional Differences in NO Pathway

To test the NO pathway separately in the HP/LF and HP/HF vasculature, isolated pulmonary small arteries from the HP/LF (caudal, banded) and HP/HF (cranial, unbanded) pulmonary lobes were pre-constricted with U46619, and subjected to incremental doses of SNP or sildenafil. SNP produced a similar dose-dependent vasodilation in pulmonary small arteries from HP/LF and HP/HF lobes of PVB animals, compared to pulmonary small arteries from corresponding lobes of sham animals (Figure 4). PDE5 inhibition with sildenafil produced a similar vasodilation in pulmonary small arteries between PVB HP/LF lobes and sham. However, pulmonary small arteries from PVB HP/HF lobes showed a smaller vasodilation than sham, suggesting a lower PDE5 activity in HP/HF lobes (Figure 4). Vasodilation response to bradykinin was similar in pulmonary small arteries from PVB HP/HF and sham, but was lower in PVB HP/LF as compared to sham. Prior inhibition of eNOS by L-NAME decreased the response to bradykinin to a similar extent in all vessels from PVB and sham animals (Figure 4). Thus, the difference in response to bradykinin between pulmonary small arteries from PVB HP/LF and sham persisted, suggesting that the decreased vasodilation response to bradykinin was NO-independent.

Total eNOS expression was similar in the HP/LF (banded) lobe as compared to upper and lower lobes from sham animals, while eNOS expression was significantly higher

in the HP/HF as compared to the HP/LF lobes (Figure 5). The eNOS monomer:dimer ratio was not altered by PVB, but, due to the higher expression in HP/HF, both eNOS monomer and dimer were increased as compared to the HP/LF territory.

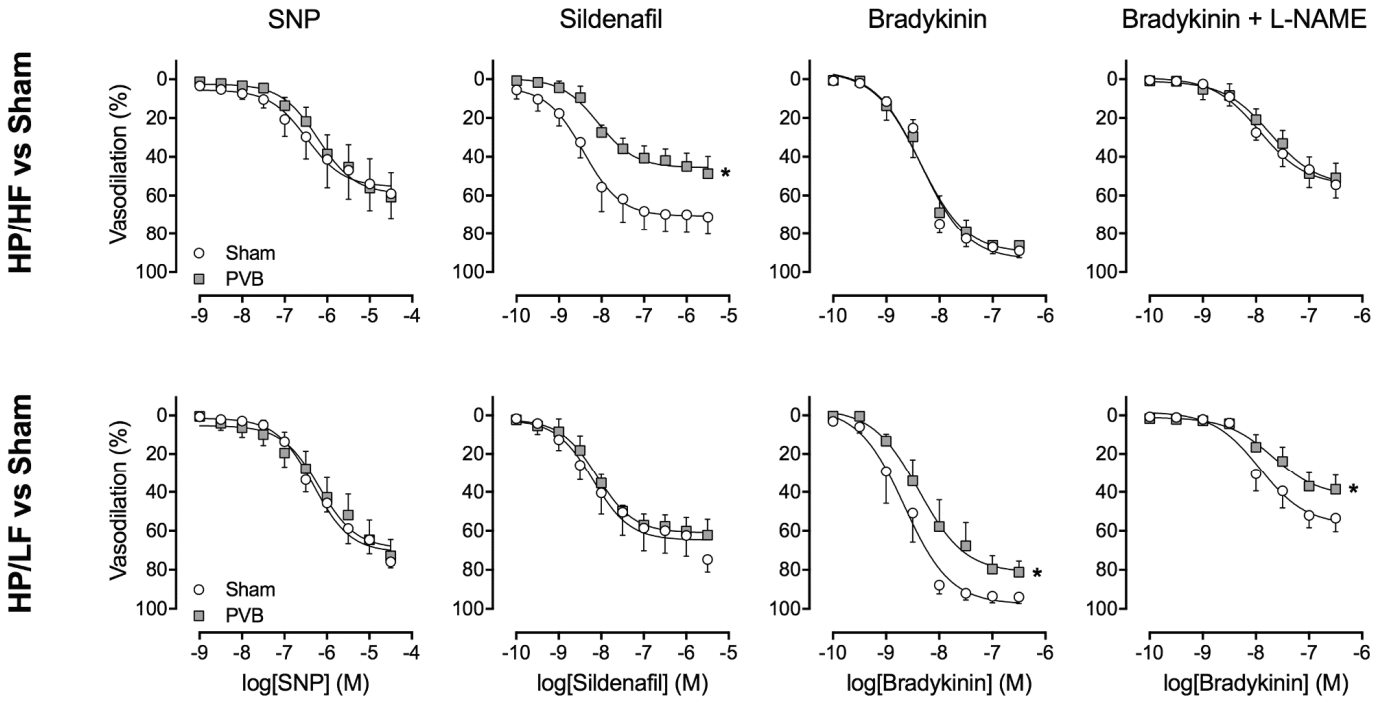

Figure 4. Ex-vivo vasodilation of small pulmonary arteries taken from different regions. Small pulmonary arteries of the high pressure/high flow (HP/HF) and high pressure/low flow (HP/LF) territories of pulmonary vein banding (PVB) swine, or small pulmonary arteries from corresponding lobes of sham animals, were isolated, pre-constricted by u46619 and exposed to incremental doses of the nitric oxide donor sodium nitroprusside (SNP), phosphodiesterase-5 (PDE5) inhibitor sildenafil or bradykinin with or without prior inhibition of endothelial nitric oxide synthase by L-N$^{\omega}$-nitroarginine methyl ester (L-NAME). Data are presented as percentages of preconstriction with U46619. * $p \leq 0.05$ vs. corresponding sham, by regression analyses. Values are means ± SEM.

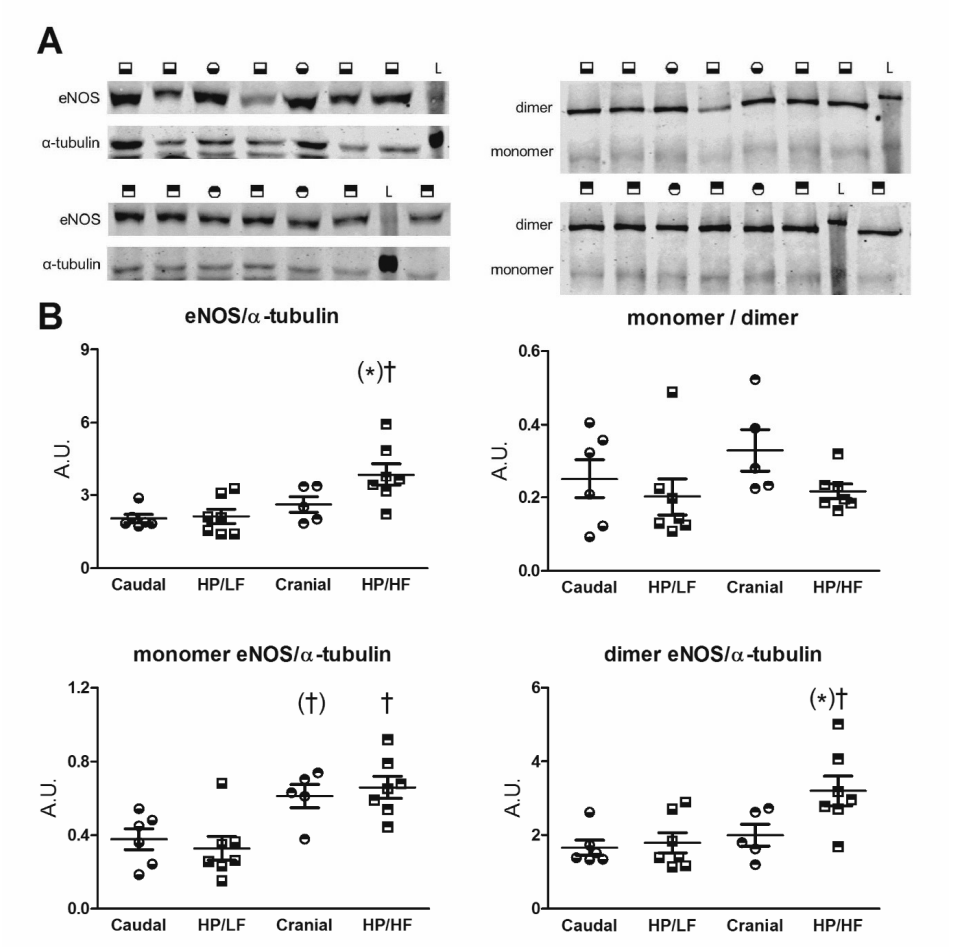

Figure 5. Gene expression in different regions of the lungs. Endothelial nitric oxide syntase eNOS protein expression in lung tissue of the high pressure/high flow (HP/HF) and high pressure/low flow (HP/LF) territories of pulmonary vein banding (PVB) swine, and corresponding caudal and cranial lobes from sham-operated swine. A) typical examples of original blots, with symbols correponding to B, denoting the different lung territories and L denoting the ladder. B) Detection of eNOS monomer and dimer fractions with low temperature sodium dodecyl sulfate–polyacrylamide gel electrophoresis (SDS-PAGE) showed that monomer:dimer ratio was unaltered, while both eNOS monomer and dimer were higher in HP/HF as compared to HP/LF, but the eNOS dimer only tended to be higher in HP/HF vs. corresponding sham. Data are presented as arbitrary units (A.U.) defined as the ratio of intensity of the eNOS band and the α-tubulin band or the eNOS monomer and dimer bands. Data are shown as dotplots. Lines denote means ± SEM. (*) $p \leq 0.10$ vs. corresponding sham (caudal or cranial), † $p \leq 0.05$, (†) $p \leq 0.10$ HP/HF vs. HP/LF or cranial vs. caudal by two-way ANOVA.

DISCUSSION

The main findings in this study were that (i) banding of the confluence of the lower pulmonary veins in swine resulted in PH; (ii) 10 weeks after banding, pulmonary vasodilation response to exogenous NO was higher in PVB as compared to sham in vivo; (iii) the endogenous NO-mediated vasodilator influence was significantly higher in the pulmonary vasculature of PVB as compared to sham animals and the difference increased over time, particularly during exercise, which was accompanied by a higher eNOS expression in the PVB HP/HF territory; (iv) the pulmonary vasodilation in response to PDE5 inhibition was enhanced in PVB as compared to sham animals both at rest and during exercise; (v) sensitivity of isolated pulmonary small arteries to NO donor SNP was similar in PVB vs. sham irrespective of HP/LF and HP/LF; (vi) sensitivity to PDE5 inhibitor sildenafil was similar in PVB HP/LF vs. sham but lower in PVB HP/HF; (vii) vasodilation to bradykinin was similar in PVB HP/HF and sham, but was lower in PVB HP/LF; (viii) this decreased response to bradykinin was NO-independent. The implications of our findings are discussed below.

Pulmonary Hypertension Associated with PVS

Although PVS is a rare phenomenon, the frequency of PH in PVS is very high, being up to 67% as reported by Mahgoub et al. (7), and right heart failure is the most common cause of death in this population. Treatment of PVS currently consists of either surgical pulmonary venoplasty, or a catheter-based approach like balloon angioplasty with or without intravascular stent placement. Unfortunately, treatment of PVS is technically challenging; restenosis is frequent and event-free survival is poor (4). A French cohort of premature infants with PVS and PH reported a 44% mortality 1 year after diagnosis (8). Despite the small number of enrolled patients, they were able to analyse 1-year survival in patients that received any type of intervention (69%) vs. patients that received no intervention (21%). A recently published multicentre retrospective cohort study of PVS affecting ex-premature infants (7) and a meta-analysis (4) found similar survival rates—between 55 and 70%. These studies identified a number of risk factors that result in decreased survival and increased risk

of restenosis; among them were the number of stenotic pulmonary veins (three or more affected veins had poorer outcome then two or fewer stenotic pulmonary veins), bilateral disease and small body size for gestational age. Another important determinant of mortality is the severity of PH and concomitant RV dysfunction (24).
PH secondary to PVS is classified as group II PH because of the post-capillary position of the stenosis, which results in a left ventricular inflow tract obstruction. The IpcPH that is the result of hampered outflow from the lungs to the LV may ultimately affect the pulmonary vasculature and lead to CpcPH, characterised by pre-capillary structural and functional vascular remodelling resembling pulmonary arterial hypertension (PAH; WHO classification group I PH) (9–11). Similarly, in our swine model, PVS led to PH and RV dysfunction (14–16). At first, PVS-induced PH was a purely passive increase in pulmonary pressure and resistance (IpcPH), but within 12 weeks, structural and functional remodelling of the pulmonary vasculature introduced a pre-capillary component, producing CpcPH (14,17).
Most patients with PVS (25), as well as swine with PVS (15), show a decrease in pulmonary artery pressure upon vasoreactivity testing with inhaled 100% oxygen. In our previous study, we showed that $ET_{A/B}$ blockade with tezosentan resulted in a decrease in tPVRi in swine with PVB, and that this vasodilator effect increased over time (17). In the present study, the NO donor SNP and the PDE5 inhibitor sildenafil both induced pulmonary vasodilation that was larger in swine with PVB. However, the effect of SNP was relatively modest as compared to the reduction in tPVRi induced by PDE5 inhibition. Although it could be suggested that the dosage of SNP should be further increased to increase its effect, this was not possible, given its potent hypotensive effect on the systemic vasculature. Together with the observations that eNOS inhibition produced a larger increase in tPVRi in PVB as compared to sham, and the relatively modest vasodilation induced by SNP as compared to PDE5 inhibition, this suggests that the NO pathway is hyperactive in PVB pulmonary vasculature, probably as a compensatory mechanism, and that adding additional NO has a very limited effect. These data are consistent with the study of Domingo et al., which showed that NO on top of 100% oxygen did not induce further pulmonary vasodilation (25). Interestingly, eNOS expression was higher in HP/HF as compared to HP/LF, and tended to be higher compared to the corresponding lung lobe of sham

animals. This increased expression predominantly involved a higher expression of the NO-producing eNOS dimer, as the superoxide-producing eNOS monomer was higher in HP/HF as compared to HP/LF, but was similar in the corresponding lobes of sham animals.

In group II PH, extreme caution should be taken in the utilisation of vasodilation therapy. The guidelines for the diagnosis and treatment of pulmonary hypertension are very clear in their advice to treat only the underlying disease in group II PH (26), because an increase in flow may result in an increase in pulmonary capillary pressure and ensuing pulmonary oedema. It is, however, important to realise that in PVS, the pulmonary vasculature comprises two territories; those draining into stenotic pulmonary veins, and those draining into unaffected pulmonary veins. While the pulmonary vasculature in the first territory will experience high pressure and low flow, the latter experiences high pressure and high flow. Issues regarding pulmonary oedema that arise in treatment of PH secondary to left heart failure may be absent when treating only the HP/HF vasculature in PVS-induced PH.

This model is unique in its ability to allow for independent interrogation of these two subsets of arteries. We have previously shown that in this model, PVB leads to increased wall thickness, increased wall:lumen ratio and a decreased relative lumen area in pulmonary small arteries from both the HP/HF and HP/LF territories (17). This structural remodelling was accompanied by increases in maximal constriction to KCl and U46619 in all pulmonary small arteries, irrespective of flow. Interestingly, in the present study, vasodilation in response to bradykinin was smaller in pulmonary small arteries from the PVB HP/LF territory than sham, while pulmonary small arteries from the HP/HF territory did not show a difference as compared to sham (Figure 4). These data are consistent with our previous observation that vasodilation to Substance P, a measure for endothelial function, was only decreased in PVB HP/LF lobes (17). These data suggest endothelial dysfunction in PVS, but mainly in the HP/LF territory. To further test whether this endothelial dysfunction comprised a change in NO, we also investigated bradykinin-induced vasodilation after administration of the eNOS inhibitor L-NAME. However, L-NAME attenuated the bradykinin-induced vasodilation to a similar extent in pulmonary small arteries from all territories, suggesting that the decreased vasodilation to bradykinin was NO-

independent. This is consistent with unchanged eNOS protein expression in the HP/LF lobes compared to sham. Bradykinin also exerts a vasodilator effect via endothelium-derived hyperpolarizing factor and via prostacyclin. The decreased vasodilation to bradykinin in the PVB HP/LF territory was thus the result of either decreased endothelium-derived hyperpolarizing factor or decreased prostacyclin. It could therefore be speculated that prostacyclin therapy would mainly target the HP/HF vasculature, and could be the therapy of choice for PVS-induced PH. As we did not directly test the effect of prostacyclin therapy in vivo or in vitro, future studies are needed to assess this possibility.

This study was the first to test the effect of two first-line therapies, i.e., the NO donor SNP and PDE5 inhibitor sildenafil, separately in the unaffected HP/HF and the affected HP/LF vasculatures. The vasodilator effect of the NO donor was not different in the HP/HF PVB upper vs. the HP/LF PVB lower lobes. There was, however, a difference in efficacy of PDE5 inhibition by sildenafil. Unfortunately, the effect was bigger in the HP/LF vasculature. Although this is theoretically unfavourable, we did not find any evidence for pulmonary oedema in vivo (no reduction in arterial pO_2, Figure 3). The reduced effect of sildenafil in vitro could potentially be explained by the lack of flow in the in vitro experiments. It is possible that in vivo, in the presence of flow, shear-stress-induced NO production is higher in the HP/HF territories as compared to the HP/LF territories, and, consequently, that an increase in cGMP in response to PDE5 inhibition may be more pronounced in the HP/HF territories. In group I PH, vascular narrowing is also believed to be heterogeneous. Rol et al. found that in idiopathic PAH patients, only 30% of the vessels have a reduced inner diameter (27). These vessels will be HP/LF, while the remaining 70% of the vasculature will be HP/HF. The difference from PVS-induced PH is that in group I PH, the HP/LF vasculature should be targeted. Extrapolation of our results could possibly explain the efficacy of PDE5 inhibition in PAH.

Clinical Relevance

Both surgical and catheter-based treatments of PVS in the paediatric population are challenging, and restenosis is frequent. However, it is currently the only option to prolong survival for severe progressive PVS. Pulmonary vasodilators could reduce RV afterload and postpone the need for surgery, but may induce pulmonary oedema, particularly when vasodilation occurs in both stenotic and unaffected territories. Currently, approximately 30% of paediatric patients with PVS are on pulmonary vasodilator treatment, with sildenafil being the most commonly administered drug (7,24). Our study showed that, although the pulmonary small arteries from the HP/LF territories respond better to sildenafil in vitro than those from HP/HF territories, sildenafil treatment did not result in overt pulmonary oedema in vivo. Currently, there have been no studies comparing the effects of different vasoactive drugs as treatment for PVS-induced PH. We previously showed that $ET_{A/B}$ blockade with tezosentan also induced pulmonary vasodilation. However, the pulmonary vasodilator effect of sildenafil in the present study was approximately twice as big as the pulmonary vasodilation induced by tezosentan. Similarly, the effect of sildenafil was larger than that of the NO donor SNP. Hence, sildenafil should be the treatment of choice for PVS-induced PH.

REFERENCES

1. Galie, N.; Humbert, M.; Vachiery, J.L.; Gibbs, S.; Lang, I.; Torbicki, A.; Simonneau, G.; Peacock, A.; Vonk Noordegraaf, A.; Beghetti, M.; et al. 2015 ESC/ERS Guidelines for the Diagnosis and Treatment of Pulmonary Hypertension. Rev. Esp. Cardiol. 2016, 69, 177.
2. Rosenkranz, S.; Gibbs, J.S.; Wachter, R.; De Marco, T.; Vonk-Noordegraaf, A.; Vachiery, J.L. Left ventricular heart failure and pulmonary hypertension. Eur. Heart J. 2016, 37, 942–954.
3. Cappato, R. Pulmonary Vein Stenosis Following Radiofrequency Ablation of Atrial Fibrillation: Has It Become a Clinically Negligible Complication? JACC Clin. Electrophysiol. 2017, 3, 599–601.
4. Backes, C.H.; Nealon, E.; Armstrong, A.K.; Cua, C.L.; Mitchell, C.; Krishnan, U.; Vanderlaan, R.D.; Song, M.K.; Viola, N.; Smith, C.V.; et al. Pulmonary Vein Stenosis in Infants: A Systematic Review, Meta-Analysis, and Meta-Regression. J. Pediatr. 2018, 198, 36–45.e3.
5. Seale, A.N.; Webber, S.A.; Uemura, H.; Partridge, J.; Roughton, M.; Ho, S.Y.; McCarthy, K.P.; Jones, S.; Shaughnessy, L.; Sunnegardh, J.; et al. Pulmonary vein stenosis: The UK, Ireland and Sweden collaborative study. Heart 2009, 95, 1944–1949.
6. Gowda, S.; Bhat, D.; Feng, Z.; Chang, C.H.; Ross, R.D. Pulmonary vein stenosis with Down syndrome: A rare and frequently fatal cause of pulmonary hypertension in infants and children. Congenit. Heart Dis. 2014, 9, E90–E97.
7. Mahgoub, L.; Kaddoura, T.; Kameny, A.R.; Lopez Ortego, P.; Vanderlaan, R.D.; Kakadekar, A.; Dicke, F.; Rebeyka, I.; Calderone, C.A.; Redington, A.; et al. Pulmonary vein stenosis of ex-premature infants with pulmonary hypertension and bronchopulmonary dysplasia, epidemiology, and survival from a multicenter cohort. Pediatr. Pulmonol. 2017, 52, 1063–1070.
8. Laux, D.; Rocchisani, M.A.; Boudjemline, Y.; Gouton, M.; Bonnet, D.; Ovaert, C. Pulmonary Hypertension in the Preterm Infant with Chronic Lung Disease can be Caused by Pulmonary Vein Stenosis: A Must-Know Entity. Pediatr. Cardiol. 2016, 37, 313–321.
9. Gerges, M.; Gerges, C.; Pistritto, A.M.; Lang, M.B.; Trip, P.; Jakowitsch, J.; Binder, T.; Lang, I.M. Pulmonary Hypertension in Heart Failure. Epidemiology, Right Ventricular Function, and Survival. Am. J. Respir. Crit. Care Med. 2015, 192, 1234–1246.
10. Miller, W.L.; Grill, D.E.; Borlaug, B.A. Clinical features, hemodynamics, and outcomes of pulmonary hypertension due to chronic heart failure with reduced ejection fraction: Pulmonary hypertension and heart failure. JACC Heart Fail. 2013, 1, 290–299.
11. Vanderpool, R.R.; Naeije, R. Progress in Pulmonary Hypertension with Left Heart Failure. Beyond New Definitions and Acronyms. Am. J. Respir. Crit. Care Med. 2015, 192, 1152–1154.
12. Lundgren, J.; Radegran, G. Pathophysiology and potential treatments of pulmonary hypertension due to systolic left heart failure. Acta Physiol. 2014, 211, 314–333.
13. Roman, K.S.; Kellenberger, C.J.; Macgowan, C.K.; Coles, J.; Redington, A.N.; Benson, L.N.; Yoo, S.J. How is pulmonary arterial blood flow affected by pulmonary venous obstruction in children? A phase-contrast magnetic resonance study. Pediatr. Radiol. 2005, 35, 580–586.

14. Aguero, J.; Ishikawa, K.; Hadri, L.; Santos-Gallego, C.; Fish, K.; Hammoudi, N.; Chaanine, A.; Torquato, S.; Naim, C.; Ibanez, B.; et al. Characterization of right ventricular remodeling and failure in a chronic pulmonary hypertension model. Am. J. Physiol. Heart Circ. Physiol. 2014, 307, H1204–H1215.

15. Garcia-Alvarez, A.; Fernandez-Friera, L.; Garcia-Ruiz, J.M.; Nuno-Ayala, M.; Pereda, D.; Fernandez-Jimenez, R.; Guzman, G.; Sanchez-Quintana, D.; Alberich-Bayarri, A.; Pastor-Escuredo, D.; et al. Noninvasive monitoring of serial changes in pulmonary vascular resistance and acute vasodilator testing using cardiac magnetic resonance. J. Am. Coll. Cardiol. 2013, 62, 1621–1631.

16. Pereda, D.; Garcia-Alvarez, A.; Sanchez-Quintana, D.; Nuno, M.; Fernandez-Friera, L.; Fernandez-Jimenez, R.; Garcia-Ruiz, J.M.; Sandoval, E.; Aguero, J.; Castella, M.; et al. Swine model of chronic postcapillary pulmonary hypertension with right ventricular remodeling: Long-term characterization by cardiac catheterization, magnetic resonance, and pathology. J. Cardiovasc. Transl. Res. 2014, 7, 494–506.

17. van Duin, R.W.B.; Stam, K.; Cai, Z.; Uitterdijk, A.; Garcia-Alvarez, A.; Ibanez, B.; Danser, A.H.J.; Reiss, I.K.M.; Duncker, D.J.; Merkus, D. Transition from post-capillary pulmonary hypertension to combined pre- and post-capillary pulmonary hypertension in swine: A key role for endothelin. J. Physiol. 2019, 597, 1157–1173.

18. Keusch, S.; Bucher, A.; Muller-Mottet, S.; Hasler, E.; Maggiorini, M.; Speich, R.; Ulrich, S. Experience with exercise right heart catheterization in the diagnosis of pulmonary hypertension: A retrospective study. Multidiscip. Respir. Med. 2014, 9, 51.

19. De Wijs-Meijler, D.P.; Stam, K.; van Duin, R.W.; Verzijl, A.; Reiss, I.K.; Duncker, D.J.; Merkus, D. Surgical Placement of Catheters for Long-term Cardiovascular Exercise Testing in Swine. J. Vis. Exp. 2016, e53772, doi:10.3791/53772.

20. Haitsma, D.B.; Merkus, D.; Vermeulen, J.; Verdouw, P.D.; Duncker, D.J. Nitric oxide production is maintained in exercising swine with chronic left ventricular dysfunction. Am. J. Physiol. Heart Circ. Physiol. 2002, 282, H2198–H2209.

21. Mulvany, M.J.; Halpern, W. Contractile properties of small arterial resistance vessels in spontaneously hypertensive and normotensive rats. Circ. Res. 1977, 41, 19–26.

22. Zhou, Z.; de Beer, V.J.; de Wijs-Meijler, D.; Bender, S.B.; Hoekstra, M.; Laughlin, M.H.; Duncker, D.J.; Merkus, D. Pulmonary vasoconstrictor influence of endothelin in exercising swine depends critically on phosphodiesterase 5 activity. Am. J. Physiol. Lung Cell Mol. Physiol. 2014, 306, L442–L452.

23. Moens, A.L.; Champion, H.C.; Claeys, M.J.; Tavazzi, B.; Kaminski, P.M.; Wolin, M.S.; Borgonjon, D.J.; Van Nassauw, L.; Haile, A.; Zviman, M.; et al. High-dose folic acid pretreatment blunts cardiac dysfunction during ischemia coupled to maintenance of high-energy phosphates and reduces postreperfusion injury. Circulation 2008, 117, 1810–1819.

24. Sykes, M.C.; Ireland, C.; McSweeney, J.E.; Rosenholm, E.; Andren, K.G.; Kulik, T.J. The impact of right ventricular pressure and function on survival in patients with pulmonary vein stenosis. Pulm. Circ. 2018, 8, doi:10.1177/2045894018776894.

25. Domingo, L.; Magdo, H.S.; Day, R.W. Acute Pulmonary Vasodilator Testing and Long-Term Clinical Course in Segmental Pulmonary Vascular Disease. Pediatr. Cardiol. 2018, 39, 501–508.

26. Galie, N.; Hoeper, M.M.; Humbert, M.; Torbicki, A.; Vachiery, J.L.; Barbera, J.A.; Beghetti, M.; Corris, P.; Gaine, S.; Gibbs, J.S.; et al. Guidelines for the diagnosis and treatment of pulmonary hypertension: The Task Force for the Diagnosis and Treatment of Pulmonary Hypertension of the European Society of Cardiology (ESC) and the European Respiratory Society (ERS), endorsed by the International Society of Heart and Lung Transplantation (ISHLT). Eur. Heart J. 2009, 30, 2493–2537.

27. Rol, N.; Timmer, E.M.; Faes, T.J.; Vonk Noordegraaf, A.; Grunberg, K.; Bogaard, H.J.; Westerhof, N. Vascular narrowing in pulmonary arterial hypertension is heterogeneous: Rethinking resistance. Physiol. Rep. 2017, 5, e13159.

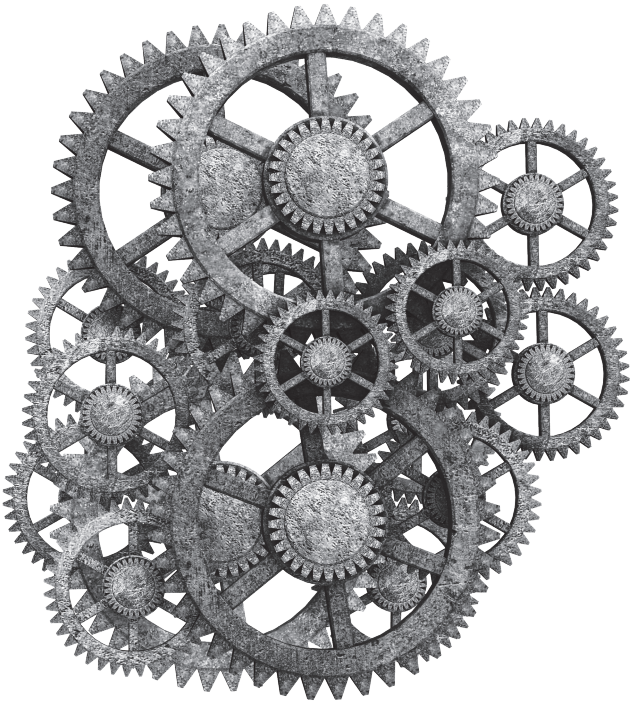

6

Chapter 6

Impaired right ventricular O_2 delivery reserve is associated with reduced right ventricular reserve in post-capillary pulmonary hypertension during exercise

Richard WB van Duin*, Zongye Cai*, Kelly Stam,
André Uitterdijk, Jolanda van der Velden,
Anton Vonk-Noordegraaf,
Dirk J Duncker, Daphne Merkus

•

THE AMERICAN JOURNAL OF PHYSIOLOGY - HEART AND CIRCULATORY PHYSIOLOGY. OCT 2019

ABSTRACT

Assessing right ventricular (RV) functional reserve is important for determining clinical status and prognosis in patients with pulmonary hypertension (PH). In this study, we aimed to establish RV-oxygen (O_2) delivery as a determinant for RV-functional reserve during exercise in swine with chronic PH.

Chronic PH was induced by pulmonary vein banding (PVB), with sham operation serving as control. RV function and RV-O_2 delivery were measured over time in chronically instrumented swine, up to 12 weeks after PVB at rest and during exercise. At rest, RV afterload (pulmonary artery pressure and Ea) and contractility (Ees and dP/dt_{max}) were higher in PH compared with control with preserved cardiac index and RV-O_2 delivery. However, RV-functional reserve, as measured by the exercise-induced relative change (Δ) in cardiac index, dP/dt_{max}, and Ees, was decreased in PH, and RV-pulmonary arterial coupling was lower both at rest and during exercise in PH. Furthermore, the increase in RV-O_2 delivery was attenuated in PH during exercise principally due to a lower systolic coronary blood flow in combination with an attenuated increase in aorta pressure while arterial O_2 content was not significantly altered in PH. Moreover, RV-O_2 delivery reserve correlated with RV-functional reserve, Δ cardiac index (R^2=0.85), ΔdP/dt_{max} (R^2=0.49), and ΔEes (R^2=0.70), all $P<0.05$.

The inability to sufficiently increase RV-O_2 supply to meet the increased O_2 demand during exercise is principally due to the reduced RV-perfusion relative to healthy control values and likely contributes to impaired RV-contractile function and thereby to the limited exercise capacity that is commonly observed in patients with PH.

New and Noteworthy

Impaired right ventricular (RV) O_2 delivery reserve is associated with reduced RV-functional reserve during exercise in a swine model of Pulmonary Hypertension (PH) induced by pulmonary vein banding. Our data suggest that RV function and exercise capacity might be improved by improving RV-O_2 delivery.

INTRODUCTION

Patients with pulmonary hypertension (PH) experience a limited exercise capacity due to the inability of the right ventricle (RV) to sufficiently increase cardiac output during exercise. Assessing RV-functional reserve during exercise is thus critical to assess the clinical status of patients with PH (1,2). RV-functional reserve is defined as the relative increase in RV-function in response to exercise. The main determinants of RV- functional reserve in patients with PH are unknown. In this study we speculate that the ability to increase oxygen (O_2) delivery to the RV-myocardium is an important determinant of RV-functional reserve.

At rest, O_2 consumption in the human heart is 40-fold and 20-fold higher as compared to skeletal muscle and the whole body respectively, reflecting the high metabolic rate of the cardiac contractile process (3). RV-coronary blood flow (CBF) under resting conditions is lower than left ventricular (LV)-CBF, but the increase in RV-CBF during exercise is twice as big as that in LV-CBF, in ponies (4), swine (5), and dogs (6). This reflects the lower myocardial O_2 demand of the RV at rest (6), and implies that the relative increase in RV-CBF, i.e. RV-CBF-reserve, should be sufficiently large to accommodate the greater increase in RV-O_2 demand during exercise, in order to maintain RV-function during exercise.

In subjects with PH, resting RV-CBF is increased compared with healthy controls (7,8), but their ability to increase RV-CBF after infusion of adenosine is reduced (7), suggesting impaired vasodilator reserve. During exercise, vasodilator reserve is particularly important since O_2 consumption is augmented, and extravascular compression of the coronary vasculature, that is already increased in resting PH patients (8), may further compromise RV-perfusion and thus RV-O_2 delivery. We hypothesize that exercise exacerbates the mismatch between RV-work and RV-O_2 delivery, thereby impairing RV function. This implies that there is a correlation between RV-O_2 delivery reserve and RV-functional reserve.

It was already shown in 1984 that, even in patients with LV-dysfunction, exercise capacity is more closely related to RV-function than to LV-function (9,10). In a subgroup of patients with LV-dysfunction, isolated post- capillary PH progresses into combined pre- and post-capillary PH, which shows reduced RV-functional reserve

and a further impairment of exercise capacity (11). These data indicate that also in patients with PH classified by the World Health Organization (WHO) as group 2 PH, RV-functional reserve is an important exercise limiting factor. To exclude a potential role for LV-dysfunction, we used a porcine model of chronic PH without LV-dysfunction produced by pulmonary vein banding (PVB) (12,13) to investigate the relationship of RV-O_2 delivery and RV-functional reserve during exercise.

METHODS

Ethics and study design

This study was performed in accordance with the "Guiding Principles in the Care and Use of Laboratory Animals" as approved by the Council of the American Physiological Society, and with the approval of the Animal Care Committee of the Erasmus Medical Center Rotterdam (3158, 109-13-09). Sixteen crossbred Landrace x Yorkshire swine of either sex obtained from a commercial breeder (3-4 weeks old, 6±1 kg) entered the study. Swine were individually housed in the animal facility of the Erasmus University Medical Center, fed age appropriate diet initially four times per day for 3 weeks (Babywean, Topwean, Denkavit, Voorthuizen, The Netherlands), afterwards twice a day and had free access to drinking water. A schematic design of the study is given in Figure 1.

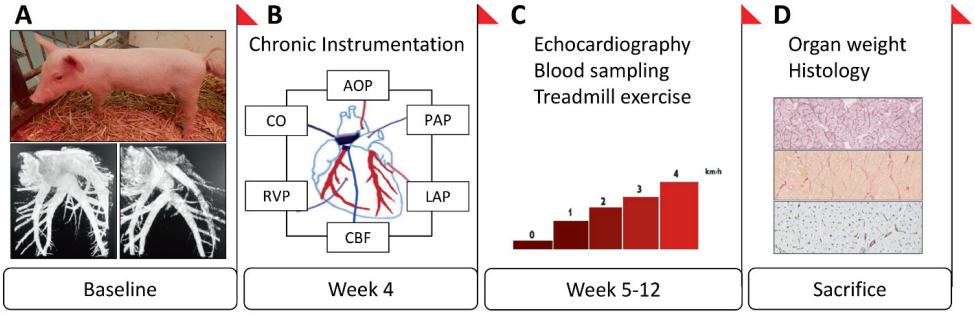

Figure 1. Schematic design of the study. A. At baseline, swine were randomized to the PH group with pulmonary vein banding of the lower (caudal) lobes (PVB, n=9) or control group with sham operation (n=5), lower panels show the 3D angiography of the control with sham operation (left) and the PH group with PVB (right). B. In week 4, swine were chronically instrumented to measure awake haemodynamics. C. From week 5, starting one week after recovery from chronic instrumentation, all swine were weekly exercised on a motor driving treadmill while measuring haemodynamics. D. In week 12, swine were sacrificed and tissues were harvested for various analyses.

Swine model

PVB was induced in swine as previously described (12,13). In brief, 10 swine (8.4±1.8 kg) were sedated (5 mg/kg Tiletamine/Zolazepam, Virbac; 2.25 mg/kg Xylazine, AST

Pharma; 0.5 mg Atropine, Teva Nederland, Netherlands), intubated and ventilated with a mixture of O_2 and N_2 (1:2) to which isoflurane (2% Pharmachemie, Haarlem, Netherlands) was added. Antibiotic prophylaxis (0.75 ml Depomycine, 200 mg/mL dihydrostreptomycin, 200,000 IU/mL procaine benzyl penicillin, Intervet Schering Plough, Netherlands) was given before the procedure. Under sterile conditions, the chest was opened via the fifth right intercostal space and a surgical loop (Braun Medical Inc., Bethlehem, USA) was passed around the confluent of the inferior pulmonary veins and secured at the resting diameter with a silk suture. The ribs were approximated using non absorbable USP6 braided polyester (Ø0.8 mm) and the wound was closed using silk sutures. Swine received analgesia (0.3 mg buprenorphine i.m. Indivior, UK) and a fentanyl slow release patch (6μg/hr, 72 hrs, Fentanyl Sandoz® Matrix, Sandoz B.V., Netherlands) and were transferred to the animal facility. One swine died of acute heart failure within 3 hours following PVB. Sham operation was performed in 6 swine (8.4±2.1 kg) as control, in which the pulmonary vein confluent was exposed and dissected, but no banding was performed. One control swine was excluded due to catheter failure, precluding haemodynamic measurements in the awake state.

Four weeks after PVB or sham-operation (Fig 1), swine were anaesthetised and ventilated as described above, and chronically instrumented as described previously (13-15). In brief, under sterile conditions, the chest and pericardium were opened via the fourth left intercostal space, and fluid-filled polyvinylchloride catheters (Braun Medical Inc., USA) were inserted into the aortic arch, the pulmonary artery, the RV, and the left atrium for pressure measurement and blood sampling (13-15). Transit time flow probes (Transonic Systems Inc., Ithaca, USA) were positioned around the ascending aorta to measure cardiac output and around the right coronary artery to determine RV-CBF. The right coronary artery perfuses the majority of the RV-free wall as well as part of the posterior LV and the interventricular septum (16). Fluid status was maintained with an intravenous glucose drip (5%, 100 mL/hr). Catheters were tunneled to the back, and the wound was closed. When fully awake, swine were transferred to the animal facility, receiving analgesia (1 mg buprenorphine i.m. Indivior, UK), and a fentanyl slow release patch (12 μg/hr), and antibiotic prophylaxis (25 mg/kg, amoxicillin i.v. Centrafarm B.V., Netherlands; 5 mg/kg, gentamycin i.v.

Eurovet, Netherlands) for 7 days. If, during follow up catheters were infected and infection precipitated in the joints and caused crippleness of the animal, this was treated by daily administration of antibiotics (enrofloxazine, 2.5 mg/kg i.m. Baytril, Bayer, Netherlands) and anti-inflammatory pain medication (flunixine, 1 mg/kg i.m., Finadyne, Schering Plough Animal Health, Netherlands) until crippleness resolved (usually within one week).

Haemodynamic evaluation of RV-function

After one week of recovery from chronic instrumentation, swine were placed on a motor driven treadmill (Fig 1). Haemodynamics consisting of heart rate (HR), cardiac output (CO), RV-CBF, and pressures in the right ventricle (RVP), aorta (MAP), pulmonary artery (PAP) and left atrium (LAP) were continuously recorded (ATCODAS, Dataq Instruments, OH) at rest and during a four stage (3 mins/stage) incremental exercise protocol (1-4 km/hr) for later off line data analysis. Blood samples were collected at rest and during the last minute of each stage from the aorta and pulmonary artery and processed for determination of pO_2, O_2 saturation, and haemoglobin (Hb, g/dL) (ABL 800, Radiometer, Denmark). Cardiac index was calculated as cardiac output/body weight. Stroke volume index was calculated as the ratio of cardiac index and heart rate. Total pulmonary vascular resistance index (tPVRi) was calculated as the ratio of mean PAP and cardiac index. Arterial O_2 content ($_AO_2C$, mM) was calculated as (Hb×0.621×O_2 saturation) + (0.00131×pO_2) (5), and RV-O_2 delivery was calculated as RV-CBF×$_AO_2C$.

RV-function was evaluated by rate pressure product (RPP=heart rate×mPAP) as an index of RV-work, cardiac index, maximal rate of RVP rise (dP/dt_{max}) and end systolic elastance (Ees). Ees was derived from RVP and stroke volume index using the single beat method (17) using mean PAP as an index of end systolic PAP (11,18). The mean of at least 10 consecutive beats was determined. Arterial elastance (Ea) was calculated as mPAP/stroke volume index (19). RV-PA coupling was calculated as Ees/Ea (17). RV-functional reserve (Δ) was defined as the fractional change from basal RV-function at rest to RV-function during exercise, and calculated by (Maximum value during exercise-value at rest)/Value at rest.

Echocardiography

Resting RV-dimensions and function were evaluated by echocardiography (ALOKA ProSound SSD 4000, Hitachi Aloka Medical, Japan) under awake resting conditions. RV-end diastolic area (EDA) and end systolic area (ESA) were obtained from the apical four chamber view, RV-fractional area change (RV-FAC) was calculated by (EDA-ESA)/EDA×100%. Tricuspid annular plane systolic excursion (TAPSE) was determined from M mode in the four-chamber view.

Sacrifice, Fulton index and RV-Histology

Swine were anaesthetised, intubated and ventilated. Subsequently, a sternotomy was performed under deep anaesthesia, the heart was fibrillated using a 9V battery, and immediately excised. The heart was sectioned into RV and LV+ interventricular septum and weighed. Fulton index (RV/LV) was used to assess RV-hypertrophy. RV-tissue was fixed using 3.5-4% formaldehyde and embedded in paraffin. 5µm sections were stained with Gomori to assess cardiomyocyte cross sectional area (CSA), Picrosirius Red to assess collagen content, and lectin to assess capillary density and analyzed as previously described (20).

Statistical analyses

Data are presented as mean±SEM. Differences between two groups and relationships between different indices were analyzed using t test and linear regression (Prism, GraphPad, La Jolla, CA, USA). Differences between PH and control over time at rest and during maximal exercise were analyzed using linear mixed model with fixed effects (time and exercise as within subject factors and banding as a between subject factor as appropriate, SPSS version 21.0 IBM, NY, USA). A P value <0.05 (two-tailed) was considered statistically significant, and a P-value <0.1 (two-tailed) was considered as a trend.

RESULTS

RV-function and O_2 delivery at rest

PVB for 12 weeks resulted in progressive PH with higher mPAP (Fig 2A), tPVRi (Fig 2B), and Ea (Fig 2C) compared with control, and increased RV-work (Fig 2D). The increased afterload resulted in gradual RV-dilation, as evidenced by a progressive enlargement of RV-EDA (Fig 2H) and ESA (Fig 2I), and hypertrophy indicated by increased Fulton index (Table 1) and bigger cardiomyocyte size (Fig 3A) and a trend towards increased interstitial collagen content (Fig 3B).

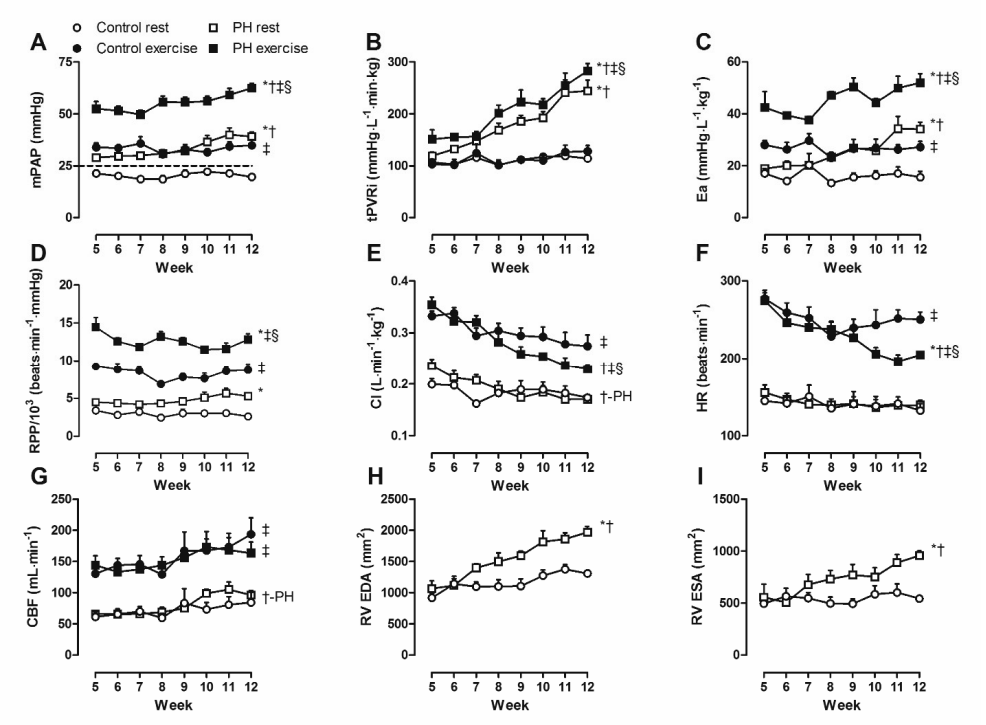

Figure 2. Haemodynamic, CBF and echocardiographic changes over time at rest and during exercise. At rest, PVB for 12 weeks resulted in progressive PH with higher mPAP (A) and tPVRi (B) compared with control. RV-afterload Ea (C) and RV-work RPP (D), and RV-EDA (H) and ESA (I) also increased progressively in PH compared with control. CI (E) decreased over time in PH, but not control, while HR (F) and CBF (G) were unchanged in PH compared with control. During exercise, the increases in mPAP (A), tPVRi (B), Ea (C), RPP (D) were enhanced in PH compared with control, while the exercise-induced increase in CI (E) and HR (F) were attenuated in PH. mPAP: mean pulmonary artery pressure, tPVRi: total pulmonary vascular resistance index, Ea:

arterial elastance, RPP: rate pressure product, CI: cardiac index, HR: heart rate, CBF: coronary blood flow, EDA: end diastolic area, ESA: end systolic area.*: p<0.05, effect of PH; †: p<0.05, effect of time; ‡: p<0.05, effect of exercise; §: p<0.05, effect of exercise different in PH.

Table 1. Resting characteristics and echocardiography at week 12.

	Control	PH	*P*-value
Subjects/Female (n/n)	5/3	9/4	
Body Weight (kg)	59±2	53±3	0.24
RV Weight (g)	84±4	97±6	0.17
RV/Body Weight (g/kg)	1.42±0.07	1.85±0.11	0.02
LV Weight (g)	193±8	166±8	0.06
LV/Body Weight (g/kg)	3.2±0.1	3.1±0.1	0.63
Fulton Index	0.44±0.02	0.58±0.02	< 0.01
Haemodynamics			
Heart Rate (beats·min^{-1})	131±9	137±5	0.57
Mean Aorta Pressure (mmHg)	94±4	87±4	0.31
Mean LAP (mmHg)	3.6±0.3	4.0±0.6	0.55
Mean PAP (mmHg)	20±1	39±2	< 0.0001
Total PVRi (mmHg·L^{-1}·min·kg)	114±9	244±21	< 0.001
RV Systolic Pressure (mmHg)	33±2	69±3	< 0.0001
RV End-diastolic Pressure (mmHg)	10±2	14±1	0.09
RV function			
Cardiac Index (L·min^{-1}·kg^{-1})	0.17±0.00	0.17±0.01	0.80
Stroke Volume Index (mL·kg^{-1})	1.3±0.2	1.2±0.2	0.29
dP/dt_{max} (mmHg·s^{-1})	1350±190	1750±400	0.06
Ees (mmHg·mL^{-1}·kg)	37±2	54±3	< 0.01
Ea (mmHg·mL^{-1}·kg)	16±2	34±3	< 0.0001
RV-PA coupling (Ees/Ea)	2.5±0.3	1.7±0.2	< 0.05
Echocardiography			
RV FAC (%)	59±1	51±1	< 0.001
TAPSE (mm)	23±1	17±1	< 0.01

Data are presented as mean±SEM. RV: right ventricle; LV: left ventricle; LAP: left atrium pressure, PAP: pulmonary artery pressure, PVRi: pulmonary vascular resistance index, dP/dt_{max}: maximum rate of RV pressure rise, Ees: end-systolic elastance, Ea: arterial elastance, RV-PA coupling: RV-pulmonary arterial coupling, FAC: fractional area change, TAPSE: tricuspid annular plane systolic excursion.

Mild RV-dysfunction, i.e. significant decreases in RV-FAC and TAPSE in PH compared with control (Table 1), was present while cardiac index (Table 1, Fig 2E&4A) and stroke volume index (Table 1) were still preserved. Global RV-contractility (Ees, P<0.01; dP/dtmax, P=0.06) was higher in PH (Table 1, Fig 4B&C).

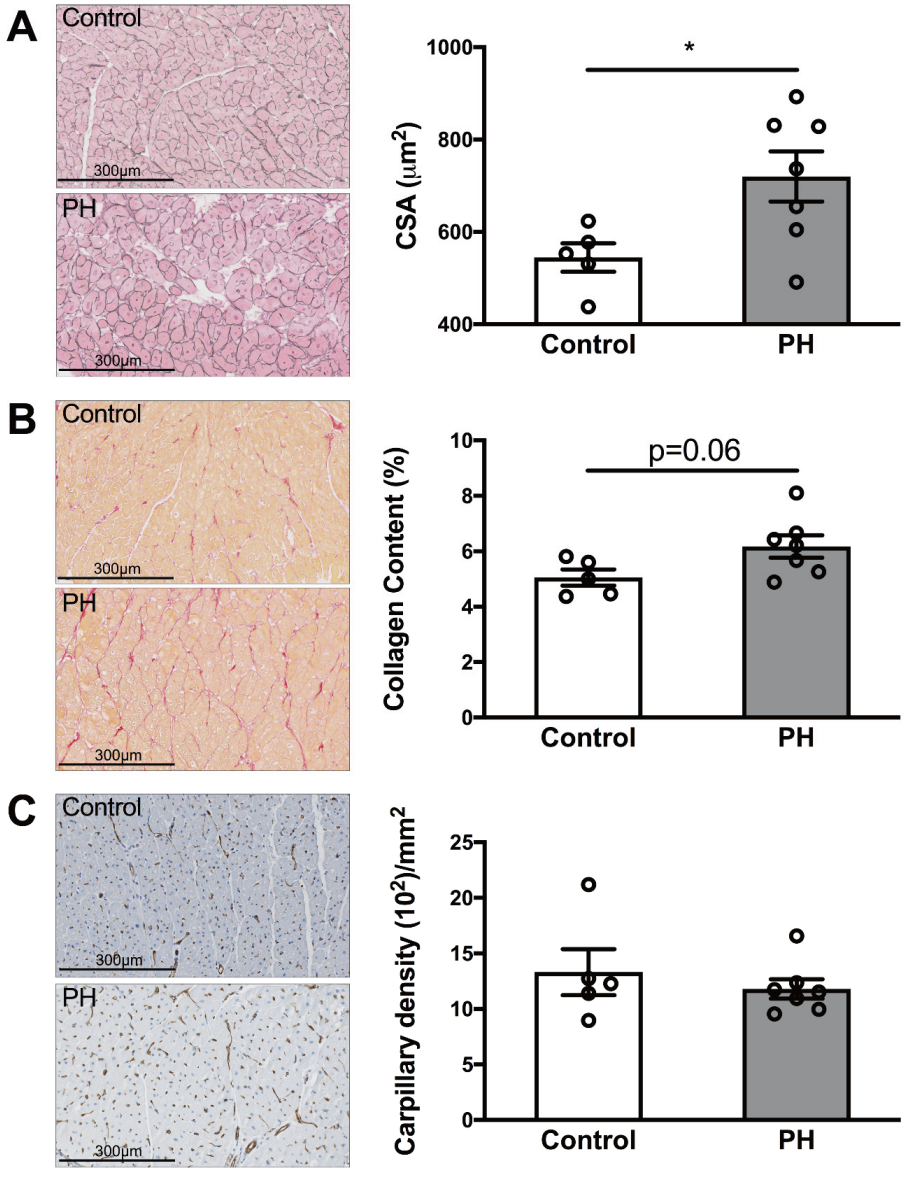

Figure 3. Histology of RV-myocardium. PH group (n=7) showed RV cardiomyocyte hypertrophy with higher CSA (A, Gomori staining) and a trend towards interstitial fibrosis (B, Picrosirius Red staining) when compared with control group (n=5), while the capillary density (C, Lectin staining) was similar in both groups. CSA: cross sectional area. *: $p<0.05$ for comparison between groups.

Nevertheless, RV-PA coupling was significantly lower in PH compared with control as Ees did not increase commensurate with the increase in Ea (Table 1, Fig 4D). RV-CBF averaged over the cardiac cycle was similar in both groups (Fig 2G, 5A). RV-O2 delivery was also similar in both groups (Fig 5H) as O2 content was unchanged (Fig 5G). Furthermore, capillary density was similar in both groups (Fig 3C).

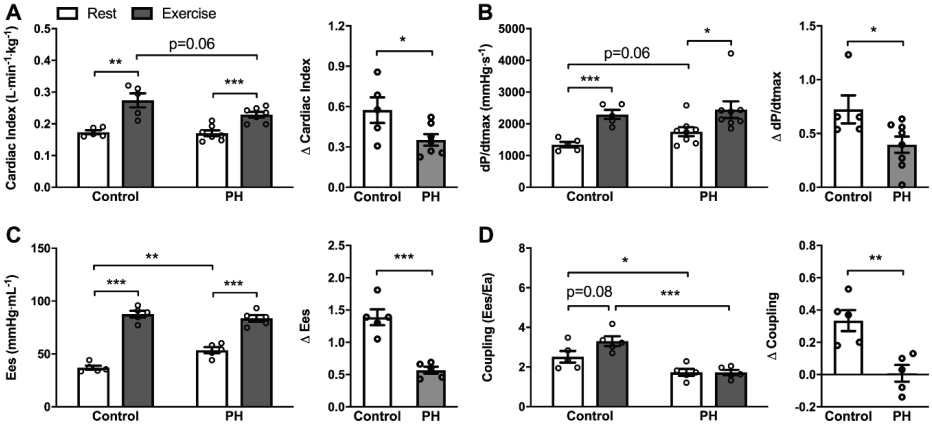

Figure 4. Assessment of RV-function at rest and during exercise at week 12. At rest, Cardiac index (A) was preserved in the PH group compared with control, while dP/dt_{max} (B) and Ees (C) were increased in PH. Conversely, coupling (D) was decreased in PH compared with control. During exercise, Cardiac index (A) and Coupling (D) were reduced in PH compared with control, while dP/dt_{max} (B) and Ees (C) were similar in both groups. RV-functional reserve, calculated as the relative increase from baseline i.e. (exercise-baseline)/baseline, ΔCardiac index (A), $\Delta dP/dt_{max}$ (B), ΔEes (C), and ΔCoupling (D), was reduced in PH compared with control. A. control: n=5, PH: n=7; B. control: n=5, PH: n=8; C. control: n=5, PH: n=5; D. control: n=5, PH: n=5. dP/dt_{max}: maximum rate of RV-pressure rise, Ees: end systolic elastance. *: p<0.05, **: p<0.01, ***: p<0.001 for comparison between groups.

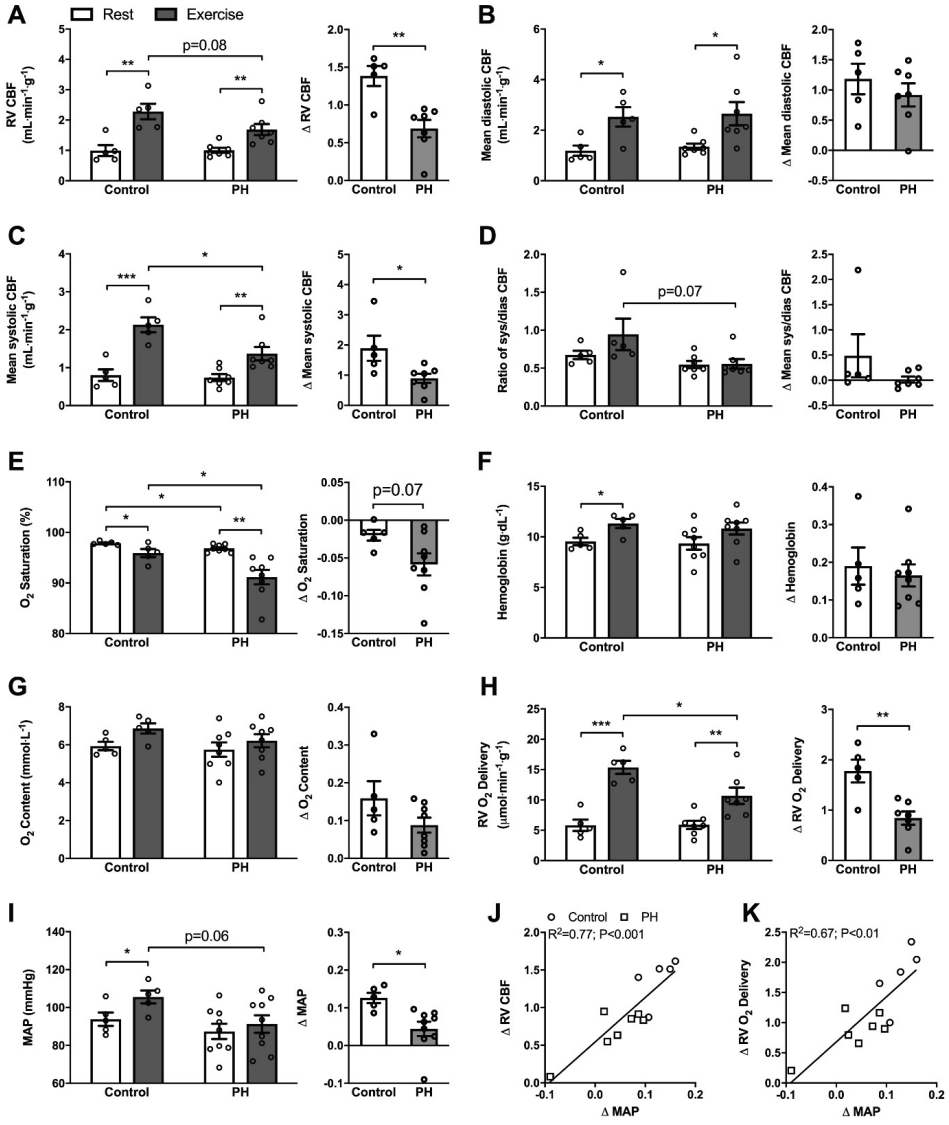

Figure 5. Assessment of determinants of RV-O_2 delivery at rest and during exercise at week 12. At rest, RV-CBF (A), mean diastolic CBF (B), mean systolic CBF (C), the ratio of systolic and diastolic CBF (D), haemoglobin (F), O_2 content (G), O_2 delivery (H) and MAP (I) were all similar between both groups despite a lower O_2 saturation in PH (E). During exercise, RV-CBF (A), mean systolic CBF (C), the ratio of systolic and diastolic CBF (D), O_2 saturation (E) and O_2 delivery (H) were reduced in PH (n=7~8) compared with control (n=5). The relative increase from baseline, i.e. (exercise-baseline)/baseline, ΔRV-CBF (A), Δmean systolic CBF (C), ΔRV-O_2 delivery (H) and ΔMAP (I) were reduced in PH compared with control. ΔMAP correlated with both ΔRV-CBF (J) and ΔRV-O_2 delivery (K). CBF: coronary blood flow, MAP: mean aortic pressure. *: p<0.05, **: p<0.01, ***: p<0.001 for comparison between groups.

RV-function and O_2 delivery during exercise

To assess RV-function and RV-functional reserve during exercise, swine were weekly exercised on a motor driven treadmill. The increased RV-afterload in PH was exacerbated during exercise, as mPAP (Fig 2A), tPVRi (Fig 2B), and Ea (Fig 2C) were higher in PH than in control. Hence, RV-work was higher in PH during exercise (Fig 2D). Global RV contractility (dP/dt_{max} and Ees) was increased during exercise in both PH and control to cope with the increased afterload (Fig 4B&C). Nevertheless, the exercise-induced increase in cardiac index was progressively attenuated in PH as compared to control (Fig 2E&4A), which resulted in a decrease in mixed venous buffer base ($HCO3^-$), in swine with PH (rest vs. exercise: 26.6±0.6 vs. 24.6±0.7 mmol/L, $p<0.05$) but not in control swine (25.8±0.6 vs. 25.2±1.1 mmol/L, $p=0.67$) suggesting that PH swine exercised closer to their anaerobic threshold. The attenuated increase in cardiac index was at least partially due to chronotropic incompetence, as the exercise-induced increase in heart rate was blunted in PH as compared to control (Fig 2F). Moreover, at week 12, exercise increased RV-PA coupling in control while it remained unchanged in PH, which resulted in a lower RV-PA coupling in PH than in control during exercise (Fig 4D), suggesting that the RV was less able to cope with the increased afterload.

Despite the higher RV-afterload and RV-work in PH than in control during exercise, RV-CBF (Fig 5A) and O_2 delivery (Fig 5H) per gram of RV-tissue were lower in PH as compared to control during exercise, which could be attributed to a lower systolic flow in PH (Fig 5C), and thus the ratio of systolic and diastolic flow tended to be decreased as well (Fig 5D). Although there was a slightly decreased O_2 saturation (Fig 5E) in PH, the O_2 content (Fig 5F) was similar in both groups. Therefore, RV-O_2 delivery reserve (Fig 5H) was impaired in PH due to impaired RV-CBF reserve (Fig 5A). This impaired RV- O_2 delivery reserve correlated strongly with a reduced exercise-induced increase in systemic blood pressure (Fig 5K), indicating that an attenuated increase in blood pressure in PH also likely contributed to the impaired RV- O_2 delivery reserve in PH during exercise.

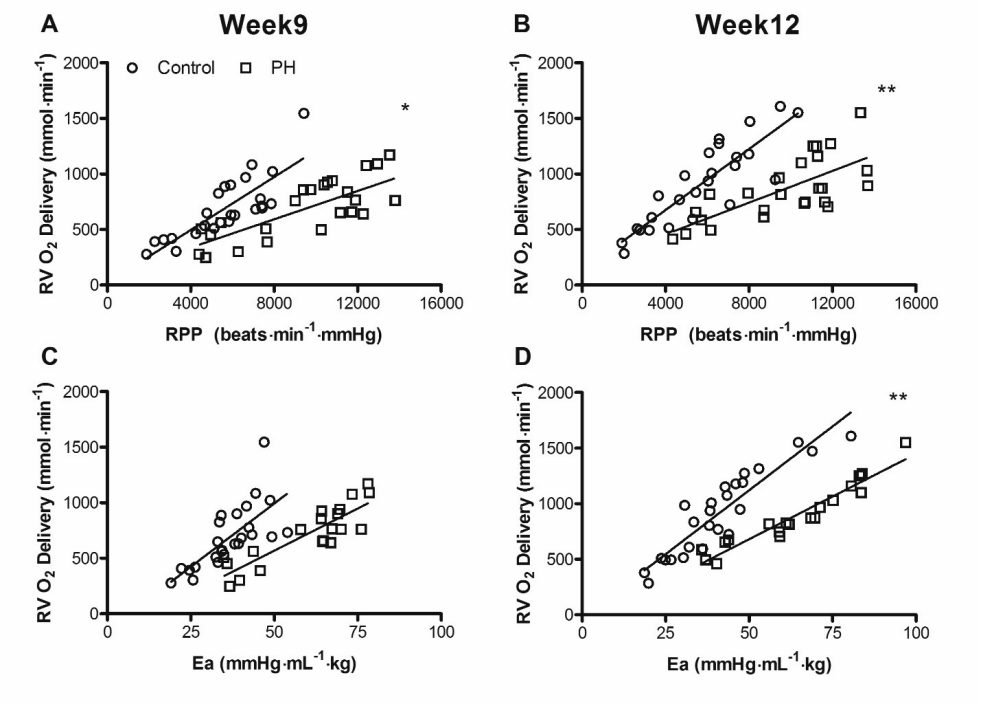

Figure 6. Relations between RV-work, RV-afterload and RV-O_2 delivery during exercise. The relation between RV-work, RPP and RV-O_2 delivery rotated clockwise in PH (n=6) at week 9 (A) and week 12 (B) compared with control (n=5). There was no significant change in the relation between RV-afterload, Ea and RV-O_2 delivery at week 9 (C), but a significant clockwise rotation at week 12 (D) in PH (n=6) compared with control (n=5). RPP: rate pressure product, Ea: arterial elastance. *: p<0.05, **: p<0.01 for comparison between groups.

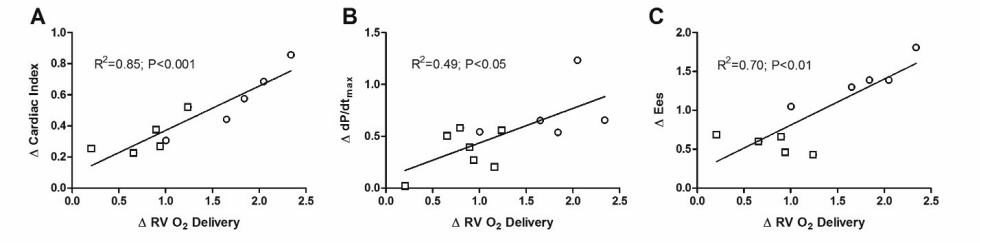

Figure 7. Relations between RV-O_2 delivery reserve and RV-functional reserve during exercise. RV-O_2 delivery reserve, i.e. the relative increase in RV-O_2 delivery from baseline, (exercise-baseline)/baseline, correlated with RV-functional reserve ΔCardiac index (A, control: n=5, PH: n=5), $\Delta dP/dt_{max}$ (B, control: n=5, PH: n=7), and Δ Ees (C, control: n=5, PH: n=5) in combined data from both groups. dP/dt_{max}: maximum rate of RV-pressure rise, Ees: end systolic elastance.

RV-O_2 delivery as determinant of RV-function

The relation between RV-work and O_2 delivery as well as the relation between afterload and O_2 delivery in the RV rotated clockwise in PH as compared to control at week 9 (Fig 6A&C), and this rotation became more pronounced at week 12 (Fig 6B&D), suggestive of progressive myocardial hypo-perfusion in PH during exercise. Furthermore, RV-O_2 delivery reserve (Fig 7) correlated with RV-functional reserve. In addition, significant correlations were observed between both RV-FAC and TAPSE at rest and RV-functional reserve as well as with O_2 delivery reserve, which was particularly strong for RV-FAC (Table 2).

Table 2. Relations between echocardiography parameters and RV-functional reserve, and RV-O_2 delivery reserve.

		RV FAC		TAPSE	
		R^2	*P* Value	R^2	*P* Value
RV-functional reserve	Δ CI	0.70	<0.01	0.58	<0.01
	Δ Ees	0.78	<0.001	0.59	<0.01
	Δ dp/dt_{max}	0.49	<0.05	0.45	<0.05
RV-O_2 delivery reserve	Δ RV-O_2 delivery	0.84	<0.001	0.48	<0.05

Relationships were analyzed using a linear regression. Δ: relative change from rest (exercise-rest)/rest, RV: right ventricle; FAC: fractional area change; TAPSE: tricuspid annular plane systolic excursion; CI: cardiac index; Ees: end-systolic elastance; dp/dt_{max}: maximum rate of RV pressure rise.

DISCUSSION

In the present study, we used exercise as a stressor to investigate RV-function and its relation to RV-O_2 delivery in a porcine model of chronic PH without LV dysfunction. Our findings indicate that in the presence of RV-hypertrophy in PH, RV-function is preserved with enhanced RV-contractile function at rest, while the exercise induced increase in RV-function is blunted, which is accompanied by an impaired increase in RV-O_2 delivery. Furthermore, the relation between RV-work and O_2 delivery rotates in a clockwise manner in PH as compared to control, and RV-O_2 delivery reserve strongly correlates with RV-functional reserve during exercise. Altogether, this is the first study showing that O_2 delivery to the RV is related to the changes of RV-function during exercise in PH.

Pulmonary vein banding and RV remodeling

WHO Group 2 PH is associated with left heart disease and/or valvular disease, resulting in impaired outflow into the left heart and an increase in pulmonary venous pressure that is transmitted backwards through the pulmonary vasculature. According to the clinical classification of PH, pulmonary vein stenosis, that is found as a congenital anomaly or that occurs as a severe complication of ablation of atrial fibrillation in humans (21), is one of the subgroups of WHO group 2 PH. Banding of the confluent of the pulmonary veins of the lower (caudal) lobes in swine results in a local stenosis (Figure 1), that progresses in relative severity with the growth of the animal. This progressive obstruction of 60-65% of the pulmonary vascular bed (22) resulted over time in isolated post-capillary PH that progresses with pulmonary microvascular remodelling into combined pre- and post-capillary PH (13,23), further contributing to the increased afterload and RV-remodelling. The gradual increase in afterload over time results in RV-hypertrophy, evidenced by an increase in Fulton index and cardiomyocyte size, a trend towards increased interstitial fibrosis, as well as RV-dilation measured by echocardiography.

RV-hypertrophy enabled the RV to cope with the increased afterload as cardiac index and stroke volume index were maintained at rest. This required recruitment of

contractile function, as evidenced by higher Ees and a trend towards an increased dP/dt_{max} in PH, while RV-PA coupling was reduced. RV-PA coupling describes the matching of RV-function and afterload. RV-PA coupling in the control swine in the present study was equal to 2.5±0.3, which is higher than the optimal coupling between 1.5 and 2 as originally proposed for humans by Suga and co-workers (24). Although human and porcine hearts are similar in size, the pigs were relatively young. With increasing age, autonomic control changes and the balance between sympathetic and parasympathetic activity changes with parasympathetic control becomes more dominant(25). It is therefore possible that the relatively high sympathetic activity resulted in a higher heart rate and higher Ees, with increased coupling. In another study in swine, in which RV-PA coupling was measured under anaesthesia using a PV loop catheter, RV-PA coupling in control swine was equal to 1.24 (26). This study reports an Ees of 0.37 mmHg/mL and an Ea of 0.32 mmHg/mL using RV-end systolic pressure in their calculation. Recalculation of Ea as mPAP/SVi, with mPAP of 14 mmHg and a stroke volume index of 44 ml/m^2, which translates into a stroke volume index of 1 ml/kg, results in an Ea of 14 mmHg·mL^{1}·kg, which is very similar to the Ea value of 16 mmHg·mL^{1}·kg in the present study. Hence, the difference in coupling between the study of Guihaire and co-workers (1.24) and our study (2.5) is likely due to a difference in sympathetic activity that impacted Ees. Indeed, following a low dose of the sympathomimetic dobutamine, heart rate increased to 130 bpm, and coupling increased to 2.14, which is closer to the value of 2.5 that we observed under awake resting conditions at similar heart rate (131 bpm).

In the present study, PH resulted in a 32% reduction in RV-PA coupling, which is similar in magnitude to the 25% reduction in RV-PA coupling observed in patients with WHO group 2 PH (27,28) and somewhat smaller as compared to the 47% reduction in RV-PA coupling in swine with chronic thromboembolic pulmonary hypertension. Consistent with the reduction in RV-PA coupling, RV-FAC and TAPSE were reduced in PH. Altogether, histological, echocardiographic, haemodynamic and RV-PA coupling data are consistent with mild RV-dysfunction at rest in PH.

RV-O_2 delivery in relation to RV-function and exercise capacity

Exercise limitation is the earliest symptom of right heart failure and is a strong predictor of survival in PH patients (29). Moreover, RV-function correlated more closely with exercise capacity than LV-function in patients with chronic left heart failure (9,10). This correlation between RV-function and exercise capacity is present in patients with left heart failure irrespective of the ejection fraction, i.e. in reduced, midrange or preserved ejection fraction (30-32). Both chronotropic incompetence and impaired stroke volume reserve may contribute to the reduction in exercise capacity (32,33). Indeed, the exercise-induced increase in cardiac index was attenuated in PH as compared to control in the present study, which, consistent with data from patients with heart failure (32), was in part due to chronotropic incompetence, potentially due to impaired autonomic control (34,35). In addition, the increased work and afterload of the RV in PH were not accompanied by an equivalent increase in RV-contractile function, particularly during exercise. The observation that maximal RV-contractility in PH during exercise was not higher than in control is consistent with a recent observation in obese patients with exercise-induced PH and reduced exercise tolerance (36). Together with data showing Ea is a robust and independent predictor of mortality in patients with WHO group 2 PH, and correlates strongly with RV-dysfunction (11,37), it appears that the reduced RV-contractile reserve, which results in a decrease in RV-PA coupling during exercise, is an important limiting factor in exercise tolerance in PH patients.

Despite the presence of hypertrophy, the RV in PH swine was unable to increase its contractile function beyond the value observed in control subjects. One potential reason may be that augmenting contractile force requires an increase in myocardial O_2 consumption. Previous work has shown that, although myocardial O_2 extraction in the RV, is lower than that in the LV, the RV also has limited O_2 extraction reserve, particularly during exercise (18). Therefore, increasing O_2 delivery is required for increasing O_2 consumption although it has also been shown that myocardial O_2 utilization efficiency can be temporarily increased (38,39). Thus, although RV-function is initially downregulated upon chronic reductions in flow (38), subsequent stimulation with dobutamine resulted in an increased function without an increase in

flow which was accompanied by an increased O_2 utilization efficiency (39). However, after 10 minutes, RV-function went back to baseline in the groups treated with high dose dobutamine, despite continued stimulation with dobutamine. Therefore, it is unlikely that an increase in myocardial work can be sustained for a prolonged period of time without an increase in myocardial perfusion. The relation between RV-O_2 delivery and work rotated clockwise during exercise in PH in the present study, suggesting impaired O_2 delivery. This impaired O_2 delivery was not sufficient to cause ischemic damage (high sensitive troponin in Control swine 0.17±0.07 ng/ml and PH 0.07±0.01 ng/ml), the impaired O_2 delivery reserve recruited during exercise correlated linearly with RV-functional reserve.

O_2 delivery is determined by arterial O_2 content and CBF. Swine in the present study have lower haemoglobin levels (9.5±0.4 g/dL) as compared to humans (normal range 12-20 g/dL), resulting in a lower arterial O_2 content and requiring a larger CBF to obtain a similar O_2 delivery. Nevertheless, RV-CBF in swine (0.99±0.17 ml/min/g) appears to be only slightly higher than the value obtained in healthy humans (0.90±0.35 ml/min/g (8)). The lower haemoglobin levels in these swine were not due to surgery or repetitive blood sampling as the values are similar to values obtained in a large cohort (>4000) swine of similar age (40). Furthermore, haemoglobin levels were similar between control and PH swine both at rest and during exercise. Also, arterial O_2 content was unchanged, despite a trend towards a larger arterial desaturation during exercise in swine with PH. This larger arterial desaturation that occurred during exercise is likely a consequence of the reduced pulmonary capillary passage time due to redistribution of CI away from the banded lower lung lobes. CBF per gram of RV-tissue tended to be lower in swine with PH during exercise, and the RV-CBF reserve was significantly reduced in PH, which is also shown in dogs with RV-hypertrophy secondary to pulmonary artery banding (41,42). It should be noted that CBF was measured in the right coronary artery, which also supplies the posterior wall of the LV. Since LV work, and hence perfusion of the LV are not expected to change in mild PH either at rest or during exercise, the reduction in RV-CBF reserve may be underestimated in the present study. The reduced RV-CBF reserve was not due to a reduction in capillary density of the RV-myocardium, but can be attributed in part to the attenuation of the exercise-induced increase in blood pressure, possibly as a result

of the attenuated increase in cardiac index due to the chronotropic incompetence. However, particularly mean *systolic* CBF was lower, while mean *diastolic* CBF remained similar between PH and control during exercise indicating that increased extravascular compression in PH is the main contributor to the reduced RV-perfusion reserve. These data are consistent with studies showing a reduced ratio of systolic and diastolic flow at rest in patients with PAH (8,43-45) and animals following pulmonary artery banding (41,42,46,47), as well as various studies showing that maximal RV-function is related to maximal RV-CBF in both healthy subjects (48-51), and in patients with PAH and chronic thromboembolic pulmonary hypertension (8,52).

CONCLUSIONS

The present study shows evidence for an impaired increase in RV-O_2 delivery in chronic PH without LV dysfunction during exercise. Although the attenuated increase in blood pressure during exercise may have contributed to the impaired increase in RV-O2 delivery, the impaired RV-O_2 delivery reserve in PH was principally due to augmented extravascular compression of the coronary vasculature, that limited particularly the exercise-induced increase in CBF during systole. The impaired RV-O_2 delivery reserve correlates with a reduced RV-functional reserve, indicating that impaired RV-O_2 delivery may limit RV-function during exercise, and thereby contribute to the limited exercise capacity that is commonly observed in patients with PH.

REFERENCES

1. Hsu S, Houston BA, Tampakakis E et al. Right Ventricular Functional Reserve in Pulmonary Arterial Hypertension. Circulation 2016;133:2413-22.
2. Naeije R, Brimioulle S, Dewachter L. Biomechanics of the right ventricle in health and disease (2013 Grover Conference series). Pulm Circ 2014;4:395-406.
3. Montgomery H. Cardiac reserve: linking physiology and genetics. Intensive Care Med 2000;26 Suppl 1:S137-44.
4. Manohar M. Transmural coronary vasodilator reserve and flow distribution during maximal exercise in normal and splenectomized ponies. J Physiol 1987;387:425-40.
5. Duncker DJ, Stubenitsky R, Tonino PA, Verdouw PD. Nitric oxide contributes to the regulation of vasomotor tone but does not modulate O(2)-consumption in exercising swine. Cardiovasc Res 2000;47:738-48.
6. Hart BJ, Bian X, Gwirtz PA, Setty S, Downey HF. Right ventricular oxygen supply/demand balance in exercising dogs. Am J Physiol Heart Circ Physiol 2001;281:H823-30.
7. Manohar M. Transmural coronary vasodilator reserve, and flow distribution during tachycardia in conscious young swine with right ventricular hypertrophy. Cardiovasc Res 1985;19:104-12.
8. van Wolferen SA, Marcus JT, Westerhof N et al. Right coronary artery flow impairment in patients with pulmonary hypertension. Eur Heart J 2008;29:120-7.
9. Baker BJ, Wilen MM, Boyd CM, Dinh H, Franciosa JA. Relation of right ventricular ejection fraction to exercise capacity in chronic left ventricular failure. Am J Cardiol 1984;54:596-9.
10. Franciosa JA, Baker BJ, Seth L. Pulmonary versus systemic hemodynamics in determining exercise capacity of patients with chronic left ventricular failure. Am Heart J 1985;110:807-13.
11. Guazzi M, Dixon D, Labate V et al. RV Contractile Function and its Coupling to Pulmonary Circulation in Heart Failure With Preserved Ejection Fraction: Stratification of Clinical Phenotypes and Outcomes. JACC Cardiovasc Imaging 2017;10:1211-1221.
12. Pereda D, Garcia-Alvarez A, Sanchez-Quintana D et al. Swine model of chronic postcapillary pulmonary hypertension with right ventricular remodeling: long-term characterization by cardiac catheterization, magnetic resonance, and pathology. J Cardiovasc Transl Res 2014;7:494-506.
13. van Duin RWB, Stam K, Cai Z et al. Transition from post-capillary pulmonary hypertension to combined pre- and post-capillary pulmonary hypertension in swine: A key role for endothelin. J Physiol 2018.
14. De Wijs-Meijler DP, Stam K, van Duin RW et al. Surgical Placement of Catheters for Long-term Cardiovascular Exercise Testing in Swine. J Vis Exp 2016:e53772.
15. Stam K, van Duin RWB, Uitterdijk A, Cai Z, Duncker DJ, Merkus D. Exercise Facilitates Early Recognition of Cardiac and Vascular Remodeling in Chronic Thrombo-Embolic Pulmonary Hypertension in a Novel CTEPH Swine Model. Am J Physiol Heart Circ Physiol 2017:ajpheart 00380 2017.

16. Malkasian S, Hubbard L, Dertli B, Kwon J, Molloi S. Quantification of vessel-specific coronary perfusion territories using minimum-cost path assignment and computed tomography angiography: Validation in a swine model. J Cardiovasc Comput 2018;12:425-435.
17. Brimioulle S, Wauthy P, Ewalenko P et al. Single-beat estimation of right ventricular end-systolic pressure-volume relationship. Am J Physiol Heart Circ Physiol 2003;284:H1625-30.
18. Zong P, Tune JD, Downey HF. Mechanisms of oxygen demand/supply balance in the right ventricle. Exp Biol Med (Maywood) 2005;230:507-19.
19. Spruijt OA, de Man FS, Groepenhoff H et al. The effects of exercise on right ventricular contractility and right ventricular-arterial coupling in pulmonary hypertension. Am J Respir Crit Care Med 2015;191:1050-7.
20. Sorop O, Heinonen I, van Kranenburg M et al. Multiple common comorbidities produce left ventricular diastolic dysfunction associated with coronary microvascular dysfunction, oxidative stress, and myocardial stiffening. Cardiovasc Res 2018;114:954-964.
21. Latson LA, Prieto LR. Congenital and acquired pulmonary vein stenosis. Circulation 2007;115:103-8.
22. VanAlstine WG. Respiratory System. In: Jeffrey J. Zimmerman LAK, Alejandro Ramirez, Kent J. Schwartz, Gregory W. Stevenson, editor Diseases of Swine 10th. 10th ed: John Wiley & Sons, 2012.
23. Aguero J, Ishikawa K, Hadri L et al. Characterization of right ventricular remodeling and failure in a chronic pulmonary hypertension model. Am J Physiol Heart Circ Physiol 2014;307:H1204-15.
24. Sagawa K ML, Suga H, Sunagava K. Cardiac Contraction and Pressure-Volume Relationship: New York: Oxford University Press, 1988.
25. Eyre EL, Duncan MJ, Birch SL, Fisher JP. The influence of age and weight status on cardiac autonomic control in healthy children: a review. Auton Neurosci 2014;186:8-21.
26. Guihaire J, Haddad F, Noly PE et al. Right ventricular reserve in a piglet model of chronic pulmonary hypertension. Eur Respir J 2015;45:709-17.
27. Naeije R, D'Alto M. The Diagnostic Challenge of Group 2 Pulmonary Hypertension. Prog Cardiovasc Dis 2016;59:22-9.
28. Gerges M, Gerges C, Pistritto AM et al. Pulmonary Hypertension in Heart Failure. Epidemiology, Right Ventricular Function, and Survival. Am J Respir Crit Care Med 2015;192:1234-46.
29. Vonk-Noordegraaf A, Haddad F, Chin KM et al. Right heart adaptation to pulmonary arterial hypertension: physiology and pathobiology. J Am Coll Cardiol 2013;62:D22-33.
30. Borlaug BA, Kane GC, Melenovsky V, Olson TP. Abnormal right ventricular-pulmonary artery coupling with exercise in heart failure with preserved ejection fraction. Eur Heart J 2016;37:3293-3302.
31. Guazzi M, Villani S, Generati G et al. Right Ventricular Contractile Reserve and Pulmonary Circulation Uncoupling During Exercise Challenge in Heart Failure: Pathophysiology and Clinical Phenotypes. JACC Heart Fail 2016;4:625-35.

32. Topilsky Y, Rozenbaum Z, Khoury S et al. Mechanisms of Effort Intolerance in Patients With Heart Failure and Borderline Ejection Fraction. Am J Cardiol 2017;119:416-422.

33. Oliveira RKF, Faria-Urbina M, Maron BA, Santos M, Waxman AB, Systrom DM. Functional impact of exercise pulmonary hypertension in patients with borderline resting pulmonary arterial pressure. Pulmonary Circulation 2017;7:654-665.

34. Wensel R, Jilek C, Dorr M et al. Impaired cardiac autonomic control relates to disease severity in pulmonary hypertension. Eur Respir J 2009;34:895-901.

35. Bristow MR, Minobe W, Rasmussen R et al. Beta-adrenergic neuroeffector abnormalities in the failing human heart are produced by local rather than systemic mechanisms. J Clin Invest 1992;89:803-15.

36. McCabe C, Oliveira RKF, Rahaghi F et al. Right ventriculo-arterial uncoupling and impaired contractile reserve in obese patients with unexplained exercise intolerance. Eur J Appl Physiol 2018;118:1415-1426.

37. Tampakakis E, Shah SJ, Borlaug BA et al. Pulmonary Effective Arterial Elastance as a Measure of Right Ventricular Afterload and Its Prognostic Value in Pulmonary Hypertension Due to Left Heart Disease. Circ Heart Fail 2018;11:e004436.

38. Bian X, Downey HF. Right coronary pressure modulates right ventricular systolic stiffness and oxygen consumption. Cardiovasc Res 1999;42:80-6.

39. Yi KD, Downey HF, Bian XM, Fu M, Mallet RT. Dobutamine enhances both contractile function and energy reserves in hypoperfused canine right ventricle. Am J Physiol-Heart C 2000;279:H2975-H2985.

40. Hermesch S, Jones RM. Genetic parameters for haemoglobin levels in pigs and iron content in pork. Animal 2012;6:1904-12.

41. Murray PA, Baig H, Fishbein MC, Vatner SF. Effects of exerimental right ventricular hypertrophy on myocardial blood flow in conscious dogs. J Clin Invest 1979;64:421-7.

42. Murray PA, Vatner SF. Reduction of Maximal Coronary Vasodilator Capacity in Conscious Dogs with Severe Right Ventricular Hypertrophy. Circulation Research 1981;48:25-33.

43. Divekar A, Auslender M, Colvin S, Artman M, Rutkowski M. Abnormal right coronary artery flow and multiple right ventricular myocardial infarctions associated with severe right ventricular systolic hypertension. J Am Soc Echocardiogr 2001;14:70-2.

44. Akasaka T, Yoshikawa J, Yoshida K, Hozumi T, Takagi T, Okura H. Comparison of relation of systolic flow of the right coronary artery to pulmonary artery pressure in patients with and without pulmonary hypertension. Am J Cardiol 1996;78:240-4.

45. Ishibashi Y, Tanabe K, Oota T et al. Phasic right coronary blood flow in a patient with right ventricular hypertension using transesophageal Doppler echocardiography. Cardiology 1995;86:169-71.

46. Archie JP, Fixler DE, Ullyot DJ, Buckberg GD, Hoffman JI. Regional myocardial blood flow in lambs with concentric right ventricular hypertrophy. Circ Res 1974;34:143-54.

47. Lowensohn HS, Khouri EM, Gregg DE, Pyle RL, Patterson RE. Phasic right coronary artery blood flow in conscious dogs with normal and elevated right ventricular pressures. Circ Res 1976;39:760-6.

48. Guyton AC, Lindsey AW, Gilluly JJ. The limits of right ventricular compensation following acute increase in pulmonary circulatory resistance. Circ Res 1954;2:326-32.

49. Salisbury PF. Coronary artery pressure and strength of right ventricular contraction. Circ Res 1955;3:633-8.

50. Brooks H, Kirk ES, Vokonas PS, Urschel CW, Sonnenblick EH. Performance of the right ventricle under stress: relation to right coronary flow. J Clin Invest 1971;50:2176-83.

51. Klima UP, Guerrero JL, Vlahakes GJ. Myocardial perfusion and right ventricular function. Ann Thorac Cardiovasc Surg 1999;5:74-80.

52. Vogel-Claussen J, Skrok J, Shehata ML et al. Right and left ventricular myocardial perfusion reserves correlate with right ventricular function and pulmonary hemodynamics in patients with pulmonary arterial hypertension. Radiology 2011;258:119-27.

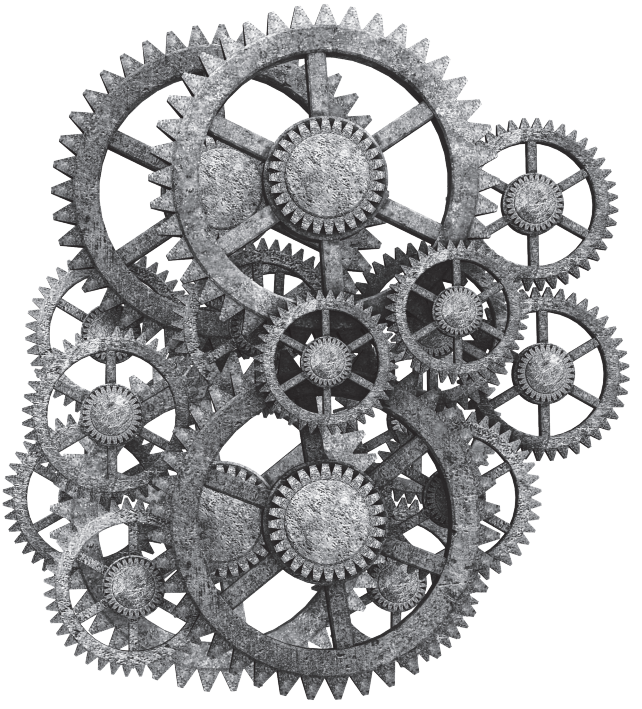

7

Chapter 7

General discussion and summary

GENERAL DISCUSSION AND SUMMARY

Cardiovascular disease remains the number one cause of death in the world. In the Netherlands it is second to cancer only. In 2018, 37.769 people died from cardiovascular diseases in the Netherlands alone (1), while globally, 17,9 million people die from cardiovascular diseases annually, representing 31% of all global deaths (2). In 1980, the main cause of death from cardiovascular disease was acute myocardial infarction. Since then, excellent science has led to innovative treatments for acute myocardial infarction (3). The most important innovation has been percutaneous coronary interventions to open up occluded coronary arteries and restore blood-flow to the heart (4). These advances, and changes in lifestyle (most importantly a reduction in smoking) have led to an 88% reduction of mortality as a direct result of acute myocardial infarction since 1980 (1). This amazing achievement has however led to a large number of patients with chronic cardiac disease. At present, one of the main causes of morbidity and mortality in cardiovascular diseases is heart failure, a condition where the heart is unable to supply the body with the necessary cardiac output. Heart failure can be attributed to either the inability of the left ventricle to contract sufficiently, or to fill sufficiently. The first being called heart failure with reduced ejection fraction (HFrEF), and the latter being called heart failure with preserved ejection fraction (HFpEF). Myocardial infarction is the primary cause of HFrEF, whereas in HFpEF old age and the metabolic syndrome are the most important risk factors (5). Heart failure affects at least 26 million people worldwide, and the prevalence is increasing (6). In 2018, 242.300 people in the Netherlands had the diagnosis of heart failure. This number is expected to increase to 342.000 people in 2030 (1).

Heart failure is the most common cause of pulmonary hypertension (PH), a pathophysiological disorder that is defined as a mean pulmonary arterial pressure of >25 mmHg at rest (7). While PH has many different aetiologies, in 65 – 80% of all cases PH is due to left heart disease, i.e. WHO classification group II (7,8). The prevalence of PH is reported to be between 40 and 75% in HFrEF and between 36 and 83% in HFpEF (8-14). A quick extrapolation of even the lowest estimates implies a prevalence of over 10 million people with heart failure related PH worldwide, and

almost 100.000 in the Netherlands alone. Another cause of group II PH is pulmonary vein stenosis. In pulmonary vein stenosis, one or more of the pulmonary veins are narrowed, hampering outflow of blood from the lungs into the left atrium. In the adult population, pulmonary vein stenosis may occur as an, albeit rare, consequence of radio-frequency ablation of atrial tissue around the pulmonary veins to treat atrial fibrillation (15-17). Pulmonary vein stenosis in the paediatric population is a severe congenital anomaly associated with poor outcome (16,18,19). Although pulmonary vein stenosis is a rare phenomenon, the frequency of pulmonary hypertension in pulmonary vein stenosis is very high, being up to 67% (20) and right heart failure is the most common cause of death in this population. In both pulmonary vein stenosis, HFpEF and HFrEF, congestion of the pulmonary venous circulation causes an increase in pulmonary venous pressure. To maintain the transpulmonary pressure gradient required for blood flow, this results in a compensatory elevation of the pre-capillary pressure. This arterial pressure increase called isolated post-capillary PH (IpcPH) is purely passive. However, when left untreated, IpcPH has the potential to progress to active, combined pre- and post-capillary PH (CpcPH), a chronic progressive disease that is subject to the vicious self-sustaining cycle that most forms of PH know (Figure 1). In this cycle, increased pulmonary arterial pressure induces vascular remodelling in the form of vascular thickening and stiffening, increasing vascular resistance, which further increases pulmonary arterial pressure.

This vicious cycle increases right ventricular afterload which promotes right ventricular remodelling and ultimately may result in right ventricular failure (10,21,22). CpcPH has a worse prognosis than IpcPH (23). While IpcPH can be treated by remedying only the underlying condition (7), CpcPH requires treatment of pulmonary vascular remodelling as well as the primary disease, as treatment of the primary disease alone does not break the vicious cycle in CpcPH (24). In group I PH, numerous treatment options promoting vasodilation and counteracting vascular remodelling are available, but the use of these drugs in group II PH can be perilous because of possible induction of pulmonary oedema (7). To assess possible treatment options, it is important to know the mechanisms by which IpcPH progresses to CpcPH and to study the most prominent vasoactive pathways.

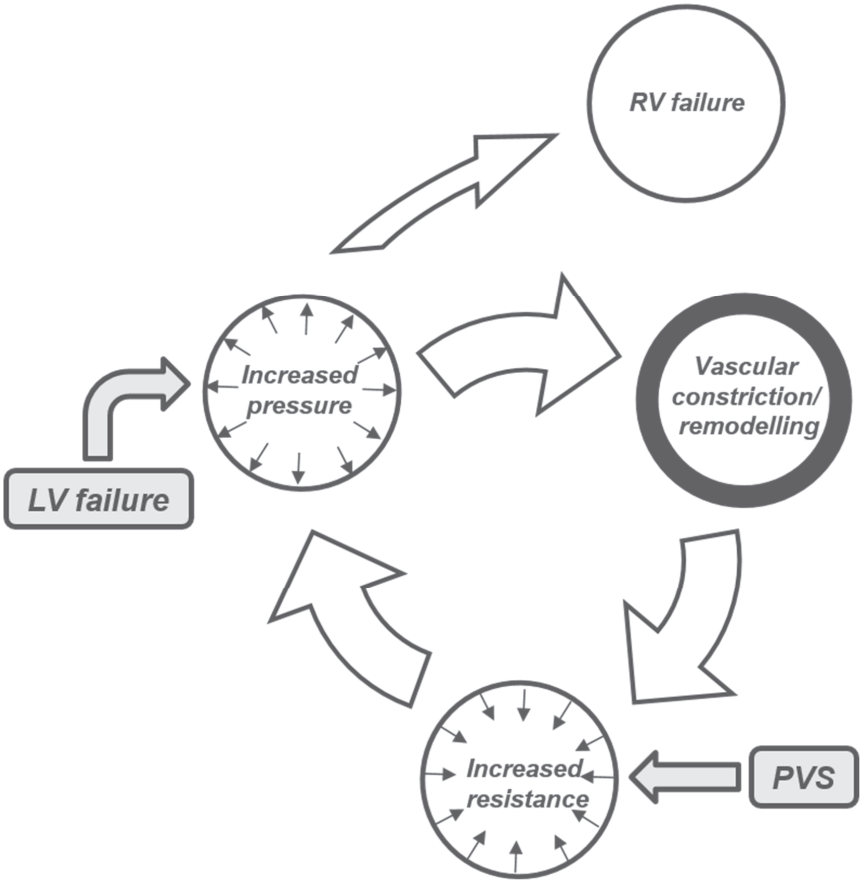

Figure 1. Vicious cycle of pulmonary hypertension. Schematic representation of the vicious self-sustaining cycle of increased pressure, vascular constriction/remodelling and increased resistance that ultimately promotes right heart (RV)-failure. The cycle is initiated by left ventricular (LV)-failure or pulmonary vein stenosis (PVS).

Considerations on experimental design and methods

The aim of this thesis was to characterize (patho-)physiological mechanisms leading to development and progression of group II PH. The disease must be studied at very early stages, and monitored as it progresses. Also monitoring of true pulmonary pressures, vascular resistance and cardiac output requires serial invasive measurements, although estimates can be made using non-invasive methods such as MRI or echo-Doppler (25-27). Because of these reasons, it is difficult to study these

phenomena in patients. Furthermore, because of the complex and unknown mechanisms underlying the pathophysiology of PH, experiments cannot be performed using isolated cells, organs or a computer model alone. To fill the gap between these fundamental techniques and human studies, animal models are an invaluable source of information. Each animal species has advantages and disadvantages as an animal model. While rodent models have considerable advantages including low housing and maintenance costs, genetic stability and the possibility of genetic engineering, results from large animal models are more easily translated to human patients. We chose to use swine as an animal model because the cardiovascular system - as well as the respiratory system - of swine closely resembles that of humans both anatomically and physiologically, making it a highly translational animal model (28). Disadvantages of domestic swine as animal models include their size and rapid growth. In commercially available swine breeds such as Yorkshire and Landrace, adults are very large and may therefore be difficult to handle. To counter these practical challenges, juvenile swine are often used. Depending on the breed, swine are born at 1-2 kg and grow to 100 kg in six to eight months. This underlines the importance of indexing haemodynamic parameters to bodyweight or body surface area when studying haemodynamics over time. Also, the heart and pulmonary vasculature of juvenile swine are still very adaptable to change and stress. Adult miniature swine such as Yucatan or Göttingen are 40 - 60 kg and can be used to circumvent these issues (29). Animal models for pulmonary hypertension are available, but cardiopulmonary function is often measured invasively, requiring anaesthesia (30-32). As many anaesthetic agents are cardio-depressive, subtle changes in cardiovascular function may be masked (33). To overcome these issues, we describe a surgical procedure to chronically instrument swine in **chapter 2**. This allows for measurement of cardiopulmonary function in the awake state, so that measurements can be obtained under quiet resting conditions, without the effects of anaesthesia and acute surgical trauma. **Chapter 2** continues with the description of the procedure to exercise instrumented swine on a motor-driven treadmill. This way, we can challenge the cardio-pulmonary system, and unmask early (patho-) physiological adaptations. We used the procedure of chronic instrumentation in **chapter 3, 4, 5 and 6**.

Early pulmonary hypertension after myocardial infarction

To assess early perturbations of vascular function in secondary PH we used a swine model for myocardial infarction in **chapter 3**. Our group characterized this swine model in previous studies, unveiling haemodynamic characteristics and neurohumoral activation similar to that seen in early secondary PH e.g. increased left atrial pressure and increased pulmonary arterial pressure (34). In these previous studies we found that these haemodynamic alterations were accompanied by increased levels of endothelin, and increased endothelin receptor activity (34). Furthermore, we have previously shown that the pulmonary vasodilator influence of nitric oxide (NO) is maintained (35,36). In **chapter 3**, we further investigated potential alterations in the NO-signalling pathway and found that pulmonary vasodilation to phosphodiesterase 5 (PDE5)-inhibition was not only maintained, but even slightly enhanced compared to normal swine, particularly during exercise, indicating that either cGMP-levels were higher or that PDE5-activity was increased. Several studies in animal models already demonstrated that cGMP and PDE5-activity are increased and hence that the NO-cGMP pathway is altered in PH (37-40). Two of these studies showed that the net result of these alterations in the NO-pathway are elevated levels of cGMP (38,39). It is important to consider the increased effect of PDE5-inhibition in perspective of the maintained contribution of the NO pathway. Indeed, elevated levels of cGMP could have resulted from increased NOS-activity, as has been reported in early stages of PH (41,42). In **chapter 3** we therefore also evaluated the effect of PDE5-inhibition in the presence of NO synthase-inhibition and found that inhibition of PDE5, in the presence of NO synthase-inhibition, still produced a greater decrease in vascular resistance compared to normal swine, suggesting that this increased response was NO-independent. Activation of particulate guanylyl cyclase, for example by natriuretic peptides such as atrial natriuretic peptides (ANP) can also produce cGMP. ANP is stored within atrial secretory granules and is released in response to increased wall stress or pressure (43). In **chapter 3** the effect of PDE5-inhibition increased during exercise, when left atrial pressure increased as well. Furthermore, there was a correlation between left atrial pressure and change in pulmonary vascular resistance as a result of PDE5-

inhibition in both normal swine and swine with myocardial infarction, consistent with the concept that ANP-signalling via particulate guanylyl cyclase could have contributed to cGMP-production. In PH secondary to myocardial infarction, atrial pressures are increased and can thereby contribute to elevated circulating levels of ANP that are found in patients with PH (44). In accordance with these findings, we have previously shown that ANP levels are elevated in our model of early PH (45,46) and we found a strong correlation between left atrial pressure and ANP in normal swine (r^2=0.90; P=0.053) and especially in swine with a myocardial infarction (r^2=0.93; P<0.05). The increased vasodilator effect on PDE5-inhibition in swine with myocardial infarction in **chapter 3** could thus have been the result of these elevated levels of ANP. These observations suggest that PDE5-inhibition holds promise as a pharmacotherapeutic strategy to normalize pulmonary haemodynamics in post-capillary PH after a recent MI, when NO is often increased, to prevent progressive CpcPH. Furthermore, PDE5-inhibition may also be an effective therapeutic strategy in more advanced PH associated with heart failure, when cGMP is increased as the result of increased ANP activity.

Progression from IpcPH to CpcPH

While the MI-model used in **chapter 3** produced a mild elevation of pulmonary artery pressure, this elevation was principally the result of a higher mean left atrial pressure after myocardial infarction, as pulmonary vascular resistance was not significantly different between normal swine and swine with a myocardial infarction. To further investigate the transition from IpcPH to CpcPH, we used a different swine model for post-capillary PH. In this model, first described by Pereda et al, pulmonary vein banding results in an obstruction of 60-65% of the pulmonary vascular bed that increases in severity when the animal grows (31). The increase in distal vascular resistance causes a passive pressure increase, that is transmitted backwards into the pulmonary vasculature, mimicking the passive pressure increase in left heart failure or pulmonary vein stenosis (31,47). This model is well suited to study the progression and pathophysiology of all forms of group II PH. With translation to PH as a result of left heart failure, both with reduced or preserved ejection fraction, it can be both a

drawback as well as an advantage that there is no actual left heart failure. This model could be missing circulating factors originating from left heart failure such as elevated natriuretic peptides and troponins (48). On the other hand, we were able to study the isolated pulmonary vascular pathogenesis of CpcPH without influence of the left side of the heart. In **chapter 4 and chapter 5**, we adapted and haemodynamically characterized this model by performing the chronic instrumentation described in **chapter 2**. We found that not only pulmonary arterial pressure, but also total pulmonary vascular resistance index increased over time. While this increased pressure and resistance started out as a direct result of pulmonary venous congestion, we found that from ten weeks after banding, changes in vasoactive pathways were eminent. Specifically, there was a substantial contribution of increased endothelin activity to the increased vascular tone, while - surprisingly - NO availability and sensitivity were increased, possibly as a compensatory mechanism. Not only functional changes were observed in these animals. After sacrifice at twelve weeks after banding, histology on pulmonary small arteries in **chapter 4** demonstrated muscularisation and thickening of the vascular wall, resulting in a relative reduction of the vascular lumen. This finding is consistent with the observation that pulmonary vascular remodelling in group II PH mainly consists of medial hypertrophy and muscularisation of arterioles (49). Although this model has been known to lead to not only increased medial thickness, but also increased intimal thickness and fibrosis in previous studies with four months follow up (31). Consistent with the increased muscularisation, we found that maximal contraction of these vessels was increased. These structural vascular changes could have been caused by the increased ET-activity, as ET is a well-known mediator of vascular remodelling (50-52). With the observed structural vascular remodelling, and functional remodelling evidenced by alterations in the ET and NO pathways, we characterized the transition from IpcPH to CpcPH in this swine model.

Endothelin as a therapeutic target for heart failure related PH

The increased endothelin activity in **chapter 4** was evidenced by increased vasodilation to in-vivo dual receptor blocking, increased expression of pre-pro

endothelin and endothelin converting enzyme in lung tissue, and increased circulating levels of endothelin. Because of the abluminal release, circulating plasma levels of endothelin are thought to be the result of spillover from the junctions between endothelial and smooth muscle cells and can therefore not be equated to endothelin activity in pathological states (53). However, plasma endothelin levels are upregulated in group I PH (pulmonary arterial hypertension; PAH) and in chronic heart failure, and correlate with the severity of symptoms and pulmonary haemodynamics (54-57). The fact that a purely mechanical increase of pulmonary pressure and resistance induces over-activation of the endothelin pathway in this animal model suggests that this pathway might be an interesting target for therapy in patients suffering from group II PH, in which activation of the endothelin pathway may be further exacerbated by neurohumoral activation. To date, a number of clinical trials have been performed with a variety of endothelin receptor antagonists in chronic heart failure, with generally rather disappointing results (58-66). The 18 months follow up ENABLE study failed to show a significant reduction in mortality or heart failure-related hospitalisation with bosentan vs placebo in HFrEF patients (60). Also, already after 2 weeks, bosentan treatment was associated with fluid retention, peripheral oedema, anaemia and abnormal liver function. The REACH study utilized a higher dose of bosentan (2x500mg/day vs 125mg/day in ENABLE) and was terminated early because of early deterioration of heart failure in the bosentan group (64). In the subset of patients who did complete follow up at 6 months, the detrimental effect in the bosentan group was only evident in the first few weeks of the study while later in the trial, the risk of deteriorating heart failure was higher in the placebo group. This beneficial effect of long term treatment with bosentan came, however, with increased liver transaminases and mild anaemia. Selective endothelin-A receptor blockade with darusentan (30, 100 or 300 mg/day) increased cardiac index in de three-week follow up period of the HEAT trial (62). While systemic vascular resistance decreased in this trial, pulmonary capillary wedge pressure, pulmonary arterial pressure, pulmonary vascular resistance, right atrial pressure, heart rate and mean arterial pressure did not. Also, all except the 30 mg/day dose were accompanied by headaches, and the 300 mg/day dose was associated with worsening heart failure. Despite preservation of the endothelin-B receptor which can

act as a clearance receptor, endothelin-1 levels increased in the darusentan groups at 3 weeks follow up. The 24 weeks follow up EARTH trial did not show clinical benefit in any of the 5 darusentan groups (10, 25, 50, 100 or 300 mg/day) and no change in left ventricular end-systolic volume, which was the primary endpoint in that study. The RITZ trials assessed the use of intravenous dual endothelin receptor blockade by tezosentan, as used in **chapter 4**. In RITZ-1, 669 patients with acute decompensated heart failure received 50 mg/hr tezosentan or placebo (59). Neither the primary endpoint of reduction of dyspnoea at 24 hours of therapy nor the secondary endpoint of time to death or worsening heart failure showed any difference between tezosentan or placebo treatment groups. Tezosentan was however associated with increased risk of adverse effects (hypotension, nausea, headache, dizziness, renal failure/impairment). RITZ-2 assessed the haemodynamic effect of, and outcome after 50 or 100 mg/hr tezosentan treatment in patients with chronic heart failure (61). Contrary to RITZ-1, the results of the RITZ-2 trial were very positive, with increased cardiac index, decreased pulmonary capillary wedge pressure and improved dyspnoea in tezosentan groups. Also, time to death, and worsening heart failure tended to be better in the tezosentan groups. Adverse effects (mainly hypotension) only seemed to be increased in the 100 mg/hr tezosentan group. In the VERITAS study, a low dose of tezosentan (5 mg/hr for 30 minutes followed by 1 mg/hr for 24-72 hours) successfully decreased pulmonary capillary wedge pressure, right atrial pressure, pulmonary vascular resistance and systemic vascular resistance, with a trend towards an increased cardiac index. However, these haemodynamic changes failed to improve dyspnoea or other symptoms, or clinical outcome. Again, hypotension was more common in the tezosentan group than in placebo. While these six clinical trials involve three different types of ET-receptor antagonists, they have some things in common. In all studies, experimental ET-receptor antagonists were tested in the presence of continued conventional medicine, including ACE-inhibitors, ß-blockers and angiotensin-II- and aldosterone receptor antagonists. It is possible that the added effect of ET-receptor antagonists is limited because of its use in an already highly medicated system which collectively impair the 'natural defence mechanisms' against hypotension. In an acute clinical study, darusentan showed a dose-dependent decrease in cardiac index, systemic vascular resistance, pulmonary

vascular resistance, mean arterial pressure, pulmonary arterial pressure and pulmonary capillary wedge pressure when conventional medicine was halted. This is in contrast with the HEAT and EARTH trials, where medication was continued, and darusentan produced no additional pulmonary haemodynamic effect. It could even be speculated that the continuation of conventional medicine is an aggressor of the recurrent systemic hypotension found in many Endothelin trials. Another possible factor which could cause a discrepancy between studies is the presence or absence of measurement of haemodynamic parameters. McMurray et al. stated that the knowledge of haemodynamic parameters could possibly influence the assessment of dyspnoea (63). This could explain the positive results from the RITZ-2 trial, where haemodynamic parameters were obtained compared to the negative RITZ-1 and VERITAS trials, which did not monitor haemodynamics, and could not reproduce the beneficial effects of tezosentan from the RITZ-2 study. A well-designed future clinical trial with endothelin receptor antagonists in a population with CpcPH without influence of conventional medicine would be interesting from a fundamental scientific point of view. The observation in **chapter 4** that ET-induced vasoconstriction in isolated pulmonary small arteries appeared to be entirely dependent on ET_A-receptors, suggests ET_A-blockade alone might be preferable over dual ERA's. However, discontinuation of conventional medicine is not without risk. Thus, great caution should be taken when designing and conducting such a study.

Nitric oxide as a therapeutic target for heart failure related PH

In **chapter 5** we investigated the changes in the NO pathway in the pulmonary vein banded swine model in the same timeframe as studied in **chapter 4**. We found that already 10 weeks after banding, at the same time that ET activity increases, both NO availability and sensitivity were increased. The NO-donor SNP induced a bigger pulmonary vasodilation response in banded swine than in sham swine. This increased sensitivity was not driven by a decreased PDE5-activity, as the PDE5-inhibitor Sildenafil also induced a bigger pulmonary vasodilation response in banded swine. The effect of SNP was relatively modest as compared to the reduction in total pulmonary vascular resistance index induced by PDE5-inhibition. Together with the

observations that eNOS-inhibition produced a larger increase in pulmonary vascular resistance as compared to sham, this suggests that, like in **chapter 3**, the NO-pathway is hyperactive in the pulmonary vasculature of banded swine in **chapter 5**, probably as a compensatory mechanism for the increased ET-activity as found in **chapter 4**. Adding additional NO therefore has a very limited effect. These data are consistent with the study of Domingo et al, showing that NO on top of 100% oxygen did not induce further pulmonary vasodilation (67). Based on **chapter 5**, the most effective anchor point for NO-related therapy is PDE5-inhibition. PDE5-inhibitors are already widely used to reduce pulmonary vascular resistance and pulmonary arterial pressure and thereby alleviate the workload of the right ventricle in patients with PAH. While many PAH-therapies have proven ineffective (63,64,68) or even detrimental (69,70) for other forms of PH, recent trials showed decreased pulmonary arterial pressure, pulmonary capillary wedge pressure and improved function of the right ventricle and the pulmonary vasculature with PDE5-inhibition in PH due to left heart failure with reduced ejection fraction, and also in PH due to left heart failure with preserved ejection fraction (71-73). Moreover, whereas other PAH-therapies have been associated with increased LV filling pressures, leading to acute pulmonary oedema in PH secondary to left heart failure (74,75), Guazzi et al. showed that PDE5-inhibition not only improved pulmonary haemodynamics and right ventricular function, but also had a positive effect on left ventricular structure and function (76). This crucial feature prevents pulmonary oedema and makes this vasodilator therapy particularly suited for treatment of PH due to left heart failure. Interestingly, in our swine with PH as a result of myocardial infarction in **chapter 3**, PDE5-inhibition not only decreased pulmonary vascular resistance, but also improved cardiac function, indicated by an increased stroke volume. Whether this was mediated by improved left and/or right ventricular function remains to be determined although consistent with previous studies, we observed no significant changes in left ventricular contraction or relaxation rate and no change in left ventricular filling pressure upon PDE5-inhibition (77). **Chapter 3 and 5** indicate that both patients with early PH secondary to MI, as well as patients with progressive CpcPH could benefit from the pulmonary vasodilator effect of PDE5-inhibition. Especially because in both states, the vasodilator effect is enhanced in comparison with normal healthy conditions,

probably as a result of increased cGMP availability. The fact that in early PH after myocardial infarction, the increased vasodilator effect is independent of NO-signalling, suggest that even when PH progresses to a state where endothelial dysfunction causes decreased NO-activity, inhibition of PDE5 can still result in pulmonary vasodilation and decrease pulmonary arterial pressure and resistance and alleviate right ventricular afterload. When looking at clinical trials, the RELAX-trial, did not show significant improvement in exercise capacity or clinical status in HFpEF patients with 24 weeks of PDE5-inhibition (78). Also in HFpEF patients with IpcPH, 12 weeks of treatment with PDE5-inhibition did not improve pulmonary haemodynamics or other clinical parameters (79). It must be noted however, that the true target population within group II PH are patients with left heart failure and CpcPH, not IpcPH. It is the pre-capillary aspect that should be targeted with vasodilator therapy, whereas in IpcPH, the primary cause should be targeted. Recently, Kramer et al did a retrospective study in 40 patients with HFpEF and CpcPH that received PDE5-inhibition for at least 12 months. This study showed significant improvement in exercise capacity, NTproBNP levels, and measures of RV-function (80). A randomized, placebo-controlled, double-blind study in HFpEF patients with CpcPH is currently conducted (PASSION trial). Hopefully, this trial will have the statistical power to prove a beneficial effect of PDE5-inhibition in this challenging group of patients. Regarding LHF patients with IpcPH, PDE5-inhibition does not seem to have a direct effect on pulmonary haemodynamics or other clinical parameters. However, it remains to be determined to what extent PDE5-inhibition inhibits or even reverses pulmonary vascular remodelling in group II PH. PDE5-inhibition might prove a successful strategy to prevent CpcPH.

Treatment of pulmonary vein stenosis and related PH

Treatment of pulmonary vein stenosis currently consists of either surgical pulmonary venoplasty, or a catheter-based approach like balloon angioplasty with or without intravascular stent placement. Unfortunately, treatment of pulmonary vein stenosis is technically challenging, restenosis is frequent and event-free survival is poor (18). A French cohort of premature infants with pulmonary vein stenosis and PH reported

56% survival 1 year after diagnosis (81). Despite the small number of enrolled patients, they were able to analyse 1-year survival in patients that received any type of intervention (1-year survival 69%) vs patients that received no intervention (1-year survival 21%). A recently published multicentre retrospective cohort study of pulmonary vein stenosis affecting ex-premature infants (20) and a meta-analysis (18) found similar survival rates between 55% and 70%. An important determinant of mortality is the severity of PH and concomitant RV-dysfunction (82). Lowering the pulmonary arterial resistance and pressure is therefore an increasingly popular therapeutic target. Most patients with pulmonary vein stenosis (67), as well as swine with pulmonary vein stenosis (83) show a decrease in pulmonary artery pressure upon vasoreactivity testing with inhaled 100% oxygen. In **chapter 4**, we showed that $ET_{A/B}$ blockade with tezosentan resulted in a decrease in pulmonary vascular resistance in swine with pulmonary hypertension as a result of pulmonary vein banding, and that this vasodilator effect increased over time. In **chapter 5**, also the NO-donor SNP as well as the PDE5-inhitor Sildenafil induced pulmonary vasodilation that was larger in swine with pulmonary hypertension. In the search for the best vasodilation therapy in pulmonary vein stenosis-induced PH, it is important to realize that in pulmonary vein stenosis, the pulmonary vasculature comprises two territories; those draining into stenotic pulmonary veins, and those draining into unaffected pulmonary veins. The high resistance of the stenosis causes a redistribution of flow from the stenosis lobes to the lobes without stenosis. Thus, the pulmonary vasculature in the first territory will experience high pressure and low flow (HP/LF), whereas the latter experiences high pressure and high flow (HP/HF) (84). Issues regarding pulmonary oedema that arise in treatment of PH secondary to left heart failure may be absent when treating only the HP/HF vasculature in pulmonary vein stenosis-induced PH. The swine model used in **chapter 4 and 5** is unique in its ability to allow for independent interrogation of these two subsets of arteries as these vessels can be separately assessed in vitro at the end of follow-up. Interestingly, in **chapter 5**, vasodilation in response to bradykinin was smaller in pulmonary small arteries from the HP/LF-territory, than sham while pulmonary small arteries from HP/HF-territory did not show a difference as compared to sham. These data are consistent with data from **chapter 4**, showing that vasodilation to

Substance P, another endothelium-dependent vasodilator used to measure endothelial function, was only decreased in HP/LF lobes of swine with pulmonary hypertension. These data suggest endothelial dysfunction in pulmonary vein stenosis, but mainly in the HP/LF-territory. This endothelial dysfunction did not encompass a change in NO, as the eNOS-inhibitor L-NAME attenuated the bradykinin-induced vasodilation to a similar extent in pulmonary small arteries from all territories. This is consistent with unchanged eNOS protein expression in the HP/LF lobes compared to sham. Bradykinin also exerts a vasodilatory effect via endothelium derived hyperpolarizing factor and via prostacyclin. The decreased vasodilation to bradykinin in the HP/LF-territory of swine with pulmonary hypertension is thus either the result of decreased endothelium derived hyperpolarizing factor or decreased prostacyclin. It could therefore be speculated that prostacyclin therapy would mainly target the HP/HF vasculature, and be the therapy of choice for pulmonary vein stenosis-induced PH. As we did not directly test the effect of prostacyclin therapy in-vivo or in-vitro, future studies are needed to assess this possibility. Interestingly, eNOS-expression was higher in HP/HF as compared to HP/LF and tended to be higher as compared to the corresponding lung lobe of sham animals. This increased expression predominantly involved a higher expression of the NO-producing eNOS dimer, as the superoxide producing eNOS monomer was higher in HP/HF as compared to HP/LF, but was similar to the corresponding lobes of sham animals. The vasodilator effect of the NO-donor SNP was not different in the HP/HF upper vs the HP/LF lower lobes of swine with pulmonary hypertension. There was however a difference in efficacy of PDE5-inhibition by Sildenafil. Unfortunately, the effect was bigger in the HP/LF vasculature. Although this is theoretically unfavourable, we did not find any evidence for pulmonary oedema in-vivo (i.e. no reduction in arterial pO_2). The reduced effect of sildenafil in vitro could potentially be explained by the lack of flow in the in-vitro experiments. It is possible that in-vivo, in the presence of flow, shear stress induced NO-production is higher in the HP/HF-territories as compared to the HP/LF-territories, and consequently that an increase in cGMP in response to PDE5-inhibition may be more pronounced in the HP/HF-territories. When comparing the effect of the vasodilators studied in this thesis, the pulmonary vasodilator effect of Sildenafil in **chapter 5** is approximately twice as big as the pulmonary vasodilation induced by

tezosentan in **chapter 4**. Similarly, the effect of Sildenafil was larger than that of the NO-donor SNP. Hence, based on results of this thesis, sildenafil should be the treatment of choice for pulmonary vein stenosis-induced PH. Currently, approximately 30% of paediatric patients with pulmonary vein stenosis are on pulmonary vasodilator treatment with Sildenafil being the most commonly administered drug (20,82).

Right ventricular adaptations in group II pulmonary hypertension

The right ventricle (RV) has not evolved to work at high pressures. The gradual increase in afterload over time in animals with pulmonary vein stenosis (or PH in general) results in structural remodelling of the RV. This can be either adaptive remodelling, or maladaptive remodelling. Adaptive remodelling comprises concentric hypertrophy, and unchanged systolic and diastolic function. Maladaptive remodelling comprises eccentric remodelling, RV dilatation and reduced RV function (85). Maladaptive remodelling ultimately leads to RV failure. Even in group II PH as a result of left heart failure, the function of the right ventricle may determine the fate of the patient (86). In **chapter 6** we investigated RV-function and assessed if the RV showed signs of remodelling. We found that the gradual increase in afterload over time resulted in RV-hypertrophy, evidenced by an increase in Fulton index and cardiomyocyte size, a trend towards an increased interstitial fibrosis, as well as RV-dilation measured by echocardiography. RV-hypertrophy enabled the RV to cope with the increased afterload as cardiac index and stroke volume index were maintained at rest. This required recruitment of contractile function, as evidenced by higher Ees and a trend towards an increased dP/dt-max in PH, while RV-PA coupling was reduced. RV-PA coupling describes the matching of RV-function and afterload (86). In **chapter 6**, PH resulted in a 32% reduction in RV-PA coupling, which is similar in magnitude to the 25% reduction in RV-PA coupling observed in patients with WHO group II PH (21,87). Consistent with the reduction in RV-PA coupling, RV-fractional area change and Tricuspid annular plane systolic excursion (TAPSE) were reduced in PH. Altogether histological, echocardiographic, haemodynamic and RV-PA coupling data were consistent with mild RV-dysfunction at rest.

Right ventricular function during exercise

Exercise challenges the RV. Exercise limitation is the earliest symptom of right heart failure and is a strong predictor of survival in PH patients (88). Patients with PH, even those with PH related to left heart failure, experience a limited exercise capacity due to the inability of the RV to sufficiently increase cardiac output during exercise (89-91). The correlation between RV-function and exercise capacity in patients with left heart failure is irrespective of the ejection fraction, and found in patients with reduced, midrange or preserved ejection fraction (92-94). Together with data showing Ea is a robust and independent predictor of mortality in patients with WHO group II PH, and correlates strongly with RV-dysfunction (95,96), it appears that the reduced RV-contractile reserve, which results in a decrease in RV-PA coupling during exercise, is an important limiting factor in exercise-tolerance in PH patients. The main determinants of RV-functional reserve in patients with PH are unknown. The inability to sufficiently increase cardiac output may be partly due to chronotropic incompetence and partly due to impaired stroke volume reserve (94,97). In **chapter 6**, we found that the exercise-induced increase in cardiac index was indeed attenuated, partly because of chronotropic incompetence, potentially due to impaired autonomic control (98,99). Furthermore, despite the presence of hypertrophy, the RV in PH swine was unable to increase its contractile function beyond the value observed in control subjects. We tested the hypothesis that this inability to augment the contractile force was at least partly due to the inability to increase myocardial O_2 consumption. Although myocardial O_2 extraction in the RV is lower than that in the LV, the RV has limited O_2 extraction reserve, particularly during exercise (100), and myocardial O_2 utilisation efficiency can only be temporarily increased (101,102). Thus to increase O_2 consumption, O_2 delivery must increase. Indeed, in **chapter 6** we found that the relation between RV-O_2 delivery and work rotated clockwise during exercise in PH, suggesting impaired O_2 delivery. This impaired O_2 delivery was not sufficient to cause ischemic damage (high sensitive troponin was not increased in PH), but did correlate linearly with RV-functional reserve. The impaired O_2 delivery reserve was not due to a reduction in capillary density of the RV-myocardium, but can be attributed in part to the attenuation of the exercise-induced increase in blood

pressure, possibly as a result of the attenuated increase in cardiac index due to the chronotropic incompetence. However, particularly mean systolic CBF was lower, while mean diastolic CBF remained similar between PH and control during exercise indicating that increased extravascular compression in PH is the main contributor to the reduced RV-perfusion reserve. These data are consistent with studies showing a reduced ratio of systolic and diastolic flow at rest in patients with PAH (103-106) and animals following pulmonary artery banding (107-110), as well as various studies showing that maximal RV-function is related to maximal RV-CBF in both healthy subjects (111-114), and in patients with PAH and chronic thromboembolic PH (103,115).

The findings in **chapter 6** suggest that O_2 delivery reserve could potentially be used to assess the clinical status of patients with PH. Furthermore, our data suggest that RV function and exercise capacity could be improved by improving RV-O_2 delivery.

Future perspectives

The studies provided in this thesis aimed to provide novel insights in pathophysiological mechanisms in cardiopulmonary disease. Although this thesis indeed provides novel insights, these insights raise a number of new questions that should be addressed in future studies.

First, in **chapter 3**, we found that pulmonary vasodilation to PDE5-inhibition is enhanced and NO-independent in resting and exercising swine with PH as a result of myocardial infarction. We hypothesize that in PH, atrial natriuretic peptide is an alternative source for cGMP via the activation of particulate guanylyl cyclase. Although we provide indirect evidence for this hypothesis, with a correlation between atrial natriuretic peptide plasma levels and left atrial pressure, and a correlation between vasodilation through PDE5-inhibition and left atrial pressure, future studies with an ANP receptor antagonist (116-120) are needed to test our hypothesis.

Second, there is evidence that there are significant sex differences in the prevalence and severity of PH. In our studies, group size should be increased in order to gain

enough statistical power to assess sex-differences in the MI-animals. We recently collected historical data from swine studies performed by our group, which show a different correlation between ANP levels and left atrial pressure in male and female swine (Figure 2, unpublished data from our laboratory).

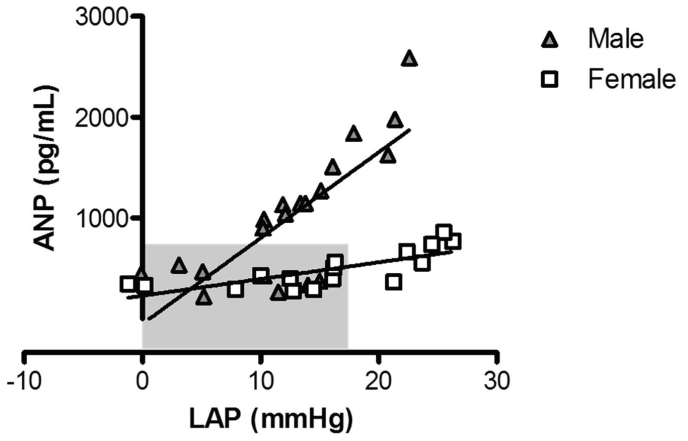

Figure 2. Correlations with ANP levels and left atrial pressures (LAP) of swine with myocardial infarction. A clear difference can be observed between male and female animals. Male P<0.0001, R2=0.61, Female P<0.001, R2=0.56. Grey area shows the range of data from normal swine. Unpublished data

Third, there is an ongoing debate regarding the reversibility of pulmonary vascular changes following chronic exposure to elevated pulmonary artery pressures. Future studies with the pulmonary vein banding model should elucidate the reversibility of the changes observed in our porcine model. Removal of the pulmonary vein banding at different time points, followed by additional weeks of follow-up and assessment of vasoactive pathways and vascular morphology could provide a 'point of no return'. If the pulmonary vein banding were to be removed at 12 weeks, would vasoactive pathways normalize? Or would the vicious cycle sustain itself to deteriorate further? Finding the point of no return could help in determining whether to start vasodilatory therapy, or only treat the underlying condition (pulmonary vein stenosis, heart failure).

Fourth, the pulmonary vein banding swine model should be used to test prostacyclin therapy and new therapeutics such as ROCK-inhibitors. The hypotheses that emerged from the results of **chapter 5** that prostacyclin therapy would mainly target the HP/HF vasculature, and be the therapy of choice for pulmonary vein stenosis-induced PH should be tested.

Fifth, future studies in the pulmonary vein banding model should include long term drug testing. Thus, it would be interesting to see if pulmonary pressures and resistance would stabilize, or even normalize when PDE5 is inhibited chronically, or endothelin is blocked chronically. Furthermore, it would be interesting to see if vascular morphometry would stabilize or normalize. In future experiments, experimental design and methods should be carefully reconsidered. While methods described in **chapter 2** are elegant and provide us with a complete haemodynamic profile, catheter-based measurement methods can only be performed for a limited number of weeks. Follow up period could be extended when haemodynamic data would be acquired by wireless techniques like the Cardiomems system (121,122). Utilisation of such a system would enable us to use long time follow up and study disease progression and long-term drug testing.

Sixth, a large international randomised double blind prospective clinical trial should be conducted with PDE5-inhibition. While there appears to be some benefit from PDE5-inhibition in group II PH secondary to LHF, the mostly small, short-term studies fail to show which type of LHF will benefit at which stage. A trial on large populations of HFrEF with IpcPH, HFrEF with CpcPH, HFpEF with IpcPH and HFpEF with CpcPH should be conducted. The last group will already be investigated in the PASSION trial. The trial should be sufficiently powered, with long-term follow-up, and endpoints should not only include WHO functional class, six-minute walk distance, and clinical worsening, but also pulmonary vascular resistance, pulmonary capillary wedge pressure and transpulmonary pressure gradient. Beside a possible direct beneficial effect, this should also elucidate any protective or preventive features of PDE5-inhibition in these groups of patients.

REFERENCES

1. de Boer AR BM, van Dis I, Vaartjes I, Visseren FLJ. Hart- en vaatziekten in Nederland, 2019. Nederlandse Hartstichting, 2020.
2. Organization WH. Factsheet on Cardiovascular diseases. https://wwwwhoint/en/news-room/fact-sheets/detail/cardiovascular-diseases-(cvds): World Health Organization, 2017.
3. Van de Werf F. The history of coronary reperfusion. Eur Heart J 2014;35:2510-5.
4. Zijlstra F. Primary angioplasty is the most effective treatment for an acute myocardial infarction. British heart journal 1995;73:403-4.
5. Gevaert AB, Boen JRA, Segers VF, Van Craenenbroeck EM. Heart Failure With Preserved Ejection Fraction: A Review of Cardiac and Noncardiac Pathophysiology. Front Physiol 2019;10:638.
6. Savarese G, Lund LH. Global Public Health Burden of Heart Failure. Card Fail Rev 2017;3:7-11.
7. Galie N, Humbert M, Vachiery JL et al. 2015 ESC/ERS Guidelines for the Diagnosis and Treatment of Pulmonary Hypertension. Rev Esp Cardiol (Engl Ed) 2016;69:177.
8. Rosenkranz S, Gibbs JS, Wachter R, De Marco T, Vonk-Noordegraaf A, Vachiery JL. Left ventricular heart failure and pulmonary hypertension. Eur Heart J 2016;37:942-54.
9. Ghio S, Gavazzi A, Campana C et al. Independent and additive prognostic value of right ventricular systolic function and pulmonary artery pressure in patients with chronic heart failure. J Am Coll Cardiol 2001;37:183-8.
10. Miller WL, Grill DE, Borlaug BA. Clinical features, hemodynamics, and outcomes of pulmonary hypertension due to chronic heart failure with reduced ejection fraction: pulmonary hypertension and heart failure. JACC Heart Fail 2013;1:290-299.
11. Tampakakis E, Leary PJ, Selby VN et al. The diastolic pulmonary gradient does not predict survival in patients with pulmonary hypertension due to left heart disease. JACC Heart Fail 2015;3:9-16.
12. Lam CS, Roger VL, Rodeheffer RJ, Borlaug BA, Enders FT, Redfield MM. Pulmonary hypertension in heart failure with preserved ejection fraction: a community-based study. J Am Coll Cardiol 2009;53:1119-26.
13. Leung CC, Moondra V, Catherwood E, Andrus BW. Prevalence and risk factors of pulmonary hypertension in patients with elevated pulmonary venous pressure and preserved ejection fraction. Am J Cardiol 2010;106:284-6.
14. Shah AM, Claggett B, Sweitzer NK et al. Cardiac structure and function and prognosis in heart failure with preserved ejection fraction: findings from the echocardiographic study of the Treatment of Preserved Cardiac Function Heart Failure with an Aldosterone Antagonist (TOPCAT) Trial. Circ Heart Fail 2014;7:740-51.
15. Cappato R. Pulmonary Vein Stenosis Following Radiofrequency Ablation of Atrial Fibrillation: Has It Become a Clinically Negligible Complication? JACC Clin Electrophysiol 2017;3:599-601.
16. Latson LA, Prieto LR. Congenital and acquired pulmonary vein stenosis. Circulation 2007;115:103-8.

17. Fender EA, Packer DL, Holmes DR, Jr. Pulmonary vein stenosis after atrial fibrillation ablation. EuroIntervention 2016;12 Suppl X:X31-X34.
18. Backes CH, Nealon E, Armstrong AK et al. Pulmonary Vein Stenosis in Infants: A Systematic Review, Meta-Analysis, and Meta-Regression. J Pediatr 2018;198:36-45 e3.
19. Manzar S. Congenital pulmonary vein stenosis. J Coll Physicians Surg Pak 2007;17:374-5.
20. Mahgoub L, Kaddoura T, Kameny AR et al. Pulmonary vein stenosis of ex-premature infants with pulmonary hypertension and bronchopulmonary dysplasia, epidemiology, and survival from a multicenter cohort. Pediatr Pulmonol 2017;52:1063-1070.
21. Gerges M, Gerges C, Pistritto AM et al. Pulmonary Hypertension in Heart Failure. Epidemiology, Right Ventricular Function, and Survival. Am J Respir Crit Care Med 2015;192:1234-46.
22. Vanderpool RR, Naeije R. Progress in Pulmonary Hypertension with Left Heart Failure. Beyond New Definitions and Acronyms. Am J Respir Crit Care Med 2015;192:1152-4.
23. Tatebe S, Fukumoto Y, Sugimura K et al. Clinical significance of reactive post-capillary pulmonary hypertension in patients with left heart disease. Circ J 2012;76:1235-44.
24. Lundgren J, Radegran G. Pathophysiology and potential treatments of pulmonary hypertension due to systolic left heart failure. Acta Physiol (Oxf) 2014;211:314-33.
25. Stam K, Chelu RG, van der Velde N et al. Validation of 4D flow CMR against simultaneous invasive hemodynamic measurements: a swine study. Int J Cardiovasc Imaging 2019;35:1111-1118.
26. Finkelhor RS, Lewis SA, Pillai D. Limitations and strengths of doppler/echo pulmonary artery systolic pressure-right heart catheterization correlations: a systematic literature review. Echocardiography 2015;32:10-8.
27. Chinen D, Nagai T, Uemura K et al. Clinical Usefulness of an Echo-Doppler Model in Predicting Elevated Pulmonary Capillary Wedge Pressure in Patients With Heart Failure. Am J Cardiol 2019;123:1464-1469.
28. Swindle MM, Makin A, Herron AJ, Clubb FJ, Jr., Frazier KS. Swine as models in biomedical research and toxicology testing. Vet Pathol 2012;49:344-56.
29. Bender SB, van Houwelingen MJ, Merkus D, Duncker DJ, Laughlin MH. Quantitative analysis of exercise-induced enhancement of early- and late-systolic retrograde coronary blood flow. Journal of applied physiology 2010;108:507-14.
30. Mercier O, Sage E, Izziki M et al. Endothelin A receptor blockade improves regression of flow-induced pulmonary vasculopathy in piglets. The Journal of thoracic and cardiovascular surgery 2010;140:677-83.
31. Pereda D, Garcia-Alvarez A, Sanchez-Quintana D et al. Swine model of chronic postcapillary pulmonary hypertension with right ventricular remodeling: long-term characterization by cardiac catheterization, magnetic resonance, and pathology. J Cardiovasc Transl Res 2014;7:494-506.
32. Pak O JW, Ghofrani HA, Seeger W, Grimminger F, Schermuly RT, Weissmann N. Animal models of pulmonary hypertension: role in translational research. Drug Discovery Today: Disease Models 2010;7:89-97.

33. Barker SJ, Gamel DM, Tremper KK. Cardiovascular effects of anesthesia and operation. Crit Care Clin 1987;3:251-68.

34. Houweling B, Merkus D, Sorop O, Boomsma F, Duncker DJ. Role of endothelin receptor activation in secondary pulmonary hypertension in awake swine after myocardial infarction. J Physiol 2006;574:615-26.

35. Haitsma DB, Merkus D, Vermeulen J, Verdouw PD, Duncker DJ. Nitric oxide production is maintained in exercising swine with chronic left ventricular dysfunction. Am J Physiol Heart Circ Physiol 2002;282:H2198-209.

36. Merkus D, Houweling B, de Beer VJ, Everon Z, Duncker DJ. Alterations in endothelial control of the pulmonary circulation in exercising swine with secondary pulmonary hypertension after myocardial infarction. J Physiol 2007;580:907-23.

37. Hanson KA, Ziegler JW, Rybalkin SD, Miller JW, Abman SH, Clarke WR. Chronic pulmonary hypertension increases fetal lung cGMP phosphodiesterase activity. Am J Physiol Lung Cell Mol Physiol 1998;275:L931-941.

38. Cohen AH, Hanson K, Morris K et al. Inhibition of cyclic 3'-5'-guanosine monophosphate-specific phosphodiesterase selectively vasodilates the pulmonary circulation in chronically hypoxic rats. The Journal of clinical investigation 1996;97:172-9.

39. Black SM, Sanchez LS, Mata-Greenwood E, Bekker JM, Steinhorn RH, Fineman JR. sGC and PDE5 are elevated in lambs with increased pulmonary blood flow and pulmonary hypertension. Am J Physiol Lung Cell Mol Physiol 2001;281:L1051-1057.

40. Li D, Zhou N, Johns RA. Soluble guanylate cyclase gene expression and localization in rat lung after exposure to hypoxia. Am J Physiol 1999;277:L841-7.

41. Archer S, Rich S. Primary Pulmonary Hypertension : A Vascular Biology and Translational Research "Work in Progress". Circulation 2000;102:2781-2791.

42. Hampl V, Herget J. Role of nitric oxide in the pathogenesis of chronic pulmonary hypertension. Physiological reviews 2000;80:1337-72.

43. de Bold AJ, Ma KK, Zhang Y, de Bold ML, Bensimon M, Khoshbaten A. The physiological and pathophysiological modulation of the endocrine function of the heart. Can J Physiol Pharmacol 2001;79:705-14.

44. Nootens M, Kaufmann E, Rector T et al. Neurohormonal activation in patients with right ventricular failure from pulmonary hypertension: relation to hemodynamic variables and endothelin levels. J Am Coll Cardiol 1995;26:1581-5.

45. van Kats JP, Duncker DJ, Haitsma DB et al. Angiotensin-converting enzyme inhibition and angiotensin II type 1 receptor blockade prevent cardiac remodeling in pigs after myocardial infarction: role of tissue angiotensin II. Circulation 2000;102:1556-63.

46. Haitsma DB, Bac D, Raja N, Boomsma F, Verdouw PD, Duncker DJ. Minimal impairment of myocardial blood flow responses to exercise in the remodeled left ventricle early after myocardial infarction, despite significant hemodynamic and neurohumoral alterations. Cardiovasc Res 2001;52:417-28.

47. VanAlstine WG. Respiratory System. In: Jeffrey J. Zimmerman LAK, Alejandro Ramirez, Kent J. Schwartz, Gregory W. Stevenson, editor Diseases of Swine 10th. 10th ed: John Wiley & Sons, 2012.

48. Gaggin HK, Januzzi JL, Jr. Biomarkers and diagnostics in heart failure. Biochim Biophys Acta 2013;1832:2442-50.

49. Dickinson MG, Bartelds B, Borgdorff MA, Berger RM. The role of disturbed blood flow in the development of pulmonary arterial hypertension: lessons from preclinical animal models. Am J Physiol Lung Cell Mol Physiol 2013;305:L1-14.
50. Shimoda LA, Laurie SS. Vascular remodeling in pulmonary hypertension. J Mol Med (Berl) 2013;91:297-309.
51. Shao D, Park JE, Wort SJ. The role of endothelin-1 in the pathogenesis of pulmonary arterial hypertension. Pharmacol Res 2011;63:504-11.
52. Shimoda LA, Sham JS, Liu Q, Sylvester JT. Acute and chronic hypoxic pulmonary vasoconstriction: a central role for endothelin-1? Respir Physiol Neurobiol 2002;132:93-106.
53. Kawanabe Y, Nauli SM. Endothelin. Cell Mol Life Sci 2011;68:195-203.
54. Cody RJ, Haas GJ, Binkley PF, Capers Q, Kelley R. Plasma endothelin correlates with the extent of pulmonary hypertension in patients with chronic congestive heart failure. Circulation 1992;85:504-9.
55. Pacher R, Stanek B, Hulsmann M et al. Prognostic impact of big endothelin-1 plasma concentrations compared with invasive hemodynamic evaluation in severe heart failure. J Am Coll Cardiol 1996;27:633-41.
56. Giaid A, Yanagisawa M, Langleben D et al. Expression of endothelin-1 in the lungs of patients with pulmonary hypertension. N Engl J Med 1993;328:1732-9.
57. Stewart DJ, Levy RD, Cernacek P, Langleben D. Increased plasma endothelin-1 in pulmonary hypertension: marker or mediator of disease? Ann Intern Med 1991;114:464-9.
58. Anand I, McMurray J, Cohn JN et al. Long-term effects of darusentan on left-ventricular remodelling and clinical outcomes in the EndothelinA Receptor Antagonist Trial in Heart Failure (EARTH): randomised, double-blind, placebo-controlled trial. Lancet 2004;364:347-54.
59. Coletta AP, Cleland JG. Clinical trials update: highlights of the scientific sessions of the XXIII Congress of the European Society of Cardiology--WARIS II, ESCAMI, PAFAC, RITZ-1 and TIME. Eur J Heart Fail 2001;3:747-50.
60. Kalra PR, Moon JC, Coats AJ. Do results of the ENABLE (Endothelin Antagonist Bosentan for Lowering Cardiac Events in Heart Failure) study spell the end for non-selective endothelin antagonism in heart failure? Int J Cardiol 2002;85:195-7.
61. Louis A, Cleland JG, Crabbe S et al. Clinical Trials Update: CAPRICORN, COPERNICUS, MIRACLE, STAF, RITZ-2, RECOVER and RENAISSANCE and cachexia and cholesterol in heart failure. Highlights of the Scientific Sessions of the American College of Cardiology, 2001. Eur J Heart Fail 2001;3:381-7.
62. Luscher TF, Enseleit F, Pacher R et al. Hemodynamic and neurohumoral effects of selective endothelin A (ET(A)) receptor blockade in chronic heart failure: the Heart Failure ET(A) Receptor Blockade Trial (HEAT). Circulation 2002;106:2666-72.
63. McMurray JJ, Teerlink JR, Cotter G et al. Effects of tezosentan on symptoms and clinical outcomes in patients with acute heart failure: the VERITAS randomized controlled trials. JAMA 2007;298:2009-19.

64. Packer M, McMurray J, Massie BM et al. Clinical effects of endothelin receptor antagonism with bosentan in patients with severe chronic heart failure: results of a pilot study. J Card Fail 2005;11:12-20.

65. Koller B, Steringer-Mascherbauer R, Ebner CH et al. Pilot Study of Endothelin Receptor Blockade in Heart Failure with Diastolic Dysfunction and Pulmonary Hypertension (BADDHY-Trial). Heart Lung Circ 2017;26:433-441.

66. Vachiery JL, Delcroix M, Al-Hiti H et al. Macitentan in pulmonary hypertension due to left ventricular dysfunction. Eur Respir J 2018;51.

67. Domingo L, Magdo HS, Day RW. Acute Pulmonary Vasodilator Testing and Long-Term Clinical Course in Segmental Pulmonary Vascular Disease. Pediatr Cardiol 2018;39:501-508.

68. McLaughlin V, Channick RN, Ghofrani HA et al. Bosentan added to sildenafil therapy in patients with pulmonary arterial hypertension. Eur Respir J 2015;46:405-13.

69. Califf RM, Adams KF, McKenna WJ et al. A randomized controlled trial of epoprostenol therapy for severe congestive heart failure: The Flolan International Randomized Survival Trial (FIRST). Am Heart J 1997;134:44-54.

70. Gottlieb SS. The impact of finally publishing a negative study: new conclusions about endothelin antagonists. J Card Fail 2005;11:21-2.

71. Reichenbach A, Al-Hiti H, Malek I et al. The effects of phosphodiesterase 5 inhibition on hemodynamics, functional status and survival in advanced heart failure and pulmonary hypertension: a case-control study. Int J Cardiol 2013;168:60-5.

72. Guazzi M, Vicenzi M, Arena R, Guazzi MD. Pulmonary hypertension in heart failure with preserved ejection fraction: a target of phosphodiesterase-5 inhibition in a 1-year study. Circulation 2011;124:164-74.

73. Lewis GD, Shah R, Shahzad K et al. Sildenafil improves exercise capacity and quality of life in patients with systolic heart failure and secondary pulmonary hypertension. Circulation 2007;116:1555-62.

74. Moraes DL, Colucci WS, Givertz MM. Secondary pulmonary hypertension in chronic heart failure: the role of the endothelium in pathophysiology and management. Circulation 2000;102:1718-23.

75. Rich S, Rabinovitch M. Diagnosis and treatment of secondary (non-category 1) pulmonary hypertension. Circulation 2008;118:2190-9.

76. Guazzi M, Vicenzi M, Arena R, Guazzi MD. PDE5 inhibition with sildenafil improves left ventricular diastolic function, cardiac geometry, and clinical status in patients with stable systolic heart failure: results of a 1-year, prospective, randomized, placebo-controlled study. Circ Heart Fail 2011;4:8-17.

77. Merkus D, Visser M, Houweling B, Zhou Z, Nelson J, Duncker DJ. Phosphodiesterase 5 inhibition-induced coronary vasodilation is reduced after myocardial infarction. Am J Physiol Heart Circ Physiol 2013;304:H1370-81.

78. Redfield MM, Chen HH, Borlaug BA et al. Effect of phosphodiesterase-5 inhibition on exercise capacity and clinical status in heart failure with preserved ejection fraction: a randomized clinical trial. JAMA 2013;309:1268-77.

79. Hoendermis ES, Liu LC, Hummel YM et al. Effects of sildenafil on invasive haemodynamics and exercise capacity in heart failure patients with preserved ejection fraction and pulmonary hypertension: a randomized controlled trial. Eur Heart J 2015;36:2565-73.

80. Kramer T, Dumitrescu D, Gerhardt F et al. Therapeutic potential of phosphodiesterase type 5 inhibitors in heart failure with preserved ejection fraction and combined post- and pre-capillary pulmonary hypertension. Int J Cardiol 2019;283:152-158.

81. Laux D, Rocchisani MA, Boudjemline Y, Gouton M, Bonnet D, Ovaert C. Pulmonary Hypertension in the Preterm Infant with Chronic Lung Disease can be Caused by Pulmonary Vein Stenosis: A Must-Know Entity. Pediatr Cardiol 2016;37:313-21.

82. Sykes MC, Ireland C, McSweeney JE, Rosenholm E, Andren KG, Kulik TJ. The impact of right ventricular pressure and function on survival in patients with pulmonary vein stenosis. Pulmonary Circulation 2018;8.

83. Garcia-Alvarez A, Fernandez-Friera L, Garcia-Ruiz JM et al. Noninvasive monitoring of serial changes in pulmonary vascular resistance and acute vasodilator testing using cardiac magnetic resonance. J Am Coll Cardiol 2013;62:1621-31.

84. Roman KS, Kellenberger CJ, Macgowan CK et al. How is pulmonary arterial blood flow affected by pulmonary venous obstruction in children? A phase-contrast magnetic resonance study. Pediatr Radiol 2005;35:580-6.

85. van de Veerdonk MC, Bogaard HJ, Voelkel NF. The right ventricle and pulmonary hypertension. Heart failure reviews 2016;21:259-71.

86. Vonk Noordegraaf A, Chin KM, Haddad F et al. Pathophysiology of the right ventricle and of the pulmonary circulation in pulmonary hypertension: an update. Eur Respir J 2019;53.

87. Naeije R, D'Alto M. The Diagnostic Challenge of Group 2 Pulmonary Hypertension. Prog Cardiovasc Dis 2016;59:22-9.

88. Vonk-Noordegraaf A, Haddad F, Chin KM et al. Right heart adaptation to pulmonary arterial hypertension: physiology and pathobiology. J Am Coll Cardiol 2013;62:D22-33.

89. Franciosa JA, Baker BJ, Seth L. Pulmonary versus systemic hemodynamics in determining exercise capacity of patients with chronic left ventricular failure. Am Heart J 1985;110:807-13.

90. Kim J, Di Franco A, Seoane T et al. Right Ventricular Dysfunction Impairs Effort Tolerance Independent of Left Ventricular Function Among Patients Undergoing Exercise Stress Myocardial Perfusion Imaging. Circ Cardiovasc Imaging 2016;9.

91. Baker BJ, Wilen MM, Boyd CM, Dinh H, Franciosa JA. Relation of right ventricular ejection fraction to exercise capacity in chronic left ventricular failure. Am J Cardiol 1984;54:596-9.

92. Borlaug BA, Kane GC, Melenovsky V, Olson TP. Abnormal right ventricular-pulmonary artery coupling with exercise in heart failure with preserved ejection fraction. Eur Heart J 2016;37:3293-3302.

93. Guazzi M, Villani S, Generati G et al. Right Ventricular Contractile Reserve and Pulmonary Circulation Uncoupling During Exercise Challenge in Heart Failure: Pathophysiology and Clinical Phenotypes. JACC Heart Fail 2016;4:625-35.

94. Topilsky Y, Rozenbaum Z, Khoury S et al. Mechanisms of Effort Intolerance in Patients With Heart Failure and Borderline Ejection Fraction. Am J Cardiol 2017;119:416-422.

95. Tampakakis E, Shah SJ, Borlaug BA et al. Pulmonary Effective Arterial Elastance as a Measure of Right Ventricular Afterload and Its Prognostic Value in Pulmonary Hypertension Due to Left Heart Disease. Circ Heart Fail 2018;11:e004436.

96. Guazzi M, Dixon D, Labate V et al. RV Contractile Function and its Coupling to Pulmonary Circulation in Heart Failure With Preserved Ejection Fraction: Stratification of Clinical Phenotypes and Outcomes. JACC Cardiovasc Imaging 2017;10:1211-1221.

97. Oliveira RKF, Faria-Urbina M, Maron BA, Santos M, Waxman AB, Systrom DM. Functional impact of exercise pulmonary hypertension in patients with borderline resting pulmonary arterial pressure. Pulmonary Circulation 2017;7:654-665.

98. Wensel R, Jilek C, Dorr M et al. Impaired cardiac autonomic control relates to disease severity in pulmonary hypertension. Eur Respir J 2009;34:895-901.

99. Bristow MR, Minobe W, Rasmussen R et al. Beta-adrenergic neuroeffector abnormalities in the failing human heart are produced by local rather than systemic mechanisms. J Clin Invest 1992;89:803-15.

100. Zong P, Tune JD, Downey HF. Mechanisms of oxygen demand/supply balance in the right ventricle. Exp Biol Med (Maywood) 2005;230:507-19.

101. Bian X, Downey HF. Right coronary pressure modulates right ventricular systolic stiffness and oxygen consumption. Cardiovasc Res 1999;42:80-6.

102. Yi KD, Downey HF, Bian XM, Fu M, Mallet RT. Dobutamine enhances both contractile function and energy reserves in hypoperfused canine right ventricle. Am J Physiol-Heart C 2000;279:H2975-H2985.

103. van Wolferen SA, Marcus JT, Westerhof N et al. Right coronary artery flow impairment in patients with pulmonary hypertension. Eur Heart J 2008;29:120-7.

104. Divekar A, Auslender M, Colvin S, Artman M, Rutkowski M. Abnormal right coronary artery flow and multiple right ventricular myocardial infarctions associated with severe right ventricular systolic hypertension. J Am Soc Echocardiogr 2001;14:70-2.

105. Akasaka T, Yoshikawa J, Yoshida K, Hozumi T, Takagi T, Okura H. Comparison of relation of systolic flow of the right coronary artery to pulmonary artery pressure in patients with and without pulmonary hypertension. Am J Cardiol 1996;78:240-4.

106. Ishibashi Y, Tanabe K, Oota T et al. Phasic right coronary blood flow in a patient with right ventricular hypertension using transesophageal Doppler echocardiography. Cardiology 1995;86:169-71.

107. Archie JP, Fixler DE, Ullyot DJ, Buckberg GD, Hoffman JI. Regional myocardial blood flow in lambs with concentric right ventricular hypertrophy. Circ Res 1974;34:143-54.

108. Lowensohn HS, Khouri EM, Gregg DE, Pyle RL, Patterson RE. Phasic right coronary artery blood flow in conscious dogs with normal and elevated right ventricular pressures. Circ Res 1976;39:760-6.

109. Murray PA, Baig H, Fishbein MC, Vatner SF. Effects of exerimental right ventricular hypertrophy on myocardial blood flow in conscious dogs. J Clin Invest 1979;64:421-7.

110. Murray PA, Vatner SF. Reduction of Maximal Coronary Vasodilator Capacity in Conscious Dogs with Severe Right Ventricular Hypertrophy. Circulation Research 1981;48:25-33.

111. Guyton AC, Lindsey AW, Gilluly JJ. The limits of right ventricular compensation following acute increase in pulmonary circulatory resistance. Circ Res 1954;2:326-32.

112. Salisbury PF. Coronary artery pressure and strength of right ventricular contraction. Circ Res 1955;3:633-8.

113. Brooks H, Kirk ES, Vokonas PS, Urschel CW, Sonnenblick EH. Performance of the right ventricle under stress: relation to right coronary flow. J Clin Invest 1971;50:2176-83.

114. Klima UP, Guerrero JL, Vlahakes GJ. Myocardial perfusion and right ventricular function. Ann Thorac Cardiovasc Surg 1999;5:74-80.

115. Vogel-Claussen J, Skrok J, Shehata ML et al. Right and left ventricular myocardial perfusion reserves correlate with right ventricular function and pulmonary hemodynamics in patients with pulmonary arterial hypertension. Radiology 2011;258:119-27.

116. Delporte C, Winand J, Poloczek P, Von Geldern T, Christophe J. Discovery of a potent atrial natriuretic peptide antagonist for ANPA receptors in the human neuroblastoma NB-OK-1 cell line. Eur J Pharmacol 1992;224:183-8.

117. Poirier H, Labrecque J, Deschenes J, DeLean A. Allotopic antagonism of the non-peptide atrial natriuretic peptide (ANP) antagonist HS-142-1 on natriuretic peptide receptor NPR-A. Biochem J 2002;362:231-7.

118. Zhang PL, Jimenez W, Mackenzie HS et al. HS-142-1, a potent antagonist of natriuretic peptides in vitro and in vivo. J Am Soc Nephrol 1994;5:1099-105.

119. Toki S, Morishita Y, Sano T, Matsuda Y. HS-142-1, a novel non-peptide ANP antagonist, blocks the cyclic GMP production elicited by natriuretic peptides in PC12 and NG108-15 cells. Neurosci Lett 1992;135:117-20.

120. Norling LL, von Geldern T, Chevalier RL. Maturation of A71915-dependent inhibition of atrial natriuretic peptide-stimulated cyclic GMP production in isolated rat glomeruli. Biol Neonate 1994;66:294-301.

121. Brugts JJ, Manintveld OC, van Mieghem N. Remote monitoring of pulmonary artery pressures with CardioMEMS in patients with chronic heart failure and NYHA class III: first experiences in the Netherlands. Neth Heart J 2018;26:55-57.

122. Ayyadurai P, Alkhawam H, Saad M et al. An update on the CardioMEMS pulmonary artery pressure sensor. Ther Adv Cardiovasc Dis 2019;13:1753944719826826.

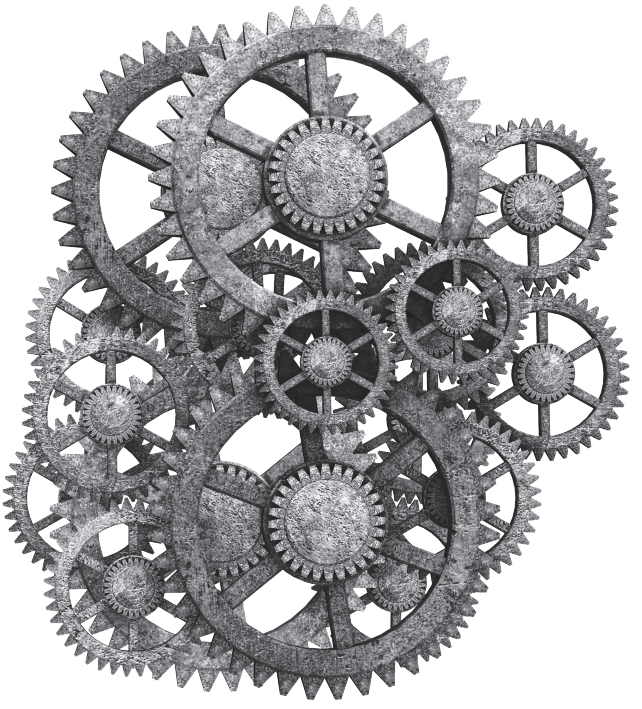

8

Chapter 8

Nederlandse samenvatting

NEDERLANDSE SAMENVATTING

Elke levende cel heeft zuurstof en voedingsstoffen nodig als bron van energie. Eéncellige organismen kunnen deze simpelweg opnemen uit hun omgeving. Ons lichaam bestaat echter uit ongeveer 100 biljoen cellen en slechts een klein percentage hiervan heeft direct contact met de buitenwereld. Om toch al onze cellen van zuurstof en voedingsstoffen te voorzien zijn er drie dingen nodig: bloed, als medium om zuurstof en voedingsstoffen te vervoeren; het bloedvatenstelsel, dat als een uitgebreid wegennetwerk elke cel bereikt; en het hart, dat door krachtig samen te knijpen ervoor zorgt dat het bloed door het bloedvatenstelsel wordt rondgepompt.

Het bloed wordt vanuit het *rechter ventrikel* (hartkamer) de *pulmonale circulatie* (kleine bloedsomloop) ingepompt. In de kleinste bloedvaatjes van de longen neemt het bloed zuurstof op vanuit de lucht in de longblaasjes. Ook geeft het bloed koolstofdioxide af aan de lucht. Het zuurstofrijke bloed komt door de *pulmonaal vene* (longader) terug bij het hart in het *linker atrium* (boezem) en vervolgens in het linker ventrikel. Deze knijpt krachtig samen en pompt zo het bloed de *systemische circulatie* (grote bloedsomloop) in, om alle organen en omliggende weefsels van zuurstof te voorzien en koolstofdioxide op te nemen. Hierna stroomt het bloed door de aders terug naar het rechter atrium. Het grote verschil tussen de systemische en pulmonale circulatie is de bloeddruk. Die is hoog (~95 mmHg) in de systemische circulatie, zodat het bloed elke cel kan bereiken, en laag (~15 mmHg) in de pulmonale circulatie, zodat er vrije uitwisseling van gassen met de lucht mogelijk is.

Wanneer de bloeddruk in de pulmonale circulatie te hoog is (≥25 mmHg) spreekt men van *pulmonale hypertensie*. Dit is een complexe, levensbedreigende ziekte. Mensen met pulmonale hypertensie ervaren klachten als kortademigheid, ongewone vermoeidheid, flauwvallen, vocht vasthouden, verslechterende conditie, hartkloppingen of pijn op de borst. Hoewel deze klachten erg vervelend zijn, zijn ze niet specifiek voor pulmonale hypertensie. Ook gaat de ziekte vaak gepaard met andere aandoeningen die soortgelijke klachten kunnen veroorzaken. Hierdoor wordt pulmonale hypertensie vaak pas in een laat stadium opgemerkt.

Er zijn verschillende vormen van pulmonale hypertensie, elk met hun eigen oorzaak en ziekteverloop. *Pulmonale arteriële hypertensie* ontstaat bijvoorbeeld door vernauwing en verstijving van de bloedvaten in de pulmonale circulatie en *chronisch trombo-embolische pulmonale hypertensie* ontstaat wanneer er bloedstolsels vastlopen in de longslagaders. Verreweg de meest voorkomende vorm is *pulmonale hypertensie als gevolg van linker hartfalen*. Wanneer het linker ventrikel zijn pompkracht verliest, ontstaat er stuwing in de bloedvaten die het bloed aan het linker ventrikel aanleveren: het pulmonale vaatbed. Hierdoor ontstaat er een passieve drukverhoging in de pulmonale circulatie. De longvaten reageren hierop door samen te knijpen. Dit verkleint het risico op *longoedeem* (vocht in de longen), maar zorgt ook voor een verhoging van de vaatweerstand. Dit resulteert in een verdere drukverhoging en zo ontstaat er een neerwaartse spiraal van drukverhoging, vaatvernauwing en weerstandsverhoging. Uiteindelijk kan de rechter hartkamer, die ontworpen is voor de lage druk van de pulmonale circulatie, deze hoge druk niet meer aan. Het zal zich aan proberen te passen, maar in de meeste gevallen uiteindelijk falen met de dood als gevolg.

Op dit moment is er voor geen enkele vorm van pulmonale hypertensie een genezende therapie. Wel zijn er medicijnen die de klachten kunnen verminderen en kunnen zorgen dat de ziekte minder snel verergert, veelal door de vaten te laten ontspannen zodat zij weer toenemen in diameter. Dit kan echter gevaarlijk zijn bij pulmonale hypertensie als gevolg van linker hartfalen, omdat deze medicijnen de kans op longoedeem vergroten. Het advies bij deze vorm van pulmonale hypertensie is dan ook om enkel de onderliggende aandoening te behandelen. Door de functie van het linker ventrikel te verbeteren zal de pulmonale bloeddruk stabiliseren. In de praktijk zien we echter dat dit slechts bij een deel van de patiënten werkt. Bij andere patiënten loopt zelfs bij (gedeeltelijk) herstel van de linkerventrikelfunctie de pulmonale bloeddruk op. Dit komt doordat de bloedvaten door de aanhoudende hoge bloeddruk zijn verdikt en verstijfd. Hierdoor houdt de neerwaartse spiraal zichzelf in stand, zelfs als de initiële oorzaak weggenomen wordt. Om eerste stappen te kunnen zetten richting een betere behandeling bij deze vorm van pulmonale hypertensie is het belangrijk dat we de mechanismen die een rol spelen in de progressie van deze

ziekte kennen en begrijpen. We moeten weten welke mechanismen ervoor zorgen dat zelfs wanneer de oorzaak weggenomen wordt, de ziekte blijft verergeren en de conditie van de patiënt blijft verslechteren.

Het doel van dit proefschrift was dan ook inzicht verkrijgen in de pathofysiologie van pulmonale hypertensie als gevolg van linker hartfalen. Specifiek hebben we onderzocht 1) hoe gezonde longvaten reageren op een pulmonale drukverhoging, 2) of er bij aanhoudende drukverhoging iets gebeurt met de regulatie van vaatverwijding en vaatvernauwing in de longvaten, 3) of er structurele veranderingen in de longvaten optreden zoals verdikking van de vaatwand en 4) hoe het rechter ventrikel zich aanpast aan de verhoogde pulmonale bloeddruk.

De aard van het onderzoek dat nodig is om deze vragen te beantwoorden maakt dat we dit niet kunnen onderzoeken in patiënten. Daarom onderzoeken we de ziekte bij een dier dat, zeker wat anatomie en -fysiologie betreft, erg lijkt op de mens: het varken. In **hoofdstuk 2** beschrijven we een methode waarmee we chronische katheters in en om het hart plaatsen. Hiermee kunnen we de bloeddrukken in verschillende delen van het hart en de grote vaten meten, en ook het hartminuutvolume en de zuurstofopname en –consumptie. Dit alles kunnen we meten over een periode van enkele maanden terwijl de dieren wakker zijn en zelfs tijdens inspanning.

In **hoofdstuk 3** hebben we dezelfde methode gebruikt om de hemodynamiek te bestuderen in varkens met een recent hartinfarct. Een hartinfarct beschadigt een deel van het linker ventrikel, waardoor de pompkracht minder wordt. We zagen een verhoogde druk in het linker atrium wat resulteerde in milde pulmonale hypertensie. Uit eerder onderzoek met dit diermodel weten we dat de vaatvernauwer *endotheline* in deze dieren extra actief is, waardoor de vaten zichzelf dichtknijpen. Ook weten we dat de vaatverwijder *stikstofoxide*, nog onverminderd actief is om de vaten juist te ontspannen. Binnen het onderzoek beschreven in **hoofdstuk 3** hebben we getest of we met het medicijn *Sildenafil* het vaat-ontspannende effect van stikstofoxide konden vergroten. Dit werkte zelfs nog beter dan bij gezonde dieren. Omdat we vanuit de

literatuur weten dat in gevorderde stadia van pulmonale hypertensie stikstofoxide minder actief kan zijn, hebben we dit medicijn ook getest in combinatie met een stof die stikstofoxide remt. Ook in deze situatie werkte het medicijn goed, wat kan betekenen dat zelfs bij patiënten met minder stikstofoxide, dit medicijn goed zou kunnen werken.

Voor het onderzoek beschreven in **Hoofdstuk 4** hebben we een varkensmodel met een ernstigere vorm van pulmonale hypertensie gebruikt. Dit hebben we opgewekt door een bandje te plaatsen om de pulmonaal vene. Dit is de ader waardoor zuurstofrijk bloed van de longen naar het linker atrium stroomt. Het bandje zorgt voor een hoge weerstand en dezelfde passieve drukverhoging als bij linker hartfalen. Met behulp van de chronische instrumentatietechniek uit **hoofdstuk 2** hebben we in **hoofdstuk 4** de progressie van pulmonale hypertensie en daarbij behorende mechanismen bestudeerd. We volgden de dieren tot 12 weken na de plaatsing van het bandje en zagen dat in die tijd de druk en de vaatweerstand in de pulmonale circulatie steeds hoger werden. Vanaf week 10 zagen we dat de vaatvernauwer endotheline extra actief werd. Hierdoor stegen de vaatweerstand en bloeddruk nog harder dan daarvoor. Naast deze functionele veranderingen was er ook sprake van structurele veranderingen. We zagen dat de vaatwand van de longvaatjes verdikt was en dat de vaten vernauwd waren. We hebben zowel in rust als tijdens inspanning gekeken wat het effect is van *Tezosentan*. Deze stof remt endotheline en zorgt daarmee voor vaatontspanning. We zagen dat hoe ernstiger de pulmonale hypertensie werd, hoe effectiever Tezosentan werd. Toch zorgde Tezosentan slechts voor een bescheiden drukverlaging.

In het onderzoek beschreven in **hoofdstuk 5** hebben we in hetzelfde varkensmodel als in **hoofdstuk 4** de vaatverwijder stikstofoxide verder onderzocht. We zagen dat 12 weken na de plaatsing van het bandje, stikstofoxide verhoogd was. Waarschijnlijk als compensatie voor de verhoogde endotheline. We hebben vervolgens verschillende medicijnen getest. Medicijnen die zorgen dat er meer stikstofoxide is en medicijnen die zorgen dat het lichaam gevoeliger is voor stikstofoxide. Dit laatste medicijn, *Sildenafil*, zoals ook gebruikt in **hoofdstuk 3** gaf de sterkste daling in pulmonale

bloeddruk. Bovendien zagen we geen tekenen van longoedeem bij het gebruik van Sildenafil. Dit zou kunnen komen omdat eerder is bewezen dat Sildenafil ook een positief effect heeft op de functie van het linker ventrikel. Dat zagen we ook in **hoofdstuk 3**.

In **hoofdstuk 6** hebben we het effect van pulmonale hypertensie op het rechter ventrikel bestudeerd. We zagen een toename in wanddikte, met name door verdikte spiercellen. Ook was het rechter ventrikel verwijd en was er sprake van een licht verminderde hartfunctie in rust. Inspanning zorgde voor verdere achteruitgang in hartfunctie. Dit kwam door twee dingen: de hartfrequentie kon niet genoeg toenemen tijdens inspanning en ondanks de gespierdere wand, kon de knijpkracht van het rechter ventrikel niet toenemen. Dit laatste lijkt te komen doordat de hartspier tijdens inspanning niet genoeg doorbloed wordt. Deze informatie kunnen we mogelijk gebruiken om bij patiënten in te schatten hoe ernstig de ziekte op dat moment is. Ook zou therapie gericht op een toename van de hartspierdoorbloeding effectief kunnen zijn in de behandeling van pulmonale hypertensie.

Samengevat heeft het onderzoek dat beschreven wordt in dit proefschrift, mechanismen geïdentificeerd die een rol spelen in de pathofysiologie van pulmonale hypertensie als gevolg van linker hartfalen. Het testen van verschillende medicamenten om farmacologisch in te grijpen op deze mechanismen heeft geleid tot een aanbeveling voor de optimale medicatie om de longvaten te verwijden. Daarnaast heeft het onderzoek aangetoond dat de achteruitgang van de rechter ventrikelfunctie in deze ziekte gepaard gaat met verminderde doorbloeding van de hartspier. Deze bevinding kan leiden tot verbeterde diagnostiek en therapie. Concluderend brengt de kennis, die is vergaard in dit onderzoek, ons dichter bij een genezende therapie voor pulmonale hypertensie als gevolg van linker hartfalen. Alhoewel hier nog veel vervolgonderzoek voor nodig is.

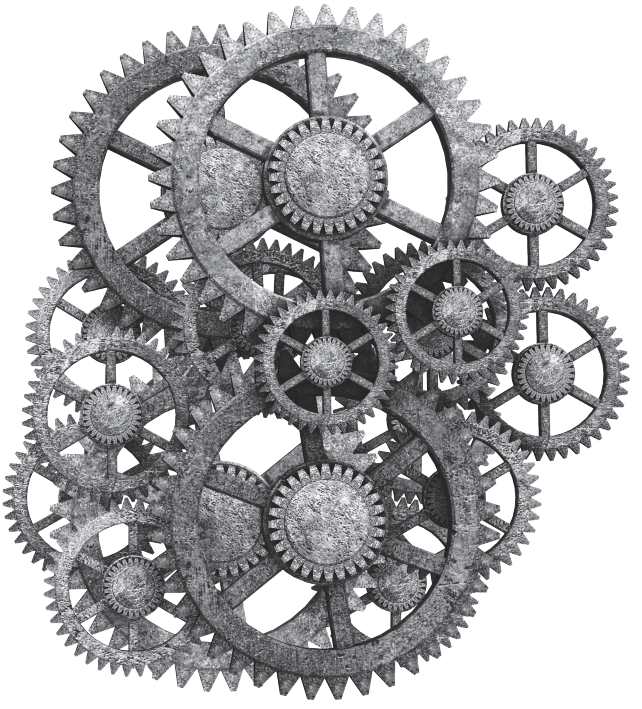

A

Appendices

List of publications

PhD portfolio

About the author

LIST OF PUBLICATIONS

1. **Cellular, mitochondrial and molecular alterations associate with early left ventricular diastolic dysfunction in a porcine model of diabetic metabolic derangement**
   Heinonen I, Sorop O, van Dalen BM, Wüst RCI, van de Wouw J, de Beer VJ, Octavia Y, **van Duin RWB**, Hoogstrate Y, Blonden L, Alkio M, Anttila K, Stubbs A, van der Velden J, Merkus D, Duncker DJ
   Sci Rep. 2020 Aug 6;10(1):13173

2. **Perturbations in myocardial perfusion and oxygen balance in swine with multiple risk factors: a novel model of ischemia and no obstructive coronary artery disease**
   van de Wouw J, Sorop O, van Drie RWA, **van Duin RWB**, Nguyen ITN, Joles JA, Verhaar MC, Merkus D, Duncker DJ
   Basic Res Cardiol. 2020 Feb 25;115(2):21

3. **Endovascular procedures cause transient endothelial injury but do not disrupt mature neointima in Drug Eluting Stents**
   Autar A, Taha A, **van Duin RWB**, Krabbendam-Peters I, Duncker DJ, Zijlstra F, van Beusekom HMM
   Sci Rep. 2020 Feb 7;10(1):2173

4. **Intervening with the Nitric Oxide Pathway to Alleviate Pulmonary Hypertension in Pulmonary Vein Stenosis**
   van Duin RWB, Stam K, Uitterdijk A, Bartelds B, Danser AHJ, Reiss IKM, Duncker DJ, Merkus D
   J Clin Med. 2019 Aug 12;8(8):1204

5. **Right ventricular oxygen delivery as a determinant of right ventricular functional reserve during exercise in juvenile swine with chronic pulmonary hypertension**
   van Duin RWB*, Cai Z*, Stam K, Uitterdijk A, van der Velden J, Vonk Noordegraaf A, Duncker DJ, Merkus D
   Am J Physiol Heart Circ Physiol. 2019 Oct 1;317(4):H840-H850

6. **Cardiac remodelling in a swine model of chronic thromboembolic pulmonary hypertension: comparison of right vs. left ventricle**
   Stam K, Cai Z, van der Velde N, **van Duin RWB**, Lam E, van der Velden J, Hirsch A, Duncker DJ, Merkus D
   J Physiol. 2019 Sep;597(17):4465-4480

7. **Validation of 4D flow CMR against simultaneous invasive hemodynamic measurements: a swine study**
   Stam K, Chelu RG, van der Velde N, **van Duin RWB**, Wielopolski P, Nieman K, Merkus D, Hirsch A
   Int J Cardiovasc Imaging. 2019 Jun;35(6):1111-1118

8. **Pulmonary microvascular remodeling in chronic thrombo-embolic pulmonary hypertension**
   Stam K, **van Duin RWB**, Uitterdijk A, Krabbendam-Peters I, Sorop O, Danser AHJ, Duncker DJ, Merkus D
   Am J Physiol Lung Cell Mol Physiol. 2018 Dec 1;315(6):L951-L964

9. **Transition from post-capillary pulmonary hypertension to combined pre- and post-capillary pulmonary hypertension in swine: a key role for endothelin**
   van Duin RWB, Stam K, Cai Z, Uitterdijk A, Garcia-Alvarez A, Ibanez B, Danser AHJ, Reiss IKM, Duncker DJ, Merkus D
   J Physiol. 2019 Feb;597(4):1157-1173

10. **Multiple common comorbidities produce left ventricular diastolic dysfunction associated with coronary microvascular dysfunction, oxidative stress, and myocardial stiffening**
    Sorop O, Heinonen I, van Kranenburg M, van de Wouw J, de Beer VJ, Nguyen ITN, Octavia Y, **van Duin RWB**, Stam K, van Geuns RJ, Wielopolski PA, Krestin GP, van den Meiracker AH, Verjans R, van Bilsen M, Danser AHJ, Paulus WJ, Cheng C, Linke WA, Joles JA, Verhaar MC, van der Velden J, Merkus D, Duncker DJ
    Cardiovasc Res. 2018 Jun 1;114(7):954-964

11. **The effect of bioresorbable vascular scaffold implantation on distal coronary endothelial function in dyslipidemic swine with and without diabetes**
    van den Heuvel M, Sorop O, van Ditzhuijzen NS, de Vries R, **van Duin RWB**, Peters I, van Loon JE, de Maat MP, van Beusekom HM, van der Giessen WJ, Jan Danser AH, Duncker DJ
    Int J Cardiol. 2018 Feb 1;252:44-51

12. **Exercise facilitates early recognition of cardiac and vascular remodeling in chronic thromboembolic pulmonary hypertension in swine**
    Stam K, **van Duin RWB**, Uitterdijk A, Cai Z, Duncker DJ, Merkus D
    Am J Physiol Heart Circ Physiol. 2018 Mar 1;314(3):H627-H642

13. **Structural and functional changes of the pulmonary vasculature after hypoxia exposure in the neonatal period: a new swine model of pulmonary vascular disease**
de Wijs-Meijler DPM, **van Duin RWB**, Duncker DJ, Scherrer U, Sartori C, Reiss IKM, Merkus D
Am J Physiol Heart Circ Physiol. 2018 Mar 1;314(3):H603-H615

14. **Pulmonary vasodilation by phosphodiesterase 5 inhibition is enhanced and nitric oxide independent in early pulmonary hypertension after myocardial infarction**
van Duin RWB, Houweling B, Uitterdijk A, Duncker DJ, Merkus D
Am J Physiol Heart Circ Physiol. 2018 Feb 1;314(2):H170-H179

15. **Neoatherosclerosis development following bioresorbable vascular scaffold implantation in diabetic and non-diabetic swine**
van Ditzhuijzen NS, Kurata M, van den Heuvel M, Sorop O, **van Duin RWB**, Krabbendam-Peters I, Ligthart J, Witberg K, Murawska M, Bouma B, Villiger M, Garcia-Garcia HM, Serruys PW, Zijlstra F, van Soest G, Duncker DJ, Regar E, van Beusekom HMM
PLoS One. 2017 Sep 12;12(9):e0183419

16. **Echocardiographic-Derived Strain-Area Loop of the Right Ventricle is Related to Pulmonary Vascular Resistance in Pulmonary Arterial Hypertension**
Hulshof HG, van Dijk AP, George KP, Merkus D, Stam K, **van Duin RWB**, van Tertholen K, Hopman MTE, Haddad F, Thijssen DHJ, Oxborough DL
JACC Cardiovasc Imaging. 2017 Oct;10(10 Pt B):1286-1288

17. **The microcirculation: a key player in obesity-associated cardiovascular disease.**
Sorop O, Olver TD, van de Wouw J, Heinonen I, **van Duin RWB**, Duncker DJ, Merkus D
Cardiovasc Res. 2017 Jul 1;113(9):1035-1045

18. **Coronary microvascular dysfunction after long-term diabetes and hypercholesterolemia**
Sorop O, van den Heuvel M, van Ditzhuijzen NS, de Beer VJ, Heinonen I, **van Duin RWB**, Zhou Z, Koopmans SJ, Merkus D, van der Giessen WJ, Danser AH, Duncker DJ
Am J Physiol Heart Circ Physiol. 2016 Dec 1;311(6):H1339-H1351

19. **Surgical Placement of Catheters for Long-term Cardiovascular Exercise Testing in Swine**
De Wijs-Meijler DP, Stam K, **van Duin RWB**, Verzijl A, Reiss IK, Duncker DJ, Merkus D
J Vis Exp. 2016 Feb 9;(108):e53772

20. **VEGF165A microsphere therapy for myocardial infarction suppresses acute cytokine release and increases microvascular density but does not improve cardiac function**
Uitterdijk A, Springeling T, van Kranenburg M, **van Duin RWB**, Krabbendam-Peters I, Gorsse-Bakker C, Sneep S, van Haeren R, Verrijk R, van Geuns RJ, van der Giessen WJ, Markkula T, Duncker DJ, van Beusekom HMM
Am J Physiol Heart Circ Physiol. 2015 Aug 1;309(3):H396-406

21. **Serial measurement of hFABP and high-sensitivity troponin I post-PCI in STEMI: how fast and accurate can myocardial infarct size and no-reflow be predicted?**
Uitterdijk A, Sneep S, **van Duin RWB**, Krabbendam-Peters I, Gorsse-Bakker C, Duncker DJ, van der Giessen WJ, van Beusekom HMM
Am J Physiol Heart Circ Physiol. 2013 Oct 1;305(7):H1104-10

22. **Invasive coronary imaging in animal models of atherosclerosis**
van Ditzhuijzen NS, van den Heuvel M, Sorop O, **van Duin RWB**, Krabbendam-Peters I, van Haeren R, Ligthart JM, Witberg KT, Duncker DJ, Regar E, van Beusekom HMM, van der Giessen WJ
Neth Heart J. 2011 Oct;19(10):442-6

PHD PORTFOLIO

Name PhD student:	Richard W B van Duin
ErasmusMC department:	Experimental Cardiology
PhD Period:	2014-2021
Promotor (1):	Prof. dr. D.J. Duncker
Promotor (2):	Prof. dr. D. Merkus

Courses and training	**Date**	**ECTS**
COEUR course: "Heart failure research"	13-14 feb 2014	1.5
DHF PhD course "Atherosclerosis and Thrombosis"	13-17 oct 2014	2
COEUR course "Pathophysiology of ischemic heart disease"	22+23 sep 2016	1.2
Basic Training and Intensive-Course - Sonography	9-11 may 2017	0.9
Career guidance program	sept 2017 - mar 2018	2
Blogging for scientists	nov 2017	0.3
COEUR course "Myocardial function in health & disease"	16 mar 2018	0.5
COEUR course "Cardiac myocytes and coronary vasculature in health & disease"	23 mar 2018	0.5
COEUR course "Congenital Cardiology in children and adults"	25 may 2018	0.5

COEUR Research seminars	**Date**	**ECTS**
Non-invasive imaging of myocardial ischemia	17 jan 2014	0.3
Specific Molecular Pathways and Targeted Therapy of Right Heart Failure	26 may 2014	0.3
Ischemic Heart Disease: Adaptations and Treatment	10 jun 2014	0.3
Current Cardiac and Vascular Aging Research at EMC	20 jun 2014	0.3
Translational research	14 jan 2016	0.3
Heart failure	12 feb 2016	0.3
Double COEUR seminar: Stuart Foster & James Muller	15 jun 2016	0.3

Conferences and meetings	Date	ECTS
LICR TGF-beta meeting	8-10 may 2014	0.9
Joint DEBS-MiVab meeting (+oral)	30-31 oct 2014	0.9
NVF "Exercise Physiology" (+oral)	27-28 nov 2014	0.9
Thalys meeting	20-21 feb 2015	0.6
DPD "Body-Brain Physiology" (+poster)	26-27 nov 2015	0.9
DPD "Nutrition and Metabolism" (+poster)	24-25 nov 2016	0.9
ExCOEURsion to Philips Healthcare (+organization)	17 feb 2017	0.3
Experimental Biology (+poster)	22-26 April 2017	1.9
1st Translational cardiovascular research meeting (+poster)	29-30 jun 2017	0.9
3rd EU conference on neonatal and peadiatric pulmonary vascular disease (+poster and oral)	12+13 oct 2017	1.2
PHAEDRA Summer School (Organization 2015)	2014-2017	3.5
PHAEDRA quarterly consortium meetings (+orals)	2014-2018	4
6th World Symposium on Pulmonary Hypertension (+poster)	27-28 mar, 1 apr 2018	1.2
ErasmusMC Pulmonary Hypertension Symposium	29 mar 2018	0.3
FCVB Vienna (+poster)	20-22 apr 2018	1.2
2nd Translational cardiovascular research meeting (+poster)	28+29 jun 2018	0.9
COEUR PhD-days (organization 2016-2018)	2014-2018	2.3
3rd Translational cardiovascular research meeting	27+28 jun 2019	0.6

Teaching and board activities:	Date	ECTS
Student education Histology	2015-2018	1
Coeur PhD-committee	2015-2018	1
Supervising Internship Biology and medical laboratory research (Macha Dreu, Denise Verbeek, Angelique Kooijman, Janneke Vos)	2014-2018	4
Supervising Internship Life Science (pre-med, Juliette van Laack)	2016	1
Supervising Internship Medical biology technician (Jessica Lange)	2017	1
	Total	**42.9**

ABOUT THE AUTHOR

Richard Willem Benjamin van Duin was born on the 27th of January, 1987 in Spijkenisse. He attended higher education at CSG Angelus Merula in Spijkenisse. Next he studied Biology and Medical Research at the Rotterdam University of Applied Sciences. During the final year of his studies, he started his research internship at the Thorax Centre, division of Experimental Cardiology at the Erasmus MC. Here he investigated acute and prolonged coronary endothelial injury as a result of repeated intravascular imaging, guidewire use and stenting under the supervision of prof. dr. Wim van der Giessen and dr. Heleen van Beusekom. After obtaining his bachelor's degree, he continued working at the Erasmus MC as a research technician for four years, during which he focused on percutaneous transluminal coronary interventions, intracoronary imaging, and vascular wound healing in large animal models with and without co-morbidities. Although the practical work was a welcome challenge and the focus of the research in line with his interests, he increasingly aspired to a role that would better satisfy his natural curiosity and challenge him on a more intellectual level. He started his PhD-traineeship under supervision of prof. dr. Dirk Jan Duncker and prof. dr. Daphne Merkus. His research was focused on defining pathophysiological mechanisms in group II pulmonary hypertension. The results of this research are described in this thesis.